ABSTRACT

Title of dissertation: The Antiviral Roles of Atg1
Against *Drosophila* X Virus
in *Drosophila melanogaster*

Qian Wang, Doctor of Philosophy, 2014

Dissertation directed by: Professor Louisa Wu
Department of Cell Biology and Molecular Genetics

In mammals, autophagy is important for the immune response against select viruses and is responsible for delivering virus to the lysosome for degradation. In *Drosophila melanogaster*, the roles of autophagy genes in an antiviral immune response are not fully understood. Here we identify a novel antiviral role for *Atg1* in *Drosophila melanogaster* upon infection with *Drosophila* X virus (DXV). Flies with a decreased level of *Atg1* expression in the fat body developed an increased susceptibility to DXV and have a higher viral load compared to wildtype. However, silencing of other autophagy components (*Atg7, Atg8*) does not have the same effect. Moreover, we could find no evidence that classical autophagy is directly associated with DXV upon viral infection. This suggests that the antiviral function of *Atg1* may be independent of classical autophagy. To address this, we examined the effect of *Atg1* knockdown on the fly transcriptome in both DXV infected and uninfected flies. Interestingly, lipid droplet lipolysis and β-oxidation, two major processes responsible for energy production, are induced upon DXV infection. Facilitating lipolysis by knocking down *lsd2*, a positive regulator of lipase *bmm*, results in

an increased host susceptibility to DXV, together with an increased viral load. In contrast, blocking lipolysis in the negative regulator *lsd1* null mutant renders the host more resistant to the virus. This indicates that the increased energy production favors the virus for active replication and does not favor the elimination of virus. Surprisingly, silencing of *Atg1*, even in the absence of infection, also increases the rates of lipolysis and β-oxidation, shown by an increased expression of genes that are involved in lipid metabolism and an decreased lipid droplet size in the *Atg1*-silenced flies. The differences in gene expression and lipid droplet size between *Atg1* RNAi flies and WT flies become more apparent as the infection progresses. In summary, we identify a novel role for *Atg1* in restricting energy production and limiting DXV replication. This finding may shed light on antiviral studies against other dsRNA viruses that manipulate host energy homeostasis. Finally, our data reveal an important and unexpected role for *Atg1* in innate immune antiviral responses independent of autophagy.

THE ANTIVIRAL ROLES OF ATG1 IN *DROSOPHILA MELANOGASTER*: IMMUNE RESPONSES AGAINST *DROSOPHILA* X VIRUS

by

Qian Wang

Dissertation submitted to the Faculty of the Graduate School of the
University of Maryland, College Park in partial fulfillment
of the requirements for the degree of
Doctor of Philosophy
2014

Advisory Committee:
Professor Louisa Wu, Chair/Advisor
Professor Najib M. El-Sayed
Professor Michael Ma
Professor David Mosser
Professor Steve Mount

Dedication

To my Mom and Dad.

Acknowledgments

I owe my gratitude to all the people who have made this thesis possible and because of whom my graduate experience has been one that I will cherish forever.

I would like to first thank my thesis adviser Dr. Louisa Wu, who has been very supportive through the years. Your "Try it" attitude encourages me to explore various research ideas and experiments, which lead me to become an independent researcher. Your spirit for innovation guides me towards investigating novel and interesting research topics. And I specifically appreciate your tremendous patience and devoted efforts in honing my writing skills through modifying various writing scripts over and over.

Secondly, I would love to thank my labmates Dr. Javier Robalino, Dr. Jahda Hill, Dr. Elizabeth Anne Gonzalez, Dr. Jessica Tang, Dr. Aprajita Garg, Ashley Nazario and our past lab technician Mr. Junlin Wu. Dr. Javier Robalino had genuinely offered great advice and coached me on various experimental techniques that I had no prior experience in. I also could not forget the many times when you patiently discussed research problems with me. I cannot imagine finishing the project without your help. I also thank Dr. Jahda Hill for being such a wonderful labmate and a friend. As the only autophagy expert in the lab, you've offered great suggestions and also provide me with numerous useful research materials. Without you, my project to study autophagy wouldn't be possible. Dr. Jahda Hill is also a cheerful and energetic person, whose curiosity and adventurous spirit have lead us to great moments from cultural discussion, Mandarin lessons, American cuisine cooking events and even a band performance. I also want to thank Dr. Jessica Tang, who has been so sweet and diligent in helping to develop our lab into a better place. Also in

the same class, Jessica has been very supportive from the very first day since I was on campus. To Dr. Elizabeth Anne Gonzalez, thank you for being so sweet and I enjoyed the company of you not only as a labmate, an officemate but also a friend. To Ashley Nazario, thank you for being so organized and volunteering for a lot of the lab duties after Junlin's leave.

Thirdly, I would love to give my special thanks to all my committee members and collaborators: Dr. Najib M. El-Sayed, Dr. Michael Ma, Dr. David Mosser, Dr. Steve Mount, Dr. Héctor Corrada Bravo and his graduate student Kwame Okrah. Without your constructive suggestions on the research projects in and out of the committee meetings, I can not be where I am now. Specifically, I'd love to thank Dr. Michael Ma, Dr. Steve Mount and Dr. Najib M. El-Sayed for your help on the bioinformatics project. Without those detailed instructions, I would not be able to finish the RNA-seq analysis in a timely manner. To Dr. David Mosser, thank you for taking me as a rotation student and inspiring me to explore the host-pathogen interactions. To Dr. Héctor Corrada Bravo and Kwame Okrah, thank you for your advise on statistical analyses and contribution on the generation of statistical figures such as the PCA plots, scatter plots and heatmaps (Figure 3.3, Figure 3.4, Figure 3.5, Figure 3.6A-C, Figure 3.7A-C, Figure 3.8A-C) on the RNA-seq data.

Finally, I would love to thank my family and friends for your unconditional love and support. To my mom and dad, thank you for being so supportive to allow me to explore an academic life in the United States. Life in graduate school is not smooth and I apologize for causing you stresses and concerns. But I appreciate your belief in me through all of my ups and downs. To my boyfriend Dr. Qi Hu, thank you for being there

for me providing not only emotional support but also critical advice. To my best friends at University of Maryland, Dr. Vivian Guo, Dr. Qiang Li, Tao Liu, Jia Wen, Zhe Chen, Lvyuan Chen, Yinghui Zheng and Zongzhong Peng and Nan Zhou, thank you for your years of company. To my old friends, Dr. Chun Chen, Dr. Ran An, Naji Liu, Minmin Pan, Lei Zhao, and Shi Yan, thank you for your continuous support no matter where I am.

Table of Contents

List of Tables ix

List of Figures x

List of Abbreviations xii

1 Introduction 1
- 1.1 The innate immune system in *Drosophila melanogaster* . . . 1
  - 1.1.1 Microbial Recognition . . . 2
- 1.2 *Drosophila* viruses . . . 3
  - 1.2.1 *Drosophila* X virus . . . 3
    - 1.2.1.1 Taxonomy . . . 4
    - 1.2.1.2 Viral genome and proteins . . . 5
    - 1.2.1.3 Virus cycle . . . 9
- 1.3 Antiviral responses in *Drosophila melanogaster* . . . 9
  - 1.3.1 The Toll Signaling Pathway . . . 11
  - 1.3.2 The Imd Signaling Pathway . . . 13
  - 1.3.3 JAK-STAT Signaling Pathway . . . 17
  - 1.3.4 RNA interference pathway . . . 19
  - 1.3.5 JNK Signaling Pathway . . . 21
  - 1.3.6 Autophagy . . . 22
    - 1.3.6.1 Autophagy signaling pathway . . . 24
    - 1.3.6.2 Signaling regulation of autophagy . . . 29
    - 1.3.6.3 The immune function of autophagy . . . 30
    - 1.3.6.4 Crosstalk between autophagy and other immune signaling 33
- 1.4 Lipid Metabolism . . . 37
  - 1.4.1 Lipid droplets as energy storage compartments . . . 37
  - 1.4.2 The Perilipin family proteins in the regulation of LDs . . . 40
  - 1.4.3 β-Oxidation . . . 48

2 Atg1 plays an antiviral role against *Drosophila* X Virus, but this effect appears to be independent of classical autophagy 51
2.1 Results . . . 51
2.1.1 Atg1 plays an antiviral role against DXV infection in the fat body 51
2.1.2 Autophagy does not appear to be specifically activated by DXV in both larval hemocytes and adult fat body . . . 59
2.1.3 Autophagy is not induced in *ex vivo* hemocytes upon DXV infection 62
2.1.4 Autophagy is not induced in *Drosophila* S2 cells . . . 65
2.1.5 Autophagy is not induced in GFP-Atg8 *Drosophila* S2R+ cells . . 72
2.1.6 The antiviral function of Atg1 is not through regulating RNA interference pathway upon DXV infection . . . 74
2.2 Materials and methods . . . 77
2.2.1 Fly stocks. . . . 77
2.2.2 Cell lines. . . . 77
2.2.3 Virus infections. . . . 77
2.2.4 Survival analyses. . . . 78
2.2.5 RT-PCR. . . . 78
2.2.6 Protein extraction and Western blot. . . . 78
2.2.7 Staining and confocal imaging. . . . 79
2.2.8 Electron Microscopy . . . 80

3 Transcriptome Profiling of WT and *Atg1* RNAi flies upon DXV infection 81
3.1 Introduction to RNA-seq . . . 81
3.1.1 Pipeline for RNA seq analysis . . . 82
3.1.1.1 Generation of RNA seq data set . . . 84
3.1.1.2 RNA seq data analysis . . . 85
3.2 Differential expression analysis . . . 87
3.2.1 Normalization . . . 88
3.2.2 Statistical modeling of gene expression . . . 89
3.2.3 Test for differential expression . . . 89
3.3 Exploratory studies . . . 90
3.3.1 Scatter plot . . . 90
3.3.2 Clustering and visualization . . . 91
3.3.3 Principle component analysis and its visualization . . . 92
3.4 Results . . . 92
3.4.1 Statistics diagnostics . . . 94
3.4.2 Differential expression analysis in wildtype flies upon DXV infection at day 3 and day 5 . . . 100
3.4.3 Differential expression analysis in wildtype flies upon DXV infection at day 7 . . . 103
3.4.4 Differential expression analysis between wildtype and *Atg1* RNAi flies without infection . . . 107
3.5 Materials and methods . . . 109

4 Atg1 is playing an antiviral role against DXV by regulating lipid metabolism 111
4.1 Results . . . 111
4.1.1 DXV infection induces lipolysis in the lipid droplet . . . 111
4.1.2 Atg1 regulates lipid metabolism even in the absence of DXV infection . . . 114
4.1.3 Lipid metabolism is important for DXV infection . . . 116
4.2 Materials and Methods . . . 120
4.2.1 Fly stocks. . . . 120
4.2.2 Lipid staining and confocal imaging. . . . 120

5 Conclusions and discussions 121

A Appendix A 126
A.1 Differentially expressed genes between uninfected WT flies and DXV-infected flies at day 7 post infection . . . 126
A.2 Differentially expressed genes between wildtype flies and *IR-Atg1* flies without DXV infection . . . 161

List of Tables

3.1 Differentially expressed genes between uninfected WT flies and DXV-infected flies at day 3 post infection. Genes presented in the table are selected by log_2 fold Change > 0.5 and p value < 0.05. Gene list is sorted by log_2 fold Change from the largest to the smallest. 102
3.2 Differentially expressed genes between uninfected WT flies and DXV-infected flies at day 5 post infection. Genes presented in the table are selected by log_2 fold Change > 0.5 and p value < 0.05. Gene list is sorted by log_2 fold Change from the largest to the smallest. 102
3.3 Immune genes that are responsive to DXV infection in WT flies. 106

A.1 Differentially expressed genes between uninfected WT flies and DXV-infected flies at day7 post infection. Genes presented in the table are selected by log_2 fold Change > 0.5 and p value < 0.05. Gene list is sorted by log_2 fold Change from the largest to the smallest. 160
A.2 Differentially expressed genes between wildtype flies and *IR-Atg1* flies without DXV infection. Genes presented in the table are selected by log_2 fold Change > 0.5 and p value < 0.05. Gene list is sorted by log_2 fold Change from the largest to the smallest. 179

List of Figures

1.1 DXV viron structure. 5
1.2 DXV Genome Structure. 6
1.3 Immune signaling against virus. 11
1.4 Schematic representation of the Imd signaling pathway and TNF-α pathway. 14
1.5 Diagram of the RNA interference pathway in fighting against invading virus. 20
1.6 Diagram of the Autophagy process. 23
1.7 The signaling components of Autophagy. 25
1.8 Schematic representation of the lipid storage tissues in the *Drosophila*. . . 38
1.9 Schematic representation of the core enzymes in the *Drosophila* lipid metabolism. 39
1.10 Diagram of Lipid droplet metabolism. 47
1.11 Lipid metabolism and β-oxidation. 49

2.1 Silencing of *Atg1* renders flies more susceptible to DXV. 53
2.2 Fat body is the tissue important for the *Atg1*-dependent immune response. 55
2.3 Western blots of DXV viral proteins in the dissected tissues of adult flies. 57
2.4 *Atg* genes are not important for the host response against CrPV and DCV. 58
2.5 Autophagy does not appear to be activated directly by DXV. 61
2.6 Autophagy is not induced in *ex vivo* hemocytes upon TS-DXV infection. . 64
2.7 A representative picture showing DXV in multi-membraned vesicles by electron microscopy-I. 66
2.8 A representative picture howing DXV in multi-membraned vesicles by electron microscopy-II. 67
2.9 DXV replicates in S2 cells and forms array-like structures. 68
2.10 Autophagy is induced to eliminate mitochondria. 69
2.11 Electron Microscopy of an S2 cell upon DXV infection: Virus particles within ER-like structures. 70
2.12 Magnified picture from Figure 2.11. 71
2.13 DXV does not induce autophagosome formation in S2R+ cells. 73
2.14 Ago2 is important for antiviral response against DXV. 75

2.15 Loss of autophagy does not render the RNAi pathway ineffective against DXV 76

3.1 Diagram of RNA-seq analysis workflow 83
3.2 Experimental design of the RNA seq experiment. 93
3.3 Normalization of RNA-seq data sets. 95
3.4 Voom. 97
3.5 Principle component analysis. 99
3.6 Differential expression analysis in wildtype flies upon DXV infection at day 3 and day 5. 101
3.7 DXV infection induces genes important for lipid droplet lipolysis and β-oxidation. 105
3.8 Silencing of *Atg1* in the fat body induces lipid droplet lipolysis and β-oxidation genes in the absence of infection. 108

4.1 DXV infection decreases lipid droplet size. 113
4.2 Loss of *Atg1* decreases lipid droplet size. 115
4.3 *plin1*^{38} null mutants have bigger lipid droplet size and are not susceptible to *Drosophila* C virus. 118
4.4 Lipid metabolism genes are important regulators for fly survival upon DXV infection. 119

List of Abbreviations

α	alpha
β	beta
γ	gamma
Δ	delta
Atgs	Autophagy related genes
LD	Lipid Droplet
RNA-Seq	RNA Sequencing
MEF	Mouse embryonic fibroblasts
NLR	NOD-like receptors: The nucleotide-binding oligomerization domain receptors
NLRP3	NLR family, pyrin domain containing 3
RLR	RIG-I-like receptors
IκK	Inhibitor of κB kinase
TCT	Tracheal Cytotoxin
PGN	Peptidoglycan
PLIN	Perilipins
PGRP	PGN-recognition Proteins
PRR	Pattern Recogonition Receptor
TOR	Target of Rapamycin
TLR	Toll-like Receptor
VSV	Vesicular stomatitis virus
HCV	Hepatitis C virus
DENV	Dengue virus
JEV	Japanese encephalitis virus
MAVS	Mitochondrial antiviral-signaling protein

Chapter 1: Introduction

1.1 The innate immune system in *Drosophila melanogaster*

Drosophila is a good model for the study of innate immunity because the cellular and signaling events are conserved with mammalian systems (Anderson, 2000). In addition, *Drosophila* does not have an adaptive immune system, making it a good model to study innate immunity specifically. With the advantage of powerful genetics toolkits in *Drosophila*, novel genes can be identified and further characterized *in vivo*, which can lead to functional discoveries of the mammalian homologs. For example, *Drosophila* Toll was originally found as a protein required for the establishment of the dorsal-ventral axis in the embryo (Morisato and Anderson, 1995). It was later demonstrated as a critical receptor controlling antimicrobial peptide gene expression in response to fungal infection (Lemaitre et al., 1995a, 1996). The sequence homology study of *Drosophila* Toll led to the discovery of the mammalian Toll-Like Receptors (TLRs), which turn out to be one of the major pattern recognition receptors (PRRs) in the mammalian innate immune system (Medzhitov et al., 1997; Rock et al., 1998; Takeuchi et al., 1999).

Upon infection, the epithelial barrier serves as the first physical defense against the invading pathogens (Ferrandon et al., 1998). When pathogens are internalized, both cellular and humoral responses are activated to fight the pathogens. In *Drosophila*, cellular

immunity is functionally executed by three types of hemocytes: plasmatocytes, crystal cells and lamellocytes. These cells function by phagocytosis, melanization and encapsulation, respectively (Williams, 2007). The humoral response is induced in the fat body, an organ that is equivalent to the liver in mammals. Upon infection, large amounts of antimicrobial peptides (AMPs) are produced by the fat body and secreted into the hemolymph. Some studies also show that AMPs can break the bacteria cell wall to kill them (Brogden, 2005).

1.1.1 Microbial Recognition

Following infection, the host initiates immune responses first by detecting specific microbial pattern molecules. The host encoded pattern recognition receptors (e.g. PGN-recognition proteins or PGRPs) can specifically bind to conserved structures (e.g. Peptidoglycan) that are found in the pathogens but absent in the host (Janeway, 2013). Peptidoglycan (PGN) is present on most bacteria and is composed of conserved polymers of β -1,4-linked N-acetylglucosamine and N-acetylmuramic acid cross-linked by short stem peptides, which vary between different types of bacteria. Mammals have a family of four PGRPs, whereas insects have more (with 13 genes coding for 19 proteins in *Drosophila*) (Werner et al., 2003, 2000). The mammalian PGRPs are secreted proteins that bind bacterial muramyl peptides. Some mammalian PGRPs have an amidase activity, probably to eliminate the proinflammatory PGN, whereas others are more diverged from the insect genes and function directly as bactericidal proteins (Dziarski and Gupta, 2006; Liu et al., 2000; Swaminathan et al., 2006). Mammalian PGRPs do not appear to possess signaling

activity.

Insect PGRPs can act as amidases to degrade PGN and also activate of signal-transduction pathways and proteolytic cascades. Insect PGRPs are classified as short (S) or long (L), according to their transcript size: short PGRPs have signal peptides and can be extracellular proteins, whereas long PGRPs can be intracellular, extracellular, or trans-membrane proteins. In *Drosophila*, PGRP-SA and PGRP-SD are required for the Toll signaling pathway (Bischoff et al., 2004; Michel et al., 2001; Valanne et al., 2011). No immunological *in vivo* phenotype has been observed for the amidases PGRP-SB1 and PGRP-SB2, even though PGRP-SB1 is strongly induced post-infection, and its bactericidal activity has been shown *in vitro* (Mellroth and Steiner, 2006; Paredes et al., 2011; Zaidman-Rémy et al., 2011). The function of PGRP-LD is unclear. The other PGRPs either positively or negatively regulate the Imd pathway.

1.2 *Drosophila* viruses

1.2.1 *Drosophila* X virus

Drosophila X virus was initially observed during the studies of Sigma Virus. Flies infected with rhabdovirus Sigma virus developed anoxia sensitivity such that infected flies would die after 15 mins of pure CO_2 exposure (L'Heritier, 1958). However, in the course of a control uninfected passage, Teninges et al. found that uninfected flies also develop anoxia sensitivity occasionally. This made the scientists suspect that the anoxia sensitivity does not come from Sigma virus but from other sources. By negative contrast electron microscopy, it was found that a group of icosahedral viral particles were present that

are morphologically distinct from Sigma virus. Without information of the relationship between this newly-discovered virus and other viruses, it was named *Drosophila* X virus (Teninges et al., 1978).

1.2.1.1 Taxonomy

Drosophila X virus is a non-enveloped virus with a linear double stranded RNA genome. It belongs to the Family Birnaviridae. This family is composed of three genera (i) Genus Aquabirna-virus, represented by the type species infectious pancre- atic necrosis virus (IPNV); (ii) Genus Avibirnavirus, type species infectious bursal disease virus (IBDV); and (iii) Genus Entomobirnavirus, type species *Drosophila* X virus (Dobos, 1995). Birnaviruses are medium sized (60 nm), unenveloped viruses with an icosahedral nucleocapsid that contains a bisegmented dsRNA genome.

DXV has a single-shelled T=13 icosahedral symmetry capsid of about 60 nm in diameter, that is composed of 260 trimers of VP2 that form spikes projecting radially from the capsid (**Figure 1.1**). The peptides derived from pre-VP2 C-terminal cleavages remain associated within virion. VP3 forms a ribonucleoprotein complex with the genomic RNA. Minor amounts of VP1 are also incorporated in the virion. Based on morphological properties, DXV is similar to several ungrouped vertebrate and invertebrate viruses like Infectious pancreatic necrosis virus (IPNV) , infectious bursal disease virus (IBDV) and Tellina tenuis virus.

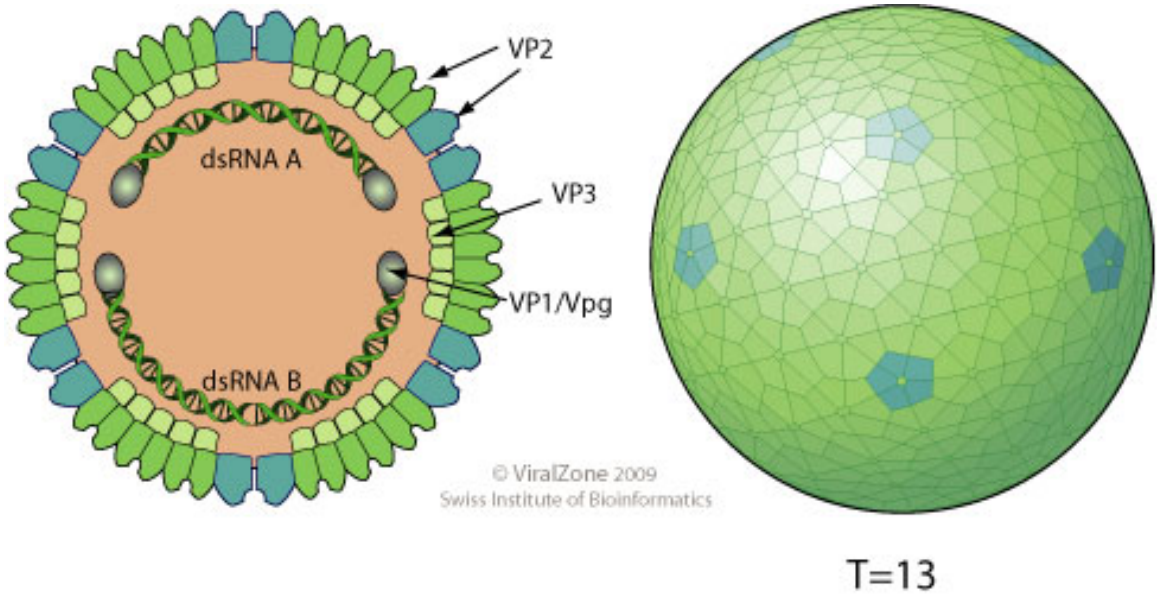

Figure 1.1: DXV viron structure.
DXV has a single-shelled T=13 icosahedral symmetry capsid, which is composed of VP1, VP2 and VP3. The dsRNA genome has two segments A and B.

1.2.1.2 Viral genome and proteins

Drosophila X virus has a two-segment dsRNA genome. These two segment dsRNA are translated into two separate polypeptides (A and B) before mature viral proteins are processed from the polypeptides. A representation of the viral protein polypeptides are shown in **Figure 1.2**.

The Segment B includes only VP1, a 112kDa protein that encodes for the RNA-dependent RNA polymerase (RdRp). VP1 is present not only in a free form but can be found covalently attached to the 5' genomic RNA end of both segments (VPg) (Kibenge and Dhama, 1997; Nagy and Dobos, 1984a,b; Revet and Delain, 1982). As an internal protein within the viron, VP1 has a low copy number and represents only 4% of total protein present in the virion.

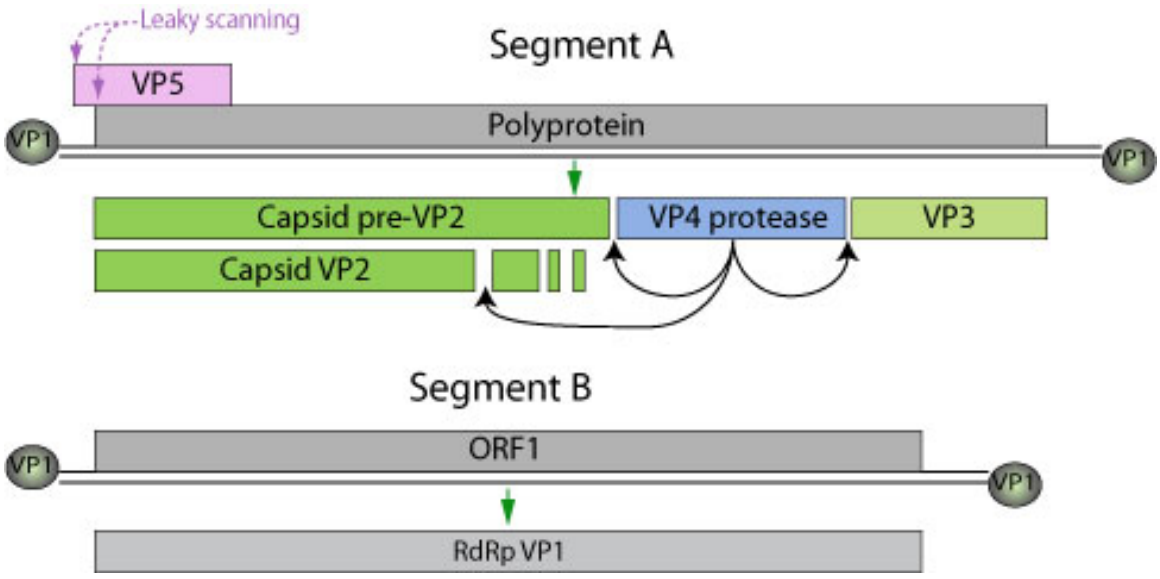

Figure 1.2: DXV Genome Structure.
DXV genome has two segments: A and B. Segment B encodes the RNA-dependent RNA polymerase (RdRP). Segment A encodes the capsid proteins VP2 and VP3 and the protease VP4. It also encodes an alternative ORF translated possibly by leaky scanning (VP5) (Hulo et al., 2011).

The structural properties of VP1 from DXV were predicted based on studies of other Birnavirus including infectious bursal disease virus (IBDV) and infectious pancreatic necrosis virus (IPNV) since a close homology is shared between the viruses within this family (Dobos, 1995; Müller et al., 2003). The IBDV RdRp contains several structural motifs (I, II, III and IV) that are common to RNA-dependent RNA polymerases (RdRp) of positive-strand RNA (ssRNA+) viruses (Bruenn, 1991; Gorbalenya and Koonin, 1988; von Einem et al., 2004). VP1 can catalyze RNA dependent RNA polymerization *in vitro*. During *in vitro* RNA transcription, VP1 serves as a primer and remains attached to the 5' end of the RNA. Viral RNA transcribes in a semi-conservative, strand-displacement mechanism (Dobos, 1995). Different from HCV RdRp, IBDV VP1 requires specific template features to function. Experiments with various truncated RNA templates indicate

that the 3' noncoding region (NCR) of segments A and B was critical for VP1-directed RNA polymerization (von Einem et al., 2004).

.

Segment A is 3360bp-nucleotide in length and contains two overlapping open reading frames (ORFs). The large ORF is composed of 3096 nucleotides, which is flanked by a 107-bp 5' and a 157-bp 3'-untranslated region. The small ORF is 711-nucleotide-long and located within the carboxy half of the large ORF but in a different reading frame. The large ORF encodes a 114kDa polyprotein (NH2-preVP2-VP4-VP3-COOH), which is cotranslationally cleaved by viral-encoded protease VP4 to generate the major outsider capsid protein VP2 (45kDa) and internal structual protein VP3 (34kDa) (Birghan et al., 2000; Nagy and Dobos, 1984a,b). The small ORF starts at the junction of VP4 and VP3, and is capable of encoding a basic, arginine-rich 27kDa polypeptide which so far has not been detected in infected cells (Chung et al., 1996).

VP2 is the major outer capsid protein of DXV and represents approximately 60% of a virions total protein (Dobos, 1995). Its mature form is processed through two protease cleavages, from preVP2 to pVP2 (49kDa) and finally to VP2 (Chung et al., 1996). As a result of these two cleavages and another one that hasn't been fully characterized, four peptides are generated. Associated with the virion, these peptides were proposed to facilitate cell membrane destabilization during viral entry (Coulibaly et al., 2005; Da Costa et al., 2002).

VP3 is the inner capsid structural protein of birnaviruses and composes 34% of the total virion (Dobos, 1995). Crystal structure data suggests that VP3 is important for the viral coat assembly (Coulibaly et al., 2005). VP3 has been shown to bind to dsRNA and

form a threadlike ribonucleoprotein complex. In addition, the positively charged C terminus of VP3 has been shown to interact with VP1 that is critical for the encapsidation into virus-like particles (VLPs) (Böttcher et al., 1997; Hjalmarsson et al., 1999; Hudson et al., 1986; Lombardo et al., 1999). The interactions between VP3 and other viral proteins have been detected in multiple birnaviruses. This might indicate that VP3 is a crucial for the birnavirus structure, assembly, and replication.

VP4 encodes for the viral protease that is responsible for the proteolytic maturation of the polyprotein A (Fahey et al., 1985; Hudson et al., 1986). It has been shown that VP4 forms a non-canonical RNA viral Lon protease, even though it does not contain an ATPase domain (Birghan et al., 2000). In the birnavirus protease, two residues, conserved across the Lon/VP4 protease family, form a Ser-Lys catalytic dyad and are critical for the cleavage activity (Birghan et al., 2000). VP4 is responsible for the cleavage at the pVP2-VP4 and VP4-VP3 junctions.

In addition to the 128kDa polyprotein ORF, birnavirus genome segment A also encodes other smaller reading frames. In IPNV, a 17kDa nonstructural protein (VP5) is encoded and is present in IPNV-infected cells (Magyar and Dobos, 1994). However, IPNV VP5 is not required for viral replication in cell culture and that VP5-deficient mutant viruses have replication kinetics similar to that of wild type virus (Mundt et al., 1997; Weber et al., 2001; Yao et al., 1998). The function of this VP5 is still unknown. Although no effect is observed *in vitro*, it could possibly have a role *in vivo*. In IBDV-infected cells, VP5 has also been detected but it is not present in the virion (Mundt et al., 1995).

1.2.1.3 Virus cycle

The complete virus cycle for DXV is not fully elucidated yet. In *Drosophila* S2 cells, DXV can replicate and cause pathology such as a cytopathic effect (CPE). Preliminary siRNA experiments in S2 cell lines indicate that endocytosis is important for viral infection. Silencing the core components of the endocytoic pathway, including Rab5, and clathrin inhibit DXV replication (Javier Robalino, unpublished).

In *Drosophila*, virus particles were found in larval hemocytes 30 mins after DXV infection. However, the replication of DXV takes time to reach other tissues. Within a week, virus can be found in multiple tissues including the digestive tracts, fat body, brain muscle and ovaries (Teninges et al., 1978).

1.3 Antiviral responses in *Drosophila melanogaster*

Viruses are among the most threatening pathogens that cause human diseases. For example, dengue virus, hepatitis C virus (HCV) and human immunodeficiency virus (HIV) put millions of people at risk every year. However, the mechanisms of pathogenesis and replication strategies often vary for different viruses, and the host utilizes a variety of antiviral responses to combat different viral pathogens. Thus, it is critical to establish infection models to understand the underlying mechanisms *in vivo*. *Drosophila melanogaster* can be infected with a variety of insect viruses. Some are natural pathogens found in wild *Drosophila* population including sigma virus, *Drosophila* C Virus (DCV), and flock house virus (FHV) (Carpenter et al., 2007; Jovel and Schneemann, 2011; Kapun et al., 2010). Some are viruses that can infect *Drosophila* and cause pathogenesis in lab-

oratories, for example, *Drosophila* X virus (DXV) and vesicular stomatitis virus (VSV) (Périès et al., 1966; Zambon et al., 2005). To combat invading viral pathogens, *Drosophia* also initiate different immune responses against the pathogens. This makes *Drosophila* a good host-pathogen model to study the antiviral response. So far, in addition to the Toll and Imd pathways, two of the best characterized immune pathways in *Drosophila*, RNAi interference, JAK-STAT, autophagy pathways have also been suggested to play an antiviral role in *Drosophila* (**Figure 1.3**). In our lab, we show that energy homeostasis is closely related with viral replication that modulation of lipid metabolism and β-oxidation could be crucial for antiviral responses. We will present and discuss about this discovery in detail in this thesis.

The Toll and Imd signaling pathways are the best characterized immune signaling pathways in the *Drosophila* immune responses (De Gregorio et al., 2002). Although both pathways were first identified to fight against fungi or bacteria, they also play roles against virus infections (Costa et al., 2009; Lloyd and Taylor, 2010; Zambon et al., 2005). Recently, other pathways such as autophagy, RNA interference, JAK-STAT and JNK, have also been found to participate in antiviral responses (Dostert et al., 2005; Lee et al., 2005; Sabin et al., 2009; Shelly et al., 2009). Here we will briefly review the immune functions of these pathways and specifically the roles they play when the host is infected with virus.

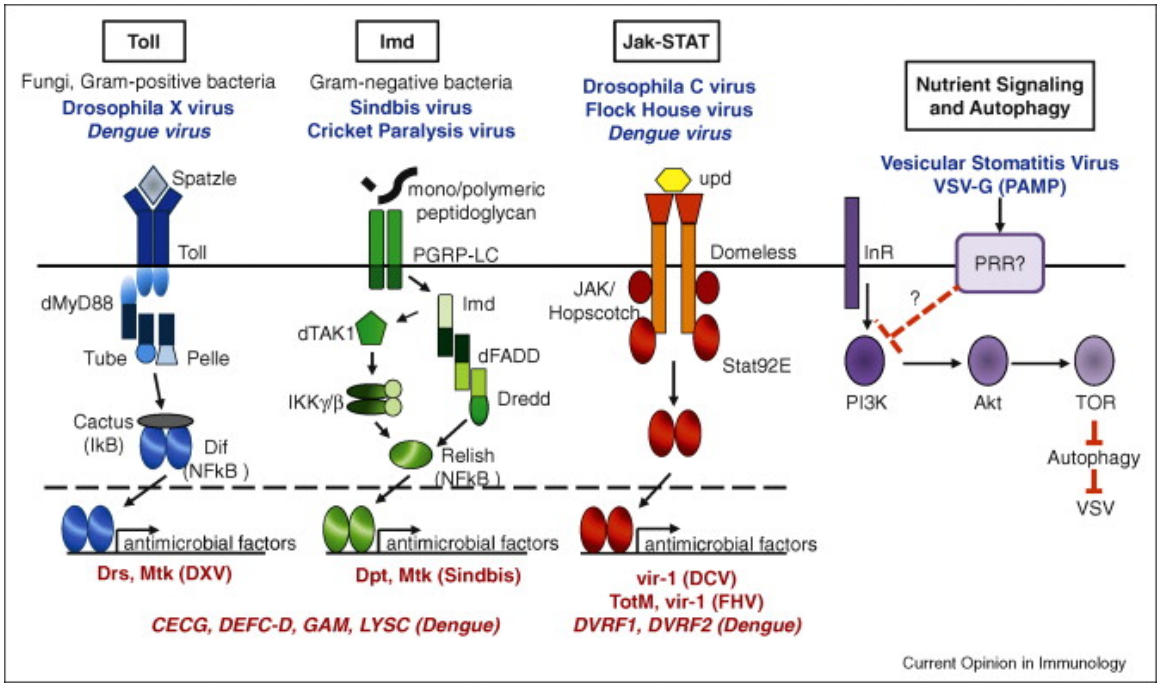

Figure 1.3: Immune signaling against virus.
The Toll pathway is important in the immune defense against fugi, Gram-positive bacteria, *Drosophila* X virus and dengue virus. The Imd pathway is important for defense against Gram-negative bacteria, sindbis virus, cricket paralysis virus (CrPV). The JAK-STAT pathway is critical for the response against *Drosophila* C virus, flock house virus and dengue virus. Autophagy has been shown to play a role against vesicular stomatitis virus (Sabin et al., 2010).

1.3.1 The Toll Signaling Pathway

Toll was first identified for its role in establishing the dorsal-ventral pattern in the *Drosophila* embryo (Morisato and Anderson, 1995). It was later shown to be responsive to Gram-positive bacteria and fungi (Lemaitre et al., 1996, 1997; Rutschmann et al., 2002). The Toll pathway is highly conserved with the Toll-like receptor pathways in mammals. The transmembrane protein Toll is activated by a proteolytically processed form of the Spätzle protein, a cystine-knot-cytokine-growth-factor-like polypeptide (Lemaitre et al., 1996; Mizuguchi et al., 1998). The extracellular domain of Toll is composed largely of

leucine-rich repeats, and the cytoplasmic domain of Toll is similar to the cytoplasmic domain of the mammalian IL-1 receptor (Schneider et al., 1994). Toll activation results in the phosphorylation of the downstream proteins Tube and Pelle, which regulate degradation of the Cactus protein. Cactus, the Iκ-B homolog, holds the transcription factors Dif and Dorsal in the cytoplasm by forming a Cactus-Dif / Cactus-Dorsal complex. The degradation of Cactus results in the nucleus translocation of Dif and Dorsal, which lead to expression of antimicrobial peptide genes (Ip et al., 1993; Lemaitre et al., 1995b). The antimicrobial peptides are produced in the fat body and secreted into the hemolymph for immune functions. Currently, there are seven characterized AMPs in *Drosophila*: Drosomycin, Diptericin, Attacin, Drosocin, Cecropin, Defensin, Metchnikowin. Toll activation usually leads to high upregulation of Defensin, Metchnikowin and Drosomycin.

The Toll pathway was discovered to be important for the antiviral response against *Drosophila* X virus (DXV) (Zambon et al., 2005). The *Toll*^{10b} mutant, which carries a constitutively activated form of Toll, was susceptible to DXV infection. The *Dif* mutant is also susceptible to DXV infection. This evidence suggests that Toll is important in the antiviral response in insects. However, the downstream targeted AMPs genes do not appear to affect the viral response. Overexpression of single AMPs does not cause resistance to DXV (Zambon et al., 2005). Additional studies have shown the importance of Toll during the infection of dengue virus in mosquito. Silencing of the positive regulator *dMyD88* results in an increase of viral load, whereas silencing of the negative regulator *cactus* results in an decreased load of virus (Xi et al., 2008).

1.3.2 The Imd Signaling Pathway

The Imd pathway was found to be responsive to Gram-negative bacteria (Lemaitre et al., 1995a). Unlike the Toll Pathway, the Imd pathway is activated through the transmembrane receptor PGRP-LC, which recognizes diaminopimelic acid-type peptidoglycan on Gram-negative bacteria and certain Gram-positive bateria such as *Bacillus spp* (Choe et al., 2005, 2002; Gottar et al., 2002; Lemaitre et al., 1997; Leulier et al., 2003; Rämet et al., 2002b; Zaidman-Rémy et al., 2006). PGRP-LC is spliced into several isoforms, three of which have been characterized. For example, PGRP-LCx recognizes polymeric PGN; PGRP-LCa does not directly bind PGN, but it acts as a coreceptor with PGRP-LCx to bind monomeric PGN fragments called tracheal cytotoxin (TCT) (Chang et al., 2006; Kaneko et al., 2004; Lim et al., 2006). A diagram of the Imd pathway is shown in **Figure 1.4**.

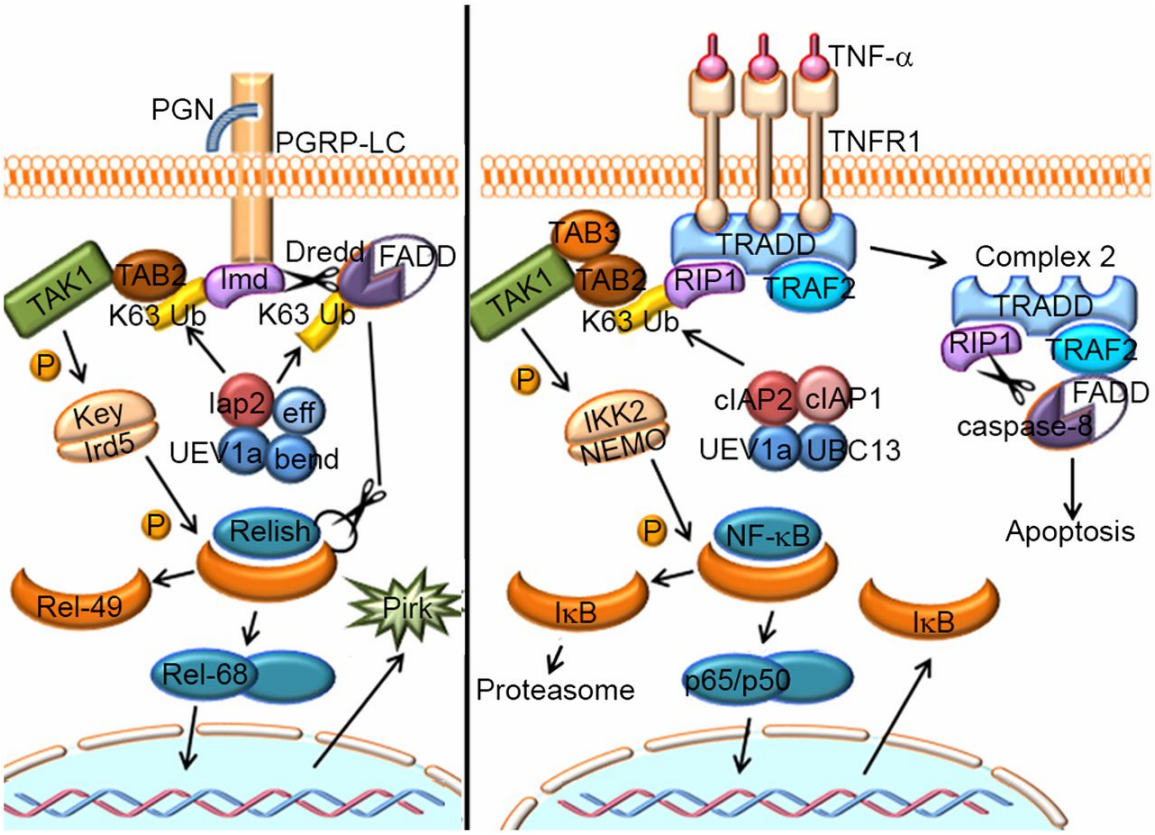

Figure 1.4: Schematic representation of the Imd signaling pathway and TNF-α pathway. The *Drosophila* Imd pathway is equivalent to the mammalian TNF-α pathway. Activation of both pathways results in the translocations of NF-κB transcription factors, Relish in *Drosophila* and P65/P50 in mammals. Conserved components are represented by similar shapes and colors. bend, bendless; eff, effete; Key, Kenny; K63 Ub, K63 polyubiquitination; NEMO, NF-κB essential modulator; TAB, TAK1-binding protein; TRADD, TNFR1-associated death domain (Myllymäki et al., 2014).

Recognition of PGN by PGRP-LC results in the recruitment of the 25kDa death domain protein Imd, whose death domain is homologous to that of mammalian RIP1, a TNF-receptor interacting protein. Imd further associates with the mammalian homolog of FADD (dFADD) and the caspase-8 homolog Dredd (Leulier et al., 2000, 2002). Dredd becomes activated through ubiquitination by the E3-ligase Inhibitor of apoptosis 2 (Iap2) , which associates with the E2-ubiquitin-conjugating enzymes UEV1a, Bendless (Ubc13), and Effete (Ubc5) (Meinander et al., 2012; Zhou et al., 2005).

When activated, Dredd cleaves Imd, removing a 30-aa N-terminal fragment, and creates a novel binding site for Iap2, which can then K63-ubiquitinate Imd (Meinander et al., 2012; Paquette et al., 2010). This leads to activation of the TAB2/TAK1 complex, composed of a homolog of mammalian transforming growth factor-activated kinase 1 (TAK-1) and TAB2. Downstream of dTAK1, a signalosome equivalent, composed of Ird5 (the IκBKβ homolog) and Kenny (the IκBKγ homolog), phosphorylates Relish, leading to the proteolytic cleavage of the inhibitory carboxyl-terminal fragment (Rutschmann et al., 2000; Stöven et al., 2000; Wu and Anderson, 1998). Activated Relish translocates into the nucleus and induces a large number of genes including antimicrobial peptide genes, such as *diptericin*, *cecropin*, *drosocin* and *attacin*. It is proposed that Dredd, after its initial interaction with the death domain protein dFADD, is responsible for cleavage of Relish (Stoven et al., 2003).

In addition to PGRP-LC, PGRP-LE can also regulate the Imd pathway. PGRP-LE exists in two forms (Kaneko et al., 2006; Neyen et al., 2012). The short form is secreted into the hemolymph and can stimulate the Imd signaling by binding and presenting PGN to PGRP-LC. However, the secretion mechanism of PGRP-LE is not yet well understood

(Takehana et al., 2002). The full-length PGRP-LE remains in the cytoplasm, where it is thought to recognize TCT fragments that reach the inside of a cell. Binding of TCT leads to the oligomerization of cytoplasmic PGRP-LE in a head-to-tail fashion (Lim et al., 2006). Ectopic expression of PGRP-LE in the fat body is sufficient to activate AMP expression, in a cell-autonomous manner, even in the absence of infection. Cytoplasmic PGRP-LE can activate the Imd pathway, independently of PGRP-LC, by interacting with Imd (Kaneko et al., 2006; Neyen et al., 2012; Takehana et al., 2002; Yano et al., 2008). PGRP-LE is the only intracellular microbial receptor identified in *Drosophila* (Choe et al., 2005; Takehana et al., 2002). The intracellular form is able to activate autophagy, whereas the transmembrane form can, together with PGRP-LC, activate a prophenoloxidase cascade (Kurata, 2014; Schmidt et al., 2008; Takehana et al., 2002). However, the activation of autophagy through PGRP-LE does not appear to involve the Imd pathway (Yano et al., 2008).

PGRP-LF is a transmembrane protein that resembles PGRP-LC but lacks the intracellular signaling domain and does not bind PGN. PGRP-LF acts as an inhibitor of Imd signaling by binding PGRP-LC and preventing its dimerization (Basbous et al., 2011; Maillet et al., 2008; Persson et al., 2007). PGRP-LA is also predicted not to bind PGN and recently was shown to be dispensable for systemic infections. However, consistent with its expression profile, PGRP-LA appears to positively regulate the Imd pathway in barrier epithelia, such as the trachea and the gut (Gendrin et al., 2013). PGRP-LB, PGRP-SC1A, PGRP-SC1B, and PGRP-SC2 have amidase activity and are shown to play somewhat redundant roles in downregulating the Imd pathway during a systemic response. PGRP-LB is the major regulator in the gut. The amidase PGRPs digest PGN into short, nonimmuno-

genic or less immunogenic fragments and, therefore, prevent or reduce the activation of defense mechanisms (Paredes et al., 2011; Zaidman-Rémy et al., 2011).

Recent studies have suggested that the Imd pathway might have other roles in addition to the immune response. For example, antimicrobial peptides are upregulated during metamorphosis in the absence of infection (Lee et al., 2003). In addition, overexpression of *imd* can promote apoptosis and induce expression of the pro-apoptotic *Drosophila reaper* gene due to the death domain of Imd. Both the apoptosis and the antimicrobial peptide gene expression induced by Imd activation can be blocked by the caspase inhibitor p35 (Georgel et al., 2001).

Recently, the Imd pathway was shown to be important in the antiviral response against Cricket Paralysis Virus and Sindbis Virus (Avadhanula et al., 2009; Costa et al., 2009). Loss-of-function mutations in several Imd pathway genes (*PGRP-LC, Tak1, ird5, kenny, relish, imd, dFADD*) displayed increased sensitivity to CrPV infection and higher CrPV loads, while mutations in the Toll pathway fail to affect replication (Costa et al., 2009). Similar results were obtained from Sindbis virus (SINV) infection both in *Drosophila* (*Rel, Imd, Fadd, Dredd, Tab2, Ird5, Key*) and in the cultured mosquito cells (Avadhanula et al., 2009).

1.3.3 JAK-STAT Signaling Pathway

The JAK/STAT (JAK: Janus Kinase, STAT: signal transducers and activators of transcription) signal transduction pathway is conserved throughout evolution such that structural and functional homologs of components originally identified in vertebrates are

also present in the model organism *Drosophila melanogaster*. The JAK-STAT pathway is a key regulator of proliferation and differentiation of larval hematopoietic cells (Harrison et al., 1995; Hou et al., 1996; Luo et al., 1997; Yan et al., 1996). In addition to its role during larval hematopoiesis, the JAK/STAT pathway in *Drosophila* is also involved in other developmental processes such as sexual identity, the segmentation of the embryo and the establishment of polarity within the adult compound eye (Agaisse and Perrimon, 2004; Harrison et al., 1998; Jinks et al., 2000).

Recent studies have revealed novel immune functions of JAK-STAT pathway in both the cellular and humoral responses. Upon infection, a cytokine-like protein Upd3 produced by hemocytes activates JAK-STAT signaling in the fat body, which results in transcriptional expression of *tot* genes and *tep1* (Agaisse et al., 2003). Specifically, *totA* is a stress induced gene of unknown function, and *tep1* is a thiolester-containing protein that possibly acts as an opsonin (Agaisse et al., 2003; Boutros et al., 2002; Lagueux et al., 2000). Additionally, the JAK-STAT target genes have shown a delayed and transient expression pattern compared to the Toll- and Imd-dependent genes, although the reason why still remains to be identified (Boutros et al., 2002).

JAK-STAT signaling has also been implicated in the activation of blood cells and possibly important as an antiviral response in *Drosophila* against *Drosophila* C Virus. Loss-of-function $hop^{M38/msvl}$ flies are more susceptible to *Drosophila* C Virus compared to wildtype and there is an increased viral RNAs in the mutants compared to wildtype as well (Dostert et al., 2005).

1.3.4 RNA interference pathway

RNA interference (RNAi) is a targeted gene silencing pathway that controls gene expression by sequence-specific small RNAs. RNA silencing regulates the expression of endogenous genes, and can also modulate exogenous gene expression. For example, small RNAs generated by the RNAi pathway can specifically target viral genome sequence to degrade viral RNAs, which is an effective antiviral strategy widely used in plants and invertebrates (Aliyari and Ding, 2009; Bronkhorst and van Rij, 2014; van Rij et al., 2006). Accumulating evidence suggests that most of virus-derived siRNAs are processed by Dicer proteins, members of the RNase III family, which generate a 21-23nt RNA duplex from a larger dsRNA precursor molecule (Aliyari and Ding, 2009; Bernstein et al., 2001; Jaskiewicz and Filipowicz, 2008). Upon infection, the virus-derived dsRNA molecules (e.g., the dsRNA genome or dsRNA intermediates generated through single strand RNA replication) are processed into viral siRNAs. The small interfering RNA duplex (siRNA) is incorporated into the effector complex, in a sequence specific manner, and followed by the recruitment of the RNA-induced silencing complex (RISC) to cleave the complementary sequence on the mRNA target (**Figure 1.5**). Mutants of the core siRNA machinery (*dcr2, r2d2, ago2*) showed increased sensitivity to infection by several RNA viruses, such as Flock House virus (FHV), *Drosophila* C virus (DCV), Cricket Paralysis virus (CrPV), Sindbis virus (SINV), Vesicular Stomatitis virus (VSV), *Drosophila* X virus (DXV), West Nile virus (WNV), and Rift Valley Fever virus (RVFV) (Chotkowski et al., 2008; Galiana-Arnoux et al., 2006; Li et al., 2002; Sabin et al., 2009; van Rij et al., 2006; Wang et al., 2006; Zambon et al., 2006). To combat the RNA in-

terference, some viruses encode viral suppressors of RNA silencing (VSRs) to deactivate the RNAi pathway (Li and Ding, 2006). For example, FHV infection requires an FHV-encoded protein B2 to suppress RNA silencing (Aliyari et al., 2008; Li et al., 2002). B2 also inhibits RNA silencing in transgenic plants and *Caenorhabditis elegans*, providing evidence for a conserved RNA silencing pathway in the plant and animal kingdoms (Guo and Ding, 2002; Guo and Lu, 2013; Li et al., 2002).

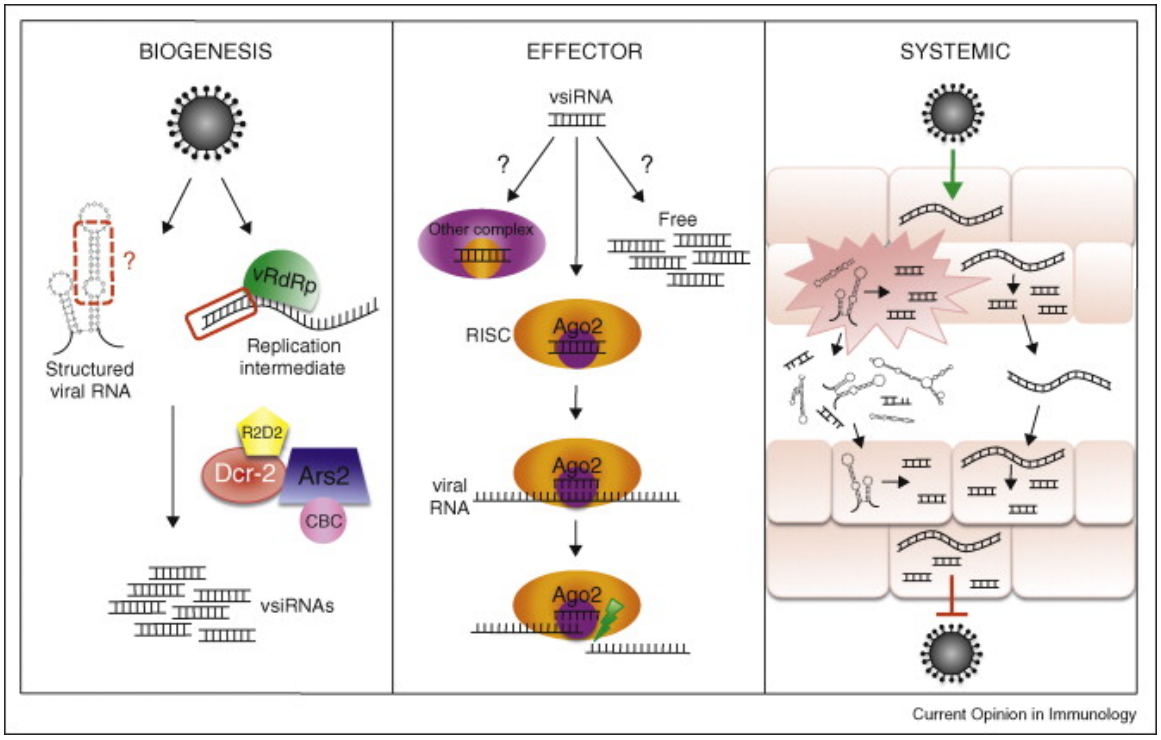

Figure 1.5: Diagram of the RNA interference pathway in fighting against invading virus. A systemic RNAi response against virus comprises two steps: biogenesis of vsiRNAs and a vsiRNA-dependent effector response. The biogenesis of vsiRNA is initiated by the enzyme Dicer, which detects dsRNA genome or dsRNA replication intermediates and cleave them into short double stranded fragments of $\sim$21 nucleotide vsiRNAs. Each vsiRNA is unwound into two single-stranded (ss) ssRNAs, the passenger strand and the guide strand. The passenger strand is degraded and the guide strand is incorporated into the RNA-induced silencing complex (RISC). When the guide strand pairs with a viral RNA molecule, argonaute (Ago2), the catalytic component of the RISC complex can facilitate the cleavage of the viral RNAs (Sabin et al., 2010).

1.3.5 JNK Signaling Pathway

The c-Jun NH2-terminal kinases (JNK) are central components of signal transduction pathways in the regulation of cell proliferation and differentiation, cytokine production, apoptosis, and cell survival in mammals (Arthur and Ley, 2013; Garrington and Johnson, 1999; Lamb et al., 2003). c-Jun N-terminal kinases (JNKs) bind and phosphorylate c-Jun on Ser-63 and Ser-73 within its transcriptional activation domain. Activated JNK can bind and phosphorylate a variety of downstream substrates such as the transcription factors c-Jun and ATF-2 (Dérijard et al., 1994; Kyriakis et al., 1994).

It is well established that JNK signaling is important in the *Drosophila* innate immune response. Particularly it is involved in cellular processes such as phagocytosis, wound healing, melanization, and defense against extracellular pathogens (Bidla et al., 2007; Kim et al., 2005; Park et al., 2004; Rämet et al., 2002a; Schneider et al., 2007; Silverman et al., 2003). However, there is discrepancy on whether JNK is positively or negatively regulating AMP gene expression. One proposal is that JNK is a negative regulator of the transcription factor Relish. This is supported by evidence that the JNK-dependent transcription factors *Drosophila* activator protein 1 (dAP-1) and Stat92E form a repressosome complex in response to continuous immune signaling (Kim et al., 2007). The alternative proposal suggests that JNK signaling is essential for AMP gene induction since the expression of a JNK inhibitor and an induction of JNK loss-of-function clones suppress AMP gene expression (Delaney et al., 2006). Additional studies are required in order to differentiate between these contradictory hypotheses.

Studies have also shown that many viruses can manipulate the JNK signaling path-

way to regulate viral replication and gene expression. These viruses include human immunodeficiency virus type 1 (HIV-1), echovirus 1, herpes simplex virus type 1 (HSV-1), Kaposi's sarcoma-associated herpes virus, coxsackievirus B3, varicella-zoster virus and infectious bursal disease virus (IBDV) (Huttunen et al., 1998; Kumar et al., 1998; Pan et al., 2006; Si et al., 2005; Wei et al., 2011; Xie et al., 2005; Zachos et al., 1999; Zapata et al., 2007). In addition, the JNK pathway is involved in cell apoptotic death induced by some viruses, including HSV-1, coxsackievirus B3, reovirus, swine influenza virus and poliovirus (Autret et al., 2007; Choi et al., 2006; Clarke et al., 2004; Kim et al., 2004; Perkins et al., 2003). For example, the activated JNK1/2, induced by IBDV, phosphorylates the downstream target c-Jun. Inhibition of JNK1/2 activation leads to reduced viral progeny release, which is associated with decreased viral transcription and lower virus protein expression. A decrease in apoptotic cell death is also observed since Bax activation, cytochrome c release, and caspase activation are all blocked. These data suggest that the JNK pathway plays an important role in viral replication and contributes to virus-mediated changes in host cells (Wei et al., 2011).

1.3.6 Autophagy

Autophagy is a cell intrinsic mechanism for the degradation of cytoplasmic contents (**Figure 1.6**). It was originally discovered as a starvation-induced response, that delivers long-lived proteins and entire organelles for lysosomal degradation, so that cytoplasmic contents can be recycled for new synthesis (Klionsky and Emr, 2000).

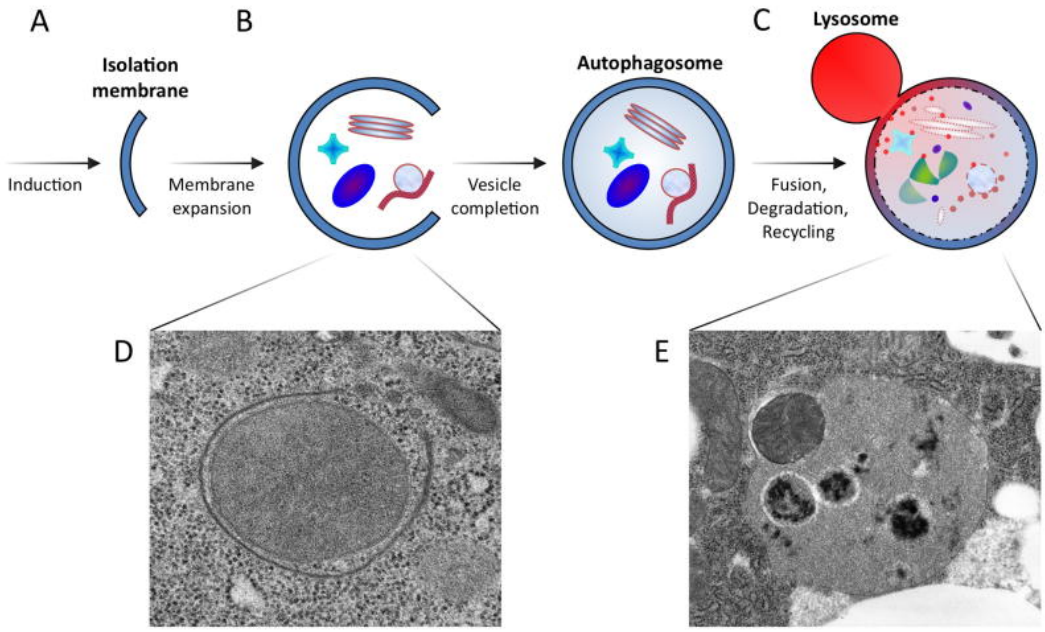

Figure 1.6: Diagram of the Autophagy process.
(A-C)The induction of autophagy starts with isolation membrane formation, followed by membrane expansion, vesicle completion, autophagosome formation, fusion and degradation of cargo proteins within autolysosomes. (D-E) Electron microscopy pictures showing autophagosome and autolysosome, respectively (Meléndez and Neufeld, 2008).

Three types of autophagy have been defined: microautophagy, chaperone-mediated autophagy (CMA) and macroautophagy (Mizushima and Klionsky, 2007). Microautophagy is characterized by budding into the lysosome so that cytoplasmic contents are incorporated for degradation. The CMA pathway initiates protein degradation with the recognition of a signaling motif, KFERQ, by the chaperone protein Hsc70. Hsc70 then interacts with the lysosomal membrane protein (LAMP) and directs the targeted proteins for degradation (Cuervo and Dice, 2000; Massey et al., 2006). Macroautophagy, also termed autophagy, is the main pathway for degradation of cytoplasmic contents. When it is activated, the initiation sites form preautophagosomal assembly sites (PAS). By membranous expansion, the phagophore will form double membrane vesicles called autophagosomes. The autophagosome then fuses with the lysosome to become an autolysosome that eventually results in degradation of the incorporated contents. More than twenty autophagy related genes (*Atg*) have been identified from the studies in yeast (Mizushima et al., 1998). Most Atg homologs are also found in higher organisms, such as *Drosophila melanogaster* and mammals.

1.3.6.1 Autophagy signaling pathway

Although autophagy was initially identified in mammals, the understanding of the *Atg* genes mostly comes from the yeast screens (Tsukada and Ohsumi, 1993). The *Atg* proteins can be divided into four groups: 1) the Atg1-Atg13-Atg17 kinase complex; 2) the class III phosphatidylinositol 3-kinase (PtdIns3K) complex, consisting of Vps34, Vps15, Atg6 and Atg14; 3) two ubiquitin-like protein conjugations systems (Atg8 and Atg12);

4) Atg9 and its cycling system (Yang and Klionsky, 2010). The signaling components of autophagy are shown in **Figure 1.7**.

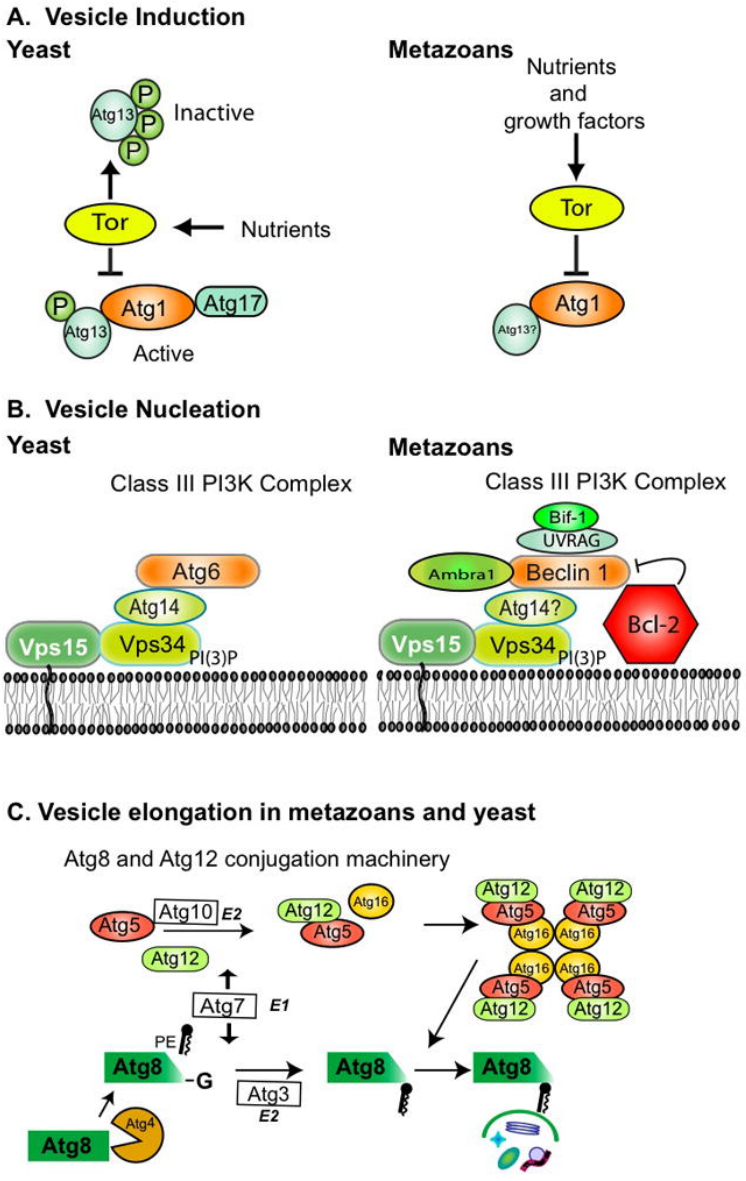

Figure 1.7: The signaling components of Autophagy.
The autophagy pathway is conserved from yeast to metazoans. The core regulators include the Atg1-Atg13-Atg17 kinase complex, the class III phosphatidylinositol 3-kinase (PtdIns3K) complex (Vps34, Vps15, Atg6 and Atg14), two ubiquitin-like protein conjugations systems (Atg8 and Atg12) and the membrane cycling system (Atg9) (Meléndez and Neufeld, 2008).

The Atg1-Atg13-Atg17 kinase complex is involved in the induction of autophagy. The target of rapamycin kinase (TOR), negatively regulates autophagy, andnphosphorylates Atg13 (Funakoshi et al., 1997). In nutrient-rich conditions, Atg13 is highly phosphorylated and has a lower affinity towards Atg1. When there is a lack of nutrients, Atg13 is rapidly dephosphorylated and has a higher affinity with Atg1 that results in the activation of autophagy (Kamada et al., 2000). Among all the Atg proteins, Atg1 is the sole serine/threonine protein kinase (Matsuura et al., 1997). The downstream targets of Atg1 are not known.

The class III phosphatidylinositol 3-kinase (PtdIns3K) complex is important in numerous membrane trafficking events, and is involved in autophagic vesicle nucleation. PtdIns3k is a lipid kinase and its activity is essential for autophagy. One possible role of PtdIns3k is to generate PtdIn(3)P at the Pre-autophagosomal Structure (PAS) to recruit PtdIn(3)P binding proteins such as Atg18 and Atg21 (Guan et al., 2001; Strømhaug et al., 2004). In yeast, VPS34 is the only PtdIns3k, and it forms two distinct Atg6/Vps34 complexes: complex I is composed of Vps34, Vps15, Vps30/Atg6 and Atg14, and complex II contains the same proteins except that Atg14 is replaced by Vps38. The first complex is thought to localize other Atg proteins to the pre-autophagosomal structure or PAS and thus has a stimulating role in autophagy; the second complex is involved in vacuolar protein sorting of carboxypeptidase Y (CPY), which is normally transported from the late Golgi to the vacuole (Kihara et al., 2001). However, in metazoans, two kinds of PtdIns3Ks are involved: Class I and Class III PtdIns3Ks. Similar to yeast VPS34, VPS34 in the metazoan is a Class III PtdIns3K and plays a stimulating role in autophagy. But Class I PtdIns3K, downstream of the insulin signaling pathway, functions at the plasma

membrane and activate TOR; hence it inhibits autophagy (Jacinto and Hall, 2003).

There are two conjugation systems led by Atg5-Atg12 and Atg8, respectively. In the Atg5-Atg12 system, Atg12 interacts with Atg5 through an irreversible isopeptide bond that is formed between a C-terminal glycine residue of Atg12 and a central lysine residue of Atg5 (Mizushima et al., 1998). Two other proteins are required for this process: Atg7, a homolog of the E1 ubiquitin-activating enzyme, and Atg10, a homolog of the E2 ubiquitin-activating enzyme (Kim et al., 1999; Mizushima et al., 1999; Shintani et al., 1999). Atg7 transiently binds to the C-terminal glycine of Atg12 through its active site cysteine through a thioester bond. After ATP hydrolysis, Atg12 is activated and then temporarily interacts with Atg10. Finally, a covalent bond is formed between Atg5 and Atg12. Atg 16 is also involved in the Atg5-Atg12 complex. Atg16 can form a homo-oligomer to mediate the formation of a higher multimeric structure with Atg12, Atg5, and Atg16 (Kuma et al., 2002).

The Atg8 conjugation system modifies a lipid called phosphatidylethanolamine (PE) (Ichimura et al., 2000; Kirisako et al., 2000). Initially, the cysteine protease Atg4 proteolytically removes a C-terminal arginine residue from Atg8, exposing a glycine that can be accessed by the E1-like Atg7. Atg8 is activated by Atg7 and then is transferred to another E2-like enzyme, Atg3, and eventually conjugates to PE through an amide bond. Atg8 conjugated to PE behaves like a membrane protein and can form protein aggregates on the surface of the autophagosome. Under stress conditions, the ratio of Atg8-PE/Atg8 is increased and this has been widely applied as an indication of autophagy induction. Unlike the Atg12-Atg5 conjugation, modification of PE with Atg8 is reversible, in that Atg4 can cleave Atg8 after the glycine residue to remove it from the lipid (Kirisako et al.,

2000).

Atg9 is a transmembrane protein that is important for the autophagosomal retrieval (Noda et al., 2000). Different from most Atg proteins that mainly localize to the PAS, Atg9 displays a distribution at multiple punctate structures (Reggiori et al., 2005; Tucker et al., 2003). The cycling event between PAS and non-PAS is essential for autophagy. The recruitment of Atg9 to the PAS requires several Atg proteins, such as Atg11, Atg23 and Atg23 (He et al., 2006; Legakis et al., 2007; Shintani and Klionsky, 2004). The retrieval of Atg9 from PAS to other membrane structures requires the Atg1-Atg13 complex, Atg2, Atg18 and the PtdIns3K complex I. Loss of any of these proteins will result in accumulation of Atg9 at the PAS and thus block the autophagosomal activity (Reggiori et al., 2004). Both Atg2 and Atg18 are peripheral membrane proteins that bind to Atg9, and the interaction of Atg18 with Atg9 requires Atg2 and Atg1 (Reggiori et al., 2004; Suzuki et al., 2007; Wang et al., 2001). To localize to the PAS, Atg2 and Atg18 depend on each other, Atg1, Atg13, Atg9 and the PtdIns3K complex I. Atg18 can bind to PtdIns(3)P, which is generated by VPS34, and the binding is essential for autophagy function (Strømhaug et al., 2004). One model is that Atg9 could shuttle between the peripheral structures and the PAS, which is regulated by the Atg1-Atg13 kinase complex. This complex mediates the interaction of Atg9 with Atg2 and Atg18 and the formation of this ternary complex allows Atg9 to be retrieved from the PAS back to the peripheral sites (Reggiori et al., 2004).

1.3.6.2 Signaling regulation of autophagy

The understanding of autophagy signaling pathways was expanded after the identification of the target of rapamycin kinase (TOR), which regulates cell growth, cell proliferation, cytoskeletal rearrangement and protein synthesis (Brown et al., 1994; Kunz et al., 1993). Since TOR negatively regulates autophagy, treatment with rapamycin, the inhibitor of TOR, can induce autophagy (Noda and Ohsumi, 1998). This result was shown both in rat hepatocytes (Blommaart et al., 1995) and in yeast (Noda and Ohsumi, 1998). Downstream of TOR, the ribosomal protein S6 is phosphorylated when nutrition is sufficient (Blommaart et al., 1995). Phosphorylation of S6 blocks autophagy and this suppression can be reversed by rapamycin (Blommaart et al., 1995).

Both Class I and Class III PtdIns3K function as regulating complexes in autophagy (Klionsky, 2005). Class I PtdIns3K activates TOR and thus has an inhibitory role. Consistent with this result, overexpression of PTEN, which inactivates Class I PtdIns3K can induce autophagy (Arico et al., 2001). In contrast, Class III PtdIns3K positively regulates the VPS34/Atg6 complex and hence stimulates autophagy (Petiot et al., 2000). PtdIns3K inhibitors such as wortmannin, LY294002 and 3-methyladenine have been used to modulate autophagy (Blommaart et al., 1997; Seglen and Gordon, 1982) However, recent studies suggest that 3-MA could increase autophagosomal influx yet eventually still suppress autophagy because it interacts with both PI3Ks, but with different efficacy (Seglen and Gordon, 1982; Wu et al., 2010). This indicates that caution should be applied when interpreting results with 3-MA in the study of autophagy.

The insulin pathway has been shown to inhibit autophagy through the activation of

Class I PtdIns3K products. Activation of the insulin pathway by overexpressing protein kinase B (Akt) or a constitutively active form of 3-phosphoinositide-dependent protein kinase 1 (PDK1) leads to suppression of autophagy (Arico et al., 2001; Meijer and Codogno, 2004).

1.3.6.3 The immune function of autophagy

Genetic studies in *Drosophila* have deepened our understanding of autophagy and its role in development (Berry and Baehrecke, 2007; Scott et al., 2004). Cumulative evidence also connects autophagy to neurodegenerative diseases, cancer and immune diseases (Liang et al., 1999; Lipinski et al., 2010; Orvedahl et al., 2010). In fly and mouse Huntington disease models, induction of autophagy can protect neurons from accumulation of toxic polyglutamine protein aggregates, while suppression of autophagy has the converse effect (Ravikumar et al., 2004). Beclin-1, the mammalian homolog of Atg6, was found to be a tumor suppressor since *beclin1*$^{+/-}$ mutant mice suffered from a high incidence of spontaneous tumors (Yue et al., 2003). However, the role of autophagy in immunity is complex since autophagy responds differently towards different pathogens.

The role of autophagy in immunity can be divided to two groups: (1) Autophagy can serve as a defense mechanism to target pathogens for degradation. (2) The pathogens can subvert autophagic machinery for their own benefit so autophagy can facilitate pathogen replication and expansion (Lin et al., 2010).

Autophagy as a defense mechanism Autophagy has been shown as antiviral against some viruses. Beclin-1, the Atg6 homolog, was shown to be antiviral when mice were

infected with the Neurotropic Sindbis Virus (SINV) (Liang et al., 1998). Overexpression of Beclin-1 increased the viability of mice infected with SINV, and also reduced the neuronal apoptosis and viral titers in the mouse brain (Liang et al., 1998).

In *Drosophila*, autophagy was also found to be important in restricting the infection of intracellular pathogen *Listeria monocytogenes* in a PGRP-LE (pattern-recognition receptor)-dependent manner (Yano et al., 2008). However, the mechanisms underlying cytoplasmic infection-induced autophagy and the function of autophagy in host survival after infection with intracellular pathogens (especially viruses) are far from clear.

Pathogen manipulation of autophagy for their own benefit Previous studies suggest that autophagy is a critical antiviral defense mechanism (Orvedahl et al., 2010; Tallóczy et al., 2006). However, the role of autophagy in virus infection is complicated and it may facilitate viral pathogenesis. Many viruses manipulate autophagy for their own benefit by one of the following mechanisms.

1. Using Membrane-Bound Replication Compartments for Viral Replication The subversion of autophagy by poliovirus (PV) is a classic model of viral exploitation of the autophagy pathway (Suhy et al., 2000). Polio virus infection can induce autophagosome formation, and knockdown of *Atg* genes (*Atg12, LC3*) reduces viral titers (Jackson et al., 2005). Many other RNA viruses including Coxsackievirus B3 (CVB3), Japanese encephalitis virus (JEV), HCV, Coronavirus mouse hepatitis virus (MHV), vesicular stomatitis virus (VSV), and rhinoviruses 2 and 14 also exploit autophagic membrane scaffolds for RNA replication (Jackson et al., 2005; Jounai et al., 2007; Ke and Chen, 2011; Li et al.,

2012b; Prentice et al., 2004; Tang et al., 2007). In addition, the physical structure of a double membrane compartment is proposed to allow efficient fusion of the autophagosomal membrane with the cytoplasmic membrane. Thus, an emerging concept is that autophagy may play a role in the nonlytic release of cytoplasm during autophagosome maturation, namely autophagic exit without lysis (AWOL). This machinery can also be used in the release of PV (Kirkegaard and Jackson, 2005; Taylor et al., 2009).

2. Increased Viral Infectivity by Blocking Autophagic Flux Virus can induce incomplete autophagy by blocking the later stage of autophagic fusion with the lysosome. This was reported in cells infected with CVB3, rotavirus, and Influenza A Virus (IAV) (Alirezaei et al., 2012; Crawford et al., 2012; Gannagé et al., 2009; Kemball et al., 2010). In CVB3-infected pancreatic acinar cells, an increase in the number of double-membraned autophagic-like vesicles was observed upon infection. However, the accumulation of the autophagic substrate p62 and the formation of large autophagy-related structures named megaphagosomes indicate that CVB3 blocks a later stage of the autophagic pathway (Kemball et al., 2010). This induction of autophagosome serves as a niche for CVB3 RNA replication and translation (Alirezaei et al., 2012). In rotavirus infected cells, it was reported that the NSP4 viroporin releases endoplasmic reticulum calcium into the cytoplasm, thereby activating a CaMKK-βAMPK pathway to initiate autophagy (Crawford et al., 2012). However, autophagosome maturation is impeded. By hijacking this membrane trafficking pathway, rotavirus transport viral proteins from the ER to the site of infection to produce viral particles. In addition, several studies suggest that M2, HA, and NS1 proteins of Influenza A Virus (IAV) are involved in the induction

of autophagy, but only M2 has been identified as a critical factor in preventing fusion of autophagosomes with lysosomes (Gannagé et al., 2009; Sun et al., 2012; Zhirnov and Klenk, 2013).

3. Escaping the Host Immune Response Viruses like VSV, HCV, DENV, and JEV can evade the host immune response by activating autophagy to target immune components (Jin et al., 2013; Jounai et al., 2007; Ke and Chen, 2011). For example, in VSV infection, the Atg5-Atg12 conjugate targets RIG-I/MDA5-MAVS-dependent type I IFN production by directly interacting with MAVS and RIG-I. This results in a suppression of MAVS-mediated NF-κB and type I IFN promoters, and permits VSV replication. Furthermore, through an unidentified mechanism, HCV- or DENV-induced autophagy negatively regulates type I IFN production and promotes HCV replication (Ke and Chen, 2011). Additionally, JEV replication is impeded in autophagy-deficient cells *in vitro*. Upon infection, lack of autophagy also results in mitochondrial antiviral signaling protein (MAVS) aggregation and activation of IFN regulatory factor 3 (IRF3), markers for innate immune activation (Jin et al., 2013). This suggests that autophagy can be exploited to facilitate virus replication, partly through suppression on antiviral responses.

1.3.6.4 Crosstalk between autophagy and other immune signaling

Toll signaling and autophagy Multiple studies suggested that the immune function of autophagy is closely associated with the pattern recognition receptors (PRRs) (Oh and Lee, 2014). Specifically, PRRs are not only involved in autophagy induction but can also promote phagosomal maturation mediated by Atg proteins when pathogenic bacteria in-

vade host cells. In addition, autophagy facilitates the delivery of both viral PAMPs and TLR9 that lead to type I IFN production. Autophagy also regulates PRR-induced inflammation in various ways to prevent excessive inflammatory responses, and conversely, PRR signaling also controls autophagy.

Among all the PRRs, Toll-like receptors (TLRs) are the best characterized. The first evidence to link TLRs with autophagy is a study of TLR4, whose activation by lipopolysaccharide (LPS) induces autophagy to enhance elimination of phagocytosed mycobacteria (Xu et al., 2007). In addition to LPS-induced autophagy, ligands of TLR3 and TLR7 also induce autophagy. Single-stranded RNA (ssRNA) and imiquimod, two different ligands of TLR7, promote autophagosome formation in murine macrophages (Delgado et al., 2008). The activation of TLR7 ligand-induced autophagy results in a decreased load of *M. tuberculosis var. bovis Bacille Calmette-Gurin (BCG)* (Delgado et al., 2008).

TLR-activated autophagy can promote pathogen clearance through autophagosome degradation. In addition, autophagy also enhances antiviral defenses by facilitating delivery of cytosolic viral PAMPs to endosomal TLRs. In response to vesicular stomatitis virus (VSV) infection in plasmacytoid dendritic cells (pDCs), endosomal TLR7 recognizes the replication intermediates rather than the viral genome. The replication intermediates (recognized as PAMPs) are then delivered to the lysosomes by autophagy, further activating TLR7 signaling (Lee et al., 2007). pDCs that lack Atg5 fails to produce IFN-α or IL-12p40 following VSV infection. Furthermore, *Atg5* deficient mice are also more suceptible to VSV infection compared to WT (Lee et al., 2007). In *Drosophila*, Toll-7, was shown as the PRR to activate autophagy during vesicular stomatitis virus (VSV)

infection. Toll-7 interacted with VSV at the plasma membrane and induced antiviral autophagy independently of the canonical Toll signaling pathway (Nakamoto et al., 2012). These data indicate a conserved linkage between Toll signaling and autophagy in both mammals and invertebrates.

Autophagy and inflammation Autophagy can negatively regulate inflammatory responses (Jounai et al., 2007; Nakahira et al., 2011; Saitoh et al., 2008; Shi et al., 2012; Tal et al., 2009; Zhou et al., 2011). For example, a lack of Atg16L1, an essential component of the autophagosome, results in increased production of IL-1β and IL-18 following LPS stimulation. Since Atg16L1 plays an important role in the development of Crohn's disease, it is possible that the endotoxin-induced inflammasome activation in *Atg16L1*-deficiency could be involved in the occurrence of Crohn's disease (Saitoh et al., 2008).

Another study indicates that autophagy can suppress the NLRP3 inflammasomes, which play a major role in innate immunity by activating caspase-1 and mediating the processing and release of the leaderless cytokine IL-1β(Baroja-Mazo et al., 2014; Nakahira et al., 2011; Zhou et al., 2011). Blockage of autophagy results in the accumulation of damaged, reactive oxygen species (ROS)-generating mitochondria, which in turn activates NLRP3 inflammasomes. Furthermore, depletion of the autophagic proteins LC3B and beclin-1 also lead to excessive secretion of IL-1β and IL-18 (Nakahira et al., 2011).

In addition, autophagy can negatively regulate RLR signaling (Jounai et al., 2007; Tal et al., 2009). The RLR signaling pathway is important for cytoplasmic pathogen

recognition, which is mediated by cytosolic sensors such as RIG-I and MDA-5 (Reikine et al., 2014). In both Atg5- and Atg7-deficient mouse embryonic fibroblasts (MEFs), where the Atg5-Atg12 association is disrupted, type I IFNs are overproduced following VSV infection. In contrast, overexpression of Atg5 or Atg12 results in suppression of IFN signaling. The Atg5-Atg12 conjugates directly interact with the CARD domains of RIG-I and IPS-1, inhibiting subsequent RLR signaling (Jounai et al., 2007). Similarly, Atg5-deficient cells overproduce IFNs through enhanced RLR signaling in response to VSV infection (Tal et al., 2009).

A recent study showed that autophagy induced by inflammatory signals targets ubiquitinated inflammasomes, thereby limiting IL-1β production through inflammasome destruction (Shi et al., 2012).

In *Drosophila*, inflammation is best characterized in the intestine with a phenotype of overexpressed antimicrobial peptides (AMP) (Lee and Lee, 2014). A low AMP expression is stimulated by the gut microbiota, which is beneficial for the preservation of community structure. However, overexpression of antimicrobial peptides might be detrimental to the fly health. This is demonstrated in the *caudal*-silenced flies with a phenotype of gut cell apoptosis and early host death (Ryu et al., 2008). This is because caudal, an intestine-specific homeobox transcription factor, acts as a repressor of Relish-dependent AMP genes. Lack of caudal will results in AMP overexpression that further destroys the gut microbiota balance.

Similar to caudal knockdown flies, flies that carry mutations in negative regulators

of the Imd pathway and thus are constitutively overexpressing AMPs have a reduced survival rate in a conventional environment, when microbiota exist in flies. However, when flies were raised in a germ free environment, these mutant flies have a normal survival rate (Bischoff et al., 2006; Lhocine et al., 2008; Paredes et al., 2011). This indicates that the Imd pathway tightly controls the expression levels of AMPs stimulated by the gut microbiota. So far, it is unclear whether autophagy could play a role in causing inflammation in flies.

1.4 Lipid Metabolism

1.4.1 Lipid droplets as energy storage compartments

In recent years, *Drosophila melanogaster* has proven to be a powerful model for the studies of lipid metabolism and energy homeostasis (Liu and Huang, 2013; Schlegel and Stainier, 2007). The anatomy of organs and cell types, the signaling pathways and the genes involved are highly conserved between mammals and *Drosophila*. The *Drosophila* fat body, the equivalent of mammalian adipocytes, is the major organ for lipid storage in the form of lipid droplets (LDs). The major components of LDs are triacylglycerol (TAG) and cholesterol ester, the functions of which are storing energy, composing the cellular membranes, and serving as precursors of hormones and vitamins (**Figure 1.8**).

In addition, the recent evidence has revealed oenocytes, a cluster of large secretory cells underlying the epidermis of abdominal segments, along with the fat body are critical for the regulation of lipid metabolism (Gutierrez et al., 2007). During starvation, *Drosophila* larve release large quantities of lipid from the fat body while lipid accumu-

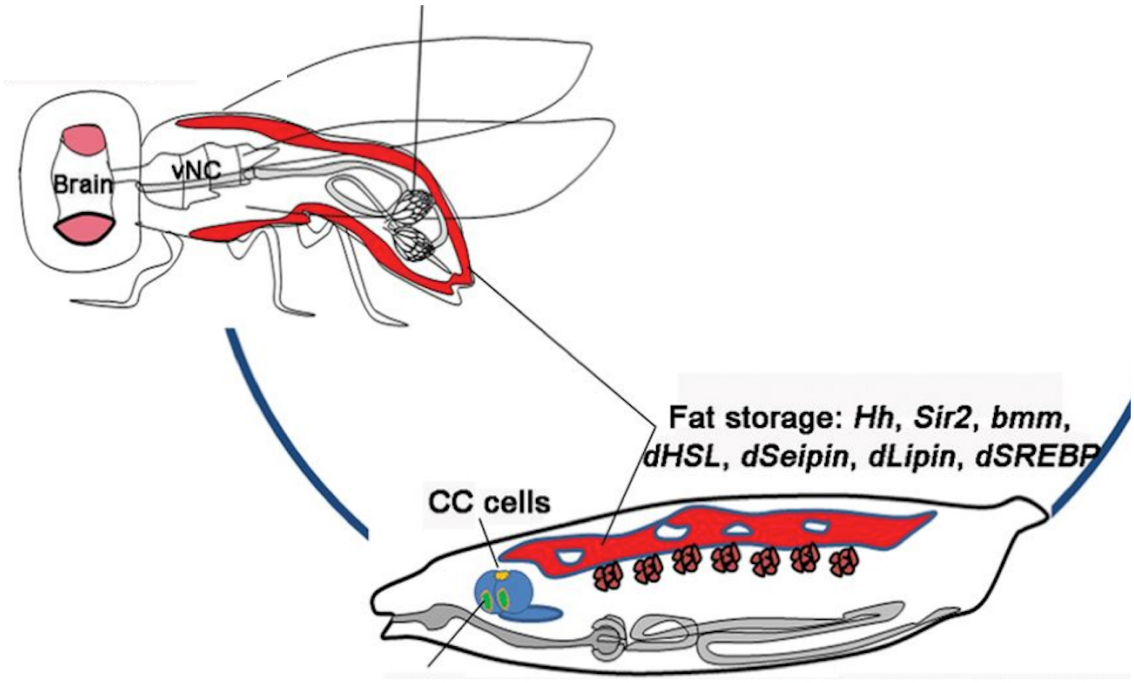

Figure 1.8: Schematic representation of the lipid storage tissues in the *Drosophila*. Red indicates larval and adult fat body (Liu and Huang, 2013).

lates in the oenocytes. Disruption of oenocyte function prevents the depletion of lipid in the fat body. This indicates that the fat body and oenocytes coordinate in lipid mobilization and that oenocytes act downstream of the fat body. It is not fully understood how the fat body communicates with oenocytes. The fat body and oenocytes also express different lipid-metabolizing proteins. For example, in the fat body, lipases such as Brummer, and lipase regulators such as Lsd-1, Lsd-2 are highly expressed. In oenocytes, Cyp4g1, an omega-hydroxylase regulating triacylglycerol composition was found to be particularly important (Gutierrez et al., 2007) (**Figure 1.9**).

The LD homeostasis is achieved by a balanced control of lipogenesis and lipolysis. Activation of lipogenesis results in an increase of LD size, which is mainly controlled by the lipid synthesis enzyme diacylglycerol O-acyltransferase 1 (DGAT1) in mammals.

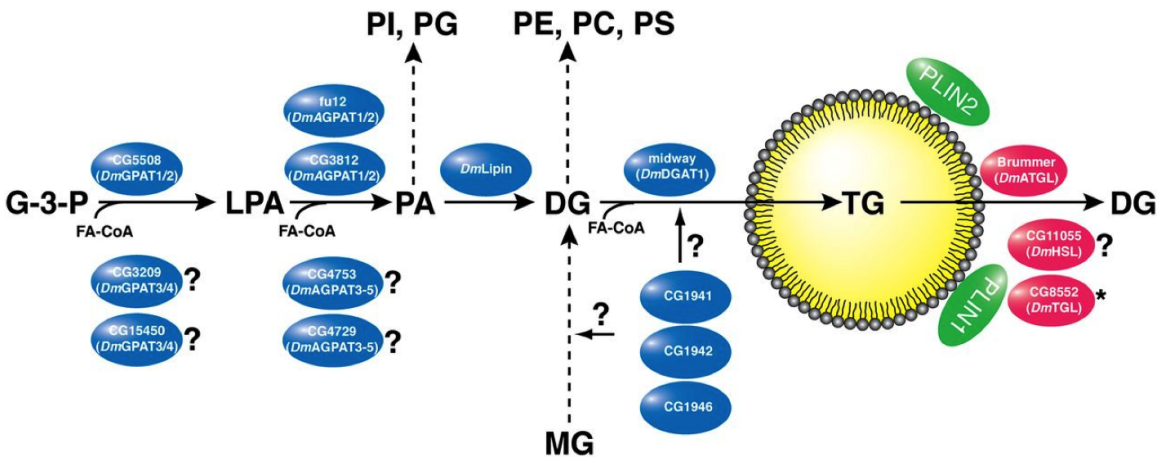

Figure 1.9: Schematic representation of the core enzymes in the *Drosophila* lipid metabolism.
Lipid metabolism is a balance between lipid synthesis and lipid mobilization. Represented are lipogenic enzymes of the glycerol-3-phosphate pathway (blue), lipases (red), and modulatory LD-associated proteins of the Perilipin family (green). The proteins marked by a question mark (?) are identified with sequence homology, while the functions of those proteins are not yet confirmed. An asterisk (*) indicates that in vitro evidence supports the involvement of the Manduca sexta CG8552 ortholog MsTGL in storage fat mobilization from LDs. ATGL: adipose triglyceride lipase; FA-CoA: fatty acid CoA ester; HSL: hormone sensitive lipase; MG: monoacylglycerol; PC: phosphatidylcholine; PE: phosphatidylethanolamine; PG: phosphatidylglycerol; PI: phosphatidylinositol; PLIN1, 2: Perilipin1, 2; PS: phosphatidylserine; TGL: triglyceride lipase (Kühnlein, 2012).

In contrast, a facilitated lipolysis will decrease the LD size, with the adipose triglyceride lipase (ATGL/PNPLA2) degrading stored lipids in the LDs. In *Drosophila*, DGAT1 and ATGL are encoded by *midway* and *brummer*, respectively (Buszczak et al., 2002; Grönke et al., 2005). Loss-of-function of *brummer* generates an obese phenotype with enlarged LDs in the fat body. In contrast, the *midway* null mutant displays a lean phenotype.

The detailed regulation of LD homeostasis is not yet well understood. Among all the regulators, the Perilipin family are the best characterized LD surface proteins (Bickel et al., 2009; Londos et al., 2005).

1.4.2 The Perilipin family proteins in the regulation of LDs

The mammalian perilipins (PLINs) include several sequence-related and evolutionarily conserved LD proteins, which have been extensively studied for their roles in LD regulation (Bickel et al., 2009; Brasaemle, 2007; Brasaemle et al., 2009; Londos et al., 2005). Among the perilipins, perilipin A is the most abundant protein on the surface of LD (Brasaemle et al., 2009). Perilipin A acts as a protein coating to prevent the access of hormone-sensitive lipase (HSL) to neutral lipids. Following β-adrenergic receptor activation, however, perilipin is phosphorylated and changes its protein conformation accordingly (Miyoshi et al., 2006). This change in conformation promotes the accessibility of HSL for lipid lipolysis (Brasaemle et al., 2009).

In *Drosophila*, only two perilipins are encoded: lipid storage droplet-1 (*lsd-1*) and lipid storage droplet-2 (*lsd-2*) (Beller et al., 2010; Grönke et al., 2003; Lu et al., 2001). Due to the recent nomenclature revision, *lsd-1* and *lsd-2* are also called *perilipin1 (plin1)*, *perilipin2 (plin2)*, respectively (Kimmel et al., 2010). Fly perilipins not only share sequence homology with mammalian perilipins, they were also shown to localize to the surface of LD by multiple studies. GFP-tagged Lsd-1 and Lsd-2 fusion proteins localize to the LD in the larval fly fat body and CHO cells (Miura et al., 2002). The lipid droplet association with *Drosophila* Perilipins has also been found in the lipid droplet fraction of fat body cells after density gradient fractionation (Beller et al., 2010; Grönke et al., 2003; Welte et al., 2005). An LD proteomics study also confirms the association of PLINs with LD (Beller et al., 2006; Cermelli et al., 2006).

Drosophila plin1 gene is expressed during all ontogenetic stages from late embryo-

genesis to adult flies. Although present in neuroendocrine cells of the ring gland during embryogenesis, *plin1* is predominantly expressed in both larval and adult fat body (Beller et al., 2010; Chintapalli et al., 2007). In addition, microarray data indicates that *plin1* is also expressed moderately in the adult gut, heart and spermatheca (Chintapalli et al., 2007).

Drosophila PLIN1 is only found in the lipid droplet fraction of fat body cells (Beller et al., 2010). GFP-tagged PLIN1 shows exclusive localization on the surface of LD. The level of PLIN1 protein also correlates with the total surface area of LDs (Beller et al., 2010). The mRNA transcripts and protein levels of PLIN1 are both sensitive to changes in lipid storage. However, pieces of data suggests that not only the transcriptional level of *plin1* is critical, but the post-translational modification of PLIN1 is essential for normal activity (Beller et al., 2010).

plin1 null mutants develop early onset obesity as adult flies. The fat content of the mutants is doubled compared to wildtype (Beller et al., 2010). The food intake of *plin1* mutants increase significantly when the files are on a high-sugar diet. However, on a low-sugar diet, mutant flies eat an equivalent amount of food as wildtype but still have a higher fat content. These data indicates that the obesity is not only attributed to an increased food intake but is also due to a slower metabolism.

PLIN1 is the downstream effector of the pro-lipolytic adipokinetic hormone (AKH)/AKH-receptor (AKHR) pathway at the LD surface. The AKH signaling is the equivalent of the mammalian β-adrenergic signaling pathway that regulates lipid mobilization. Once the AKH receptor (AKHR) is activated in the fat body, the second messenger cAMP is released to activate protein kinase A (PKA). Phosphorylation of PLIN1 by PKA is proposed

to be essential for the initiation of lipid lipolysis, however, the details needs to be further clarified. On one hand, phosphorylation of PLIN1 by PKA has been shown in both the *ex vivo Manduca* fat body and *Drosophila* PLIN1 decorated liposome *in vitro* (Arrese et al., 2008a; Patel et al., 2005). On the other hand, mutated PLIN1 with defective phosphorylation sites still functions normally in *Drosophila in vivo*. This might be due to the fact that multiple redundant phosphorylation sites exist in PLIN1. Mutation of the classical phosphorylation sites identified in *Manduca* might not be sufficient to turn off PLIN1 (Arrese et al., 2008b).

Recent studies indicate that PLIN1 is necessary to recruit hormone-sensitive lipase (HSL) to facilitate lipid mobilization during starvation (Bi et al., 2012). HSL (*Drosophila* dHSL) , along with ATGL (*Drosophila* Brummer), is one of the two key lipases for basal and stimulated lipolysis, respectively (Bi et al., 2012; Grönke et al., 2005; Schweiger et al., 2006). In normal conditions, dHSL is largely dispersed in the cytoplasm, with little dHSL localized to the surface of LD. However, in starved conditions, more dHSL localizes to the surface of LDs and appears as ring structures around the lipid droplets. This data is consistent with the role of HSL in mammals (Egan et al., 1992; Sztalryd et al., 2003). Strikingly, the localization of dHSL is abrogated in the *plin1* mutants, which indicates that PLIN1 is required for dHSL to target to the lipid droplet. Since $dHSL^{b24}$ null mutants accumulate more body fat with enlarged lipid droplets, it is highly possible that PLIN1 is facilitating dHSL lipase function (Bi et al., 2012).

Although a defect in PLIN1 displays impairment of LD lipolysis and fat mobilization, PLIN1 is not required for this process since fat mobilization is not totally blocked in the *plin1* mutant (Beller et al., 2010). Starvation-resistance is correlated to body fat

content and serves as a hallmark for fat storage. Null homozygous and heterozygous *plin1* mutants or RNAi knowdown flies are all resistant to starvation compared to WT (Beller et al., 2010). This indicates there are other parallel signaling pathways regulating a PLIN1-independent fat mobilization.

Genetic studies in *Drosophila* also reveal that the interaction between BMM, PLIN1 and dHSL are not exclusive (Bi et al., 2012). First, $dHSL^{b24};bmm^{1}$ double mutants have larger lipid droplets than any of the single mutants. This indicates that BMM and dHSL act in parallel pathways. Second, the lipid droplets in $plin1^{1}$ are larger than $dHSL^{b24};bmm^{1}$ double mutants. This indicates that PLIN1 has other functional targets rather than BMM and dHSL. Third, both $plin1^{1};bmm^{1}$ and $plin1^{1};dHSL^{b24}$double mutants have larger droplets compared to $plin1^{1}$, indicating the existence of other components controlling BMM and dHSL rather than PLIN1 (Bi et al., 2012).

Other than controlling lipid mobilization, PLIN1 is also critical for maintaining the lipid droplet structure *in vivo* (Beller et al., 2010). Lack of PLIN1 transforms the heterogeneously sized LD population of the wild-type fat body cell into a single giant LD accompanied by few small satellite droplets (Beller et al., 2010). However, the enlargement of the lipid droplets are not likely due to a lack of surface protein coverage. Overexpression of human PLIN1a, EGFP-tagged CG2254, or PLIN2 in $plin1^{1}$ mutant does not modify the size of lipid droplet (Beller et al., 2010). Additionally, it is controversial whether the enlarged size of lipid droplet in $plin1^{1}$ mutant is due to accumulated fat content. In the $mdy^{-};plin^{1}$ double mutants, the fat content is reduced compared to $plin1^{1}$ mutants whereas enlarged lipid droplets can still be observed. Moreover, $plin1^{1}$ mutants only display obesity in early adult stages but the enlarged droplets appear in the

larval stage (Beller et al., 2010). In summary, it is difficult to argue whether the change of LD structures results in the increased fat content or *vice versa*. In order to understand this, more experiments need to be done.

plin2 also expresses in all developmental stages in *Drosophila*. However, the distribution of *plin2* mRNA varies at different developmental stages. During the early embryogenesis, *plin2* is ubiquitously and uniformly present in the embryo, which is maternally provided (Edgar and Schubiger, 1986). At later stages of embryogenesis, *plin2* is predominately expressed in germline cells, specifically in the female (Teixeira et al., 2003). However, at the later stage of embryogenesis, larval and adult stages, *plin2* is relatively broadly expressed with an enrichment in the fat body and the midgut (Teixeira et al., 2003).

Although present at different tissues across developmental stages, PLIN2 is involved in regulating lipid droplet within all these tissues. For example, PLIN2 plays an important role in controlling of the movement of embryonic LDs along microtubules. Additionally, abnormal accumulation of neutral lipids is observed in the germline and eggs of *lsd2*^{1} females (Teixeira et al., 2003). In larval and adult flies, lack of PLIN2 results in decreased lipid accumulation, as characterized by a 50% and 27% decrease in the triglyceride level of the *plin2* mutant compared to WT in larvae and adults, respectively (Teixeira et al., 2003). Accordingly, the size of the lipid droplet is also smaller compared to wildtype in the fat body (Teixeira et al., 2003). These data shows the significance of PLIN2 in lipid metabolism.

However, in contrast to PLIN1, PLIN2 is required for lipid droplet transport in *Drosophila* embryos and is important for protecting lipid droplets from lipolysis (Fauny

et al., 2005; Grönke et al., 2003; Welte et al., 2005). Additionally, unlike PLIN1, PLIN2 can either localize to the surface of lipid droplet or remains in the cytoplasm (Grönke et al., 2003). However, the regulation of the exchange in localization of PLIN2 is not well known.

In *Drosophila* nurse cells, PLIN2 levels depend on the activity of cytoplasmic phosphorylated Akt in nurse cells (Vereshchagina et al., 2008; Vereshchagina and Wilson, 2006). Specifically, *pten* mutants show enlarged lipid droplets in nurse cells, an increase in activated Akt, and a high expression of *plin2* (Vereshchagina and Wilson, 2006). Furthermore, an increase in lipid droplet size was observed in the mutants of the phosphatase PP2A-B regulatory subunit Widerborst (*Wdb*), a negative regulator of cytoplasmic activated Akt. The phenotype in the*Wdb* mutant is abrogated in the *Akt* mutant (Vereshchagina et al., 2008).

PLIN2 is proposed to regulate adipose triglyceride lipase BMM, but not HSL, for lipid degradation. Evidence shows that bmm^{-} $plin2^{-}$ double mutants have wildtype TAG levels, indicating that loss of PLIN2 activity compensates for the lack of BMM (Grönke et al., 2005). Conversely, overexpression of both *bmm* and *plin2* in the fat body can partially revert the phenotypes generated by overexpressing either of the single genes. These data demonstrate that both BMM and PLIN2 play important roles in lipid metabolism, but in opposite direction.

Although PLIN1 and PLIN2 were previously demonstrated to have opposite function. A new piece of data suggests they may also have redundant roles. Overexpression of *plin1* in *plin2* mutants do not enhance the large lipid droplet phenotype but instead mildly suppresses the size of lipid droplets (Bi et al., 2012). Furthermore, $plin1^{38}$;$plin2^{KG00149}$

double mutant larvae were found to display an even smaller lipid droplet phenotype than the *plin2*^{KG00149} single mutant (Bi et al., 2012). Domain deletion and swapping experiments indicate that the C-terminal of PLIN1 is critical in determining the localization and functional difference between PLIN1 and PLIN2 (Bi et al., 2012).

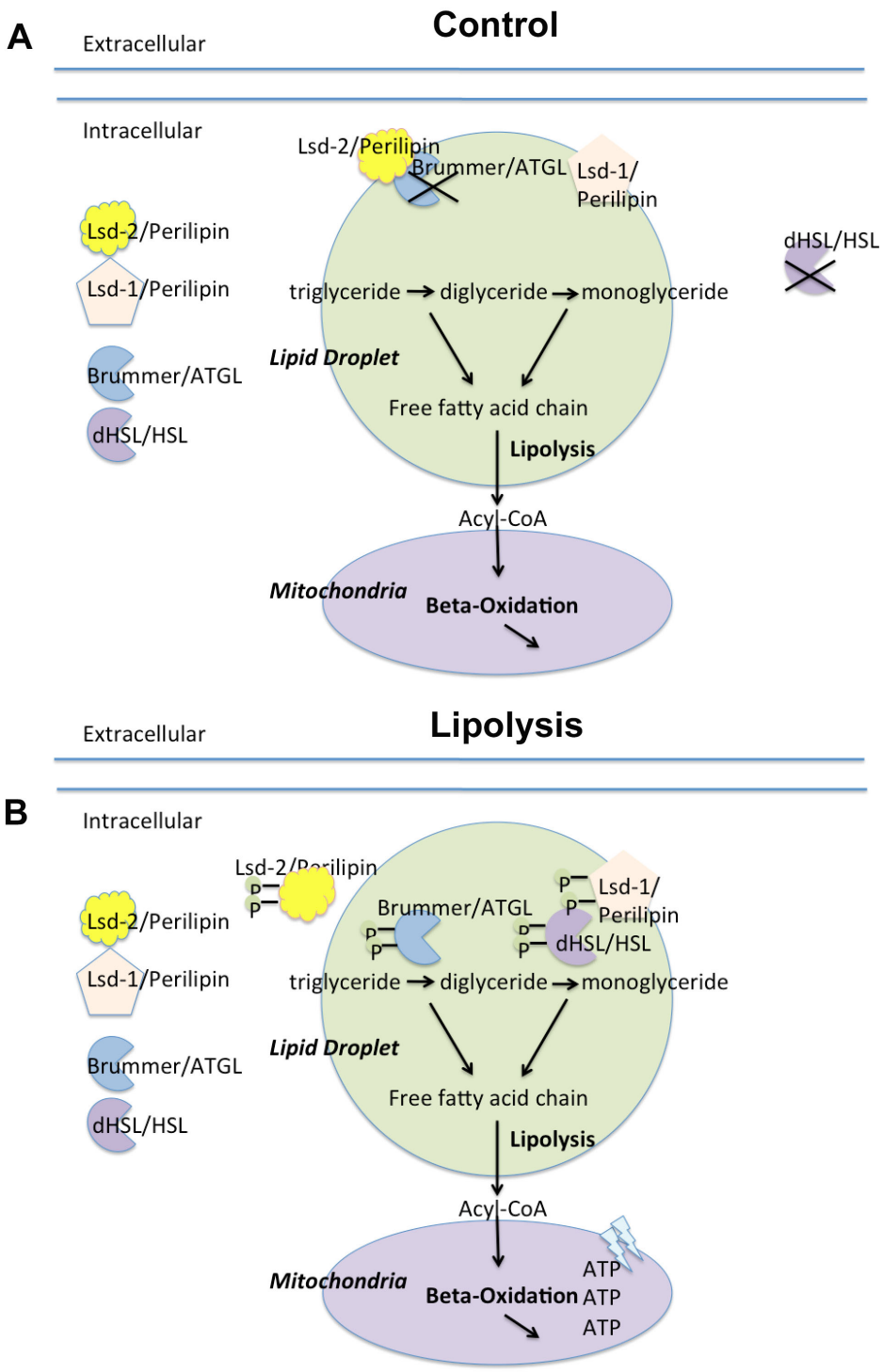

Figure 1.10: Diagram of Lipid droplet metabolism.
Under normal conditions, lipases Brummer and dHSL are inactivated. dHSL is distributed in the cytoplasm without access to the lipid droplet. Brummer is functionally inhibited by Lsd-2/PLIN2. When lipolysis is activated, Brummer and dHSL are activated through phosphorylation. This results in the degradation of triglyceride in the lipid droplet. The free fatty acids generated by lipolysis can be transported into mitochondria for ATP production.

1.4.3 β-Oxidation

Mitochondrial β-oxidation is an important system involved in the energy production of various cells. β-oxidation is a process when free amino acids are oxidized through a chain of reactions, resulting in ATP production. Disorders of β-oxidation are believed to cause about 1-3% of unexplained sudden infant deaths (SIDS). Acute fatty liver of pregnancy (AFLP) and the syndrome of hemolysis, elevated liver enzymes, and low platelets (HELLP syndrome), which have significant neonatal and maternal morbidity and mortality, have also been associated with β-oxidation deficiency in fetuses. In adults, dysfunction of β-oxidation also cause multiple heart diseases such as cardiomyopathy (**Figure 1.11**).

β-oxidation is closely associated with lipid metabolism, since the free fatty acids generated by lipid metabolism are the major substrates for β-oxidation. The free amino acid is produced through two steps of lipase hydrolysis reactions. Specifically, triglyceride is degraded by ATGL into diglyceride, which is further hydrolyzed into monoglyceride by HSL. Consistent with the mammalian system, in *Drosophila*, the hydrolysis reactions are executed by BMM and dHSL, respectively. Before translocation to the mitochondria, free fatty acids will be oxidated to acyl-CoA by acyl-CoA synthetase.

One of the rate limiting step is the transportation of acyl-CoA across the inner mitochondrial membrane from the cytoplasm. This process is controlled by the carnitine transporter system, which is comprised of Carnitine acyl transporter (CPT), Carnitine acyl transporter and L-carnitine (Bremer, 1983; Vaz and Wanders, 2002). Specifically,

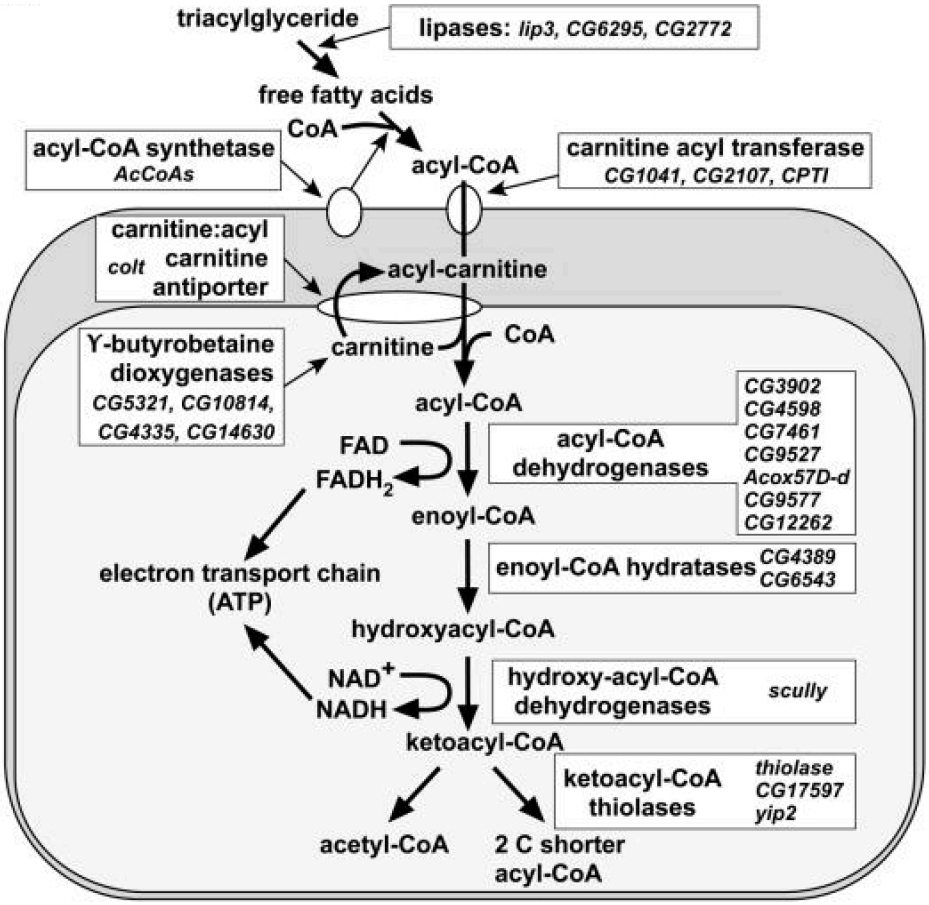

Figure 1.11: Lipid metabolism and β-oxidation.
This diagram shows the core enzymes in the β-oxidation pathway. Free fatty acids are converted to acyl-CoA by AcCoAs before entering into mitochondria. The transportation of acyl-CoA is facilitated by the carnitine carrier system. As a result of a series of oxidation reactions, two carbon bonds are oxidized in the acyl-groups. This cycle will go on until the total carbon chain is degraded (Palanker et al., 2009).

carnitine serves as a carrier to facilitate the transportation of acyl-CoA. Accumulated carnitine within the cell is conjugated with fatty acids to form acylcarnitine by carnitine palmitoyl transferase 1 (CPT1). The transfer of the acylcarnitine across the inner plasma membrane is facilitated by carnitine-acylcarnitine translocase (CACT). Once the acylcarnitine crossed the inner membrane, carnitine palmitoyl transferase 2 (CPT2) facilitates the disassociation between acyl group and carnitine and promotes the conjugation of the fatty acid back to Coenzyme A for subsequent β-oxidation. The freed carnitine is cycled out of the mitochondria inner membrane by the carnitine transporter (OCTN2). Deficiency in any part of this system can lead to multiple diseases due to β-oxidation dysfunction (Longo et al., 2006).

For example, deficiency of the OCTN2 carnitine transporter causes primary carnitine deficiency, characterized by increased loss of carnitine in the urine and decreased carnitine accumulation in tissues. Patients can develop hypoketotic hypoglycemia and hepatic encephalopathy, or with skeletal and cardiac myopathy (Scaglia et al., 1998). Defects in the liver isoform of CPT1 present with recurrent attacks of fasting hypoketotic hypoglycemia, a disease with symptoms of low levels of ketones and low blood sugars. CACT deficiency in patients results in the neonatal period with hypoglycemia, hyperammonemia, and cardiomyopathy with arrhythmia leading to cardiac arrest (Rubio-Gozalbo et al., 2004). Deficiency of CPT2 present more frequently in adults with rhabdomyolysis triggered by prolonged exercise. More severe variants of CPT2 deficiency present in the neonatal period similarly to CACT deficiency associated or not with multiple congenital anomalies (Bonnefont et al., 2004).

Chapter 2: Atg1 plays an antiviral role against *Drosophila* X Virus, but this effect appears to be independent of classical autophagy

2.1 Results

2.1.1 Atg1 plays an antiviral role against DXV infection in the fat body

To examine whether autophagy plays a role in the immune response against DXV infection, we used RNA interference to silence autophagy genes in different adult tissues with tissue specific Gal4 drivers. Among all the *Atg* genes, *Atg1* is upstream in the autophagy signaling pathway and is a critical initiator for autophagy (Chang and Neufeld, 2009). When *Atg1* is silenced in multiple tissues including the fat body and hemocytes, the major immune tissues,(Hultmark, 1993; Lemaitre and Hoffmann, 2007), flies are more susceptible to DXV infection (**Figure 2.1 A**). *Atg1* RNAi flies are not susceptible to wounding as injection of PBS does not cause fly death (**Figure 2.1 A**). Three survival experiments have been done and the median survival is 12 days and 10 days for WT and *IR-Atg1* flies, respectively (**Figure 2.1 B**). This suggests that *Atg1* is required for maintaining fly survival against DXV.

Upon infection, host can resist a pathogen by initiating an immune response to clear the pathogen or develop tolerance to the pathogen without clearing them (Schneider and

Ayres, 2008). To examine whether the immune function of *Atg1* associates with pathogen resistance or host tolerance, we examined the viral mRNA levels in both wildtype and *Atg1* RNAi flies upon infection. At day 3 post infection, VP1 (the RNA-dependent RNA polymerase) mRNA levels are $\sim$50 fold higher than in wildtype. At day 7 post infection, there is a $\sim$10 fold increase of VP1 mRNA levels (**Figure 2.1 C**). *Atg1* RNAi flies also show a higher viral protein levels by Western blot (**Figure 2.1 D**). This indicates that *Atg1* plays an antiviral role to fight against DXV.

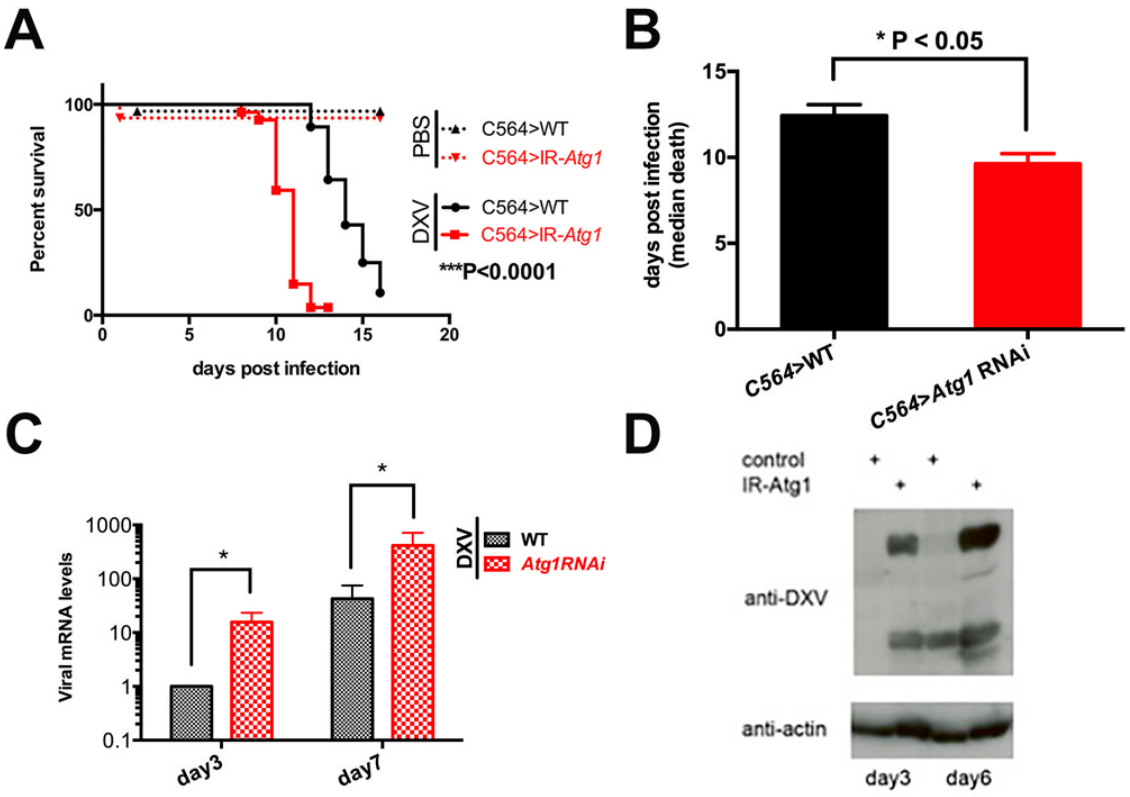

Figure 2.1: Silencing of *Atg1* renders flies more susceptible to DXV.
(A) Survival curves of wildtype and *Atg1* RNAi flies injected with PBS (dotted lines, $n > 90$ flies) or DXV (solid lines, $n > 90$ flies). Wildtype and *Atg1* RNAi lines are represented in black and red, respectively. *C564*-Gal4 is used for gene silencing in multiple tissues including fat body, hemocytes.. $^{***}P < 0.001$, (log-rank analysis). (B) Medial survival of WT and *Atg1* RNAi flies. n=3. (C) Quantitative PCR of viral RNAs in wildtype and *Atg1* RNAi flies. (D) Representative western blot of viral proteins in both wildtype and *Atg1* RNAi flies at day 3 and day 6 post infection. Proteins are extracted out of a pool of three flies. Student's t-test are used for statistical analysis in (B) and (D). All experiments were repeated at least three times.

To identify whether a particular tissue is important for this *Atg1*-dependent antiviral response, *Atg1* was silenced specifically in the hemocytes or fat body or central nervous system (CNS) using tissue specific Gal4 drivers (Georgel et al., 2001; Luo et al., 1994; Sinenko and Mathey-Prevot, 2004). Silencing of *Atg1* in the fat body results in an increased susceptibility against DXV. In contrast, silencing of *Atg1* in the hemocytes or CNS does not change fly survival. These results indicate that *Atg1* is necessary in the fat body, but not in the hemocytes or CNS for this antiviral immune response (**Figure 2.2 A-C**). To further identify the role of fat body in this *Atg1*-dependent response, adult fat tissues were dissected out for immunostaining of the virus. Our result shows that a higher level of viral proteins were detected in the fat body of *Atg1* RNAi flies compared to wildtype (**Figure 2.2 D**). The virus particles were quantified based on the fluorescence intensities. Our result shows ~ 2 fold more viral particles in the *Atg1* RNAi flies compare to wildtype (**Figure 2.2 E**).

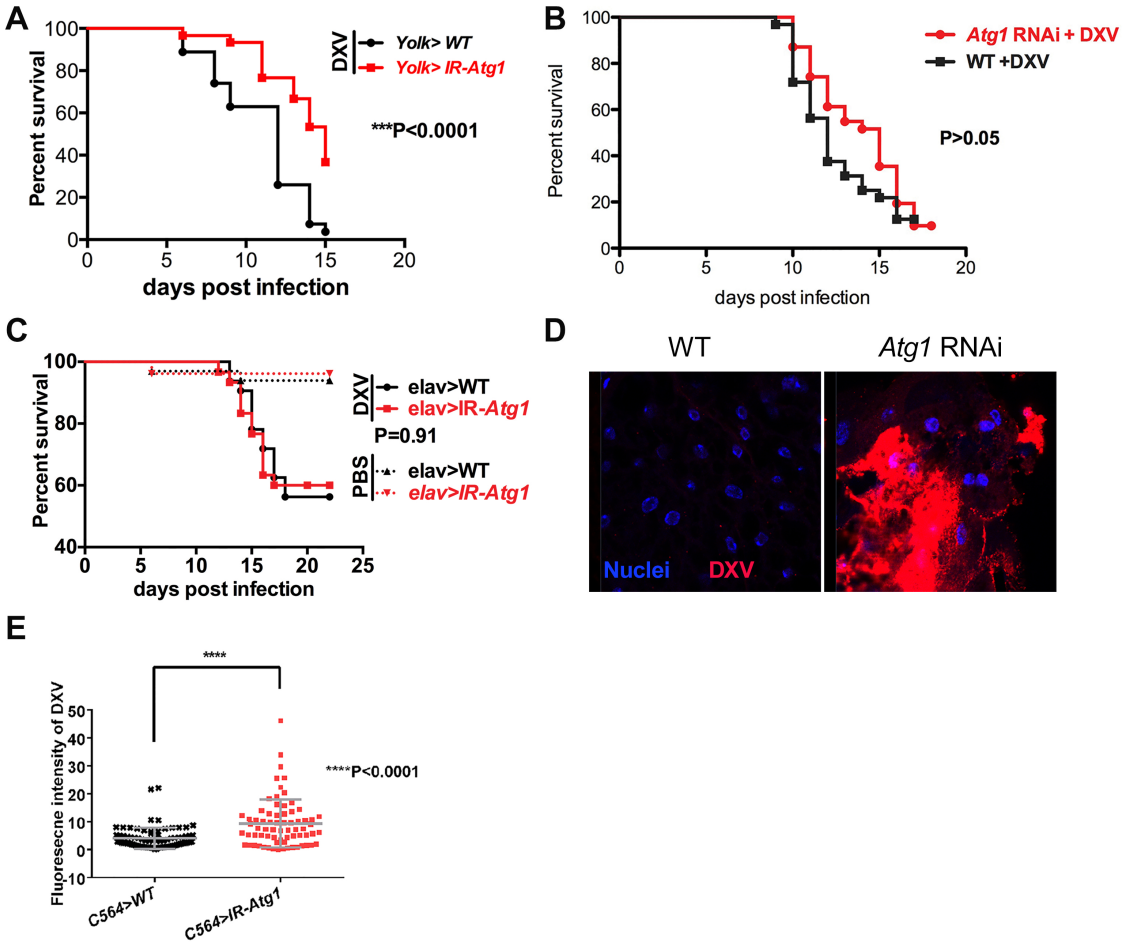

Figure 2.2: Fat body is the tissue important for the *Atg1*-dependent immune response. (A) *Atg1* was silenced in the fat body by driving the expression of IR-*Atg1* fragment using *Yolk*-Gal4 in female flies. (B) *Atg1* was silenced in the hemocytes, the cellular immune cells, by *hml*Δ-Gal4. (C) *Atg1* was silenced in the central nervous system by IR-*Atg1* fragment driven by *Elav*-Gal4. All experiments were repeated at least three times. $n > 90$ flies. Log-rank tests were used for survival analysis. (D) Confocal imaging of viral proteins in the adult fat body. Nuclei are stained with DAPI (blue). DXV is immunostained with anti-DXV primary antibody that was probed by Alexa-594 secondary antibody (red). (E) Quantification of viral proteins in adult fat body. Viral proteins levels are determined by fluorescence intensity using ImageJ software. $n > 100$ cells are examined per genotype. Student's t-test was used for statistical significance.

To further characterize the tropism of DXV in wildtype and *Atg1* RNAi flies, flies of both genotypes were infected with DXV and then were dissected into different components (head, thorax, gut, ovary, abdominal wall) at 4 and 6 days post infection. These tissues were examined for viral protein levels by Western blot. Among the five different components, abdominal wall, to which most fat body tissue attaches, shows the most viral proteins. There is also a significantly higher load of virus in the *Atg1* RNAi flies compared to wildtype (**Figure 2.3**). These data all suggest that fat body is important for the *Atg1*-dependent antiviral response against DXV.

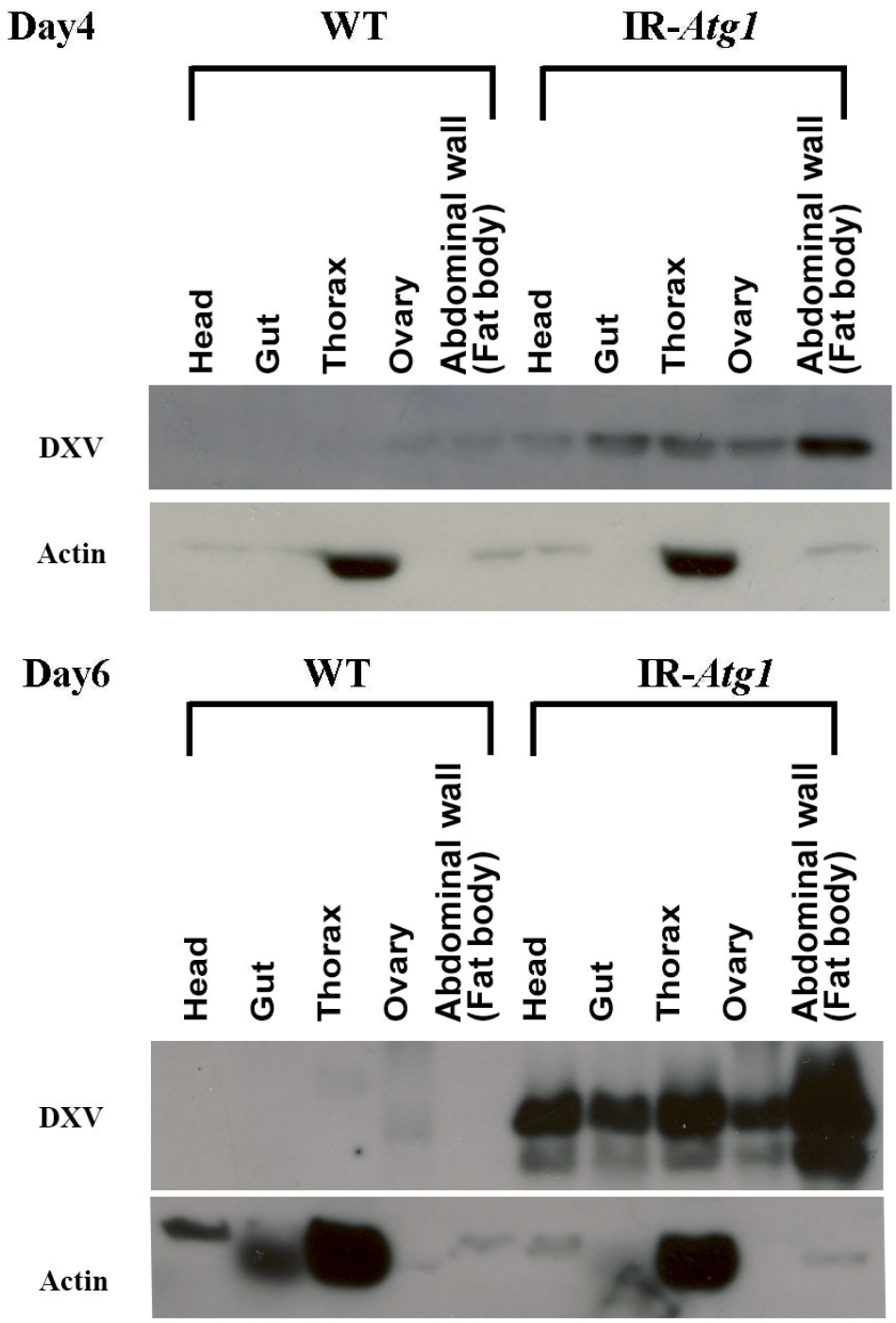

Figure 2.3: Western blots of DXV viral proteins in the dissected tissues of adult flies. WT and *IR-Atg1* flies were sacrificed, dissected into different components at day 4 and day 6 post DXV infection, respectively. Total protein from each component was extracted and western blots were performed by polyclonal antibody against DXV. In all components, a higher load of viral protein was observed in the *IR-Atg1* flies compared to wildtype. Six flies were pooled for one experiment. This experiments has been done for three times.

To test whether this protective role of *Atg1* is specific to DXV, we also infected the flies with *Drosophila* C virus or Cricket Paralysis virus (Jousset et al., 1977; Reinganum, 1975), both of which are single stranded RNA viruses. Reduced levels of *Atg1* do not render flies more susceptible to either virus (**Figure 2.4 A-B**). This indicates the Atg1-dependent protective effect is not a general antiviral mechanism but rather is specific to DXV.

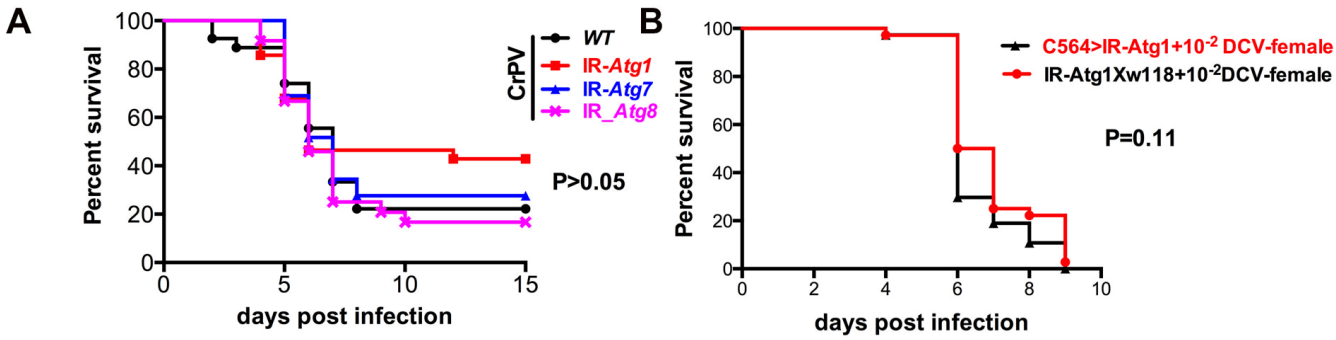

Figure 2.4: *Atg* genes are not important for the host response against CrPV and DCV. (A) Survival analyses for adult flies with *Atg1, Atg7, Atg8* silenced upon infection with Cricket Paralysis Virus (CrPV). $n > 90$. (B) Silencing of *Atg1* does not result in a survival phenotype of the flies infected with *Drosophila* C virus (DCV). $n > 90$. Log-rank statistics are used. There is no statistical difference between these lines.

2.1.2 Autophagy does not appear to be specifically activated by DXV in both larval hemocytes and adult fat body

In order to examine whether autophagy plays a role in the immune response against DXV, other than *Atg1*, we also examined other core autophagy genes, such as *Atg7* and *Atg8*. *Atg7* is a ubiquitin ligase that functions in the *Atg7-Atg5-Atg12* conjugation system. The *Atg7* null mutant shows a defect in starvation-induced autophagy in the larval fat body (Juhász et al., 2007). Upon infection with DXV, *Atg7* null mutants are not susceptible to DXV compared to wildtype (**Figure 2.5 A**). We also examined another critical *Atg* gene *Atg8*. *Atg8* is a small protein that is lipidated upon autophagy induction and thus localizes to the surface of autophagosomes. *Atg8* is not only essential for autophagy but also serves as a marker for autophagy induction when lipidated (Scott et al., 2004). When *Atg8* is silenced in the fat body, the flies only result in a slightly increased fly susceptibility (**Figure 2.5 B**). This indicates that *Atg1*, but not other core autophagy genes are important for the immune response against DXV.

If autophagy is actively playing a role during DXV infection, cellular markers for autophagy induction should be apparent in DXV infected cells. When GFP-*Atg8* transgene is expressed in the fat body, under normal condition, *Atg8* is evenly distributed in the cytoplasm (Juhász et al., 2008; Scott et al., 2004). Upon induction of autophagy, GFP-*Atg8* will form puncta. Our results show that the number of autophagosomes does not significantly increase as infection progresses (**Figure 2.5 C**). Autophagy puncta also do not specifically colocalize with DXV in the fat body cells (**Figure 2.5 C**). Once the fat body cells are overwhelmingly infected with virus, there is an increase of GFP-*Atg8* puncta,

but no colocalization of the GFP-*Atg8* puncta with DXV was observed (**Figure 2.5 D**). Autophagy is responsive to multiple kinds of stresses, including starvation, heat, reactive oxidation species (Murrow and Debnath, 2013). The activation of autophagy during the late stage of infection may be due to cellular stress induced by active viral replication, and may not be a direct immune response specific against the virus. This speculation is confirmed in electron microscopy, when autophagosomes were only observed in heavily infected S2 cells. Specifically, at the late stage of infection, mitochondria was observed in autophagososomal-like structures (**Figure 2.10**).

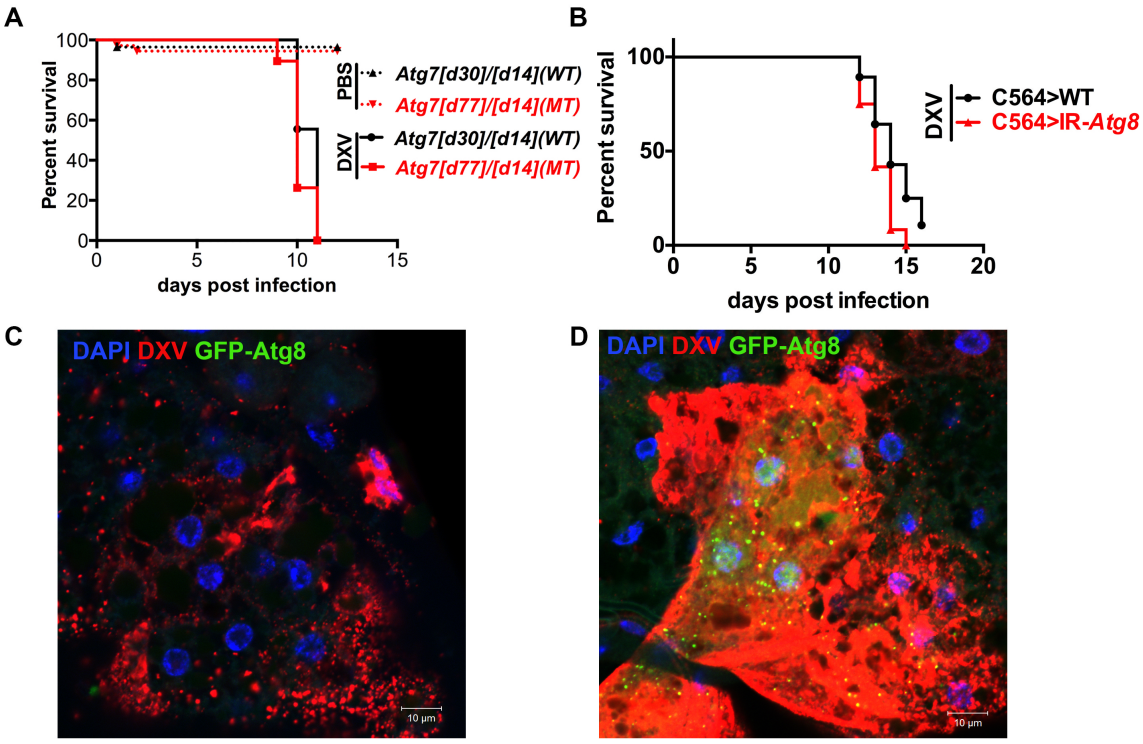

Figure 2.5: Autophagy does not appear to be activated directly by DXV. (A,B) Survival analysis of *Atg7* mutant (A) and *Atg8* RNAi lines (B). Wounding controls by injection of PBS are represented by dotted lines. The solid lines represent survival curves of wildtype and *Atg7* mutants, *Atg8* RNAi lines upon DXV infection. (C,D) GFP-*Atg8* puncta were examined in the fat body of *C564 > GFP-Atg8* flies. (C) In WT flies, at day 5 post infection, GFP-*Atg8* puncta does not seem to be induced by DXV infection. (D) In WT flies, at day 9 post infection, *Atg8* puncta are induced. The viral particles are shown in red. Nuclei are stained with DAPI (blue). *Atg8* puncta are represented by GFP (green) fluorescence. DXV is immunostained with anti-DXV primary antibody that was probed by Alexa-594 secondary antibody (red).

2.1.3 Autophagy is not induced in *ex vivo* hemocytes upon DXV infection

Hemocytes are the major immune cells responsible for cellular immune response. The plasmatocytes are professional phagocytes most similar to the mammalian monocyte/macrophage lineage and represent 95% of the total hemocyte populations (Williams, 2007). Phagoctytosis of various bacteria, such as E.Coli and Staphylococcus aureus, has been well characterized in plasmatocytes (Ulvila et al., 2011). Recently, plasmatocytes have also been shown critical for the antiviral immune responses (Costa et al., 2009; Honti et al., 2014; Shelly et al., 2009). Specifically, blocking phagocytosis prior to CrPV infection results in an increased fly sensitivity (Costa et al., 2009; Elrod-Erickson et al., 2000). *Ex vivo* larval hemocytes are also found important for the autophagic response against VSV (Shelly et al., 2009). Since DXV virus particles are taken up by larval and adult hemocytes rapidly after DXV exposure (within 30 min), we were interested in examining whether autophagy is induced in larval hemocytes upon DXV infection.

The larval hemocytes are bled out from *hml*Δ *>GFP-Atg8* transgenic flies followed by *ex vivo* infection with either live DXV virus or Texas red-tagged DXV (TR-DXV) particles. Due to a short life window for the *ex vivo* hemocytes, experiments can only be conducted within 3 hours after hemocytes isolation. *Ex vivo* hemocytes were first infected with the Texas Red fluorescent tagged virus (TR-DXV). The tagged virus particles appear in hemocytes within 30 minutes post infection. However, within a 3 hour time (checked at 30 mins, 1 hour, 2 hour, 3 hour), no autophagy puncta was observed (**Figure 2.6**). It is possible that replication intermediates, produced by active virus, are required for

autophagy induction. TR-DXV might be inactive after conjugation with Texas Red fluorescein. This could be the reason why GFP-Atg8 pucta was not observed. To evaluate whether live viruses can induce autophagy, GFP-Atg8 hemocytes were infected with live DXV particles. Within 3 hours, the number of GFP-Atg8 puncta were also not significantly increased (data not shown). Thus, we confirm that DXV, either live or not, does not induce autophagy in larval hemocytes, at least in the early stage of infection.

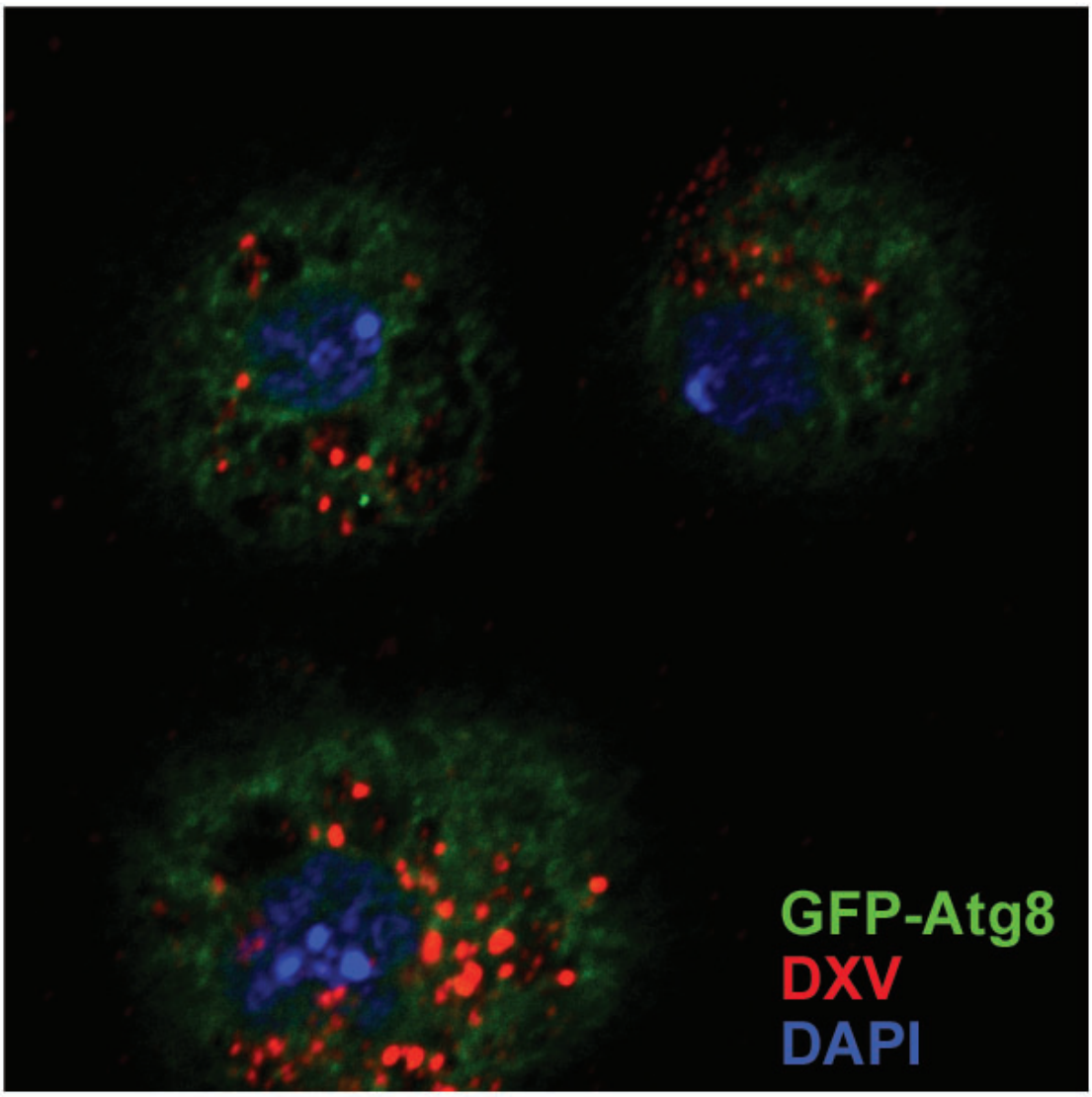

Figure 2.6: Autophagy is not induced in *ex vivo* hemocytes upon TS-DXV infection. A representative fluorescent microscopy picture showing bled-out larval hemocytes containing Texas-Red tagged DXV particles. Hemocytes from six larve were bled out into Schneider's Drosophila media for temporary culture followed by Texas-Red tagged DXV treatment for 2 hours. green, GFP-Atg8; red, TR-DXV; blue: DAPI. Experiments have been performed more than three times. n$>$ 300 cells for each condition.

2.1.4 Autophagy is not induced in *Drosophila* S2 cells

Drosophila S2 cells were examined by Transmission Electron Microscopes (TEM) following infection with live DXV virus at several doses and for different periods of time. Autophagosomes appear at a very low frequency in WT S2 cells (data not shown). Infection with DXV does not increase the number of autophagosomal structures. The virus appears in various vesicles, such as lysosome and some single membraned or multi-membraned vesicles (**Figure 2.7**, **Figure 2.8**). At the late stage of infection, DXV replicates massively, and forms array-like structures that occupies the cytoplasm (**Figure 2.9**). However, at the late stage of infection, one autophagosome structures with mitochondria within them was observed, indicating dysfunctional mitochondria are being degraded (**Figure 2.10**). This data is in agreement with our previous observation of GFP-Atg8 puncta only in heavily infected *Drosophila* adult fat cells (**Figure 2.5 D**).

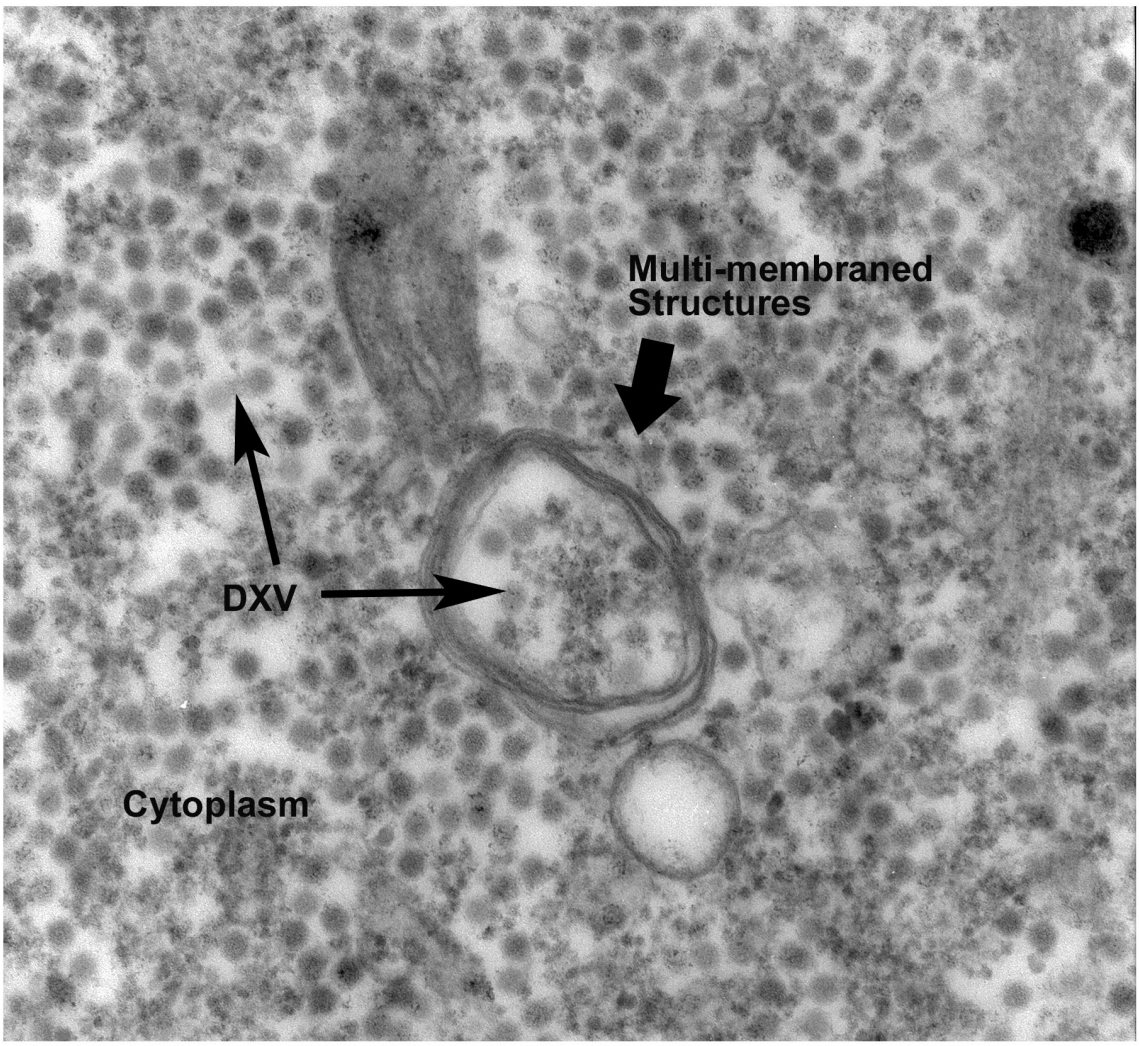

Figure 2.7: A representative picture showing DXV in multi-membraned vesicles by electron microscopy-I.
S2 cells were infected with 10^{-4} DXV for 24 hours followed by fixation, ultra-thin subsection and staining of the sample. Arrows indicate structures like DXV, multi-membraned vesicles. $>$ 60 cells were examined. The picture is taken at X 40,000 magnification.

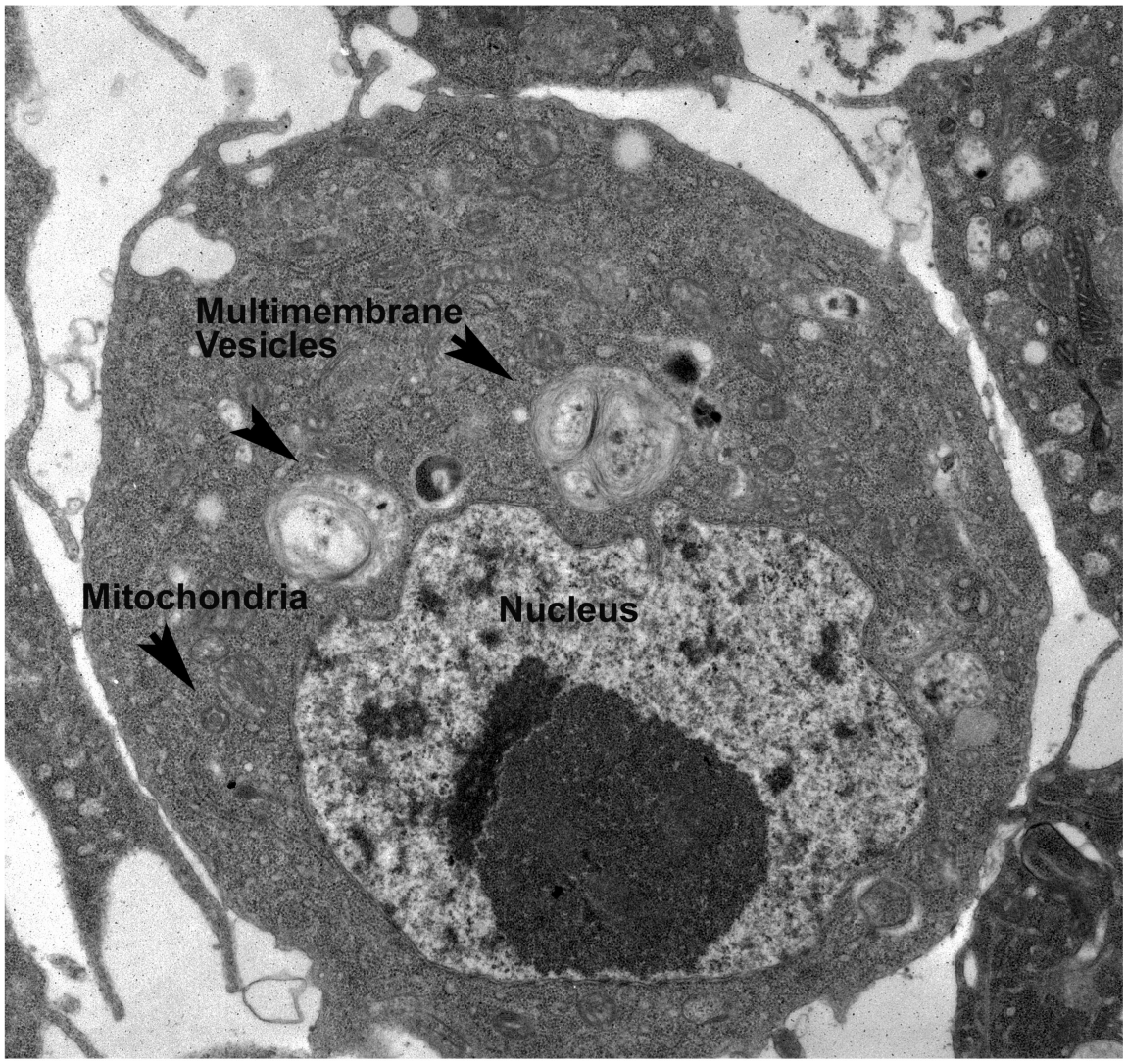

Figure 2.8: A representative picture howing DXV in multi-membraned vesicles by electron microscopy-II.
S2 cells were infected with 10^{-4} DXV for 24 hours followed by fixation, ultra-thin subsection and staining of the sample. Arrows indicate structures like nucleus, mitochondria, multi-membraned vesicles. The picture is taken at X 5,000 magnification.

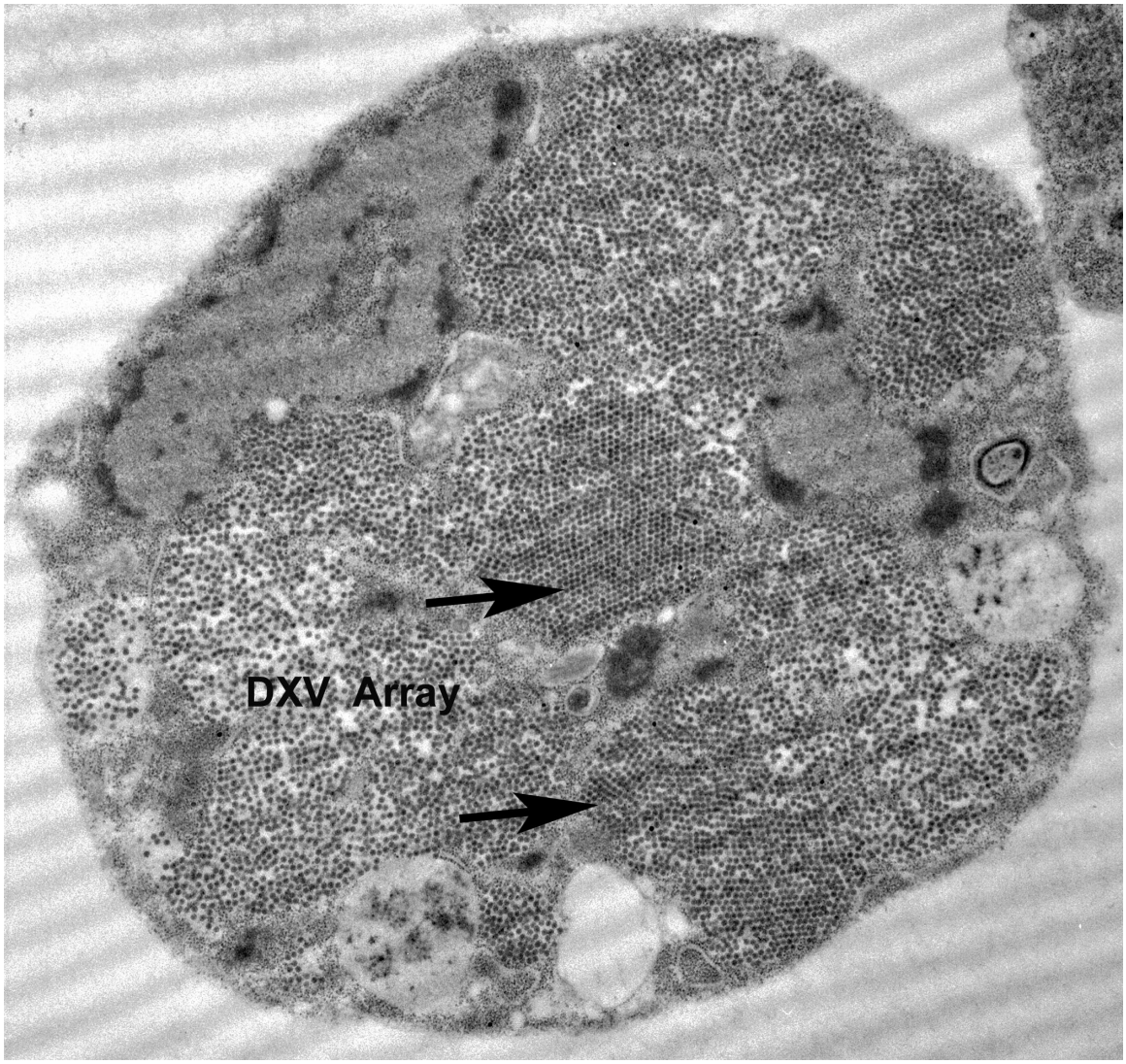

Figure 2.9: DXV replicates in S2 cells and forms array-like structures.
DXV replicates in the cytoplasm of S2 cells until they reach high concentrations that can occupy the cytoplasm. When isometric particles are crowded, they form arrays. The picture is taken at X 5,000 magnification.

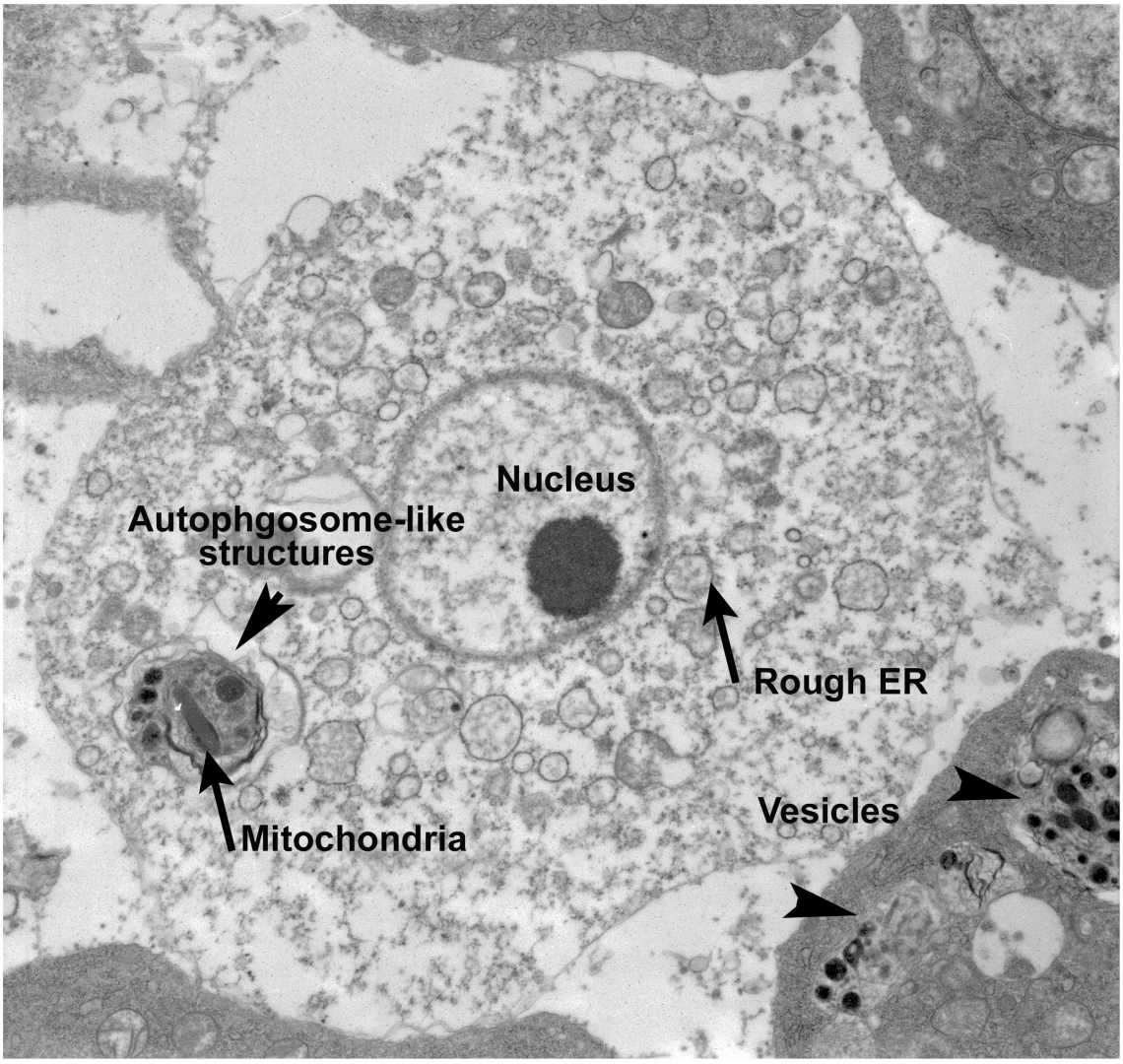

Figure 2.10: Autophagy is induced to eliminate mitochondria.
Mitochondria were digested in the autophagosomal-like structures. Arrows indicates specific structures such as mitochondria, autophagosomal-like structures, rough ER, and various vesicles. The picture is taken at X 5,000 magnification.

Interestingly, one EM picture shows contact of DXV viral particles with the endoplasmic reticulum (ER). Specifically, DXV seems to appear within the lumen of the ER (**Figure 2.11**, **Figure 2.12**). However, due to the limited number of observations of this contact, it is premature to conclude that the ER is involved in the DXV infection process.

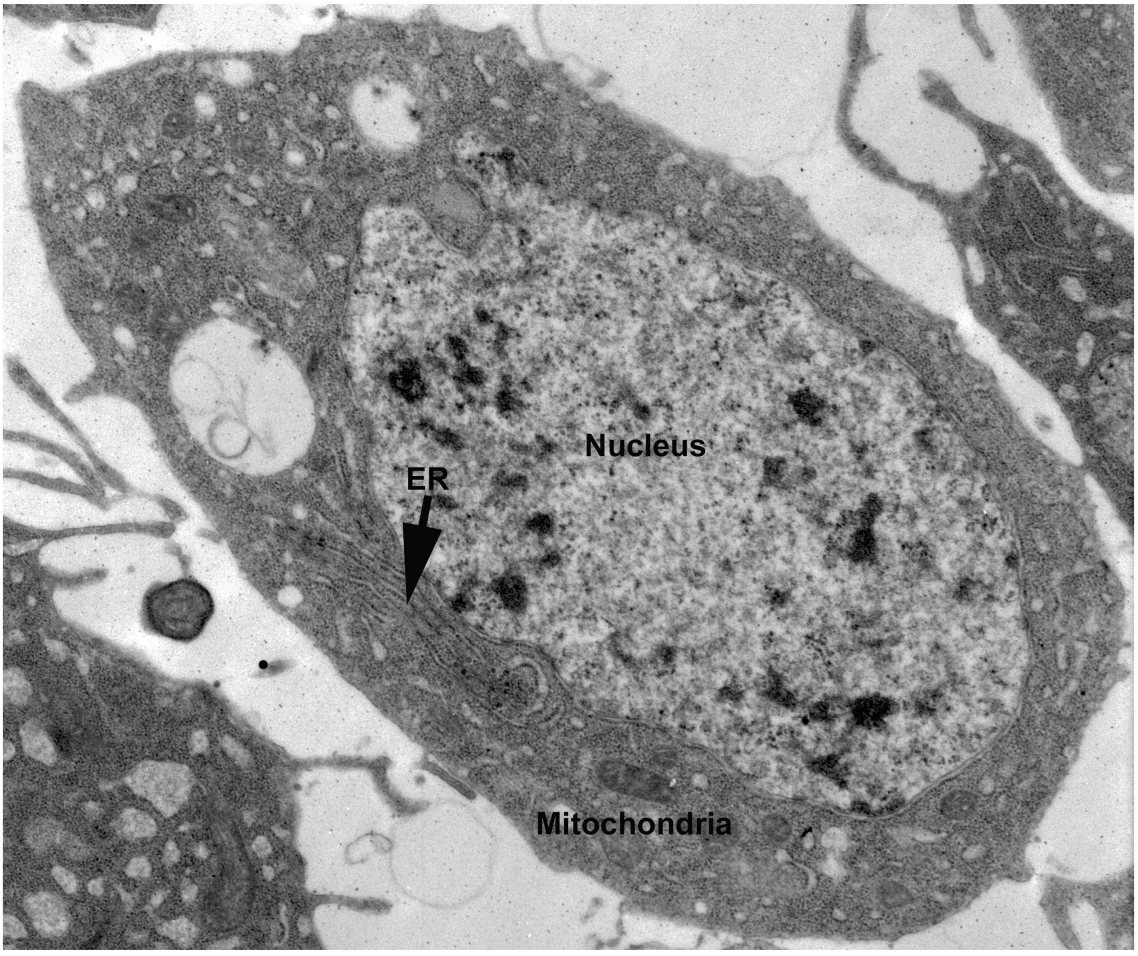

Figure 2.11: Electron Microscopy of an S2 cell upon DXV infection: Virus particles within ER-like structures.
Virus particles closely associate with ER-like structures. Arrows point to specific structures such as nucleus, ER, mitochondria. The picture is taken at X 5,000 magnification.

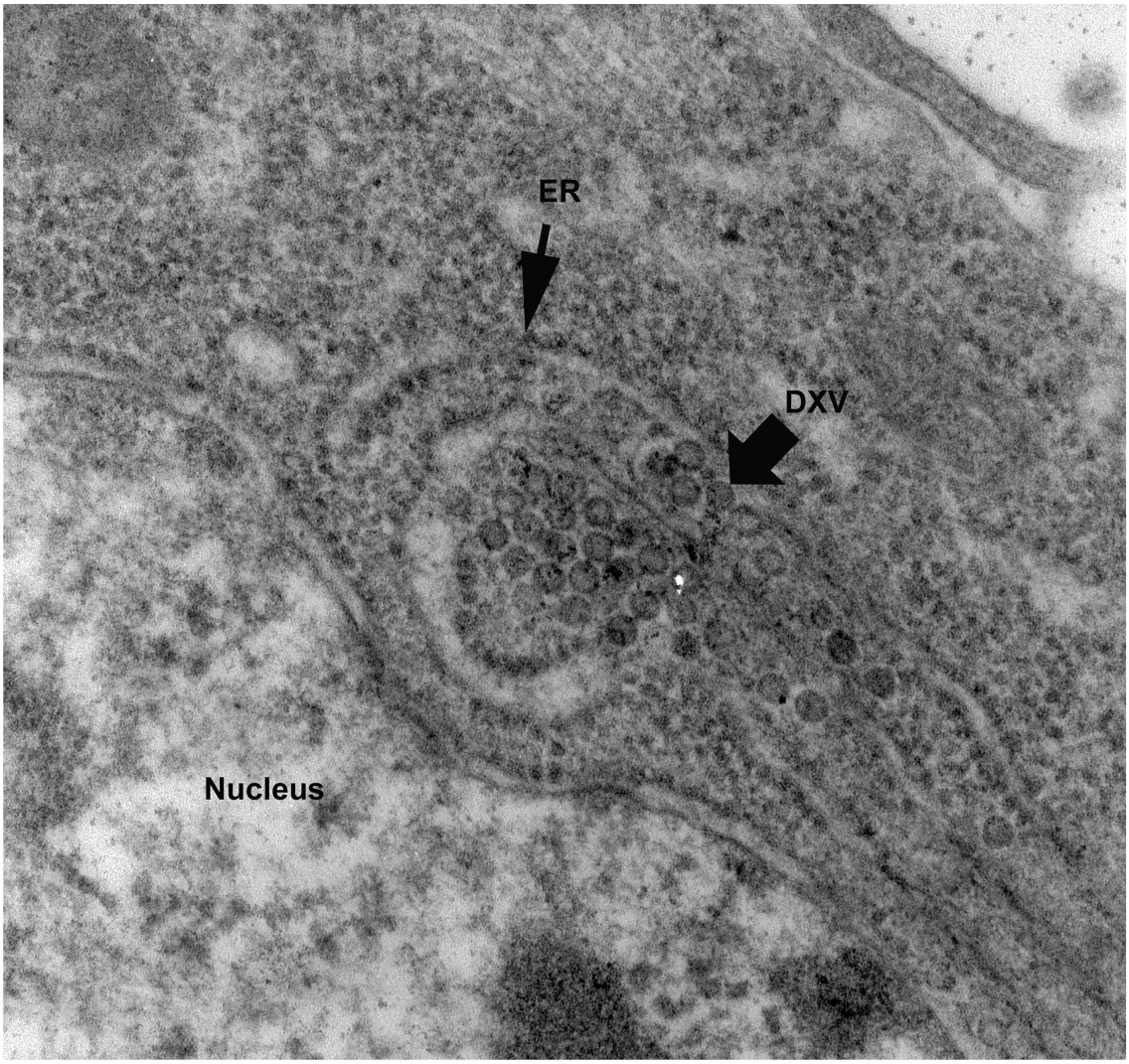

Figure 2.12: Magnified picture from Figure 2.11.
Arrows point to specific structures including nucleus, ER and DXV particles. The picture is taken at X 40,000. magnification.

2.1.5 Autophagy is not induced in GFP-Atg8 *Drosophila* S2R+ cells

To further test whether DXV induce autophagy in other cell lines, we infected GFP-Atg8-transfected *Drosophila* S2R+ cells (gift from Eric Baehrecke) with DXV while using starved cells as the positive control. After 19h of starvation, the number of Atg8 puncta significantly increased (**Figure 2.13 A, B, D**). However, GFP-Atg8 puncta are not induced in the DXV-infected cells compared to WT untreated cells (**Figure 2.13 A, C, D**). Overall, data from larval hemocytes, adult fat body, S2 cells and S2R+ cells all indicate that autophagy is not directly induced by DXV.

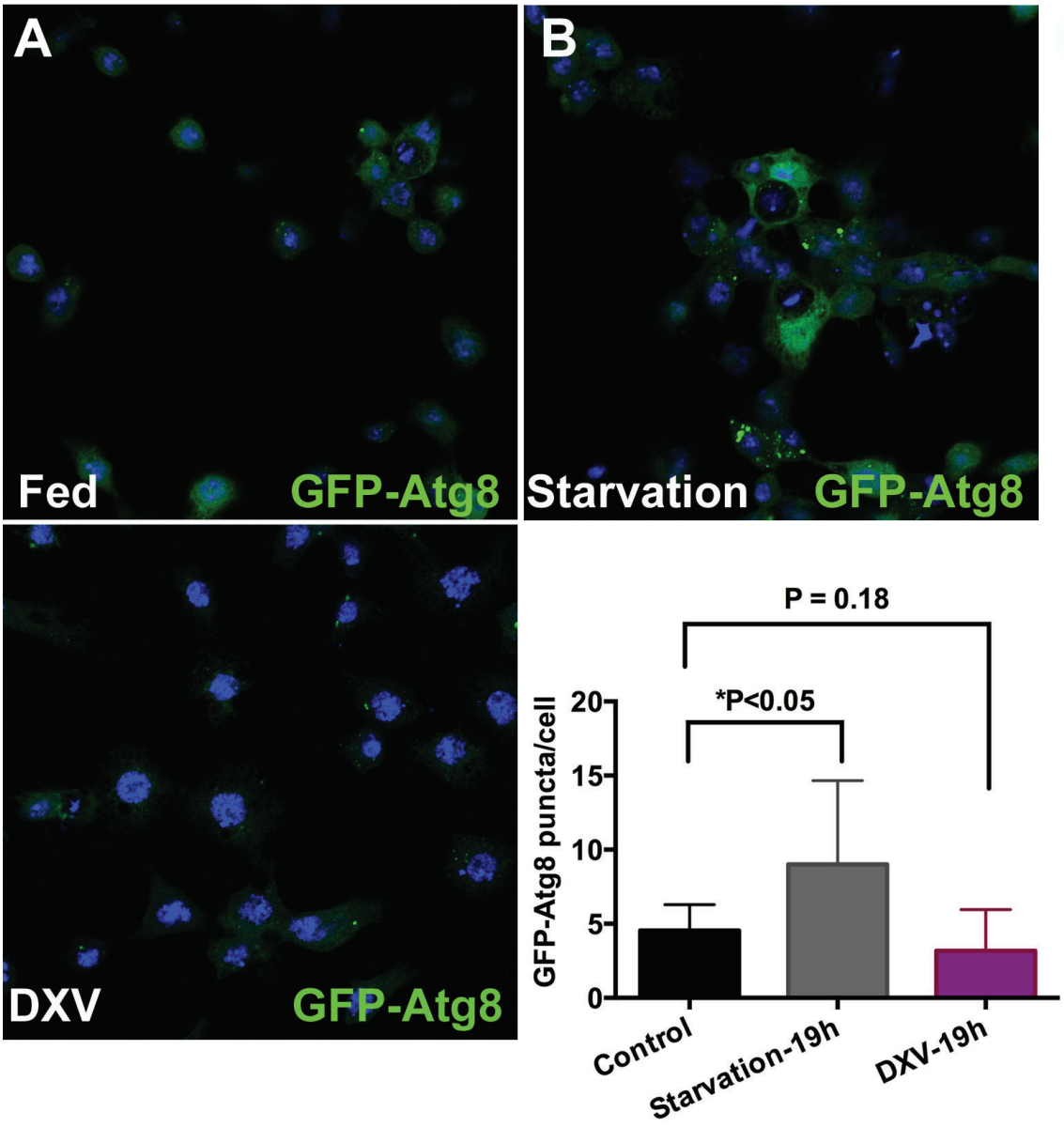

Figure 2.13: DXV does not induce autophagosome formation in S2R+ cells. GFP-Atg8 S2R+ cells are either fed (A), starved for 19 hours (B) or treated with DXV while fed (C) for 19 hours. (D) Two-tailed Student's tests were performed to test the statistical significance between groups. green: GFP-Atg8; blue: DAPI. n $>$ 250 cells for each condition.

2.1.6 The antiviral function of Atg1 is not through regulating RNA interference pathway upon DXV infection

RNA interference was previously shown to be important for the immune response against DXV (Zambon et al., 2005). In S2 cells following DXV infection, reducing the level of *Ago2*, a major component of the RNAi pathway, results in an increase level of DXV virus (Zambon et al., 2005). Silencing of *Ago2* specifically in the adult fat body also increases the fly susceptibility to DXV infection and an increased viral protein levels is also observed (**Figure 2.14**). A recent study suggests that a select autophagy can regulate the miRNA pathway by degrading Dicer and Ago2 (Gibbings et al., 2012). We were interested in determining whether the autophagy pathway can regulate the RNAi pathway upon DXV infection. By injecting *in vitro* synthesized viral dsRNA in adult flies prior to DXV infection, we observed an increased fly resistance to DXV infection compared to flies pre-injected with PBS (**Figure 2.15 A**). A decreased load of virus was also observed in the dsRNA-injected flies compared to PBS-injected flies (**Figure 2.15 B**). This indicates that viral dsRNA can act as a primer to protect DXV infection. However, *c564>IR-Atg1* flies pre-injected with dsRNA are also more resistant to DXV compared to the flies pre-injected with PBS, indicating that loss of *Atg1* does not render the RNAi pathway ineffective in fighting against DXV (**Figure 2.15 B**).

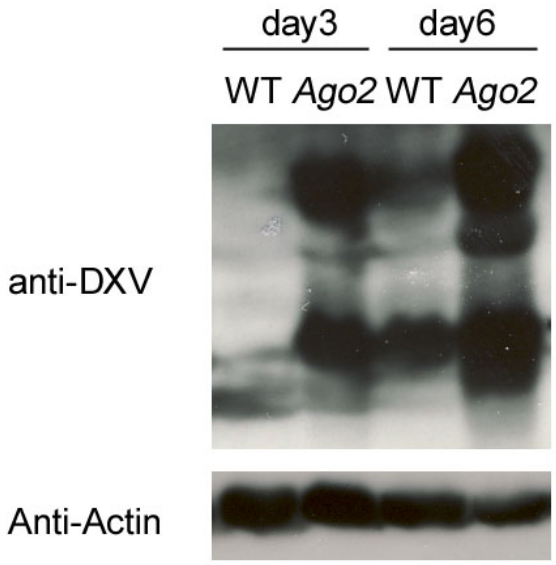

Figure 2.14: Ago2 is important for antiviral response against DXV.
IR-Ago2 flies accumulated more DXV viral proteins at day 3 and day 6 post infection. *Ago2* is silenced by *C564-Gal4* driver in the adult fat body. Western blot of viral proteins were performed on samples collected at day 3, day 6 post infection. β-actin is the loading control. Experiments are performed three times.

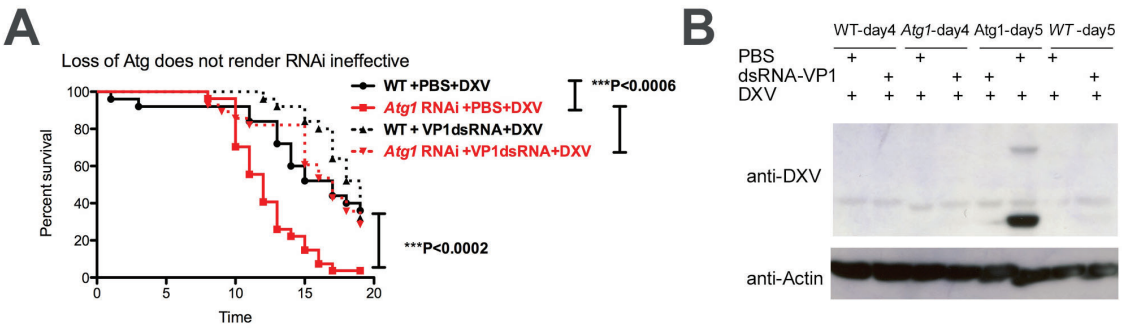

Figure 2.15: Loss of autophagy does not render the RNAi pathway ineffective against DXV .
(A) Survival curves of WT (black) and *Atg1*-RNAi flies (red) pre-injected with DXV dsRNA (dotted lines, $n > 90$ flies) or PBS (solid lines, $n > 90$ flies) prior to DXV infection. Log rank analyses were used to test statistical significance. (B) A representative western blot of viral proteins in flies in the above-mentioned conditions at day 4 and day 5 post infection. Three flies were pooled for protein extraction.

2.2 Materials and methods

2.2.1 Fly stocks.

Flies were maintained on Standard Bloomington Stock Center medium at $25\,^{\circ}\mathrm{C}$. All experiments were performed with five to seven day old female flies. RNAi flies were obtained from the Harvard TRiP Stock Center. The *Atg7* mutants were kindly provided by Dr. Tom Neufeld from University of Minnesota (Juhász et al., 2007).

2.2.2 Cell lines.

S2 cells were cultured in the Schneider's *Drosophila* Medium with 10% FBS and 1xPenicillin/Streptomycin at $25\,^{\circ}\mathrm{C}$ (Life Technologies). The *Drosophila* S2R+ cells with GFP-Atg8 stable-transfected were kindly provided by Dr. Eric Baehrecke. The cells were cultured in Schneider's Medium with 800 μg/mL G418, 10% FBS, 1X GlutaMAX and 1X Penicillin/Streptomycin (Gibco).

2.2.3 Virus infections.

Five to seven days old female flies were used for DXV infection. DXV was aliquoted and stored at $-80\,^{\circ}\mathrm{C}$. Before injection, flies were anesthetized with CO_2 followed by an injection of 27nl of DXV (10^{-5}) using individually calibrated pulled glass needles attached to a Nano injector II (Drummond Scientific). Flies were always injected in the abdomen, close to the junction with the thorax and just ventral to the junction between the ventral and dorsal cuticles. Flies were never anesthetized for longer than 10 min.

After each injection, all flies were transferred to a new vial and maintained at $25\,^{\circ}\mathrm{C}$.

2.2.4 Survival analyses.

After infection, flies were kept in vials at $25\,^{\circ}\mathrm{C}$ and transferred to a new vial every day. Flies were counted every day post infection. Log-rank survival analyses was used for statistical analysis (Prism, Graphpad).

2.2.5 RT-PCR.

Flies were challenged as described above and incubated at $25\,^{\circ}\mathrm{C}$ for the indicated time points. At a given time, triplicates of ten flies were anesthetized, placed in 1.5ml tubes. Total RNA was extracted using the standard RNeasy Mini Kit (Qiagen). Quantitative-PCR was carried out with a Applied Biosystems 7300 Real-Time PCR Machine using Maxima SYBR Green qPCR Master Mixes (Thermo Scientific) as directed by the manufacturer. The following primers below were used. Relative RNA quantities were determined with respect to *Drosophila* ribosomal protein *Rp49*, and all levels were normalized with respect to the zero time point for media injection: *VP1* (forward primer: TCAAGGCATTCGATCCCT), (reverse primer: GGCTAGCCTCTACGGCTT); *Rp49* (forward primer: GCAAGCCCAAGGGTATCGA), (reverse primer: TAACCGATGTTGGGCATCAG).

2.2.6 Protein extraction and Western blot.

Total protein was isolated from adult flies harvested and protein were denatured after extraction from a pool of three flies at $100\,^{\circ}\mathrm{C}$ for 5 minutes in Laemmli sample buffer

containing 62.5 mM Tris, pH 6.8, 2% SDS, 25% glycerol, 0.01% bromophenol blue, and 5% β-mercaptoethanol. The lysates were centrifuged and the supernatant was used for western blotting. Samples were subjected to SDS-polyacrylamide gel electrophoresis and resolved at 150 V over 1.5 hours. Proteins were transferred to a PVDF membrane (Thermo Scientific) in transfer buffer containing 25 mM Tris, pH 8.3, 192 mM glycine, 0.01% SDS, and 15% methanol using a Bio-Rad Trans-blot SD semidry transfer cell to which 70V were applied for 60 minutes. Membranes were blocked in 4% nonfat dry milk in PBS at room temperature for over 2 hours. Membranes were exposed to antibodies that recognized DXV (Zambon et al., 2005) . Equivalent protein loading between the samples was verified by reprobing membranes for β-actin (Santa Cruz Biotechnology). Primary antibodies were used at 1:5,000 to 1:10,000 dilutions in 5% BSA or nonfat milk for overnight at $4\,^{\circ}\mathrm{C}$. Membranes were exposed to anti-rabbit, anti-mouse, or anti-goat secondary antibodies conjugated with horseradish peroxidase (HRP) at a dilution of 1:10,000 in 4% nonfat milk PBS for 1 hour at room temperature. Signals were detected with a chemiluminescence detection system (Amersham ECL Western Blotting System, GE Healthcare) and exposure to x-ray film.

2.2.7 Staining and confocal imaging.

For confocal imaging, adult fat bodies were dissected in PBS and fixed in 4 % paraformaldehyde and 0.01% Tween PBS at $4\,^{\circ}\mathrm{C}$ overnight. For viral particle staining, fixed fat body tissues were blocked in PBST (3 % BSA, 0.1%Tween) for 2 hours, followed by anti-DXV antibody incubation overnight with a dilution at 1:500 at $4\,^{\circ}\mathrm{C}$. Alexa-594

or Alexa-488 secondary antibody (Invitrogen) was used at 1:250 dilutions in buffer with 0.5% BSA and 0.1% Tween for an hour. After the PBS washes, the stained fat bodies were fixed with ProLong Gold Antifade Reagent (Invitrogen). More than 800 cells were examined from either wildtype or *Atg1* RNAi fat bodies.

Confocal fluorescent images were obtained by a Zeiss LSM700 confocal scan head mounted on a Zeiss Axiovert 200M. Images were analyzed by Zeiss software. The term colocalization refers to the coincidence of green and red fluorescence, as measured by the confocal microscope. Fluorescence intensities were quantified using ImageJ software (NIH).

2.2.8 Electron Microscopy

S2 cells were cultured in 12-well plates. Cells were harvested and centrifuged in an eppendorf tube. After the PBS washes, cell pellets were fixed with 2.5% glutaraldehyde in cacodylate buffer at RT for one hour. Cell pellets were post-fixed with 1% OsO_4 and 1.5% $K_3[Fe(CN)_6]$ for one hour at $4\,^{\circ}\mathrm{C}$. Followed by PBS washes, pellets were stained with 1% uranyl acetate for one hour. After a series of washes and dehydration, samples were embedded in spurr's resin.

Chapter 3: Transcriptome Profiling of WT and *Atg1* RNAi flies upon DXV infection

3.1 Introduction to RNA-seq

RNA sequencing (RNA-seq) is a technique used to sequence the total RNAs of within a biological sample to determine the primary sequences in the transcriptome and the relative abundance of each RNA.

Compared with traditional EST sequencing by Sanger technology, which only detects transcripts that are in relative high abundance, RNA-seq can detect the transcriptional RNAs at a higher resolution with unprecedented sensitivity and accuracy, including the rare transcripts that are in low abundance (Marguerat and Bähler, 2010; Wang et al., 2009; Wilhelm and Landry, 2009). In contrast to the other high-throughput technologies, such as microarrays, which rely on pre-constructed oligonucleotide libraries, RNA-seq displays an absolute advantage by offering a near-complete snapshot of a transcriptome including transcripts that haven not previously been identified (Ozsolak and Milos, 2011). The novel transcripts can be either newly-identified splice forms from a known gene or from novel genes. Due to a high sequencing depth (100-1,000 reads per base pair of a transcript), small RNAs such as micro RNAs, PIWI-interacting RNAs (piRNAs) small

nucleolar (snoRNAs) and small interfering (siRNAs) can also be identified.

Despite all the advantages, however, the analysis of RNA-sequencing data remains a challenge, specifically the reconstruction of the transcriptome. The sequence reads generated by the common sequencing platforms, such as Illumina, SoLid and 454, are very short, between 35-500bp (Metzker, 2010). These short sequence fragments needed to be assembled and mapped to the genome annotation before quantification. Although several assembler programs, including Velvet and ABYSS have proven powerful in assembling genomes, they are not sufficient for transcriptome assembly (Simpson et al., 2009; Zerbino and Birney, 2008). The underlying reasons are: (1) The DNA sequencing depth is the same across the whole genome. Yet, the sequencing depth of transcripts could be very different since transcripts have difference abundance. (2) The existence of overlapping genes, different isoforms, strand-specific genes, and repetitive sequences adds another level of complexity in mapping the transcriptome. To tackle these problems, a complete and accurate reference genome, longer sequencing fragments, or pair-end sequencing technology can be used to resolve the ambiguities.

3.1.1 Pipeline for RNA seq analysis

RNA-seq experiments in general comprise of three steps: generation of RNA seq data set, RNA seq data analysis and statistical modeling analysis. The flow chart of the pipeline is shown in **Figure 3.1**.

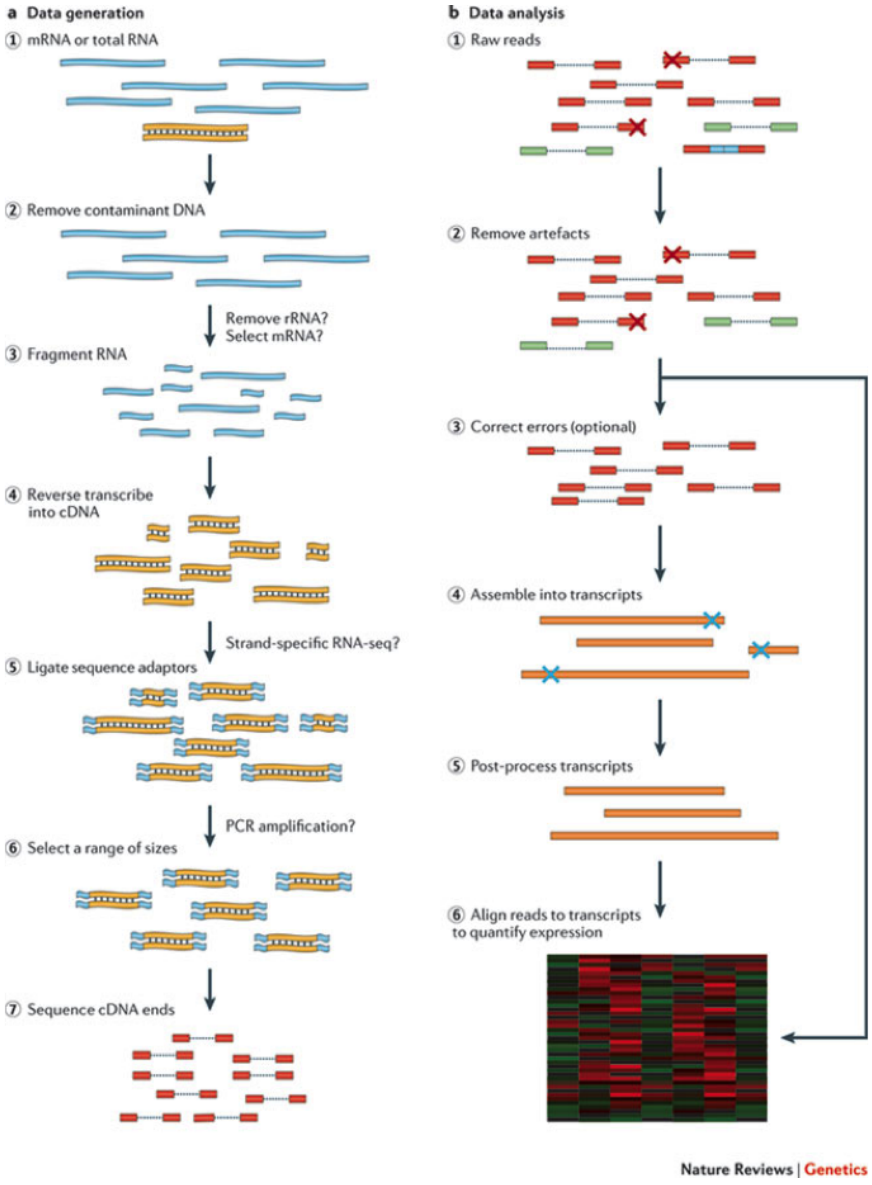

Figure 3.1: Diagram of RNA-seq analysis workflow .
Total RNAs are extracted and converted to a cDNA library. cDNAs are broken down into small fragments (200-300bp) before high throughput sequencing. The raw sequences will be either mapped to the reference genome or be assembled *de novo* into a transcriptome. The gene or transcript levels can be quantified based on how many sequences mapped to a particular gene or transcript (Martin and Wang, 2011).

3.1.1.1 Generation of RNA seq data set

Generating an RNA-sequencing data set comprises of three steps: RNA isolation, cDNA library construction and sequencing. Depending on the type of RNAs to be sequenced, the extraction procedure can vary. For example, for gene transcript sequencing, total mRNAs are extracted, followed by a poly-A tail enrichment to exclude the non-polyA transcripts. For small RNA sequencing, the RNA 3' adapter is specifically modified to target microRNAs and other small RNAs that have a 3' hydroxyl group resulting from enzymatic cleavage by Dicer or other RNA processing enzymes.

cDNA library construction is to convert RNAs to DNAs for sequencing. Due to the high representation of rRNA in a transcriptome, detection and assembly of rare transcripts could be affected. To avoid rRNA contamination, hybridization-based depletion methods can be used to eliminate the rRNAs (Chen and Duan, 2011; He et al., 2010). Another concern for library construction is whether PCR amplification should be involved. PCR amplification of the initial cDNA sample could result in a low sequencing coverage for transcripts that have a high GC-content (Kozarewa et al., 2009). This could further cause gaps in transcriptome assembly. To overcome this problem, amplification-free protocols have been developed (Kozarewa et al., 2009; Mamanova et al., 2010). One example is the single molecular sequencing technology, which does not require PCR-amplification (Sam et al., 2011). However, the sequencing rate is much higher compared to the PCR-dependent sequencing technology.

The final step is sequencing the cDNAs. To ensure a high-quality transcriptome assembly, there are several factors to consider: the length of the reads and a single-end or

pair-end protocol. Longer reads are generally more favorable for transcriptome assembly as less assembly events are needed to construct the contigs. To regions that have repetitive sequences or are at the junction sites between exons, longer reads are specifically useful. Paired-end strategy can also improve the accuracy for mapping and assembly (Rodrigue et al., 2010). However, the choice between these sequencing options largely depends on the purpose of the experiment and the budget. The longer reads and paired-end sequencing are generally more expensive. For experiments targeting for gene-level mRNA quantification, single end and shorter reads might be sufficient since distinction of various transcripts or discovery of novel transcripts are not the major concern.

3.1.1.2 RNA seq data analysis

cDNA sequencing data needs to be pre-processed to remove artifact reads such as sequencing adapters and low-complexity reads (Falgueras et al., 2010; Lassmann et al., 2009). Adapter sequences and low-complexity reads can result in misassembly of the transcriptome.

To ensure the quality of the sequencing data, quality score and k-mer (all the possible sub sequences (of length k)) frequency should be closely monitored. Low quality scores are usually associated with sequencing errors. The sequencing error rate can be inferred from the frequency of k-mers. Assuming there are no sequencing errors, a k-mer should occur multiple times as the same fragment is sequenced many times. When sequencing errors happen, there will be k-mers with very low frequencies. In order to correct the sequencing errors, the transcripts containing these low-frequency k-mers can

be removed, trimmed or corrected (Kelley et al., 2010; Miller et al., 2010). However, the side effect of removing these transcripts is eliminating the rare transcripts which also appear at low frequencies.

After trimming the data set, short sequences need to be assembled into transcriptomes. There are three strategies for transcriptome assembly: a reference-based strategy, a *de novo* strategy or a combined strategy. When there is a complete and accurate genome annotation, a reference-based method provides a reliable and accurate assembly. When no genome annotation is available, a *de novo* method is used to assemble transcripts by the overlapping sequences in the short reads. When there is an incomplete genome annotation, the combined strategy is more effective. For the sake of relevance to this research, we will only discuss the reference-based strategy.

There are three steps for a reference-based assembly. First, RNA-seq reads are aligned to a reference sequence genome using a splice-aware aligner, such as TopHat, SpliceMap, MapSplice and Blat (Au et al., 2010; Kent, 2002; Trapnell et al., 2009; Wang et al., 2010). Second, overlapping reads from each locus are clustered to build up a graph with all possible splice forms. Finally, real transcripts are resolved by eliminating the non-existent ones from the total possible transcripts. Cufflinks and Scripture are some of the programs using the reference-based strategy to assemble transcripts (Guttman et al., 2010; Trapnell et al., 2010). However, if the purpose of RNA-seq is to quantify the RNA expression on the gene level rather than on the transcript level, a splice-aware alignment by itself is sufficient.

After the sequencing reads are aligned to the reference genome, quantification of the transcripts or genes can be achieved by counting for each gene how many reads are

mapped to the reference genome. HT-seq is one of the programs using this strategy (Anders et al., 2014). Since the initial aim of the program is for gene expression quantification, the reads that map to multiple genes are not counted (Anders et al., 2014).

Recently, however, RNA-seq quantification algorithms that are alignment-free have been developed, such as Sailfish and RNA-skim (Patro et al., 2014; Zhang and Wang, 2014). This substantially decreases the amount of computing time while maintaining a comparable quantification accuracy. However, these programs can only be used to quantify the previously annotated RNA isoforms. For organisms that do not have a complete annotation, an alignment-based *de novo* strategy is required.

3.2 Differential expression analysis

RNA-seq technology enables the detailed identification of novel genes, gene isoforms, translocation events, nucleotide variations and post-transcriptional base modifications (Wang et al., 2009). However, one of the major goals of RNA-seq is to quantify differentially expressed genes. Such genes are usually selected based on the fold change of the gene expression levels and statistical significance (p value).

Since the expression signal of a gene is largely dependent on the sequencing depth and the expression levels of other transcripts, multiple statistical models and algorithms have been developed for normalization and differential expression (DE). Currently, most algorithms are based on Poisson or negative binomial distributions to model the gene count data (Auer et al., 2012; MD, 2012). Specifically, the most frequently used packages are: DESeq, PoissonSeq, edgeR, Cuffdiff, baySeq and limma (Anders and Huber, 2010;

Hardcastle and Kelly, 2010; Li et al., 2012a; Robinson et al., 2010; Smyth, 2004; Trapnell et al., 2013). These software packages mainly differ in (1) normalization methods; (2) statistical modeling of gene expression; and (3) the test for differential expression. Since this research only involves DE-seq and Limma packages, we will only review and compare these two.

3.2.1 Normalization

Due to the variability caused by RNA sample preparation, cDNA library preparation, sequencing run and nucleotide compositions, a normalization procedure is required for accurate comparisons between samples. One intuitive strategy is to divide each gene count by the total number of sequencing reads in the library, named per kilobase per million reads (RPKM) (Mortazavi et al., 2008). This method assumes that each gene count is independent of each other, which does not accurately represent the situation. Often a small fraction of genes can generate a large proportion of sequencing reads and a small expression change in these genes will affect the counts of lowly-expressed genes. This will skew the DE results (Bullard et al., 2010; Robinson and Oshlack, 2010). To consider the gene coverage differences, DESeq computes a scaling factor for a given sample by computing the median of the ratio, for each gene, of its read count over its geometric mean across all samples. It then uses the assumption that most genes are not DE and uses this median of ratios to obtain the scaling factor associated with this sample (Anders and Huber, 2010). The limma package uses quantile normalization to ensure that the counts across all samples have the same empirical distribution (Bolstad et al., 2003). An-

other normalization function termed voom, performs a LOWESS regression to estimate the mean-variance relation and transforms the read counts to the appropriate log form for linear modeling (Law et al., 2014).

3.2.2 Statistical modeling of gene expression

If each sequencing experiment of a biological sample is considered a random sampling event of a fixed group of genes, the distribution of a particular gene counts across all biological samples should conform to a Poisson distribution. Specifically, in the equation $P(x) = \frac{e^{-\lambda}\lambda^x}{x!}$, x represents the frequency of a certain read count and λ represents the expected read counts of that particular gene. An important feature of a Poisson distribution is that the variance equals the mean (λ). However, the variance of a particular gene's expression level across biological replicates is often larger than the gene expression mean. To combat this problem, DESeq uses negative binomial distribution for modeling the gene expression, where variance is equal to the Poisson estimate (λ) plus a second term representing the biological expression variability. The equation is shown as $v = \mu + \alpha\mu^2$ (Anders and Huber, 2010).

3.2.3 Test for differential expression

To test whether a gene is expressed differentially between two conditions, Fisher's exact test is used to calculate a *p*-value in the DESeq package. Limma packages, however,

uses a moderated t-statistic to compute *p*-values in which both the standard error and the degrees of freedom are modified (Smyth, 2004). The standard error is moderated across genes with a shrinkage factor, which effectively borrows information from all genes to improve the inference on any single gene. The degrees of freedom are also adjusted by a term that represents the a priori number of degrees of freedom for the model. Since there are a pool of genes to be tested, standard multiple hypothesis testing is used to control the false discovery rate (FDR), for example, by the Benjamini-Hochberg method (Benjamini, 1995).

3.3 Exploratory studies

Since the RNA-seq experiment generates a large amount of gene expression profiles from different samples, exploratory studies usually provide big pictures with critical information in terms of expression patterns within and among the biological samples. Some of the useful diagnostic and visualization tools are scatter plots, various clustering plots and principle component analysis (PCA) plots.

3.3.1 Scatter plot

A scatter plot is a direct visualization tools. In a scatter plot, usually a sample or an mRNA subject is represented by a dot on a 2D/3D coordinate systems. Some typical coordinates would be gene expression levels, *p*-values, time, drug load or other variables. Since such a plot usually does not accommodate many coordinates, some data feature

might not be best presented using this method.

3.3.2 Clustering and visualization

Clustering is a approach based on the similarity between samples. By building up the clustering tree, one can easily observe the similarity between different samples. One intuitive strategy is to measure the distance between two samples. The two groups that have the closest distance can be grouped together. As these distances are calculated between multiple pairs of samples, a clustering map can be constructed. The distance between two RNA-seq samples can be determined using this equation: $D12 = \sqrt{\sum_{i=1}^{n}(x_{1i} - x_{2i})^2}$. D12 represents the distance between two samples; x_{1i} and x_{2i} represent the ith gene in each sample, respectively.

Another measurement for similarity is the correlation coefficient. The bigger the number is, the more the two samples are correlated. This number can either be positive or negative, whereas 0 indicates no correlation. The correlation coefficient is calculated as below: $r_{xy} = \frac{n\sum_{j=1}^{n} xy - \sum_{j=1}^{n} x \sum_{j=1}^{n} y}{\sqrt{[n\sum_{j=1}^{n} x^2 - (\sum_{j=1}^{n} x)^2][n\sum_{j=1}^{n} y^2 - (\sum_{j=1}^{n} y)^2]}}$

Here r_{xy} is the correlation between genes expression profiles of samples x and y; x_{1i} and x_{2i} represent the gene counts of the ith gene in the samples x and y, respectively.

The visualization of the clustering can be represented as a heatmap, where the samples are grouped based on the similarities of their gene expression profiles. The levels of

expression counts per gene are colored in a gradient.

3.3.3 Principle component analysis and its visualization

Principle component analysis is a powerful approach to present the samples in a scatter plot format. The traditional scatter plot is supposed to contain all the variables such that an n-dimensional coordinates system (n variables) needs to be built up. While it is not possible to visualize a n-dimensional coordinates system, PCA plots can be generated instead to identify the most important principle components and projects the samples into a newly-constructed coordinate system with such principle components. The first principle component determines the most important factor that affects the gene expression profile among the samples. The second principle component is the next important factor. The other components have decreasing weights in affecting the expression profile and the least principle component can be regarded as noise. PCA is a great tool to identify the most critical factors in differentiating transcriptomes by eliminating the noise, and it can also create an accurate representation of the similarities between samples.

3.4 Results

In order to identify the genes that are important for the antiviral response against *Drosophila* X virus (DXV), we were interested to analyze the transcriptomes of the wild-type flies that are either uninfected or infected. In addition, we were interested in exploring the novel role of *Atg1* in response to DXV since classical autophagy does not seem to

Time / Genotype	uninf	day3	day5	day7
WT	1	2	3	4
Atg1 RNAi	5	6	7	8

Figure 3.2: Experimental design of the RNA seq experiment.
Wildtype and *Atg1* RNAi flies were either uninfected or infected with DXV and sacrificed for total RNA isolation at different time points. For each of the eight conditions, three biological replicates were used. Each replicate contains mRNAs from a pool of six flies.

be involved.

Atg1 is the only kinase among all of the *Atg* genes. It is possible that *Atg1* protects flies against DXV infection by phosphorylating substrates other than classical autophagy proteins. In order to identify pathways affected in an *Atg1*-dependent manner, we used RNA-Seq to analyze the transcriptomes of wildtype and *Atg1* RNAi flies without infection or with infection at day 3, day 5, and day 7 (**Figure 3.2**). The time points were chosen to take into account the kinetics of virus replication such that the relationship between the differentially expressed genes and the viral load can be determined. Three biological replicates were performed for each of the eight conditions such that the results could be presented with statistical power.

Following data pre-processing, data quality is verified by FASTQC (Andrews S.,2010). The short reads are further mapped to the *Drosophila* reference genome using Tophat (Trapnell et al., 2009). The mapped reads are quantified using HT-seq (Anders et al., 2014). Differential expression analysis was performed using the Limma and DEseq packages.

3.4.1 Statistics diagnostics

Following HT-seq count, a data matrix containing total transcriptome gene counts for 24 samples were generated. In order to minimize the variability due to the difference of library size, quantile normalization was applied to the data set. Boxplots of counts across samples in each data set, both before and after normalization should be examined to ensure the effectiveness of normalization, which should result in a stabilization of read count distributions across replicates (Dillies et al., 2013). The counts for each gene in 24 samples are transformed to its log forms. The $log_2(counts + 1)$ of each gene is presented in the box plots (**Figure 3.3A-B**). Before normalization, there is slight variability of the average $log_2(counts + 1)$ between samples. The average $log_2(counts + 1)$ number is $\sim$ 6.2 for all the samples (**Figure 3.3A**). After normalization, the distribution of the $log_2(counts + 1)$ is stabilized and the average $log_2(counts + 1)$ is even for each sample (**Figure 3.3B**).

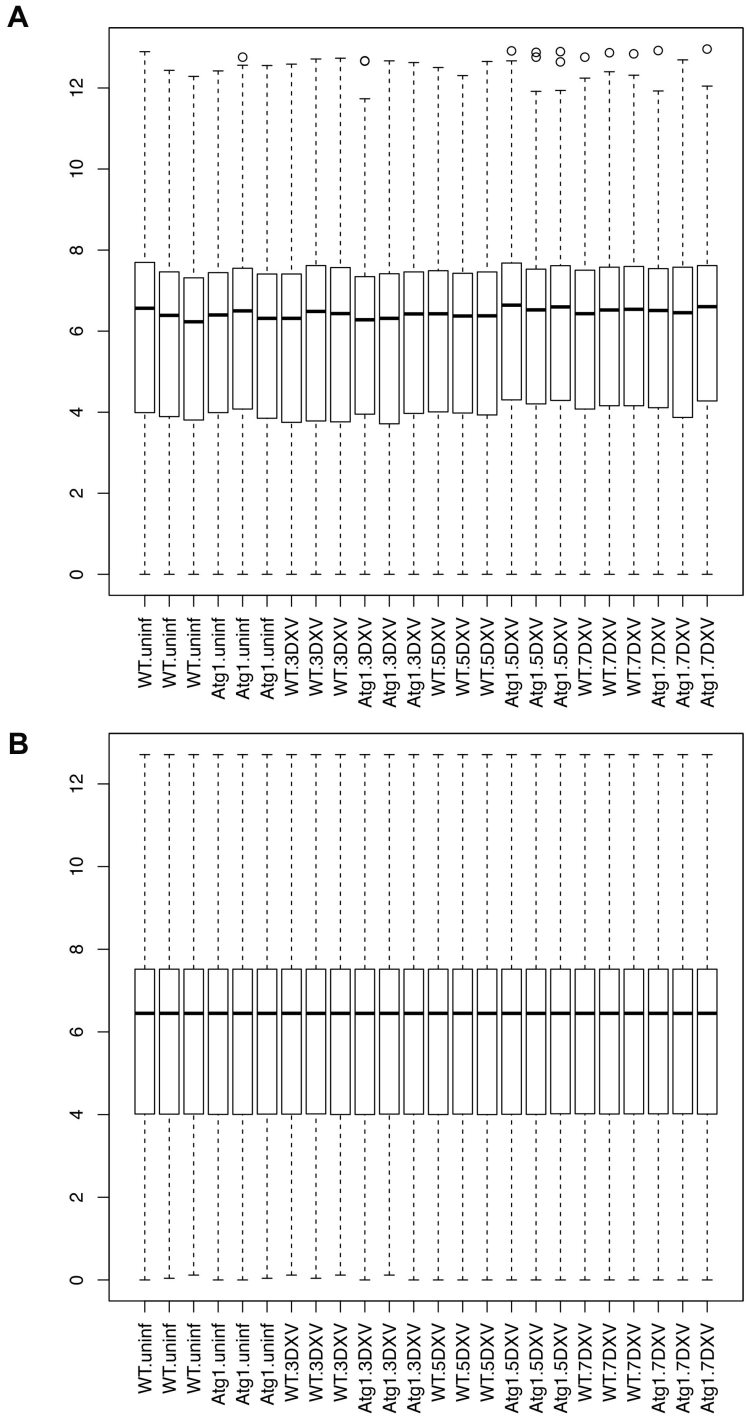

Figure 3.3: Normalization of RNA-seq data sets.
Quantile normalization to adjust the library size of 24 samples. (A) Before normalization. (B) After normalization. The x-axis represents the biological samples. The y-axis represents the box plot of all the gene read counts (in a log form) for each sample.

In the voom plot, the relationship between $log_2(counts + 1)$ and standard deviation is presented. Due to the variability of gene expression levels, the standard deviation of each gene displays a distribution that the higher the gene counts are, the smaller the standard deviations are (**Figure 3.4**). To estimate the mean-variance relation, a LOWESS regression was performed to transform the read counts to the appropriate log form for linear modeling (**Figure 3.4**).

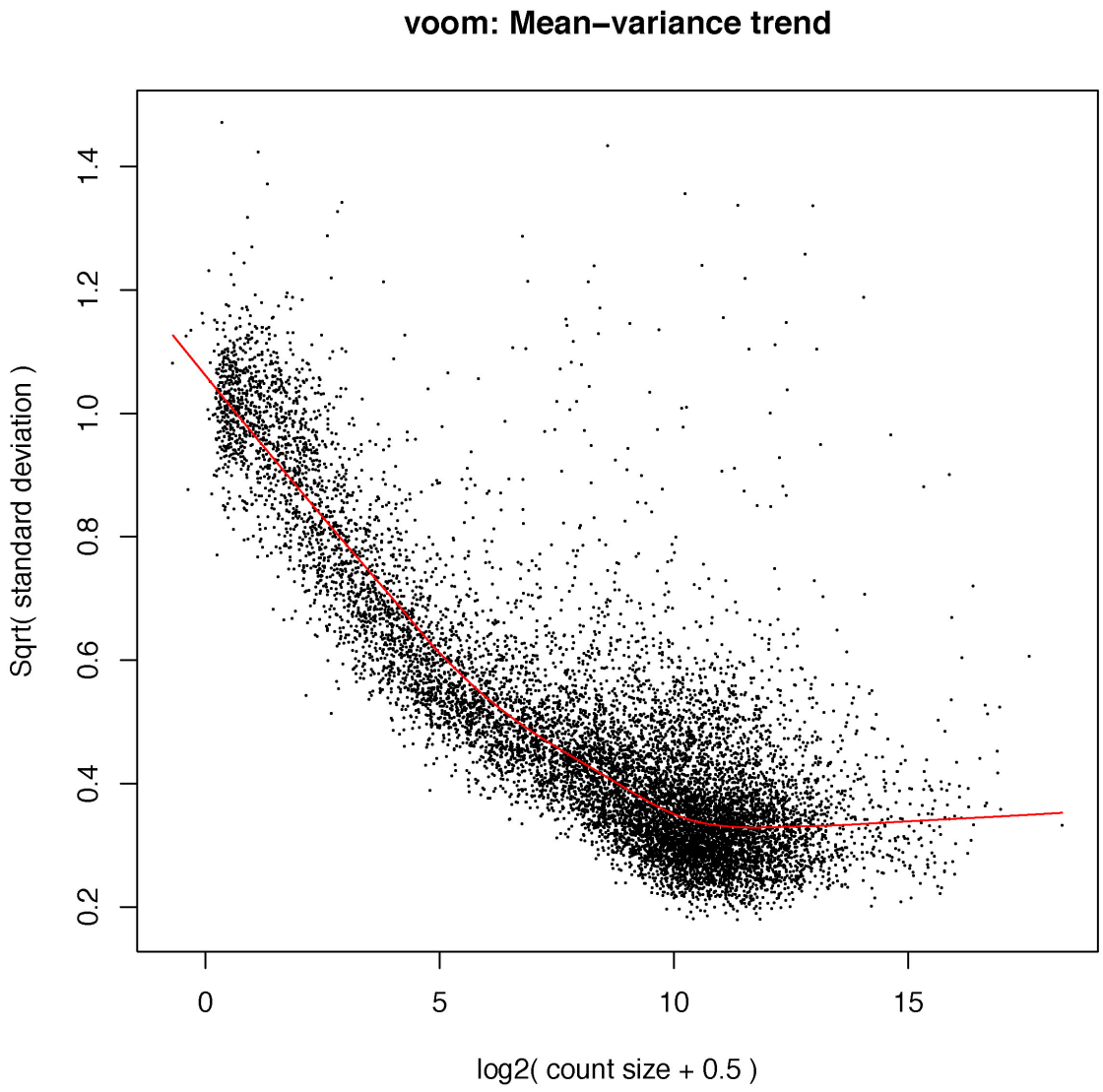

Figure 3.4: Voom.
The LOWESS regression is fitted into the data set. The x-axis represents the log_2 counts for each gene (11140 genes) in the data set. The y-axis represents the standard deviation of each gene. The red line represents the LOWESS regression line.

In order to determine the general trend and pattern of all 24 samples, principle component analysis was performed. Each dot in the PCA plots represents one transcriptome. The relative position between two dots in the PCA plot indicates the degree of similarity between the two transcriptomes. There are four observations from the PCA plots. First, all the biological replicates cluster, indicating that the reproducibility of the biological replicates is high. Second, the dots representing the wildtype and *Atg1* RNAi flies separate, indicating there is a significant difference between the transcriptomes. Third, the x-axis, representing the first principle component, corresponds to the level of DXV infection, whereas the y-axis, representing the second principle component, corresponds to genotype. Lastly, the transcriptome of the *Atg1* RNAi flies are significantly different than other transcriptomes (especially on the x-axis), and this indicates a high level of infection (**Figure 3.5**).

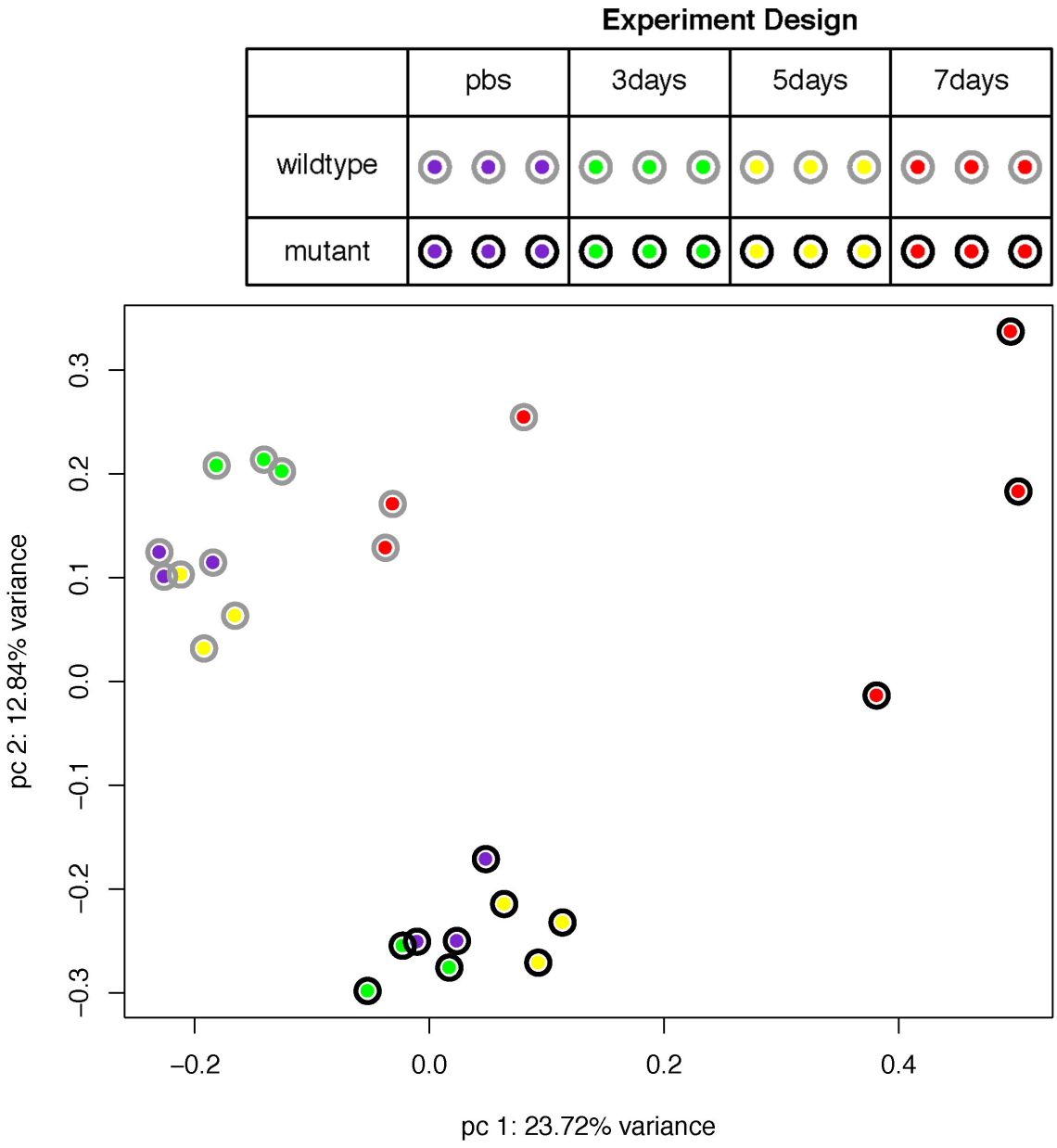

Figure 3.5: Principle component analysis.
The first principle component represents the degree of infection. The second principle component is associated with the genotype. Each biological sample is represented as a dot in the PCA plot and each color is associated with one experimental condition.

3.4.2 Differential expression analysis in wildtype flies upon DXV infection at day 3 and day 5

To identify genes important during DXV infection, differential expression analysis was applied for pairwise comparisons between infected and uninfected WT flies. Few changes in gene expression were detected in flies at days 3 and 5 post infection (dpi), compared to uninfected flies (**Figure 3.6A-B**). This might be due to the low level of DXV virus present at day 3 and day 5 in the fat body (data not shown). Specifically, there are only 4 and 3 genes that are differentially expressed in the wildtype flies upon DXV infection at 3 dpi and 5 dpi, respectively (**Table 3.1**, **Table 3.2**). In order to determine the expression of the differentially expressed genes across 24 samples, heatmaps were generated based on gene clustering (**Figure 3.6C-D**).

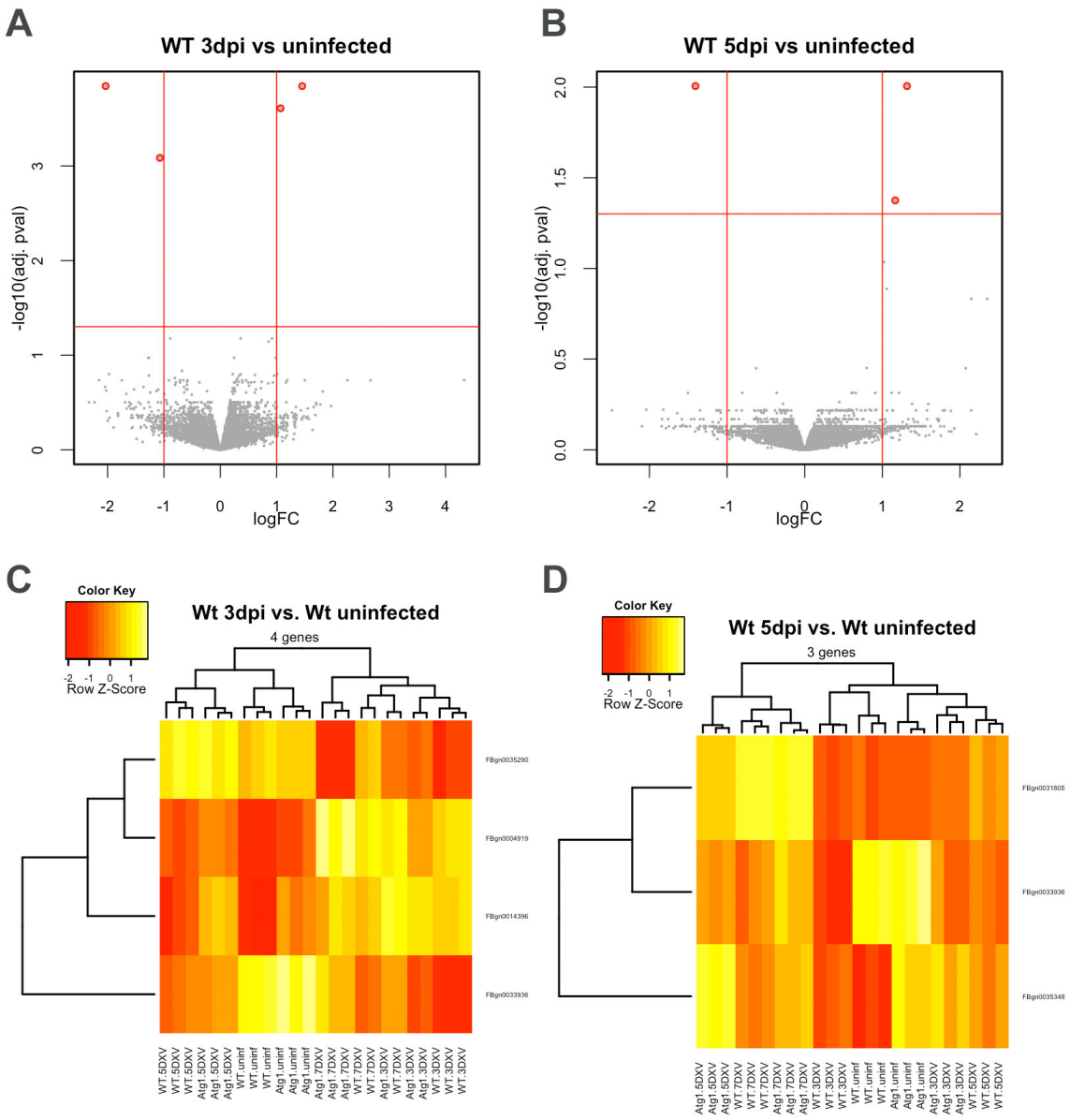

Figure 3.6: Differential expression analysis in wildtype flies upon DXV infection at day 3 and day 5.
(A-B) Scatter plots for the differential expressed genes by comparing wildtype uninfected flies vs DXV-infected flies at day 3 (A), day 5 (B). (C-D) Heatmaps for the differential expressed genes by comparing wildtype uninfected flies vs DXV-infected flies at day 3 (C), day 5 (D). The grey dots represent the total (11140) genes that are included in the analysis. The genes marked in red are differentially expressed with a log_2 fold change $>$ 0.5 and a p value $<$ 0.05.

	ID	Gene Symbol	log_2FC	AveExpr	adj.P.Val
1	FBgn0014396	tim	1.454150316	10.07824969	0.000143115
2	FBgn0004919	gol	1.07083281	7.408629419	0.000245741
3	FBgn0035290	dsb	-1.07100695	8.089983163	0.0008206
4	FBgn0033936	CG17386	-2.034002955	4.862512709	0.000143115

Table 3.1: Differentially expressed genes between uninfected WT flies and DXV-infected flies at day 3 post infection. Genes presented in the table are selected by log_2 fold Change > 0.5 and p value < 0.05. Gene list is sorted by log_2 fold Change from the largest to the smallest.

	ID	Gene Symbol	log_2FC	AveExpr	adj.P.Val
1	FBgn0031805	CG9505	1.317918736	7.485067178	0.009868327
2	FBgn0035348	CG16758	1.166306292	11.74399685	0.04215132
3	FBgn0033936	CG17386	-1.407439117	4.862512709	0.009868327

Table 3.2: Differentially expressed genes between uninfected WT flies and DXV-infected flies at day 5 post infection. Genes presented in the table are selected by log_2 fold Change > 0.5 and p value < 0.05. Gene list is sorted by log_2 fold Change from the largest to the smallest.

3.4.3 Differential expression analysis in wildtype flies upon DXV infection at day 7

At 7dpi in the wildtype flies, there were 714 genes whose change in gene expression is both large (absolute log_2 fold change $>$0.5) and significantly different (p$<$0.05) from WT flies without infection (**Figure 3.7A**).

To explore the signaling events induced by DXV infection, Gene Ontology analyses were used to perform biological function enrichment analysis in the list of differentially expressed genes (Alexa et al., 2006). In the comparison between uninfected and 7 dpi flies, the top 20 Gene Ontology Terms (GO terms) overrepresented associate with classic immune signaling pathways such as wound healing, humoral immune response, and innate immune response (**Figure 3.7C**). The genes associated with these GO terms are antimicrobial peptides, pattern associated microbial patterns (PAMPs), Toll, IMD and JAK-STAT pathway genes (**Table 3.3**). These findings are consistent with the transcriptional profiling of *Drosophila* infected with other viruses such as Flock House Virus (FHV; *Nodaviridae*), Sindbis virus (SINV; *Alphaviridae*) and *Drosophila* C Virus (DCV; *Dicistroviridae*) (Dostert et al., 2005; Kemp et al., 2013). A group of β-oxidation and lipid droplet metabolism genes are specifically upregulated in DXV-infected flies, but not in flies infected with the above mentioned viruses. For example, *lipid storage droplet-1* (*lsd1*), a positive regulator of lipid droplet lipolysis, is upregulated $\sim$2.1 fold. *AkhR* (Adipokinetic hormone receptor) and *pka* (protein kinase A), which are the upstream regulators of *lsd-1* are also upregulated more than 1.5 fold. Other upregulated genes include triglyceride lipases (*CG5966*, *CG6295*), *Acyl-CoA* dehydrogenase/oxidase (*CG9527*), and gamma-

butyrobetaine dioxygenases (*CG10814*, *CG5321*, *CG4335*) (**Figure 3.7D-E**). Triglyceride lipases can break down lipid into free fatty acids, which are then transported into mitochondria for β-oxidation by carnitine as a carrier (Bremer, 1983; McGarry and Brown, 1997; Ramsay et al., 2001; van Vlies et al., 2007). Gamma-butyrobetaine dioxygenase is the rate-limiting enzyme for carnitine synthesis (Vaz and Wanders, 2002). Since several genes in these biological processes were transcriptionally upregulated, we suspected that lipolysis and β-oxidation are induced upon DXV infection.

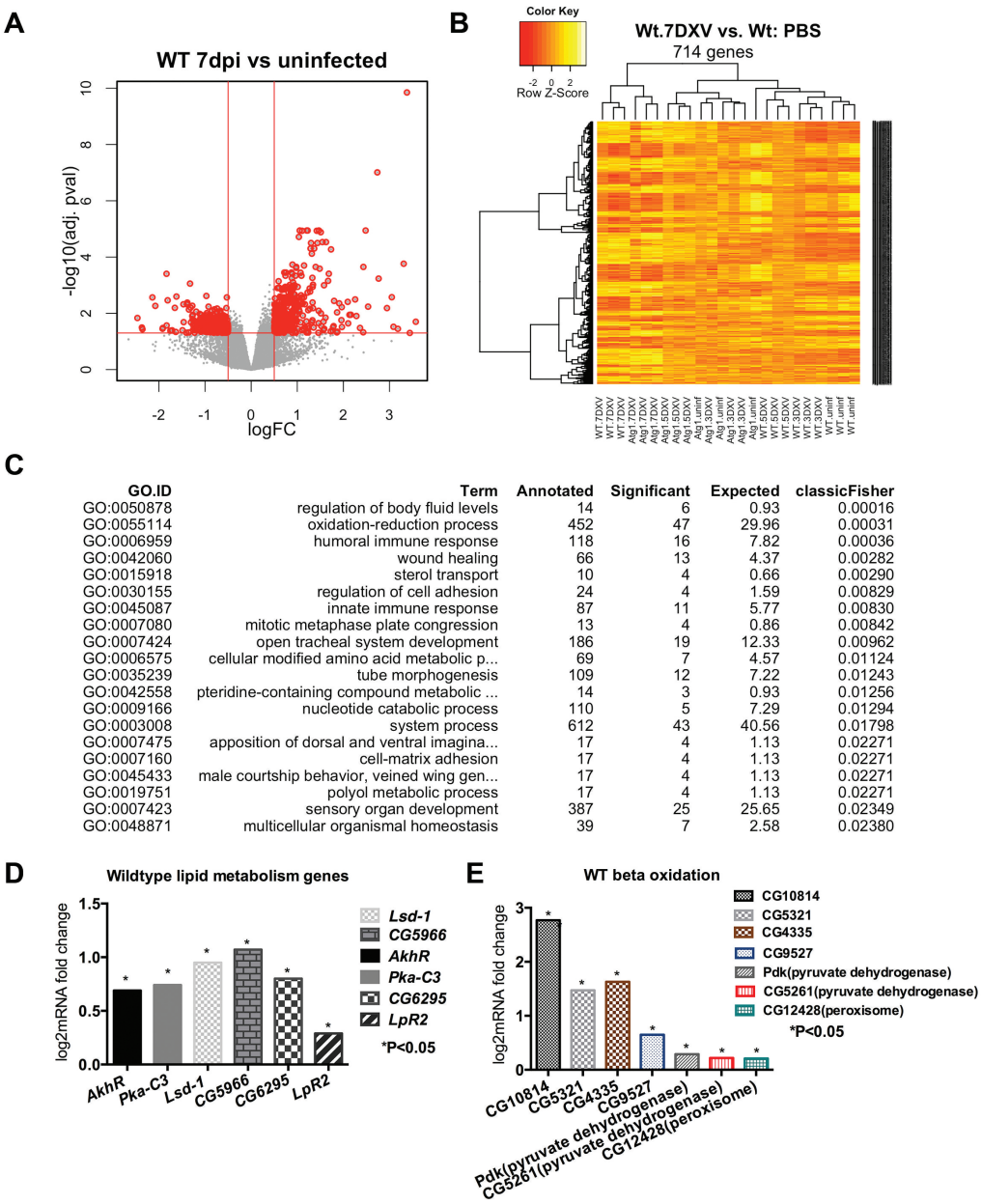

GO.ID	Term	Annotated	Significant	Expected	classicFisher
GO:0050878	regulation of body fluid levels	14	6	0.93	0.00016
GO:0055114	oxidation-reduction process	452	47	29.96	0.00031
GO:0006959	humoral immune response	118	16	7.82	0.00036
GO:0042060	wound healing	66	13	4.37	0.00282
GO:0015918	sterol transport	10	4	0.66	0.00290
GO:0030155	regulation of cell adhesion	24	4	1.59	0.00829
GO:0045087	innate immune response	87	11	5.77	0.00830
GO:0007080	mitotic metaphase plate congression	13	4	0.86	0.00842
GO:0007424	open tracheal system development	186	19	12.33	0.00962
GO:0006575	cellular modified amino acid metabolic p...	69	7	4.57	0.01124
GO:0035239	tube morphogenesis	109	12	7.22	0.01243
GO:0042558	pteridine-containing compound metabolic ...	14	3	0.93	0.01256
GO:0009166	nucleotide catabolic process	110	5	7.29	0.01294
GO:0003008	system process	612	43	40.56	0.01798
GO:0007475	apposition of dorsal and ventral imagina...	17	4	1.13	0.02271
GO:0007160	cell-matrix adhesion	17	4	1.13	0.02271
GO:0045433	male courtship behavior, veined wing gen...	17	4	1.13	0.02271
GO:0019751	polyol metabolic process	17	4	1.13	0.02271
GO:0007423	sensory organ development	387	25	25.65	0.02349
GO:0048871	multicellular organismal homeostasis	39	7	2.58	0.02380

Figure 3.7: DXV infection induces genes important for lipid droplet lipolysis and β-oxidation.
(A) Scatter plots of significantly changed genes in wildtype flies upon DXV infection at day 7 post infection. Differentially expressed genes were selected by both $p < 0.05$ and absolute log2fold change > 0.5. Significant genes are represented in red dots. Gray dots indicate all the genes involved in the analysis. (B) Heatmap of significant genes upon infection across all samples. Heat intensity is indicated by a color gradient. (C) Gene Ontology Analysis of virus induced genes. Top20 GO terms are shown in the table. (D,E) Fold change of lipid metabolism genes (D) and β-oxidation genes (E) from the RNA-seq.

Signaling pathways	Gene name	Fold change (5dpi)	Fold change (7dpi)
NF-κB pathways	Dif	1	1.43
	Imd	1	1.28
	Relish	1	1.5
	Ird1	1	0.28
	PGRP-LC	1	0.626
JAK-STAT	Upd3	1	2.64
	Socs36E	1	2.46
	Upd2	1	2.99
	Diedel	1	11.88
	TotC	1	5.13
	Tep4	1	1.43
Antiviral proteins	Vago	1	2.85
	Listericin	1	2.17
Defense against Bacterium	NimB2	1	1.71
	NimC3	1	0.37
	PPO1	1	1.5
	PPO2	1	1.58

Table 3.3: Immune genes that are responsive to DXV infection in WT flies.

All the genes shown in the table are significantly upregulated compared to uninfected WT flies. $p < 0.05$.

3.4.4 Differential expression analysis between wildtype and *Atg1* RNAi flies without infection

In order to identify genes that are important for the *Atg1*-dependent immune response, we compared the transcriptomes of wildtype and *Atg1* RNAi flies. The differential expression analysis indicates that 381 genes are differentially expressed significantly (**Figure 3.8A**). The heatmap is shown to examine the expression pattern of these 381 genes**Figure 3.8B**. Interestingly, a subset of these DE genes (upregulated in *Atg1* RNAi flies) also have upregulated expression levels as infection progresses in both the wildtype and *Atg1* RNAi flies. This indicates that a subset of the DE genes regulated in the *Atg1* RNAi flies might be overlapping with the DE genes induced by DXV infection. The top Gene Ontology term includes lipid metabolism and oxidation-reduction process (**Figure 3.8C**). In order to determine the biological events caused by the lose of *Atg1*, the differential expressed genes associated with the GO terms were examined. The lipid metabolism and β-oxidation genes are upregulated in *Atg1* RNAi flies compared to wildtype in the absence of DXV infection. These genes encode the well-characterized triglyceride lipase brummer (*bmm*), predicted triglyceride lipase CG5966, Acetyl Coenzyme A synthase (AcCoAS) and Ketoacyl-CoA thiolase (Yip2) (**Figure 3.8D**), indicating that the lipid metabolism and β-oxidation are upregulated in the *Atg1* RNAi flies.

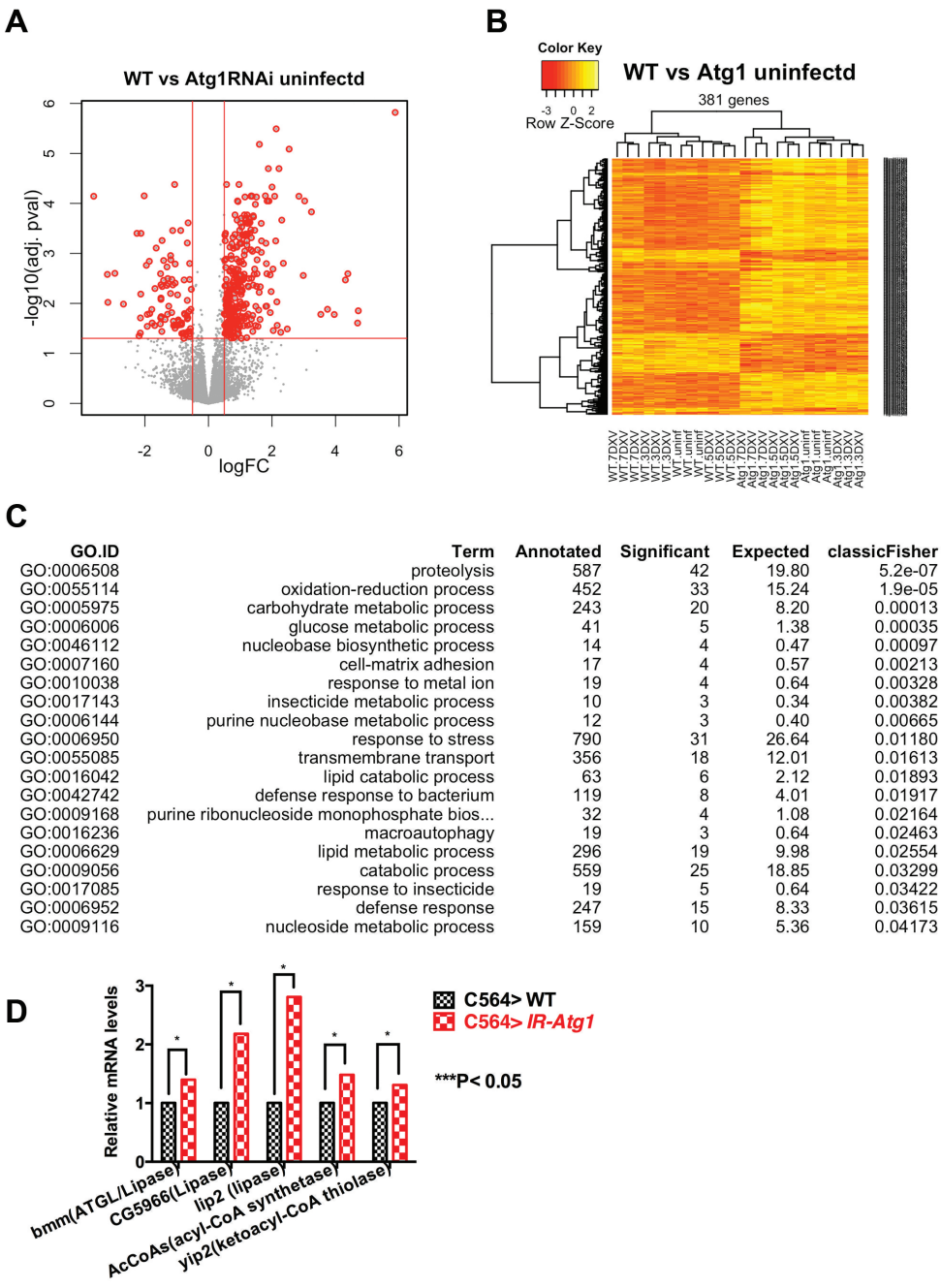

GO.ID	Term	Annotated	Significant	Expected	classicFisher
GO:0006508	proteolysis	587	42	19.80	5.2e-07
GO:0055114	oxidation-reduction process	452	33	15.24	1.9e-05
GO:0005975	carbohydrate metabolic process	243	20	8.20	0.00013
GO:0006006	glucose metabolic process	41	5	1.38	0.00035
GO:0046112	nucleobase biosynthetic process	14	4	0.47	0.00097
GO:0007160	cell-matrix adhesion	17	4	0.57	0.00213
GO:0010038	response to metal ion	19	4	0.64	0.00328
GO:0017143	insecticide metabolic process	10	3	0.34	0.00382
GO:0006144	purine nucleobase metabolic process	12	3	0.40	0.00665
GO:0006950	response to stress	790	31	26.64	0.01180
GO:0055085	transmembrane transport	356	18	12.01	0.01613
GO:0016042	lipid catabolic process	63	6	2.12	0.01893
GO:0042742	defense response to bacterium	119	8	4.01	0.01917
GO:0009168	purine ribonucleoside monophosphate bios...	32	4	1.08	0.02164
GO:0016236	macroautophagy	19	3	0.64	0.02463
GO:0006629	lipid metabolic process	296	19	9.98	0.02554
GO:0009056	catabolic process	559	25	18.85	0.03299
GO:0017085	response to insecticide	19	5	0.64	0.03422
GO:0006952	defense response	247	15	8.33	0.03615
GO:0009116	nucleoside metabolic process	159	10	5.36	0.04173

Figure 3.8: Silencing of *Atg1* in the fat body induces lipid droplet lipolysis and β-oxidation genes in the absence of infection.
(A) Scatter plots of significantly changed genes in *Atg1* RNAi flies compared to wildtype flies. Significant genes are selected by both $p < 0.05$ and absolute log_2 fold change> 0.5. Significant genes are represented in red. Gray dots indicate all the genes involved in the analysis. (B) Heatmap of significant genes dependent on *Atg1* across all samples. Heat intensity is indicated by a color gradient.(C) Gene Ontology Analysis of *Atg1*-dependent genes prior to infection. Top20 GO terms are shown in the table. (D) Fold change of lipid metabolism genes and β-oxidation genes from the RNA-seq experiment.

Brummer is a triglyceride lipase (ATGL) that can break down diglycerides into monoglycerides (Grönke et al., 2005). An increased transcriptional level of *bmm* might indicate an increased lipolysis rate. Following lipolysis, free fatty acids are produced that can be transported into the mitochondria for β-oxidation. Acyl-CoA synthetase (AcCoAS) is an catalytic enzyme that resides in the outer mitochondrial membrane, As a rate limiting factor for β-oxidation, AcCoAS is responsible for converting the free fatty acids into acyl-CoA before entry into the β-oxidation pathway. The acyl-CoA is transported through the outer and inner mitochondrial membranes via a carnitine intermediate, and then processed through four enzymatic steps for generation of ATP. The upregulation of a series of β-oxidation genes indicates that it is possible that the *Atg1*-deficient fat cells have an elevated metabolism.

3.5 Materials and methods

A pool of six flies were collected for total RNA extraction (Qiagen RNeasy kit). Three biological replicates were used for each condition. cDNA libraries were constructed using TruSeq RNA Sample Preparation Kit v2 (Illumina). 50 bp, single end sequencing was performed by Illumina HiSeq 1500 in high output mode. Six samples were sequenced per lane with an estimate of 180M reads in total. Raw sequences were aligned using the Tophat package on linux system (Trapnell et al., 2009). HTseq was used to count the the frequency of sequences that are mapped to a certain gene. Differential expression analyses were applied by using both DESeq (Anders and Huber, 2010) and Limma package (Bioconductor). The data shown were results generated by the Limma

package. Raw gene counts were log_2 transformed for linear regression modeling. TopGo R package was used for Gene Oncology analysis (Bioconductor) (Alexa et al., 2006).

Chapter 4: Atg1 is playing an antiviral role against DXV by regulating lipid metabolism

4.1 Results

4.1.1 DXV infection induces lipolysis in the lipid droplet

In Chapter 3, we have identified that the lipid metabolism and β-oxidation are significantly upregulated in wildtype flies upon DXV infection, specifically at 7 dpi. As lipid metabolism and β-oxidation are critical processes to control lipid mobilization and energy production, we were interested to determine whether lipolysis is induced in the adult fat cells upon DXV infection.

The degradation of neutral lipid is mainly controlled by triglyceride lipases and by the surface proteins that control the accessibility of lipases to the lipids (Thiam et al., 2013). When lipases are activated, lipid droplets decrease in size, and this is a key characteristic for lipolysis. As genes related to lipolysis are upregulated in DXV infected flies, we were interested to examine whether the size of lipid droplets changes over the course of infection. We stained the lipid droplets of adult fat body with Bodipy 493/503 and measured the sizes of the droplets in both uninfected and infected flies. In WT infected flies, the sizes of the lipid droplets are smaller than the ones in uninfected flies. At day

3 post infection, the number of droplets with a diameter of at least 10 μm has decreased by 50%. At day 7 post infection, almost no droplets have a diameter that is larger than 10 μm (**Figure 4.1 A-D**). Furthermore, a fat tissue infected with heterogeneous loads of virus shows a correlation between the amount of virus in a cell and the size of the lipid droplets. Individual cells with heavy infection of DXV exhibit smaller lipid droplets compared to the cells with less virus (**Figure 4.1 E**). These data suggest that lipolysis is affected during DXV infection.

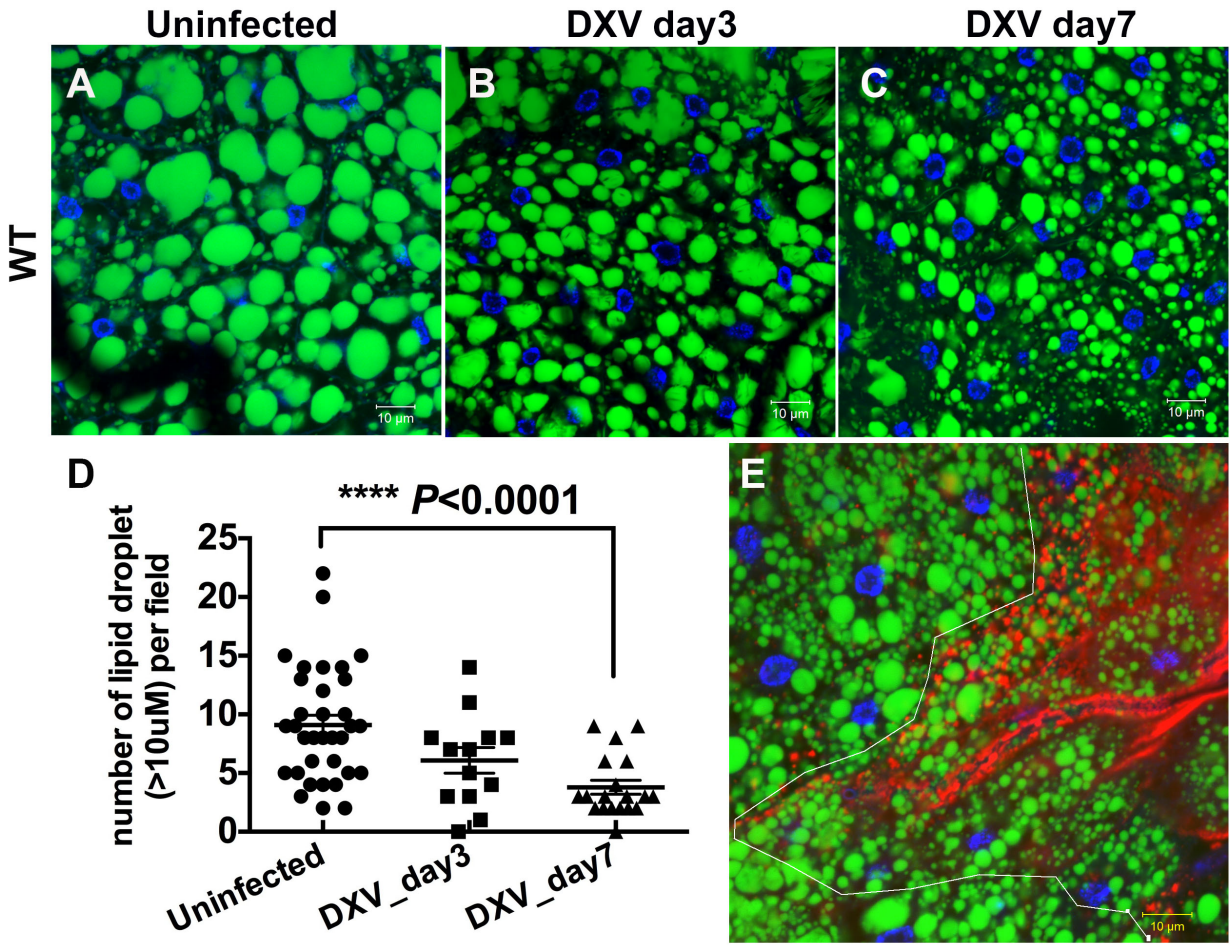

Figure 4.1: DXV infection decreases lipid droplet size.
(A-C) Lipid droplet (LD) sizes of wildtype adult fat bodies without infection, and with infection at day 3 and day 7. Lipid droplets were stained with Bodipy (Green). Nuclei are stained with DAPI (Blue). (D) Quantification of the lipid droplets sizes shown in (A-C). The number of LDs with a diameter larger than 10 μm were quantified. More than 700 cells were examined. Student's t-tests were used to test the significance. (E) Wildtype adult fat tissues were costained for DXV (red) and lipid droplets (green).

4.1.2 Atg1 regulates lipid metabolism even in the absence of DXV infection

As shown in chapter 3, prior to DXV infection, the lipid metabolism and β-oxidation genes are significantly upregulated (**Figure 3.8**). This might indicate that loss of *Atg1* results in an elevation of lipid metabolism and β-oxidation. To confirm our hypothesis, we stained the lipid droplets from adult fat body with Bodipy 493/503 and measured the sizes of the droplets. In the WT flies, the sizes of lipid droplets are mostly homogeneous with 4 to 6 large droplets in each cell. In contrast, the lipid droplets in *Atg1* RNAi flies are much smaller and the number of lipid droplets in each cell has increased (**Figure 4.2 A-C**). This suggests that reduced levels of *Atg1* facilitate lipolysis by inducing lipase activity. When flies were infected with DXV, the difference of lipid droplet size persists between WT and *Atg1* RNAi flies (**Figure 4.2 D-K**). This indicates that *Atg1* can facilitate lipid degradation and β-oxidation to produce energy.

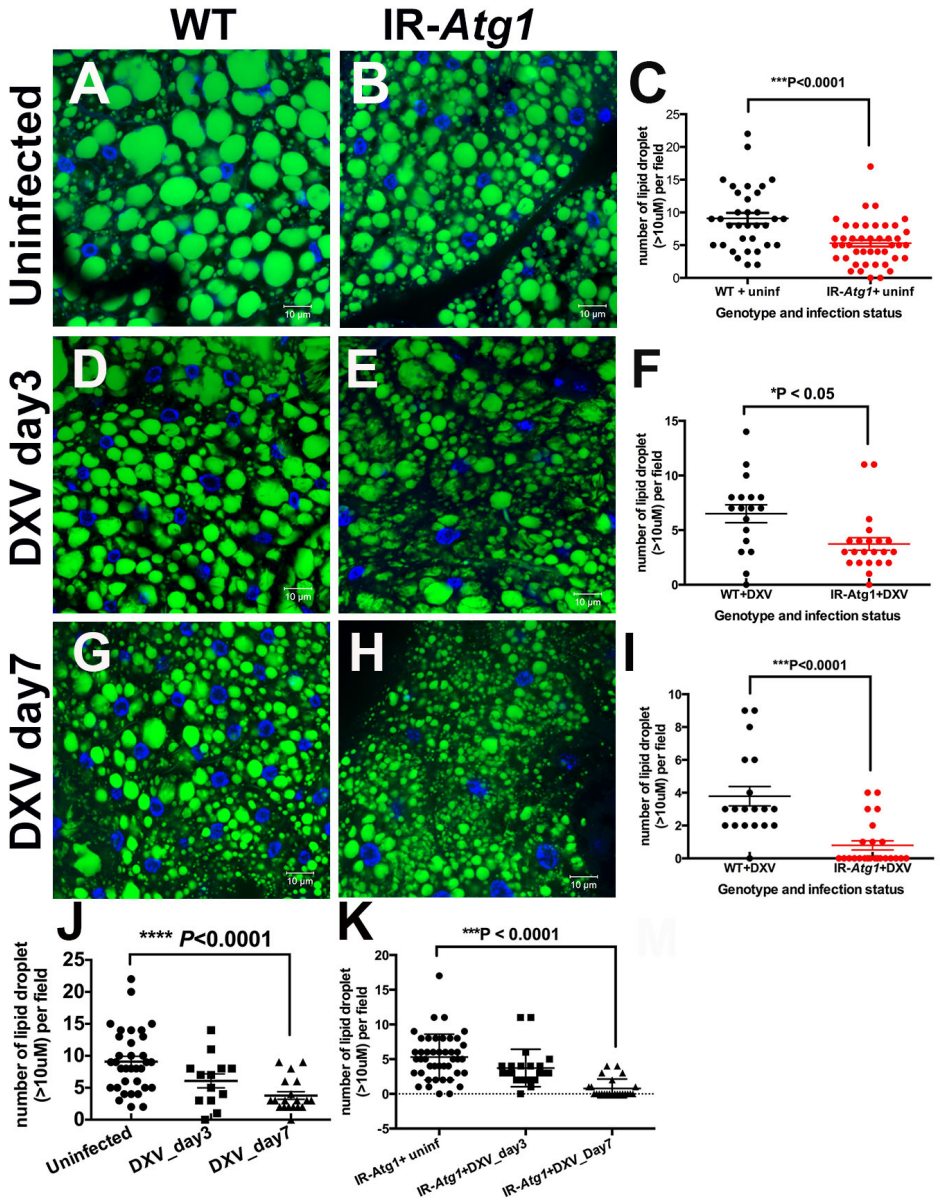

Figure 4.2: Loss of *Atg1* decreases lipid droplet size.
(A, B, D, E, G, H) Lipid droplet sizes of wildtype and *Atg1* RNAi adult fat bodies without infection (A-B), with infection at day 3 (D-E) and day 7 (G-H). Lipid droplets are stained with Bodipy (green). Nuclei are stained with DAPI (blue). (C, F, I, J, K) Quantification of the number of LDs with a diameter larger than 10 μm. More than 700 cells were examined. Student's t-tests were used to test for the significance.

4.1.3 Lipid metabolism is important for DXV infection

We have previously shown that the size of lipid droplets become smaller upon infection. We hypothesize that the lipid stored in the lipid droplets is released into the cytoplasm to generate energy.

The energy released from the lipid droplet could be utilized in two ways:1) to help initiate systemic immune responses against DXV; or 2) to facilitate DXV replication. To differentiate between these two possibilities, we applied a genetic approach to modify lipolysis and examine the effect on fly survival and DXV replication. Perilipins are proteins localized on the surface of the lipid droplets. In mammals, perilipin prevents triglyceride from being degraded by lipases (Londos et al., 2005). In *Drosophila*, two homologs, *lsd1/plin2* and *lsd2/plin2* have been characterized (Beller et al., 2010; Teixeira et al., 2003). *plin1* is required for lipolysis and a null mutant has an obese phenotype with larger lipid droplets than WT flies (Bi et al., 2012) (**Figure 4.3 A-B**). *plin2* functions as a negative regulator of lipolysis like the mammalian perilipins. *plin2* mutants have a lean phenotype together with smaller lipid droplets compared to wildtype (Beller et al., 2010). To test our hypothesis, *plin1* null mutants were infected with DXV for survival analyses. $plin1^{38}$ survive better compared to the wildtype flies upon DXV infection (**Figure 4.4 A**). Furthermore, less viral protein was detected in the *plin1* null mutant compared to wildtype by western blot (**Figure 4.4 C**). In contrast, when *plin2* was silenced in the adult fat body by *C564-Gal4*, flies become more susceptible and showed an increased amount of viral VP1 mRNA (**Figure 4.4 B,D**). Despite an increased resistance to DXV, the *plin1* null mutants were not resistant to DCV infection (**Figure 4.3 C**). This indicates that lipolysis

is facilitating viral infection, possibly by providing more energy for DXV replication.

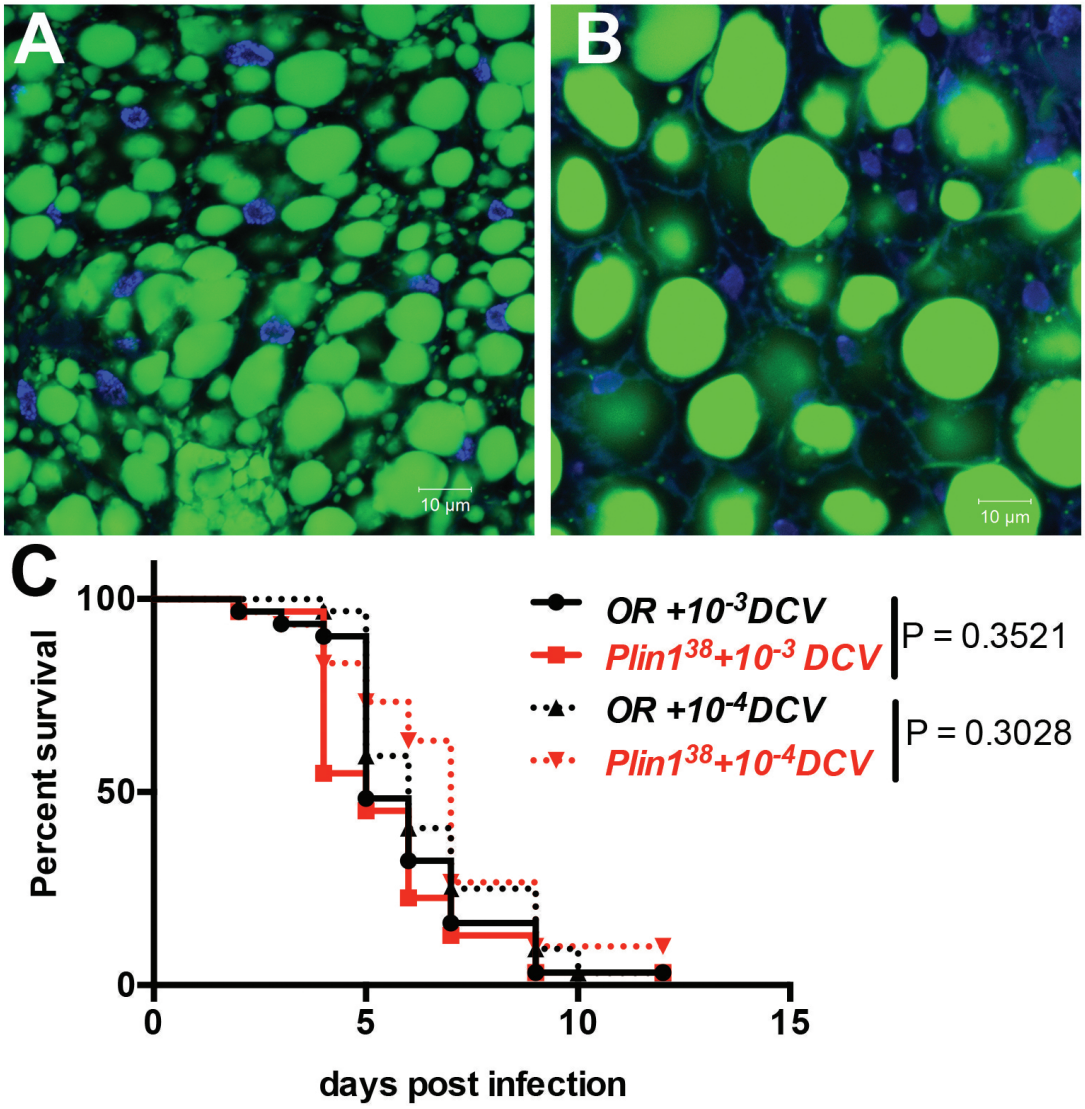

Figure 4.3: *plin1*^{38} null mutants have bigger lipid droplet size and are not susceptible to *Drosophila* C virus.
(A) In WT fat cells, most lipid droplets have a diameter of less than 10 μm. (B) In *plin1*^{38} mutant fat body cells, most lipid droplets have a diameter of more than 20 μm. More than 100 cells were measured per genotype. (C) *plin1*^{38} null mutants were not susceptible to *Drosophila* C virus in either the 10^{-3} or the 10^{-4} infectious doses. n$>$ 90 flies for each experiment.

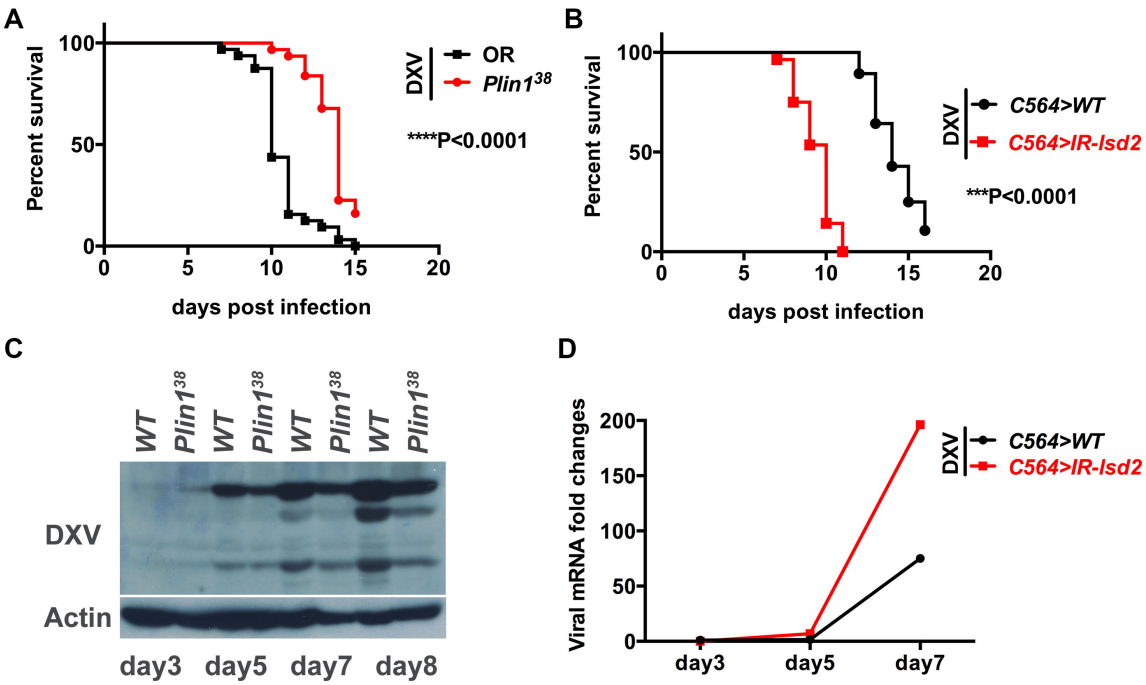

Figure 4.4: Lipid metabolism genes are important regulators for fly survival upon DXV infection.
(A-B) Survival analysis of (A) *plin1*^{38} null mutants and (B) flies with the *lsd2* gene silenced. *lsd2* was silenced in the fat body using the *C564*-Gal4 driver. n$>$ 90. Log-rank tests were used for the survival analyses (C) Western blot of DXV viral proteins in wildtype and *plin1*^{38} mutant. (D) Quantitative PCR of the viral mRNAs in wildtype and *lsd2* RNAi flies. Six flies were pooled for mRNA extraction. All experiments were repeated at least three times. Student's t-tests were used for testing statistical significance.

4.2 Materials and Methods

4.2.1 Fly stocks.

plin1^{38} was a generous gift from Dr. Xun Huang from the Chinese Academy of Sciences (Bi et al., 2012). *IR-lsd2* RNAi flies (stock number: 32846) were obtained from the TRiP *Drosophia* stock center.

4.2.2 Lipid staining and confocal imaging.

For confocal imaging, adult fly fat bodies were dissected in PBS and fixed in 4 % paraformaldehyde and 0.01% Tween PBS at $4\,^{\circ}\mathrm{C}$ overnight. After three PBS washes, fixed fat bodies were incubated in BODIPY 493/503 fluorescent stain at a concentration of 10μg/ml for an hour at room temperature (Invitrogen). The size of lipid droplets were measured by the ruler in the Zen software.

Chapter 5: Conclusions and discussions

Due to the lack of mutants available in mouse, most of the autophagy studies have focused on *Atg5, Atg6, Atg7 and Atg8* (Gutierrez et al., 2004). If a phenotype was observed when *Atg5, Atg7 and Atg8* were silenced or in these null mutants, it is generally recognized that autophagy is playing a role. However, recently, more studies have shown that autophagy genes might have roles in processes other than autophagy such as cell survival and apoptosis, modulation of cellular trafficking, protein secretion, cell signaling, transcription, translation and membrane reorganization (Subramani and Malhotra, 2013). Here we identify a novel function for *Atg1* in regulating lipid droplet metabolism in the *Drosophila* fat body. This change of lipid metabolism caused by Atg1 is closely related to the antiviral role of Atg1. Additionally, other than Atg1, the major critical regulators of lipid droplet metabolism also play important roles in controlling the DXV viral infection.

The non-canonical role of Atg1 was first discovered by the different phenotypes shown in the *IR-Atg1* and other *IR-Atg* flies upon DXV infection. Specifically, loss of *Atg1* in the fat body resulted in an increased susceptibility to DXV. In contrast, silencing of *Atg7* and *Atg8* did not lead to an increased susceptibility phenotype. *Atg1, Atg7* and *Atg8* act in the same autophagy signaling pathway. If the increased susceptibility observed in the *IR-Atg1* is attributed to autophagy, a similar effect should be observed in all

three RNAi-silenced lines. Thus, we hypothesized that Atg1 might have other functions in addition to autophagy. This hypothesis was also supported by other studies. ULK1/2, the mammalian homologs of Atg1, mediates a non-clathrin-coated endocytosis in sensory growth cones. Silencing of either *ulk1* or *ulk2* causes a defect in endocytosis of Nerve Growth Factor (NGF) that prevents filopodia extension and branching of sensory axons (Zhou et al., 2007). Furthermore, the fact that Atg1 is the only serine/threonine kinase among all the Atg proteins (e.g., 20 in *Drosophila*, and 31 in *Saccharomyces cerevisiae*) also suggests a possible role for Atg1 in phosphorylating multiple protein targets. However, as over-expression of *myc-Atg1* in the adult fat body results in fly lethality, we were not able to identify possible phosphorylation targets of Atg1 through co-immunoprecipitation (Co-IP).

Another result indicates that the the antiviral function of Atg1 is not due to autophagy. Autophagy induction is characterized by GFP-Atg8 puncta formation or an increased number of autophagosomal structures by EM (Swanlund et al., 2010). Although multiple attempts have been made by changing the infection dose or incubation time, GFP-Atg8 puncta is not significantly increased in *ex vivo* larval hemocytes or S2R+ cells upon DXV infection. Additionally, in adult fat body and S2 cells, autophagy is not induced at the early stage of infection, only at the late stages of infection. However, we come to the conclusion that the late stage induction of autophagy is not directly associated with DXV viral particles. First, in the adult fat body, GFP-Atg8 puncta only appear when the fat cells are mostly occupied by DXV particles. There is no colocalization between the virus and GFP-Atg8 puncta. This indicates that the induction of autophagy is not directly associated with DXV but rather appears to be a secondary effect (**Figure 2.5**

C,D). Second, autophagosomal-like structures are only observed in heavily infected S2 cells by EM, where mitochondria are engulfed in the autophagsosome (**Figure 2.10**).

To identify the non-canonical role of Atg1 in the antiviral response, transcriptomes of WT and *IR-Atg1* flies were compared by an RNA-seq experiment. A group of lipid metabolism and β-oxidation genes were found to be differentially expressed. For example, the adipose triglyceride lipases *brummer* and *CG5966* are upregulated in the *IR-Atg1* flies, suggesting an increased level of lipid hydrolysis. On the cellular level, lipid staining also shows a decreased size of the lipid droplets in *IR-Atg1* flies. Additionally, critical β-oxidation genes such as *AcoCOA* are also upregulated. As lipid droplets are the major energy storage organelles in flies, an elevation of lipid lipolysis and β-oxidation would result in an increased production of ATP for energy consumption.

We find that the facilitated lipid metabolism and β-oxidation are favorable for DXV replication based on three pieces of evidence. First, loss of Atg1 increases the fly sensitivity to DXV infection. This indicates that the increased production of ATP as a result of *Atg1* silencing was not used against viral replication. Although previous data has shown the importance of β-oxidation in activating the immune system, the possibility of ATP being consumed by replicating pathogen should not be ignored. For example, dengue virus can exploit autophagy to produce energy for its replication in Huh-7.5 cells (Heaton and Randall, 2010). Additionally, the expression of immune related genes are significantly higher in the *IR-Atg1* flies compared to WT upon DXV infection, indicating at least loss of *Atg1* does not block immune responses at the transcriptional level. Second, increased lipolysis and β-oxidation are observed when flies are infected with DXV. Specifically, the

upregulation of perilipin (*plin1*), triglyceride lipases, Acyl-CoA dehydrogenase/oxidase and gamma-butyrobetaine dioxygenase provides evidence on the transcriptional level. On the cellular level, the fact that the lipid droplets decrease in size as DXV infection progresses is also in agreement with our conclusion. Finally, manipulation of the lipid metabolism process by adjusting perilipin function results in changes in fly survival to DXV infection. Specifically, loss of the positive regulator, *plin1* causes the fly to be resistant to DXV. In contrast, silencing of the negative regulator *plin2* results in an increased susceptibility to DXV.

So far, we have demonstrated (1) the importance of lipid metabolism (specifically perilipins) in affecting DXV infection in the adult fat body and (2) how Atg1 regulates lipid metabolism. However, whether Atg1 and perilipin act in the same pathway is not known. Due to limited resources, epistasis experiments have not been performed. However, we speculate that Atg1 and PLIN1 acts in parallel pathways. There are two major signaling pathways controlling lipid metabolism: the pro-lipolytic adipokinetic hormone (AKH)/AKH-receptor (AKHR) pathway and the adipocyte triglyceride lipase (ATGL)-dependent pathway (Bi et al., 2012; Grönke et al., 2005, 2007). In the AKHR pathway, PLIN1 facilitates the hormone sensitive lipase (HSL), which goes on to hydrolyze lipid. In contrast, PLIN2 negatively regulates the ATGL-dependent pathway by preventing Brummer from hydrolyzing lipids. The fact that loss of *Atg1* upregulates *bmm* expression suggests that Atg1 might play a role in the Brummer-dependent lipolytic pathway. However, whether *bmm* acts in the same pathway as *plin1* should be confirmed by an epistasis experiment. Due to the weakness of adult *bmm* mutants, we were not able to perform this experiment in our system.

In summary, we have defined a novel role for Atg1 in regulating lipid metabolism in the adult fat body. We also establish a model of how lipid metabolism affects DXV infection by identifying the critical players Atg1, PLIN1 and PLIN2. Our study provides a good example of how autophagy genes could play non-autophagic roles in an immune response. As more exceptions are identified for the functions of autophagy genes, it is possible that the autophagy system is much more complex than what we already know. Furthermore, the link between lipid droplet metabolism and DXV also brings our attention to the basic metabolic processes and demonstrates how non-traditional immune pathways can play a role in host-pathogen interactions. Finally, we have proven RNA-seq as a powerful tool in identifying critical genes and pathways in the host upon viral infection.

Chapter A: Appendix A

A.1 Differentially expressed genes between uninfected WT flies and DXV-infected flies at day 7 post infection

	ID	Gene Symbol	AveExpr	log_2FC	adj.P.Val
1	FBgn0039666	Diedel	2.52E+00	3.57E+00	1.99E-02
2	FBgn0034173	CG9010	1.84E+00	3.44E+00	4.99E-02
3	FBgn0031805	CG9505	7.49E+00	3.38E+00	0.00E+00
4	FBgn0005660	Ets21C	5.05E+00	3.31E+00	2.00E-04
5	FBgn0037783	Npc2c	2.35E+00	3.18E+00	3.56E-02
6	FBgn0013278	Hsp70Bb	3.51E+00	3.09E+00	3.01E-02
7	FBgn0001230	Hsp68	8.74E+00	3.05E+00	2.70E-03
8	FBgn0052368	CG32368	8.25E+00	2.95E+00	6.50E-03
9	FBgn0033830	CG10814	7.08E+00	2.76E+00	6.00E-04
10	FBgn0034480	CG16898	8.96E+00	2.74E+00	0.00E+00
11	FBgn0037083	CG5656	1.03E+00	2.54E+00	5.80E-03
12	FBgn0010041	GstD5	5.72E+00	2.48E+00	0.00E+00

13	FBgn0002632	E(spl)m6-BFM	9.23E-01	2.43E+00	4.73E-02
14	FBgn0034741	CG4269	6.65E+00	2.43E+00	2.00E-04
15	FBgn0044812	TotC	8.24E+00	2.36E+00	3.31E-02
16	FBgn0036949	CG7290	1.03E+00	2.28E+00	1.25E-02
17	FBgn0031470	CG18557	3.43E+00	2.26E+00	3.20E-03
18	FBgn0051259	CG31259	5.65E+00	2.16E+00	1.13E-02
19	FBgn0031034	CG14205	6.92E+00	2.13E+00	1.13E-02
20	FBgn0053510	CG33510	3.03E+00	2.10E+00	2.28E-02
21	FBgn0039685	Obp99b	4.79E+00	2.09E+00	3.90E-03
22	FBgn0051041	CG31041	6.04E+00	1.97E+00	3.06E-02
23	FBgn0052107	CG32107	5.17E+00	1.96E+00	6.00E-03
24	FBgn0063388	snoRNA:U27:54Ea	8.72E-01	1.96E+00	1.75E-02
25	FBgn0003961	Uro	8.25E+00	1.91E+00	4.40E-03
26	FBgn0038526	CG14327	1.46E+00	1.87E+00	4.51E-02
27	FBgn0013277	Hsp70Ba	1.28E+00	1.86E+00	4.78E-02
28	FBgn0034289	CG10910	9.29E+00	1.86E+00	9.30E-03
29	FBgn0031490	CG17264	7.35E+00	1.80E+00	3.60E-03
30	FBgn0002732	E(spl)malpha-BFM	2.58E+00	1.79E+00	2.85E-02
31	FBgn0033355	CG13748	1.08E+00	1.77E+00	4.13E-02
32	FBgn0052751	CG32751	2.85E+00	1.77E+00	3.16E-02
33	FBgn0037225	TwdlG	2.71E+00	1.73E+00	4.36E-02

34	FBgn0038083	CG5999	7.28E+00	1.73E+00	1.00E-04
35	FBgn0033215	CG1942	6.06E+00	1.68E+00	4.00E-04
36	FBgn0034296	CG10912	1.06E+01	1.67E+00	7.00E-04
37	FBgn0038795	CG4335	6.80E+00	1.62E+00	0.00E+00
38	FBgn0035176	CG13905	8.67E+00	1.61E+00	1.43E-02
39	FBgn0030904	upd2	1.53E+00	1.58E+00	3.56E-02
40	FBgn0033388	CG8046	4.68E+00	1.58E+00	1.00E-03
41	FBgn0034880	ItgalphaPS5	3.46E+00	1.57E+00	3.92E-02
42	FBgn0036723	CG12229	3.73E+00	1.57E+00	1.98E-02
43	FBgn0033926	Arc1	1.17E+01	1.55E+00	0.00E+00
44	FBgn0038973	Pebp1	9.88E+00	1.52E+00	2.84E-02
45	FBgn0014396	tim	1.01E+01	1.51E+00	0.00E+00
46	FBgn0030262	Vago	8.70E+00	1.51E+00	1.00E-02
47	FBgn0030438	CG15721	1.12E+01	1.49E+00	3.00E-04
48	FBgn0030575	CG5321	8.25E+00	1.47E+00	0.00E+00
49	FBgn0033365	CG8170	3.82E+00	1.46E+00	8.10E-03
50	FBgn0037562	CG11671	6.14E+00	1.46E+00	4.92E-02
51	FBgn0039396	CCAP-R	2.71E+00	1.46E+00	2.24E-02
52	FBgn0033153	Gadd45	7.80E+00	1.44E+00	0.00E+00
53	FBgn0053494	CG33494	7.87E+00	1.42E+00	0.00E+00
54	FBgn0003067	Pepck	1.32E+01	1.40E+00	2.00E-04

55	FBgn0026403	Ndg	7.39E+00	1.37E+00	0.00E+00
56	FBgn0053542	upd3	3.86E+00	1.36E+00	3.20E-02
57	FBgn0003996	w	8.81E+00	1.34E+00	1.00E-03
58	FBgn0046878	Obp83cd	5.73E+00	1.34E+00	6.60E-03
59	FBgn0015035	Cyp4e3	8.20E+00	1.33E+00	4.10E-03
60	FBgn0033792	CG13325	6.26E+00	1.33E+00	1.77E-02
61	FBgn0034290	CG5773	8.52E+00	1.33E+00	5.00E-04
62	FBgn0039152	Rootletin	6.38E+00	1.33E+00	1.10E-03
63	FBgn0039319	CG13659	6.19E+00	1.32E+00	1.00E-04
64	FBgn0051901	Mur29B	8.34E+00	1.32E+00	2.06E-02
65	FBgn0041184	Socs36E	8.24E+00	1.30E+00	0.00E+00
66	FBgn0031801	CG9498	9.26E+00	1.29E+00	0.00E+00
67	FBgn0040069	vanin-like	6.89E+00	1.28E+00	1.70E-03
68	FBgn0035665	Jon65Aiii	1.29E+01	1.27E+00	1.30E-03
69	FBgn0039593	CG9989	5.43E+00	1.27E+00	6.90E-03
70	FBgn0032004	CG8292	3.52E+00	1.24E+00	3.47E-02
71	FBgn0036627	Grp	5.68E+00	1.24E+00	7.70E-03
72	FBgn0086666	snoRNA:Psi28S-2179	3.67E+00	1.24E+00	4.80E-02
73	FBgn0004919	gol	7.41E+00	1.22E+00	0.00E+00
74	FBgn0032377	CG14937	3.51E+00	1.22E+00	2.90E-02
75	FBgn0037850	CG14695	3.60E+00	1.22E+00	4.31E-02

76	FBgn0250815	Jon65Aiv	1.38E+01	1.22E+00	1.80E-03
77	FBgn0015037	Cyp4p1	8.80E+00	1.21E+00	0.00E+00
78	FBgn0035619	CG10592	8.76E+00	1.20E+00	4.83E-02
79	FBgn0259998	CG17571	1.06E+01	1.20E+00	1.94E-02
80	FBgn0038299	Spn88Eb	7.87E+00	1.17E+00	3.07E-02
81	FBgn0038717	CG17751	7.77E+00	1.17E+00	4.80E-03
82	FBgn0031645	CG3036	1.01E+01	1.15E+00	2.00E-04
83	FBgn0034295	CG10911	1.21E+01	1.15E+00	2.70E-03
84	FBgn0039316	CG11893	4.15E+00	1.14E+00	3.55E-02
85	FBgn0015038	Cyp9b1	6.01E+00	1.12E+00	4.40E-03
86	FBgn0032381	Mal-B1	1.02E+01	1.12E+00	1.21E-02
87	FBgn0020762	Atet	9.93E+00	1.10E+00	2.70E-03
88	FBgn0031249	CG11911	9.56E+00	1.10E+00	3.82E-02
89	FBgn0085419	Rgk2	5.46E+00	1.10E+00	4.70E-03
90	FBgn0261113	Xrp1	1.19E+01	1.10E+00	0.00E+00
91	FBgn0046876	Obp83ef	6.15E+00	1.09E+00	5.00E-04
92	FBgn0040060	yip7	1.37E+01	1.08E+00	2.30E-03
93	FBgn0029831	CG5966	1.09E+01	1.07E+00	4.00E-04
94	FBgn0031888	Pvf2	5.28E+00	1.07E+00	2.09E-02
95	FBgn0035623	mthl2	6.60E+00	1.06E+00	4.10E-03
96	FBgn0031520	CG8837	7.00E+00	1.05E+00	4.10E-03

97	FBgn0034335	GstE1	9.88E+00	1.05E+00	0.00E+00
98	FBgn0053281	CG33281	5.14E+00	1.05E+00	8.50E-03
99	FBgn0024290	Slob	7.72E+00	1.04E+00	7.50E-03
100	FBgn0037391	CG2017	9.62E+00	1.04E+00	0.00E+00
101	FBgn0035348	CG16758	1.17E+01	1.02E+00	4.80E-03
102	FBgn0035049	Mmp1	8.22E+00	1.01E+00	1.10E-03
103	FBgn0039798	CG11313	6.41E+00	1.01E+00	2.70E-03
104	FBgn0050280	CG30280	4.90E+00	1.01E+00	3.60E-02
105	FBgn0036321	CG14120	9.14E+00	9.92E-01	1.82E-02
106	FBgn0002543	lea	6.02E+00	9.91E-01	1.13E-02
107	FBgn0042627	v(2)k05816	1.10E+01	9.87E-01	5.50E-03
108	FBgn0032669	CG15155	8.22E+00	9.86E-01	1.89E-02
109	FBgn0015010	Ag5r	1.11E+01	9.79E-01	2.00E-04
110	FBgn0016076	vri	9.28E+00	9.76E-01	2.00E-04
111	FBgn0038658	CG14292	1.10E+01	9.76E-01	3.30E-03
112	FBgn0051233	CG31233	9.28E+00	9.71E-01	4.91E-02
113	FBgn0033913	CG8468	9.31E+00	9.66E-01	8.10E-03
114	FBgn0050277	Oatp58Da	6.77E+00	9.66E-01	7.20E-03
115	FBgn0036362	CG10725	6.39E+00	9.65E-01	1.57E-02
116	FBgn0033438	Mmp2	8.53E+00	9.63E-01	5.30E-03
117	FBgn0030261	CG15203	7.26E+00	9.61E-01	5.00E-04

118	FBgn0029896	CG3168	1.19E+01	9.59E-01	5.70E-03
119	FBgn0032136	Apoltp	1.08E+01	9.58E-01	4.40E-03
120	FBgn0039114	Lsd-1	1.07E+01	9.58E-01	4.41E-02
121	FBgn0028420	Kr-h1	8.84E+00	9.55E-01	3.50E-03
122	FBgn0010019	Cyp4g1	1.59E+01	9.50E-01	1.11E-02
123	FBgn0032773	fon	1.05E+01	9.50E-01	3.50E-03
124	FBgn0037396	CG11459	5.39E+00	9.48E-01	4.77E-02
125	FBgn0029507	Tsp42Ed	9.24E+00	9.47E-01	2.20E-03
126	FBgn0050446	Tdc2	5.48E+00	9.47E-01	2.71E-02
127	FBgn0051704	CG31704	7.05E+00	9.47E-01	2.33E-02
128	FBgn0031927	Slob	5.94E+00	9.44E-01	1.00E-03
129	FBgn0002528	LanB2	9.37E+00	9.35E-01	7.90E-03
130	FBgn0034639	CG15673	7.47E+00	9.35E-01	5.30E-03
131	FBgn0032167	CG5853	1.05E+01	9.29E-01	1.74E-02
132	FBgn0003965	v	8.45E+00	9.25E-01	1.30E-03
133	FBgn0030827	CG18258	5.64E+00	9.23E-01	3.39E-02
134	FBgn0086708	stv	9.08E+00	9.23E-01	2.00E-03
135	FBgn0034479	CG8654	8.56E+00	9.22E-01	3.60E-03
136	FBgn0031632	CG15628	9.19E+00	9.20E-01	4.20E-03
137	FBgn0036461	Zip71B	7.20E+00	9.20E-01	3.15E-02
138	FBgn0002526	LanA	1.01E+01	9.18E-01	1.60E-02

139	FBgn0034716	Oatp58Dc	8.84E+00	9.12E-01	8.60E-03
140	FBgn0261258	rgn	9.40E+00	9.10E-01	1.10E-03
141	FBgn0032322	CG16743	8.95E+00	9.09E-01	1.67E-02
142	FBgn0033710	CG17739	9.43E+00	9.07E-01	8.00E-04
143	FBgn0052669	CG32669	7.07E+00	9.03E-01	7.80E-03
144	FBgn0030482	CG1673	1.03E+01	8.97E-01	4.10E-03
145	FBgn0001168	h	8.92E+00	8.96E-01	2.00E-04
146	FBgn0085282	CG34253	6.15E+00	8.95E-01	1.14E-02
147	FBgn0085353	CG34324	1.26E+01	8.94E-01	4.92E-02
148	FBgn0053926	CG33926	1.04E+01	8.92E-01	2.38E-02
149	FBgn0035154	CG3344	8.77E+00	8.90E-01	3.77E-02
150	FBgn0003328	scb	1.05E+01	8.89E-01	4.00E-04
151	FBgn0025701	Mrp4	8.06E+00	8.89E-01	3.40E-03
152	FBgn0003888	betaTub60D	1.03E+01	8.83E-01	3.20E-03
153	FBgn0036264	CG11529	4.97E+00	8.83E-01	2.38E-02
154	FBgn0038088	CG10126	7.85E+00	8.82E-01	6.00E-04
155	FBgn0036975	CG5618	8.48E+00	8.78E-01	1.60E-03
156	FBgn0003308	ry	8.84E+00	8.77E-01	2.70E-03
157	FBgn0027585	CG8740	9.56E+00	8.77E-01	1.10E-03
158	FBgn0003137	Ppn	1.08E+01	8.74E-01	1.06E-02
159	FBgn0034312	CG10916	7.60E+00	8.72E-01	4.00E-04

160	FBgn0034709	Swim	1.02E+01	8.65E-01	1.80E-03
161	FBgn0033134	Tsp42El	9.09E+00	8.63E-01	1.70E-03
162	FBgn0031261	nAChRbeta3	7.57E+00	8.59E-01	2.30E-03
163	FBgn0050357	CG30357	4.80E+00	8.58E-01	3.89E-02
164	FBgn0023214	edl	6.61E+00	8.57E-01	3.49E-02
165	FBgn0000442	Pkg21D	6.33E+00	8.56E-01	1.57E-02
166	FBgn0033787	CG13321	9.81E+00	8.53E-01	1.45E-02
167	FBgn0036157	CG7560	7.99E+00	8.53E-01	1.40E-03
168	FBgn0039564	CG5527	6.53E+00	8.53E-01	1.05E-02
169	FBgn0037801	CG3999	7.53E+00	8.51E-01	2.46E-02
170	FBgn0051288	CG31288	7.99E+00	8.48E-01	1.30E-02
171	FBgn0030040	CG15347	9.73E+00	8.45E-01	1.06E-02
172	FBgn0016075	vkg	1.09E+01	8.40E-01	1.46E-02
173	FBgn0029526	CR18166	5.03E+00	8.40E-01	2.07E-02
174	FBgn0030993	Mec2	7.93E+00	8.39E-01	3.01E-02
175	FBgn0000395	cv-2	7.23E+00	8.37E-01	1.00E-03
176	FBgn0045761	CHKov1	6.93E+00	8.36E-01	3.60E-03
177	FBgn0036876	CG9451	7.95E+00	8.29E-01	2.90E-03
178	FBgn0036877	CG9452	5.49E+00	8.27E-01	3.84E-02
179	FBgn0051183	CG31183	7.83E+00	8.23E-01	3.70E-03
180	FBgn0250835	CG15394	5.77E+00	8.23E-01	3.15E-02

181	FBgn0025687	LKR	8.66E+00	8.22E-01	4.30E-03
182	FBgn0034758	CG13510	8.74E+00	8.22E-01	3.84E-02
183	FBgn0038842	hdly	8.92E+00	8.20E-01	3.20E-03
184	FBgn0035343	CG16762	6.71E+00	8.15E-01	3.55E-02
185	FBgn0046763	CG17278	7.68E+00	8.11E-01	1.80E-03
186	FBgn0030955	CG6891	9.43E+00	8.07E-01	3.10E-03
187	FBgn0051974	CG31974	9.16E+00	8.07E-01	2.50E-03
188	FBgn0039411	dys	4.02E+00	8.01E-01	4.02E-02
189	FBgn0039801	Npc2h	8.37E+00	8.01E-01	2.06E-02
190	FBgn0031432	Cyp309a1	9.67E+00	7.97E-01	1.35E-02
191	FBgn0053258	CG33258	9.65E+00	7.95E-01	3.57E-02
192	FBgn0001258	ImpL3	8.45E+00	7.93E-01	1.10E-03
193	FBgn0051436	CG31436	6.25E+00	7.88E-01	1.76E-02
194	FBgn0011722	Tig	8.49E+00	7.85E-01	8.40E-03
195	FBgn0004429	LysP	7.35E+00	7.83E-01	1.17E-02
196	FBgn0023549	Mct1	1.01E+01	7.83E-01	1.41E-02
197	FBgn0032116	Mco1	7.87E+00	7.81E-01	2.80E-03
198	FBgn0050273	CG30273	6.41E+00	7.78E-01	1.95E-02
199	FBgn0028543	NimB2	1.05E+01	7.76E-01	1.08E-02
200	FBgn0029639	CG14419	6.82E+00	7.74E-01	2.90E-02
201	FBgn0052834	CG32834	8.51E+00	7.71E-01	5.40E-03

202	FBgn0051547	CG31547	8.55E+00	7.69E-01	2.11E-02
203	FBgn0033188	Drat	1.03E+01	7.68E-01	1.25E-02
204	FBgn0033205	CG2064	8.34E+00	7.66E-01	3.50E-03
205	FBgn0031489	CG17224	1.04E+01	7.56E-01	1.46E-02
206	FBgn0030309	CG1572	9.59E+00	7.54E-01	4.00E-04
207	FBgn0000489	Pka-C3	9.05E+00	7.48E-01	2.70E-03
208	FBgn0036833	CG3819	1.06E+01	7.43E-01	5.00E-04
209	FBgn0038818	Nep4	7.62E+00	7.42E-01	2.63E-02
210	FBgn0052369	CG32369	8.06E+00	7.42E-01	1.00E-02
211	FBgn0261555	CG42673	8.04E+00	7.42E-01	1.79E-02
212	FBgn0011577	dally	8.83E+00	7.41E-01	3.60E-03
213	FBgn0052656	Muc11A	1.05E+01	7.41E-01	2.25E-02
214	FBgn0028424	JhI-26	9.19E+00	7.39E-01	1.10E-03
215	FBgn0050269	CG30269	7.06E+00	7.31E-01	1.31E-02
216	FBgn0025682	scf	9.92E+00	7.28E-01	3.20E-03
217	FBgn0036831	CG6839	9.41E+00	7.24E-01	1.40E-03
218	FBgn0034396	CG15097	5.17E+00	7.23E-01	1.69E-02
219	FBgn0085359	CG34330	1.02E+01	7.22E-01	3.57E-02
220	FBgn0035091	CG3829	9.67E+00	7.20E-01	8.40E-03
221	FBgn0036501	CG7272	8.76E+00	7.18E-01	4.00E-04
222	FBgn0020391	Nrk	5.50E+00	7.16E-01	4.23E-02

223	FBgn0038450	CG17560	1.12E+01	7.13E-01	1.63E-02
224	FBgn0051536	Cdep	9.50E+00	7.13E-01	5.40E-03
225	FBgn0005612	Sox14	9.45E+00	7.12E-01	1.40E-02
226	FBgn0030847	CG12991	8.41E+00	7.11E-01	1.05E-02
227	FBgn0051028	CG31028	4.70E+00	7.10E-01	4.90E-02
228	FBgn0033928	Arc2	8.17E+00	7.08E-01	1.30E-03
229	FBgn0036147	Plod	1.04E+01	7.08E-01	7.70E-03
230	FBgn0032469	CG9932	1.05E+01	7.02E-01	2.37E-02
231	FBgn0010434	cora	1.12E+01	7.00E-01	4.50E-03
232	FBgn0011695	PebIII	1.23E+01	7.00E-01	3.84E-02
233	FBgn0053301	CG33301	8.20E+00	6.98E-01	4.80E-03
234	FBgn0250871	pot	7.82E+00	6.97E-01	2.70E-03
235	FBgn0025595	AkhR	8.67E+00	6.94E-01	1.17E-02
236	FBgn0032505	CG16826	1.43E+01	6.92E-01	7.70E-03
237	FBgn0261561	CG42675	5.30E+00	6.85E-01	4.55E-02
238	FBgn0030469	IP3K2	8.56E+00	6.84E-01	1.32E-02
239	FBgn0034588	CG9394	9.83E+00	6.84E-01	1.40E-03
240	FBgn0087007	bbg	9.89E+00	6.84E-01	1.43E-02
241	FBgn0052698	CG32698	6.83E+00	6.83E-01	9.10E-03
242	FBgn0250818	Glut4EF	9.29E+00	6.83E-01	2.71E-02
243	FBgn0260952	Msp300	1.09E+01	6.83E-01	3.43E-02

244	FBgn0038718	CG17752	8.96E+00	6.80E-01	2.32E-02
245	FBgn0003997	hid	7.70E+00	6.79E-01	1.99E-02
246	FBgn0027556	CG4928	1.01E+01	6.76E-01	7.10E-03
247	FBgn0032373	Vha100-5	9.51E+00	6.76E-01	2.39E-02
248	FBgn0036106	CG6409	1.24E+01	6.76E-01	4.15E-02
249	FBgn0003651	svp	8.05E+00	6.75E-01	1.94E-02
250	FBgn0042104	CG18747	6.15E+00	6.75E-01	2.93E-02
251	FBgn0260745	mfas	1.05E+01	6.75E-01	1.25E-02
252	FBgn0030999	Mur18B	1.39E+01	6.73E-01	2.06E-02
253	FBgn0045064	bwa	9.55E+00	6.68E-01	1.48E-02
254	FBgn0259111	Ndae1	9.46E+00	6.68E-01	9.80E-03
255	FBgn0001297	kay	1.03E+01	6.64E-01	1.50E-03
256	FBgn0039776	PH4alphaEFB	9.66E+00	6.64E-01	1.43E-02
257	FBgn0000299	Cg25C	1.15E+01	6.62E-01	3.23E-02
258	FBgn0003731	Egfr	9.71E+00	6.62E-01	3.60E-02
259	FBgn0033367	PPO2	9.21E+00	6.62E-01	4.15E-02
260	FBgn0038719	CG16727	8.92E+00	6.62E-01	3.36E-02
261	FBgn0086450	su(r)	1.01E+01	6.62E-01	2.80E-03
262	FBgn0038353	CG5399	1.11E+01	6.60E-01	3.88E-02
263	FBgn0032006	Pvr	9.50E+00	6.58E-01	4.10E-03
264	FBgn0026255	clumsy	6.33E+00	6.57E-01	2.31E-02

265	FBgn0031813	CG9527	1.04E+01	6.57E-01	1.95E-02
266	FBgn0000636	Fas3	9.64E+00	6.56E-01	2.60E-03
267	FBgn0039670	CG7567	7.19E+00	6.55E-01	4.19E-02
268	FBgn0259736	CG42390	1.00E+01	6.55E-01	2.02E-02
269	FBgn0020521	pio	8.45E+00	6.53E-01	1.04E-02
270	FBgn0033504	CAP	1.02E+01	6.51E-01	1.45E-02
271	FBgn0031461	daw	7.77E+00	6.48E-01	2.43E-02
272	FBgn0033788	CG13323	1.10E+01	6.48E-01	4.41E-02
273	FBgn0050115	GEFmeso	8.79E+00	6.44E-01	2.40E-02
274	FBgn0085402	Ect4	1.21E+01	6.42E-01	7.20E-03
275	FBgn0034718	wdp	1.01E+01	6.40E-01	1.44E-02
276	FBgn0027578	CG14526	8.70E+00	6.39E-01	2.85E-02
277	FBgn0031745	rau	6.88E+00	6.38E-01	2.30E-02
278	FBgn0037853	CG14696	6.09E+00	6.36E-01	3.31E-02
279	FBgn0038631	CG7695	8.46E+00	6.36E-01	4.81E-02
280	FBgn0085408	Shroom	9.01E+00	6.35E-01	2.76E-02
281	FBgn0086901	cv-c	9.51E+00	6.35E-01	1.04E-02
282	FBgn0039620	wat	9.33E+00	6.33E-01	2.48E-02
283	FBgn0030156	CG15247	6.73E+00	6.30E-01	4.66E-02
284	FBgn0052372	ltl	8.41E+00	6.29E-01	8.10E-03
285	FBgn0259878	Fs	8.79E+00	6.29E-01	3.68E-02

286	FBgn0000635	Fas2	8.78E+00	6.28E-01	1.00E-02
287	FBgn0013988	Strn-Mlck	1.08E+01	6.28E-01	2.37E-02
288	FBgn0035976	PGRP-LC	9.02E+00	6.26E-01	2.82E-02
289	FBgn0050456	CG30456	9.10E+00	6.26E-01	2.50E-03
290	FBgn0039756	CG9743	8.82E+00	6.25E-01	7.20E-03
291	FBgn0016694	Pdp1	1.03E+01	6.19E-01	4.90E-03
292	FBgn0028859	CG42818	7.04E+00	6.18E-01	1.85E-02
293	FBgn0028859	CG42817	7.04E+00	6.18E-01	1.85E-02
294	FBgn0002527	LanB1	9.89E+00	6.16E-01	4.09E-02
295	FBgn0036806	Cyp12c1	7.35E+00	6.16E-01	1.08E-02
296	FBgn0037683	CG18473	6.95E+00	6.16E-01	4.91E-02
297	FBgn0050015	CG30015	9.84E+00	6.15E-01	2.31E-02
298	FBgn0029821	CG4020	1.02E+01	6.14E-01	7.20E-03
299	FBgn0034909	CG4797	8.85E+00	6.14E-01	8.90E-03
300	FBgn0052352	CG43078	1.02E+01	6.14E-01	3.29E-02
301	FBgn0028550	Atf3	8.12E+00	6.13E-01	1.85E-02
302	FBgn0039483	CG14259	7.10E+00	6.13E-01	1.94E-02
303	FBgn0001145	Gs2	1.16E+01	6.12E-01	1.45E-02
304	FBgn0033821	CG10799	8.95E+00	6.12E-01	7.80E-03
305	FBgn0086680	vvl	7.63E+00	6.12E-01	4.00E-03
306	FBgn0038603	PKD	8.20E+00	6.10E-01	1.04E-02

307	FBgn0050069	CG30069	8.24E+00	6.08E-01	3.25E-02
308	FBgn0037547	CG7910	1.14E+01	6.07E-01	2.29E-02
309	FBgn0051324	CG31324	7.82E+00	6.07E-01	1.81E-02
310	FBgn0024150	Ac78C	6.20E+00	6.06E-01	1.50E-02
311	FBgn0037213	CG12581	8.82E+00	6.06E-01	1.20E-03
312	FBgn0039008	CG6972	7.02E+00	6.06E-01	3.30E-02
313	FBgn0033448	hebe	9.93E+00	6.05E-01	1.17E-02
314	FBgn0037090	Est-Q	8.48E+00	6.04E-01	1.94E-02
315	FBgn0034436	CG11961	9.24E+00	6.02E-01	1.75E-02
316	FBgn0029147	NtR	8.44E+00	5.99E-01	2.01E-02
317	FBgn0030052	CG12065	9.91E+00	5.96E-01	7.00E-04
318	FBgn0032497	CG44085	9.92E+00	5.93E-01	4.27E-02
319	FBgn0050424	CG30424	6.31E+00	5.93E-01	3.07E-02
320	FBgn0015541	sda	8.64E+00	5.91E-01	2.49E-02
321	FBgn0031313	CG5080	1.02E+01	5.90E-01	1.93E-02
322	FBgn0020414	Idgf3	1.03E+01	5.87E-01	1.82E-02
323	FBgn0039789	CG9717	7.68E+00	5.87E-01	1.32E-02
324	FBgn0023129	aay	1.16E+01	5.85E-01	9.20E-03
325	FBgn0031362	CG17646	1.06E+01	5.85E-01	2.33E-02
326	FBgn0050371	CG30371	8.59E+00	5.83E-01	2.15E-02
327	FBgn0010470	Fkbp14	1.07E+01	5.82E-01	6.50E-03

328	FBgn0261362	PPO1	9.19E+00	5.82E-01	2.91E-02
329	FBgn0014018	Rel	1.12E+01	5.81E-01	1.45E-02
330	FBgn0085427	CG34398	8.10E+00	5.80E-01	9.80E-03
331	FBgn0034886	Pde8	9.00E+00	5.78E-01	1.67E-02
332	FBgn0038183	CG9286	9.02E+00	5.78E-01	1.85E-02
333	FBgn0035542	DOR	1.10E+01	5.76E-01	2.42E-02
334	FBgn0053970	CG33970	8.81E+00	5.76E-01	1.46E-02
335	FBgn0261552	ps	1.03E+01	5.76E-01	2.71E-02
336	FBgn0002733	E(spl)mbeta-HLH	6.45E+00	5.75E-01	3.84E-02
337	FBgn0004456	mew	9.23E+00	5.75E-01	2.65E-02
338	FBgn0039266	CG11791	9.67E+00	5.74E-01	1.30E-03
339	FBgn0032652	CG6870	7.91E+00	5.73E-01	2.76E-02
340	FBgn0000504	dsx	7.67E+00	5.71E-01	1.89E-02
341	FBgn0085388	IP3K2	9.17E+00	5.68E-01	1.14E-02
342	FBgn0034723	CG13506	9.40E+00	5.67E-01	1.74E-02
343	FBgn0032010	CG8086	8.62E+00	5.66E-01	3.54E-02
344	FBgn0033919	CG8547	9.67E+00	5.66E-01	2.66E-02
345	FBgn0033982	Cyp317a1	6.09E+00	5.63E-01	4.91E-02
346	FBgn0003068	per	7.76E+00	5.62E-01	2.71E-02
347	FBgn0035376	Tet	7.46E+00	5.59E-01	3.46E-02
348	FBgn0000261	Cat	1.23E+01	5.56E-01	3.04E-02

349	FBgn0003249	Rh3	9.53E+00	5.56E-01	3.33E-02
350	FBgn0038290	CG6912	7.71E+00	5.55E-01	4.91E-02
351	FBgn0029167	Hml	8.83E+00	5.53E-01	4.66E-02
352	FBgn0030251	CG2145	9.84E+00	5.52E-01	4.62E-02
353	FBgn0015221	Fer2LCH	1.36E+01	5.51E-01	6.10E-03
354	FBgn0024250	brk	7.37E+00	5.51E-01	3.60E-02
355	FBgn0015872	Drip	8.78E+00	5.50E-01	1.64E-02
356	FBgn0041712	yellow-d	9.61E+00	5.50E-01	6.00E-03
357	FBgn0031548	CG8852	6.18E+00	5.49E-01	4.51E-02
358	FBgn0031523	CG15408	7.81E+00	5.48E-01	4.08E-02
359	FBgn0031055	et	6.95E+00	5.44E-01	3.54E-02
360	FBgn0014141	cher	1.20E+01	5.43E-01	8.10E-03
361	FBgn0039800	Npc2g	1.01E+01	5.41E-01	4.55E-02
362	FBgn0034920	CG5597	9.46E+00	5.38E-01	3.78E-02
363	FBgn0035755	CG14830	7.31E+00	5.38E-01	1.63E-02
364	FBgn0038826	Syp	8.66E+00	5.38E-01	3.06E-02
365	FBgn0039022	CG4725	7.19E+00	5.35E-01	3.84E-02
366	FBgn0041180	Tep4	1.11E+01	5.32E-01	3.62E-02
367	FBgn0060296	pain	8.30E+00	5.32E-01	1.96E-02
368	FBgn0002968	Nrg	1.06E+01	5.30E-01	6.00E-03
369	FBgn0034761	CG4250	9.33E+00	5.29E-01	2.47E-02

370	FBgn0034985	CG3328	8.08E+00	5.29E-01	1.13E-02
371	FBgn0052280	CG32280	8.28E+00	5.28E-01	9.80E-03
372	FBgn0261563	wb	7.75E+00	5.28E-01	4.00E-02
373	FBgn0035710	SP1173	9.40E+00	5.24E-01	5.30E-03
374	FBgn0032156	CG13124	1.06E+01	5.23E-01	3.31E-02
375	FBgn0039208	Esyt2	8.98E+00	5.23E-01	3.62E-02
376	FBgn0013733	shot	1.22E+01	5.20E-01	2.47E-02
377	FBgn0037007	CG5059	1.12E+01	5.20E-01	7.70E-03
378	FBgn0011274	Dif	8.72E+00	5.18E-01	2.85E-02
379	FBgn0039043	CG17121	7.98E+00	5.18E-01	3.77E-02
380	FBgn0025683	CG3164	1.25E+01	5.17E-01	7.40E-03
381	FBgn0036663	CG9674	1.19E+01	5.17E-01	1.00E-02
382	FBgn0037439	CG10286	1.01E+01	5.17E-01	2.90E-03
383	FBgn0040732	CG16926	1.21E+01	5.16E-01	4.35E-02
384	FBgn0034225	veil	9.99E+00	5.14E-01	2.84E-02
385	FBgn0038465	Irc	1.13E+01	5.12E-01	1.94E-02
386	FBgn0024183	vig	1.05E+01	5.11E-01	7.80E-03
387	FBgn0038752	CG4462	6.78E+00	5.11E-01	4.34E-02
388	FBgn0051145	CG31145	9.80E+00	5.08E-01	1.61E-02
389	FBgn0083919	Zasp52	1.19E+01	5.08E-01	4.43E-02
390	FBgn0032298	CG6724	9.34E+00	5.06E-01	2.70E-02

391	FBgn0020764	Alas	1.11E+01	5.05E-01	4.90E-03
392	FBgn0022160	Gpo-1	1.07E+01	5.05E-01	2.71E-02
393	FBgn0031068	Alr	9.30E+00	5.05E-01	1.14E-02
394	FBgn0027560	Tps1	1.34E+01	5.03E-01	3.16E-02
395	FBgn0050104	NT5E-2	8.43E+00	5.03E-01	2.04E-02
396	FBgn0037796	CG12814	7.25E+00	5.02E-01	3.50E-02
397	FBgn0027864	Ogg1	8.46E+00	-5.02E-01	2.91E-02
398	FBgn0022246	Rpp30	8.55E+00	-5.03E-01	3.63E-02
399	FBgn0037535	CG14463	9.03E+00	-5.03E-01	3.97E-02
400	FBgn0040070	Trx-2	1.31E+01	-5.04E-01	3.54E-02
401	FBgn0040396	CG3939	9.39E+00	-5.06E-01	2.92E-02
402	FBgn0030048	CG12112	9.00E+00	-5.07E-01	2.38E-02
403	FBgn0036804	Sgf11	8.83E+00	-5.07E-01	2.71E-02
404	FBgn0038234	mRpL11	9.57E+00	-5.07E-01	4.54E-02
405	FBgn0051075	CG31075	1.16E+01	-5.07E-01	3.30E-02
406	FBgn0035210	msd5	9.85E+00	-5.11E-01	2.39E-02
407	FBgn0085224	CG34195	9.12E+00	-5.11E-01	4.73E-02
408	FBgn0003450	snk	8.71E+00	-5.12E-01	2.46E-02
409	FBgn0031977	baf	1.18E+01	-5.12E-01	3.54E-02
410	FBgn0037921	CG6808	7.45E+00	-5.12E-01	3.08E-02
411	FBgn0031880	CG43321	7.90E+00	-5.16E-01	3.56E-02

412	FBgn0031880	CG43322	7.90E+00	-5.16E-01	3.56E-02
413	FBgn0033294	Mal-A4	1.03E+01	-5.20E-01	1.71E-02
414	FBgn0002579	RpL36	1.60E+01	-5.27E-01	2.70E-03
415	FBgn0033366	Ance-4	8.89E+00	-5.27E-01	2.85E-02
416	FBgn0031282	Pex12	8.15E+00	-5.30E-01	3.92E-02
417	FBgn0032816	Nf-YB	8.07E+00	-5.30E-01	4.53E-02
418	FBgn0053129	CG33129	1.36E+01	-5.31E-01	4.57E-02
419	FBgn0010316	dap	1.07E+01	-5.32E-01	2.99E-02
420	FBgn0083961	CG34125	9.48E+00	-5.32E-01	3.77E-02
421	FBgn0259982	l(2)35Cc	1.00E+01	-5.33E-01	3.11E-02
422	FBgn0029915	CG14434	1.06E+01	-5.36E-01	2.76E-02
423	FBgn0033669	PI31	1.20E+01	-5.36E-01	4.43E-02
424	FBgn0034314	nopo	1.12E+01	-5.36E-01	3.46E-02
425	FBgn0010078	RpL23	1.61E+01	-5.37E-01	6.50E-03
426	FBgn0036278	CrzR	8.18E+00	-5.37E-01	2.38E-02
427	FBgn0024912	agt	9.08E+00	-5.38E-01	4.83E-02
428	FBgn0030657	cerv	9.16E+00	-5.40E-01	3.53E-02
429	FBgn0035725	Mis12	8.95E+00	-5.40E-01	2.71E-02
430	FBgn0015338	CG5861	1.15E+01	-5.43E-01	4.66E-02
431	FBgn0039766	CG15536	8.88E+00	-5.44E-01	4.62E-02
432	FBgn0035902	CG6683	8.71E+00	-5.46E-01	4.91E-02

433	FBgn0010398	Lrr47	9.87E+00	-5.47E-01	2.71E-02
434	FBgn0040477	cid	1.03E+01	-5.47E-01	3.55E-02
435	FBgn0032926	CG43346	1.04E+01	-5.48E-01	1.30E-02
436	FBgn0032926	CG43345	1.04E+01	-5.48E-01	1.30E-02
437	FBgn0035189	CG9119	1.04E+01	-5.48E-01	4.54E-02
438	FBgn0039531	CG5611	8.56E+00	-5.50E-01	2.85E-02
439	FBgn0003751	trk	7.19E+00	-5.56E-01	1.33E-02
440	FBgn0003510	Sry-alpha	6.67E+00	-5.58E-01	4.29E-02
441	FBgn0030805	wus	1.13E+01	-5.59E-01	4.66E-02
442	FBgn0033769	CG8768	8.96E+00	-5.59E-01	4.48E-02
443	FBgn0032750	CG10495	9.07E+00	-5.60E-01	1.55E-02
444	FBgn0038080	CG12279	8.65E+00	-5.60E-01	3.40E-02
445	FBgn0029800	lin-52	1.01E+01	-5.63E-01	3.84E-02
446	FBgn0038601	CG18600	1.20E+01	-5.65E-01	4.54E-02
447	FBgn0026238	gus	1.26E+01	-5.69E-01	3.58E-02
448	FBgn0031405	CG4267	1.19E+01	-5.69E-01	2.00E-02
449	FBgn0033089	CG17266	9.79E+00	-5.70E-01	4.27E-02
450	FBgn0036262	CG6910	1.33E+01	-5.72E-01	1.82E-02
451	FBgn0033429	CG12929	7.96E+00	-5.75E-01	3.75E-02
452	FBgn0035109	CG13876	8.44E+00	-5.76E-01	2.65E-02
453	FBgn0038196	CG9922	1.11E+01	-5.76E-01	4.63E-02

454	FBgn0029924	CG4586	1.24E+01	-5.84E-01	1.95E-02
455	FBgn0038586	CG7168	9.79E+00	-5.84E-01	3.23E-02
456	FBgn0004580	Cbp53E	7.05E+00	-5.87E-01	3.01E-02
457	FBgn0039970	CG17508	1.24E+01	-5.92E-01	4.90E-02
458	FBgn0052708	CG32708	9.31E+00	-5.92E-01	3.75E-02
459	FBgn0020300	gk	7.40E+00	-5.93E-01	2.71E-02
460	FBgn0030367	Cyp311a1	7.98E+00	-5.93E-01	2.78E-02
461	FBgn0028535	l(2)35Be	9.56E+00	-5.95E-01	3.21E-02
462	FBgn0027343	fz3	7.21E+00	-5.99E-01	1.25E-02
463	FBgn0037747	CG8481	1.04E+01	-5.99E-01	3.40E-02
464	FBgn0037759	CG8526	8.15E+00	-6.00E-01	1.85E-02
465	FBgn0025382	Rab27	8.00E+00	-6.01E-01	1.17E-02
466	FBgn0034918	Pym	1.06E+01	-6.01E-01	4.29E-02
467	FBgn0038428	CG14894	1.14E+01	-6.02E-01	4.66E-02
468	FBgn0034816	CG3085	7.59E+00	-6.04E-01	2.69E-02
469	FBgn0013753	Bgb	1.01E+01	-6.06E-01	4.80E-02
470	FBgn0032390	dgt2	1.08E+01	-6.07E-01	3.28E-02
471	FBgn0038490	CG5285	7.76E+00	-6.08E-01	3.40E-02
472	FBgn0050438	CG30438	7.04E+00	-6.08E-01	2.70E-02
473	FBgn0052536	CG32536	7.71E+00	-6.08E-01	2.52E-02
474	FBgn0034523	Nnf1a	7.37E+00	-6.10E-01	2.71E-02

475	FBgn0051030	CG31030	7.93E+00	-6.11E-01	3.57E-02
476	FBgn0034008	CG8152	1.06E+01	-6.15E-01	4.00E-02
477	FBgn0037634	hng2	8.86E+00	-6.15E-01	2.71E-02
478	FBgn0030011	Gbeta5	7.61E+00	-6.16E-01	2.40E-02
479	FBgn0261068	LSm7	1.09E+01	-6.17E-01	4.70E-02
480	FBgn0030099	CG12056	8.12E+00	-6.20E-01	3.03E-02
481	FBgn0036368	CG10738	8.32E+00	-6.21E-01	3.31E-02
482	FBgn0037611	CG11755	9.13E+00	-6.24E-01	2.15E-02
483	FBgn0034248	CG14483	1.02E+01	-6.28E-01	4.91E-02
484	FBgn0035120	wac	1.01E+01	-6.28E-01	2.54E-02
485	FBgn0030365	Tango4	1.18E+01	-6.30E-01	4.91E-02
486	FBgn0040823	dpr6	6.99E+00	-6.38E-01	3.00E-02
487	FBgn0050392	CG30392	1.14E+01	-6.38E-01	3.68E-02
488	FBgn0038252	BigH1	1.37E+01	-6.41E-01	3.06E-02
489	FBgn0041004	CG17715	1.15E+01	-6.42E-01	3.84E-02
490	FBgn0038739	CG4686	1.14E+01	-6.44E-01	3.84E-02
491	FBgn0039128	CG13599	1.03E+01	-6.46E-01	1.91E-02
492	FBgn0022097	Vha36-1	1.37E+01	-6.47E-01	3.27E-02
493	FBgn0030323	CG2371	1.04E+01	-6.49E-01	4.02E-02
494	FBgn0037358	elm	1.23E+01	-6.49E-01	3.11E-02
495	FBgn0002962	nos	1.26E+01	-6.50E-01	2.26E-02

496	FBgn0030322	RPA3	1.08E+01	-6.50E-01	2.60E-02
497	FBgn0032524	CG9267	9.71E+00	-6.58E-01	3.54E-02
498	FBgn0050051	CG30051	8.12E+00	-6.59E-01	4.42E-02
499	FBgn0034151	CG15617	6.89E+00	-6.63E-01	3.01E-02
500	FBgn0051032	CR31032	6.24E+00	-6.63E-01	1.70E-02
501	FBgn0032518	RpL24	1.60E+01	-6.66E-01	8.10E-03
502	FBgn0038294	Mf	1.30E+01	-6.69E-01	9.80E-03
503	FBgn0051549	CG31549	1.22E+01	-6.70E-01	3.07E-02
504	FBgn0032987	RpL21	1.65E+01	-6.73E-01	8.90E-03
505	FBgn0039932	fuss	9.03E+00	-6.74E-01	2.25E-02
506	FBgn0037728	CG16817	1.46E+01	-6.75E-01	1.71E-02
507	FBgn0014395	tilB	5.56E+00	-6.76E-01	4.48E-02
508	FBgn0031579	CG15422	7.89E+00	-6.76E-01	2.11E-02
509	FBgn0053995	CG33995	6.81E+00	-6.76E-01	3.66E-02
510	FBgn0034430	mip40	1.11E+01	-6.78E-01	4.28E-02
511	FBgn0260756	CG42554	9.57E+00	-6.82E-01	2.70E-02
512	FBgn0022359	Sodh-2	1.04E+01	-6.84E-01	3.60E-02
513	FBgn0031581	CG43773	7.94E+00	-6.84E-01	3.60E-02
514	FBgn0031581	CG43774	7.94E+00	-6.84E-01	3.60E-02
515	FBgn0032453	CG6180	1.31E+01	-6.87E-01	4.05E-02
516	FBgn0010423	TpnC47D	6.33E+00	-6.91E-01	1.89E-02

517	FBgn0000221	brn	9.79E+00	-6.92E-01	2.84E-02
518	FBgn0033520	Prx2540-1	6.81E+00	-6.94E-01	3.93E-02
519	FBgn0039332	alrm	7.46E+00	-6.94E-01	4.48E-02
520	FBgn0028738	ETH	6.52E+00	-6.95E-01	3.31E-02
521	FBgn0030345	CG1847	1.05E+01	-6.96E-01	4.54E-02
522	FBgn0032399	CG6785	6.82E+00	-6.96E-01	1.32E-02
523	FBgn0038946	rdhB	6.53E+00	-6.98E-01	4.72E-02
524	FBgn0038609	Nup43	1.17E+01	-7.00E-01	3.03E-02
525	FBgn0032171	CG5846	9.83E+00	-7.07E-01	2.15E-02
526	FBgn0010083	SmB	1.18E+01	-7.10E-01	3.97E-02
527	FBgn0030066	CG1885	9.29E+00	-7.10E-01	3.50E-02
528	FBgn0036192	Pallidin	8.02E+00	-7.10E-01	2.93E-02
529	FBgn0030776	CG4653	9.79E+00	-7.11E-01	4.01E-02
530	FBgn0037017	CG4074	8.40E+00	-7.13E-01	1.55E-02
531	FBgn0051207	CG31207	8.12E+00	-7.14E-01	3.81E-02
532	FBgn0033810	CG4646	1.04E+01	-7.17E-01	3.84E-02
533	FBgn0039881	CG1971	8.61E+00	-7.22E-01	1.36E-02
534	FBgn0030777	CG9672	9.81E+00	-7.23E-01	4.15E-02
535	FBgn0085290	CG34261	8.52E+00	-7.23E-01	3.12E-02
536	FBgn0032162	CG4592	1.06E+01	-7.26E-01	4.59E-02
537	FBgn0050042	Cpr49Ab	1.03E+01	-7.26E-01	3.83E-02

538	FBgn0036062	CG6685	9.30E+00	-7.27E-01	3.93E-02
539	FBgn0016697	Prosalpha5	1.29E+01	-7.31E-01	4.86E-02
540	FBgn0051360	CG31360	8.75E+00	-7.33E-01	4.86E-02
541	FBgn0035209	msd1	1.06E+01	-7.34E-01	2.71E-02
542	FBgn0020385	pug	1.30E+01	-7.35E-01	1.00E-02
543	FBgn0085271	CG34242	7.90E+00	-7.35E-01	4.52E-02
544	FBgn0031580	CG15423	7.88E+00	-7.36E-01	4.67E-02
545	FBgn0036847	CG11577	1.12E+01	-7.37E-01	4.71E-02
546	FBgn0053514	CG33514	8.27E+00	-7.38E-01	1.00E-02
547	FBgn0054001	CG34001	7.91E+00	-7.38E-01	6.80E-03
548	FBgn0032871	CG2611	7.64E+00	-7.40E-01	8.80E-03
549	FBgn0040718	CG15353	5.96E+00	-7.42E-01	3.45E-02
550	FBgn0036696	CG14057	8.96E+00	-7.45E-01	1.94E-02
551	FBgn0031992	CG8498	1.09E+01	-7.46E-01	2.70E-02
552	FBgn0052625	CG32625	8.81E+00	-7.46E-01	4.76E-02
553	FBgn0029134	Prosbeta5	1.38E+01	-7.50E-01	2.90E-02
554	FBgn0033348	Spt	7.86E+00	-7.51E-01	3.54E-02
555	FBgn0034705	CG11170	8.51E+00	-7.53E-01	2.15E-02
556	FBgn0086683	Spf45	1.11E+01	-7.57E-01	2.54E-02
557	FBgn0035817	CG7409	9.55E+00	-7.60E-01	2.66E-02
558	FBgn0030573	nmdyn-D6	8.11E+00	-7.63E-01	3.92E-02

559	FBgn0003480	spn-B	1.01E+01	-7.67E-01	2.25E-02
560	FBgn0033549	mms4	1.06E+01	-7.67E-01	4.05E-02
561	FBgn0051189	CG31189	5.60E+00	-7.68E-01	2.81E-02
562	FBgn0019985	mGluR	7.02E+00	-7.69E-01	1.72E-02
563	FBgn0051266	CG31266	7.16E+00	-7.79E-01	3.71E-02
564	FBgn0051812	CG31812	6.07E+00	-7.81E-01	1.45E-02
565	FBgn0029648	CG3603	1.03E+01	-7.82E-01	4.02E-02
566	FBgn0030944	CG6617	1.13E+01	-7.84E-01	3.31E-02
567	FBgn0031106	Syx16	1.07E+01	-7.85E-01	2.65E-02
568	FBgn0259832	CG34229	7.63E+00	-7.88E-01	4.66E-02
569	FBgn0040832	CG8012	7.89E+00	-7.90E-01	1.57E-02
570	FBgn0039159	mRpS24	8.47E+00	-7.92E-01	3.76E-02
571	FBgn0052220	Csas	5.73E+00	-7.94E-01	3.22E-02
572	FBgn0259112	CR42254	6.80E+00	-7.94E-01	7.20E-03
573	FBgn0031176	CG1678	1.43E+01	-7.95E-01	1.65E-02
574	FBgn0034232	CG4866	1.13E+01	-7.96E-01	2.91E-02
575	FBgn0028534	CG7916	1.14E+01	-8.01E-01	4.59E-02
576	FBgn0005633	fln	8.75E+00	-8.03E-01	1.55E-02
577	FBgn0051957	CG31957	1.02E+01	-8.04E-01	4.62E-02
578	FBgn0032945	CG8665	7.30E+00	-8.08E-01	1.80E-02
579	FBgn0040588	CG13841	6.14E+00	-8.08E-01	3.54E-02

580	FBgn0001491	l(1)10Bb	1.10E+01	-8.12E-01	4.80E-02
581	FBgn0035603	CG10635	1.12E+01	-8.12E-01	4.90E-02
582	FBgn0031040	CG14210	9.42E+00	-8.14E-01	4.16E-02
583	FBgn0037802	Sirt6	9.61E+00	-8.19E-01	3.03E-02
584	FBgn0029665	CG14270	1.09E+01	-8.20E-01	3.31E-02
585	FBgn0030294	Pa1	1.13E+01	-8.22E-01	3.76E-02
586	FBgn0062928	pncr009:3L	1.12E+01	-8.23E-01	3.03E-02
587	FBgn0043783	CG32444	1.26E+01	-8.24E-01	2.85E-02
588	FBgn0087021	Spc25	1.13E+01	-8.26E-01	2.34E-02
589	FBgn0019932	SamDC	1.09E+01	-8.27E-01	3.00E-02
590	FBgn0036546	elgi	1.23E+01	-8.30E-01	2.65E-02
591	FBgn0058045	CG40045	1.25E+01	-8.31E-01	4.00E-02
592	FBgn0086691	UK114	1.18E+01	-8.34E-01	1.14E-02
593	FBgn0031961	CG7102	6.71E+00	-8.38E-01	1.61E-02
594	FBgn0259144	CG42259	8.79E+00	-8.40E-01	2.65E-02
595	FBgn0260939	Sgt1	1.22E+01	-8.44E-01	2.47E-02
596	FBgn0034664	CG4377	1.02E+01	-8.46E-01	8.20E-03
597	FBgn0039291	CG13663	1.04E+01	-8.49E-01	3.57E-02
598	FBgn0034474	Obp56g	7.38E+00	-8.58E-01	3.84E-02
599	FBgn0052207	CR32207	1.17E+01	-8.61E-01	3.01E-02
600	FBgn0004908	Arl2	8.94E+00	-8.62E-01	2.49E-02

601	FBgn0030257	CG11160	6.09E+00	-8.68E-01	1.77E-02
602	FBgn0052230	CG32230	1.30E+01	-8.73E-01	1.25E-02
603	FBgn0032612	CG13282	4.54E+00	-8.74E-01	2.65E-02
604	FBgn0003275	RpII18	1.09E+01	-8.75E-01	3.71E-02
605	FBgn0030852	CG8316	6.67E+00	-8.75E-01	4.54E-02
606	FBgn0035754	MED4	1.02E+01	-8.75E-01	3.47E-02
607	FBgn0003482	spn-D	8.12E+00	-8.76E-01	2.70E-02
608	FBgn0037199	CG11137	1.25E+01	-8.76E-01	1.55E-02
609	FBgn0030244	CG2157	6.05E+00	-8.77E-01	3.31E-02
610	FBgn0052856	CG32856	8.72E+00	-8.78E-01	1.63E-02
611	FBgn0037263	slx1	8.51E+00	-8.81E-01	1.47E-02
612	FBgn0044872	FucTC	4.20E+00	-8.81E-01	2.15E-02
613	FBgn0039269	veli	1.10E+01	-8.87E-01	1.14E-02
614	FBgn0036887	CG9231	1.26E+01	-8.88E-01	2.25E-02
615	FBgn0036726	CG7603	1.17E+01	-8.92E-01	2.66E-02
616	FBgn0037898	CG18643	7.05E+00	-8.92E-01	4.73E-02
617	FBgn0038589	CG18598	6.24E+00	-8.93E-01	1.40E-02
618	FBgn0025839	CG3621	1.17E+01	-9.10E-01	2.46E-02
619	FBgn0033554	Lsm10	8.34E+00	-9.11E-01	2.28E-02
620	FBgn0031561	CG16712	1.29E+01	-9.12E-01	1.74E-02
621	FBgn0040532	CG8369	1.09E+01	-9.14E-01	1.55E-02

622	FBgn0051148	CG31148	7.81E+00	-9.14E-01	1.65E-02
623	FBgn0031378	CG15362	1.01E+01	-9.16E-01	3.83E-02
624	FBgn0028532	CG7968	8.34E+00	-9.25E-01	5.80E-03
625	FBgn0004087	Dhfr	1.10E+01	-9.34E-01	2.19E-02
626	FBgn0033000	CG14464	1.20E+01	-9.34E-01	3.90E-02
627	FBgn0035675	CG6610	9.95E+00	-9.35E-01	4.03E-02
628	FBgn0061198	HSPC300	1.01E+01	-9.39E-01	2.74E-02
629	FBgn0016970	l(2)k10201	1.03E+01	-9.42E-01	3.06E-02
630	FBgn0029948	CheA7a	8.17E+00	-9.43E-01	4.54E-02
631	FBgn0243513	cnir	8.41E+00	-9.43E-01	4.25E-02
632	FBgn0037751	topi	4.69E+00	-9.44E-01	4.69E-02
633	FBgn0040751	CG13018	7.64E+00	-9.45E-01	4.10E-02
634	FBgn0015299	Ssb-c31a	1.19E+01	-9.46E-01	1.58E-02
635	FBgn0029712	CG15912	6.94E+00	-9.51E-01	2.81E-02
636	FBgn0033723	CG13155	8.20E+00	-9.51E-01	3.27E-02
637	FBgn0032202	CG18619	1.03E+01	-9.56E-01	2.99E-02
638	FBgn0042119	Cpr65Au	9.61E+00	-9.57E-01	1.35E-02
639	FBgn0013981	His4r	1.42E+01	-9.60E-01	1.16E-02
640	FBgn0050096	CG30096	7.59E+00	-9.61E-01	9.80E-03
641	FBgn0085279	CG34250	7.85E+00	-9.65E-01	2.71E-02
642	FBgn0040007	RpL38	1.58E+01	-9.72E-01	2.40E-03

643	FBgn0261508	CG42656	6.42E+00	-9.74E-01	4.52E-02
644	FBgn0013749	Arf102F	1.20E+01	-9.76E-01	3.98E-02
645	FBgn0261534	l(2)34Fc	8.58E+00	-9.77E-01	3.07E-02
646	FBgn0031505	CG12400	1.20E+01	-9.78E-01	1.63E-02
647	FBgn0038654	CG14298	5.97E+00	-9.81E-01	4.34E-02
648	FBgn0024196	robl	1.19E+01	-9.91E-01	1.95E-02
649	FBgn0034578	CG15653	8.30E+00	-9.94E-01	2.06E-02
650	FBgn0032593	Trpgamma	3.88E+00	-9.99E-01	4.52E-02
651	FBgn0044511	mRpS21	1.09E+01	-9.99E-01	3.00E-02
652	FBgn0032088	CG13102	7.05E+00	-1.00E+00	1.45E-02
653	FBgn0031560	CG16713	9.89E+00	-1.01E+00	2.99E-02
654	FBgn0036105	Blos4	9.20E+00	-1.02E+00	4.15E-02
655	FBgn0052069	CG32069	9.21E+00	-1.02E+00	2.71E-02
656	FBgn0086608	CG34112	5.56E+00	-1.02E+00	2.59E-02
657	FBgn0032055	CG13091	1.00E+01	-1.03E+00	1.43E-02
658	FBgn0037015	cmpy	3.49E+00	-1.04E+00	4.12E-02
659	FBgn0031157	CG1503	6.59E+00	-1.06E+00	3.54E-02
660	FBgn0039679	ppk19	5.24E+00	-1.07E+00	2.76E-02
661	FBgn0030676	CG12379	6.17E+00	-1.08E+00	1.96E-02
662	FBgn0031558	CG16704	9.24E+00	-1.08E+00	1.13E-02
663	FBgn0083983	mRpL34	9.18E+00	-1.08E+00	1.44E-02

664	FBgn0032266	CG18302	5.29E+00	-1.09E+00	4.52E-02
665	FBgn0053977	CG33977	8.80E+00	-1.09E+00	2.91E-02
666	FBgn0051715	CG31715	1.12E+01	-1.10E+00	2.08E-02
667	FBgn0083990	sphinx	6.21E+00	-1.10E+00	1.55E-02
668	FBgn0013303	Nca	1.06E+01	-1.11E+00	3.54E-02
669	FBgn0015316	Try29F	5.64E+00	-1.11E+00	3.86E-02
670	FBgn0038257	smp-30	1.15E+01	-1.12E+00	1.05E-02
671	FBgn0052205	CR32205	8.14E+00	-1.12E+00	1.91E-02
672	FBgn0033871	CG13339	9.19E+00	-1.13E+00	2.38E-02
673	FBgn0036926	CG7646	7.72E+00	-1.13E+00	2.37E-02
674	FBgn0058439	CG40439	1.11E+01	-1.16E+00	3.84E-02
675	FBgn0053177	CG33177	2.91E+00	-1.17E+00	2.37E-02
676	FBgn0030187	Ipod	6.29E+00	-1.19E+00	8.70E-03
677	FBgn0036324	CG12520	6.55E+00	-1.19E+00	3.03E-02
678	FBgn0053481	dpr7	6.85E+00	-1.19E+00	1.94E-02
679	FBgn0029690	CG6414	4.88E+00	-1.21E+00	2.06E-02
680	FBgn0050285	CG30285	7.44E+00	-1.21E+00	3.37E-02
681	FBgn0040575	CG15922	8.29E+00	-1.22E+00	2.47E-02
682	FBgn0016053	pgc	1.35E+01	-1.23E+00	1.89E-02
683	FBgn0037742	Rpt3R	4.78E+00	-1.23E+00	4.91E-02
684	FBgn0038481	CG17475	8.57E+00	-1.23E+00	3.66E-02

685	FBgn0041005	pncr013:4	1.05E+01	-1.25E+00	2.70E-02
686	FBgn0020506	Amyrel	5.75E+00	-1.26E+00	1.65E-02
687	FBgn0031957	TwdlE	5.00E+00	-1.26E+00	2.56E-02
688	FBgn0051029	CG31029	3.79E+00	-1.26E+00	3.93E-02
689	FBgn0026563	CG1979	7.27E+00	-1.27E+00	1.61E-02
690	FBgn0085475	CG34446	5.49E+00	-1.27E+00	1.13E-02
691	FBgn0040349	CG3699	1.07E+01	-1.28E+00	5.40E-03
692	FBgn0052448	CG32448	7.02E+00	-1.28E+00	1.25E-02
693	FBgn0039761	CG18404	8.48E+00	-1.30E+00	2.10E-02
694	FBgn0040733	CG15068	1.17E+01	-1.31E+00	6.30E-03
695	FBgn0033936	CG17386	4.86E+00	-1.33E+00	9.00E-04
696	FBgn0013348	TpnC41C	8.47E+00	-1.35E+00	7.40E-03
697	FBgn0040634	CG4186	6.98E+00	-1.36E+00	4.80E-02
698	FBgn0085201	CG34172	9.20E+00	-1.38E+00	4.20E-03
699	FBgn0002565	Lsp2	1.26E+01	-1.39E+00	4.80E-03
700	FBgn0001967	NimC3	1.38E+00	-1.41E+00	4.89E-02
701	FBgn0058298	CG40298	5.16E+00	-1.46E+00	2.06E-02
702	FBgn0046776	CR14033	7.01E+00	-1.47E+00	4.80E-03
703	FBgn0039676	ppk20	4.33E+00	-1.49E+00	4.01E-02
704	FBgn0051636	CG31636	5.66E+00	-1.62E+00	2.50E-03
705	FBgn0061196	SIP3	1.08E+00	-1.63E+00	4.59E-02

706	FBgn0085209	CG34180	4.39E+00	-1.66E+00	6.40E-03
707	FBgn0036656	CG13026	2.66E+00	-1.71E+00	4.02E-02
708	FBgn0052831	CG33695	1.63E+00	-1.75E+00	4.15E-02
709	FBgn0051279	CG31279	5.66E+00	-1.81E+00	3.50E-03
710	FBgn0050334	CG30334	6.03E+00	-1.83E+00	2.71E-02
711	FBgn0040705	CG15434	7.73E+00	-1.84E+00	4.00E-04
712	FBgn0039002	CG17625	2.45E+00	-1.92E+00	3.54E-02
713	FBgn0039811	CG15550	9.95E-01	-1.92E+00	3.31E-02
714	FBgn0028853	CG15263	6.69E+00	-2.08E+00	5.40E-03
715	FBgn0054040	CG34040	8.84E+00	-2.14E+00	2.70E-03
716	FBgn0051225	Ir94f	1.46E+00	-2.36E+00	3.68E-02
717	FBgn0031554	CG15418	3.61E+00	-2.37E+00	3.20E-02
718	FBgn0034052	CG8299	5.51E+00	-2.47E+00	1.47E-02

Table A.1: Differentially expressed genes between uninfected WT flies and DXV-infected flies at day7 post infection. Genes presented in the table are selected by log_2 fold Change > 0.5 and p value < 0.05. Gene list is sorted by log_2 fold Change from the largest to the smallest.

A.2 Differentially expressed genes between wildtype flies and *IR-Atg1* flies without DXV infection

	ID	Gene Symbol	AveExpr		log_2FC adj.P.Val
1	FBgn0011832	Ser12	3.18E+00	5.88E+00	1.51E-06
2	FBgn0040725	CG13946	2.43E+00	4.72E+00	1.41E-02
3	FBgn0032549	CG4650	3.23E+00	4.69E+00	2.47E-02
4	FBgn0031276	CG12506	2.14E+00	4.39E+00	2.55E-03
5	FBgn0052198	CG32198	2.49E+00	4.31E+00	3.40E-03
6	FBgn0036068	CG42825	7.59E+00	3.96E+00	1.67E-02
7	FBgn0036068	CG42826	7.59E+00	3.96E+00	1.67E-02
8	FBgn0052071	CG32071	2.20E+00	3.75E+00	1.31E-02
9	FBgn0013278	Hsp70Bb	3.51E+00	3.54E+00	1.66E-02
10	FBgn0010197	Gyc32E	3.41E+00	3.24E+00	1.48E-04
11	FBgn0035941	CG13313	3.58E+00	3.03E+00	8.93E-05
12	FBgn0036468	CG13461	2.43E+00	2.99E+00	2.76E-03
13	FBgn0052302	CG32302	8.24E+00	2.85E+00	7.19E-05
14	FBgn0034296	CG10912	1.06E+01	2.54E+00	8.20E-06
15	FBgn0051809	CG31809	2.30E+00	2.48E+00	3.25E-02
16	FBgn0040503	CG7763	4.99E+00	2.36E+00	1.58E-03
17	FBgn0037724	Fst	8.62E+00	2.31E+00	2.16E-04

18	FBgn0036466	CG18581	1.56E+00	2.28E+00	3.79E-02
19	FBgn0015035	Cyp4e3	8.20E+00	2.22E+00	2.01E-05
20	FBgn0034288	CG5084	1.70E+00	2.16E+00	2.76E-02
21	FBgn0036467	CG12310	5.32E+00	2.15E+00	9.33E-03
22	FBgn0003067	Pepck	1.32E+01	2.13E+00	3.23E-06
23	FBgn0040730	CG15127	4.08E+00	2.12E+00	5.63E-04
24	FBgn0013772	Cyp6a8	5.49E+00	2.08E+00	7.19E-05
25	FBgn0036226	CG7252	1.98E+00	2.04E+00	3.49E-02
26	FBgn0039694	fig	2.95E+00	2.03E+00	2.06E-03
27	FBgn0083972	CG34136	7.49E+00	2.00E+00	4.71E-05
28	FBgn0085319	CG34290	4.36E+00	1.97E+00	5.81E-03
29	FBgn0031412	CG16995	4.06E+00	1.95E+00	1.53E-02
30	FBgn0036419	CG13482	7.61E+00	1.94E+00	2.69E-03
31	FBgn0032381	Mal-B1	1.02E+01	1.91E+00	8.93E-05
32	FBgn0035348	CG16758	1.17E+01	1.89E+00	2.01E-05
33	FBgn0034279	CG18635	6.01E+00	1.85E+00	8.93E-05
34	FBgn0259232	Dscam4	6.80E+00	1.84E+00	2.55E-03
35	FBgn0036181	Muc68Ca	2.98E+00	1.83E+00	1.14E-02
36	FBgn0033789	CG13324	8.27E+00	1.82E+00	1.60E-03
37	FBgn0030928	CG15044	6.06E+00	1.81E+00	6.26E-04
38	FBgn0051427	CG31427	3.44E+00	1.81E+00	1.15E-02

39	FBgn0035949	CG13314	5.54E+00	1.79E+00	7.06E-05
40	FBgn0003719	tld	6.25E+00	1.67E+00	5.63E-04
41	FBgn0038074	Gnmt	9.48E+00	1.66E+00	9.53E-04
42	FBgn0036836	CG11619	6.57E+00	1.66E+00	2.51E-04
43	FBgn0033659	Damm	8.87E+00	1.63E+00	4.65E-03
44	FBgn0035790	Cyp316a1	2.90E+00	1.62E+00	2.10E-02
45	FBgn0037684	CG8129	9.21E+00	1.60E+00	6.58E-06
46	FBgn0028899	CG31817	4.00E+00	1.60E+00	6.01E-03
47	FBgn0040958	Peritrophin-15b	4.98E+00	1.58E+00	1.36E-02
48	FBgn0034160	CG5550	5.65E+00	1.56E+00	2.88E-02
49	FBgn0033521	CG12896	5.67E+00	1.55E+00	8.48E-04
50	FBgn0033065	Cyp6w1	1.17E+01	1.53E+00	1.34E-03
51	FBgn0013811	Dhc62B	5.44E+00	1.53E+00	2.55E-03
52	FBgn0085285	CG34256	4.83E+00	1.52E+00	4.57E-03
53	FBgn0038172	Adgf-D	9.58E+00	1.51E+00	7.44E-05
54	FBgn0024740	Lip2	6.27E+00	1.49E+00	1.15E-02
55	FBgn0035176	CG13905	8.67E+00	1.48E+00	2.77E-02
56	FBgn0038353	CG5399	1.11E+01	1.48E+00	1.05E-04
57	FBgn0030774	spheroide	9.48E+00	1.46E+00	3.44E-04
58	FBgn0030929	CG15043	1.00E+01	1.45E+00	2.06E-03
59	FBgn0051004	mesh	1.01E+01	1.44E+00	2.63E-03

60	FBgn0063499	GstE10	7.02E+00	1.42E+00	1.86E-04
61	FBgn0085261	CG34232	7.33E+00	1.41E+00	1.77E-04
62	FBgn0035663	CG6462	4.29E+00	1.41E+00	4.30E-03
63	FBgn0032049	Bace	1.22E+01	1.40E+00	3.64E-02
64	FBgn0031906	CG5160	4.16E+00	1.39E+00	1.74E-02
65	FBgn0034758	CG13510	8.74E+00	1.39E+00	9.08E-04
66	FBgn0030999	Mur18B	1.39E+01	1.37E+00	7.19E-05
67	FBgn0062961	pncr016:2R	5.33E+00	1.36E+00	3.14E-03
68	FBgn0033190	CG2137	3.99E+00	1.35E+00	2.06E-02
69	FBgn0051106	CG31106	8.69E+00	1.35E+00	7.07E-05
70	FBgn0085419	Rgk2	5.46E+00	1.35E+00	4.86E-04
71	FBgn0024361	Tsp2A	8.36E+00	1.34E+00	8.48E-04
72	FBgn0041194	Prat2	1.16E+01	1.34E+00	7.19E-05
73	FBgn0025454	Cyp6g1	1.18E+01	1.34E+00	3.36E-04
74	FBgn0037727	CG8358	6.84E+00	1.31E+00	2.41E-04
75	FBgn0031690	CG7742	3.38E+00	1.31E+00	2.65E-02
76	FBgn0051445	CG31445	8.24E+00	1.30E+00	3.97E-04
77	FBgn0029091	CS-2	9.14E+00	1.29E+00	2.48E-04
78	FBgn0033926	Arc1	1.17E+01	1.28E+00	1.98E-04
79	FBgn0038658	CG14292	1.10E+01	1.27E+00	2.34E-04
80	FBgn0039809	CG15547	6.84E+00	1.27E+00	3.18E-03

81	FBgn0035933	CG13309	8.70E+00	1.26E+00	4.65E-03
82	FBgn0054054	CG34054	6.41E+00	1.25E+00	1.64E-02
83	FBgn0041337	Cyp309a2	8.62E+00	1.24E+00	4.52E-03
84	FBgn0033271	CG8708	6.39E+00	1.23E+00	4.08E-04
85	FBgn0039452	CG14245	1.04E+01	1.23E+00	2.51E-04
86	FBgn0034291	CG5770	6.76E+00	1.23E+00	2.76E-02
87	FBgn0038194	Cyp6d5	1.18E+01	1.23E+00	2.48E-04
88	FBgn0037065	CG12974	8.73E+00	1.22E+00	4.28E-04
89	FBgn0032613	CG13283	6.97E+00	1.22E+00	1.70E-04
90	FBgn0030157	CG1468	9.75E+00	1.21E+00	5.58E-04
91	FBgn0033787	CG13321	9.81E+00	1.21E+00	6.80E-04
92	FBgn0035439	CG14961	4.59E+00	1.21E+00	4.86E-02
93	FBgn0054040	CG34040	8.84E+00	1.19E+00	1.03E-02
94	FBgn0035360	CG1246	8.43E+00	1.19E+00	2.46E-04
95	FBgn0013771	Cyp6a9	7.85E+00	1.18E+00	1.03E-02
96	FBgn0085265	CG34236	5.51E+00	1.18E+00	1.80E-02
97	FBgn0031432	Cyp309a1	9.67E+00	1.18E+00	4.08E-04
98	FBgn0029507	Tsp42Ed	9.24E+00	1.17E+00	1.98E-04
99	FBgn0034140	CG8317	1.04E+01	1.15E+00	7.44E-05
100	FBgn0029826	CG6041	6.94E+00	1.14E+00	8.98E-04
101	FBgn0034294	Muc55B	4.01E+00	1.14E+00	2.03E-02

102	FBgn0029831	CG5966	1.09E+01	1.13E+00	1.70E-04
103	FBgn0039629	CG11842	7.34E+00	1.13E+00	3.02E-03
104	FBgn0024293	Spn43Ab	1.16E+01	1.13E+00	4.28E-04
105	FBgn0031580	CG15423	7.88E+00	1.13E+00	1.08E-03
106	FBgn0085227	CG34198	6.14E+00	1.12E+00	2.60E-03
107	FBgn0032908	CG9270	5.44E+00	1.11E+00	2.81E-02
108	FBgn0085205	CG34176	6.92E+00	1.11E+00	1.26E-02
109	FBgn0033788	CG13323	1.10E+01	1.11E+00	1.63E-03
110	FBgn0035583	CG13704	7.49E+00	1.10E+00	1.09E-02
111	FBgn0033820	CG4716	1.30E+01	1.09E+00	4.36E-04
112	FBgn0035094	CG9380	9.62E+00	1.09E+00	3.40E-03
113	FBgn0000406	Cyt-b5-r	1.27E+01	1.08E+00	4.28E-04
114	FBgn0034295	CG10911	1.21E+01	1.07E+00	3.40E-03
115	FBgn0028518	CG18480	7.53E+00	1.07E+00	5.56E-03
116	FBgn0040733	CG15068	1.17E+01	1.06E+00	2.17E-02
117	FBgn0040723	CG5011	9.60E+00	1.06E+00	5.40E-03
118	FBgn0026760	Tehao	5.92E+00	1.05E+00	1.84E-02
119	FBgn0053307	CG33307	8.21E+00	1.05E+00	2.96E-04
120	FBgn0028940	Cyp28a5	9.34E+00	1.05E+00	1.44E-03
121	FBgn0034480	CG16898	8.96E+00	1.04E+00	1.02E-02
122	FBgn0031910	CG15818	7.11E+00	1.04E+00	1.98E-02

123	FBgn0037090	Est-Q	8.48E+00	1.03E+00	1.98E-04
124	FBgn0046689	Takl1	6.11E+00	1.03E+00	4.98E-02
125	FBgn0033786	CG44250	1.02E+01	1.03E+00	3.36E-03
126	FBgn0033786	CG44251	1.02E+01	1.03E+00	3.36E-03
127	FBgn0030985	Obp18a	8.34E+00	1.03E+00	6.61E-03
128	FBgn0031695	Cyp4ac3	5.61E+00	1.03E+00	5.95E-03
129	FBgn0051272	CG31272	8.92E+00	1.03E+00	6.39E-04
130	FBgn0035623	mthl2	6.60E+00	1.02E+00	4.53E-03
131	FBgn0032088	CG13102	7.05E+00	1.02E+00	2.69E-03
132	FBgn0050489	Cyp12d1-p	7.19E+00	1.01E+00	6.15E-04
133	FBgn0043806	CG32032	8.15E+00	1.01E+00	2.48E-04
134	FBgn0033815	CG4676	7.16E+00	1.00E+00	2.79E-03
135	FBgn0259714	CG42368	5.92E+00	1.00E+00	1.16E-02
136	FBgn0033124	Tsp42Ec	8.21E+00	9.96E-01	9.24E-03
137	FBgn0031976	CG7367	4.68E+00	9.92E-01	2.89E-02
138	FBgn0040732	CG16926	1.21E+01	9.84E-01	6.35E-04
139	FBgn0028542	NimB4	7.10E+00	9.84E-01	3.44E-04
140	FBgn0040256	Ugt86Dd	7.97E+00	9.83E-01	3.32E-03
141	FBgn0028543	NimB2	1.05E+01	9.78E-01	1.52E-03
142	FBgn0032235	CG5096	9.46E+00	9.74E-01	3.53E-03
143	FBgn0032435	Oatp33Eb	7.76E+00	9.70E-01	3.93E-03

144	FBgn0051326	CG31326	9.47E+00	9.68E-01	4.82E-04
145	FBgn0014396	tim	1.01E+01	9.66E-01	1.45E-03
146	FBgn0051704	CG31704	7.05E+00	9.65E-01	2.67E-02
147	FBgn0039241	CG11089	1.22E+01	9.62E-01	4.18E-05
148	FBgn0032436	CG5418	3.79E+00	9.51E-01	3.98E-02
149	FBgn0036945	Ssk	9.77E+00	9.48E-01	3.27E-03
150	FBgn0030747	CG4301	7.90E+00	9.47E-01	2.73E-02
151	FBgn0034512	CG18067	1.23E+01	9.45E-01	3.21E-02
152	FBgn0033047	CG7882	9.37E+00	9.39E-01	2.11E-03
153	FBgn0037683	CG18473	6.95E+00	9.38E-01	4.61E-03
154	FBgn0038466	CG8907	8.43E+00	9.33E-01	1.44E-02
155	FBgn0042105	CG18748	7.07E+00	9.31E-01	4.37E-03
156	FBgn0000053	ade3	1.24E+01	9.31E-01	9.17E-05
157	FBgn0040299	Myo28B1	7.73E+00	9.28E-01	1.23E-02
158	FBgn0004885	tok	9.69E+00	9.23E-01	2.32E-02
159	FBgn0028936	NimB5	7.55E+00	9.14E-01	8.93E-05
160	FBgn0011822	pcl	6.70E+00	9.13E-01	4.19E-02
161	FBgn0037751	topi	4.69E+00	9.11E-01	3.25E-02
162	FBgn0040850	CG15210	8.08E+00	9.10E-01	2.32E-02
163	FBgn0030334	Karl	8.02E+00	9.04E-01	2.16E-04
164	FBgn0037548	CG7900	8.17E+00	9.03E-01	5.69E-03

165	FBgn0031579	CG15422	7.89E+00	8.99E-01	7.47E-04
166	FBgn0051414	CG31414	8.23E+00	8.85E-01	1.30E-03
167	FBgn0259896	NimC1	8.14E+00	8.84E-01	5.44E-03
168	FBgn0029766	CG15784	1.06E+01	8.79E-01	3.20E-03
169	FBgn0030160	CG9691	1.10E+01	8.77E-01	2.06E-03
170	FBgn0000473	Cyp6a2	7.55E+00	8.70E-01	7.47E-04
171	FBgn0054043	CG34043	7.43E+00	8.66E-01	2.67E-02
172	FBgn0039023	CG4723	7.05E+00	8.64E-01	2.67E-02
173	FBgn0038346	CG44014	9.25E+00	8.62E-01	1.16E-02
174	FBgn0038346	CG44013	9.25E+00	8.62E-01	1.16E-02
175	FBgn0039307	CR13656	5.36E+00	8.61E-01	1.90E-02
176	FBgn0041182	Tep2	1.08E+01	8.50E-01	2.26E-02
177	FBgn0034664	CG4377	1.02E+01	8.49E-01	2.47E-03
178	FBgn0033764	nemy	8.30E+00	8.49E-01	2.09E-02
179	FBgn0035587	CG4623	5.81E+00	8.43E-01	1.26E-02
180	FBgn0028381	Decay	8.42E+00	8.43E-01	2.83E-03
181	FBgn0044047	Ilp6	7.13E+00	8.39E-01	2.19E-02
182	FBgn0016684	NaPi-T	9.34E+00	8.37E-01	1.70E-04
183	FBgn0034493	CG8908	7.15E+00	8.36E-01	2.67E-02
184	FBgn0034717	CG5819	9.61E+00	8.35E-01	7.81E-03
185	FBgn0038465	Irc	1.13E+01	8.33E-01	4.19E-04

186	FBgn0030482	CG1673	1.03E+01	8.26E-01	6.29E-03
187	FBgn0033913	CG8468	9.31E+00	8.17E-01	2.73E-02
188	FBgn0030040	CG15347	9.73E+00	8.12E-01	1.43E-02
189	FBgn0032282	CG7299	6.63E+00	8.10E-01	4.57E-03
190	FBgn0036968	Spn77Ba	8.95E+00	8.09E-01	2.37E-03
191	FBgn0031012	CG8051	7.85E+00	8.09E-01	4.49E-03
192	FBgn0029896	CG3168	1.19E+01	8.08E-01	1.78E-02
193	FBgn0050026	CG30026	7.72E+00	7.97E-01	4.87E-02
194	FBgn0085313	CG34284	7.46E+00	7.93E-01	3.41E-03
195	FBgn0010225	Gel	1.23E+01	7.87E-01	7.93E-04
196	FBgn0040350	CG3690	8.49E+00	7.86E-01	1.31E-02
197	FBgn0031645	CG3036	1.01E+01	7.85E-01	4.65E-03
198	FBgn0039290	CG13654	6.43E+00	7.85E-01	2.59E-02
199	FBgn0053494	CG33494	7.87E+00	7.84E-01	5.23E-03
200	FBgn0015336	CG15865	7.11E+00	7.76E-01	1.23E-02
201	FBgn0002652	squ	1.06E+01	7.70E-01	4.82E-04
202	FBgn0032075	Tsp29Fb	1.08E+01	7.69E-01	2.60E-03
203	FBgn0039564	CG5527	6.53E+00	7.67E-01	2.30E-02
204	FBgn0026721	fat-spondin	1.00E+01	7.61E-01	3.86E-03
205	FBgn0085282	CG34253	6.15E+00	7.60E-01	3.76E-02
206	FBgn0042104	CG18747	6.15E+00	7.57E-01	2.03E-02

207	FBgn0034454	CG15120	6.33E+00	7.57E-01	3.76E-02
208	FBgn0038719	CG16727	8.92E+00	7.55E-01	2.22E-02
209	FBgn0029990	CG2233	1.39E+01	7.54E-01	2.74E-02
210	FBgn0053346	CG33346	9.53E+00	7.41E-01	4.30E-02
211	FBgn0032074	Tsp29Fa	9.49E+00	7.41E-01	1.59E-02
212	FBgn0020513	ade5	1.29E+01	7.36E-01	6.39E-04
213	FBgn0027070	CG17322	1.04E+01	7.27E-01	1.30E-03
214	FBgn0034501	CG13868	1.27E+01	7.27E-01	1.97E-03
215	FBgn0001208	Hn	1.15E+01	7.23E-01	1.02E-02
216	FBgn0020416	Idgf1	9.50E+00	7.21E-01	2.27E-02
217	FBgn0046302	CG10650	9.85E+00	7.19E-01	4.92E-02
218	FBgn0086450	su(r)	1.01E+01	7.10E-01	1.11E-03
219	FBgn0028526	CG15293	1.19E+01	6.98E-01	2.05E-02
220	FBgn0032774	CG17549	1.15E+01	6.95E-01	3.70E-02
221	FBgn0035076	Ance-5	8.71E+00	6.91E-01	1.68E-02
222	FBgn0085241	CG34212	1.01E+01	6.88E-01	1.90E-02
223	FBgn0039817	CG15553	6.44E+00	6.85E-01	4.28E-02
224	FBgn0037517	CG10086	7.81E+00	6.82E-01	2.16E-03
225	FBgn0051778	CG31778	8.32E+00	6.81E-01	2.24E-02
226	FBgn0023507	CG3835	1.18E+01	6.81E-01	5.31E-03
227	FBgn0032382	Mal-B2	1.26E+01	6.80E-01	1.19E-02

228	FBgn0035431	CG14968	7.83E+00	6.80E-01	3.19E-02
229	FBgn0034356	CG10924	7.49E+00	6.78E-01	4.01E-02
230	FBgn0028540	CG9008	9.30E+00	6.77E-01	7.47E-04
231	FBgn0015040	Cyp9c1	8.65E+00	6.75E-01	4.34E-03
232	FBgn0034005	ItgalphaPS4	4.97E+00	6.74E-01	3.79E-02
233	FBgn0033520	Prx2540-1	6.81E+00	6.69E-01	3.69E-02
234	FBgn0032820	fbp	1.13E+01	6.68E-01	2.27E-03
235	FBgn0045761	CHKov1	6.93E+00	6.67E-01	1.81E-02
236	FBgn0036587	CG4950	7.45E+00	6.56E-01	2.22E-02
237	FBgn0035300	CG1139	7.69E+00	6.56E-01	3.02E-02
238	FBgn0027073	CG4302	9.85E+00	6.55E-01	5.60E-03
239	FBgn0034638	CG10433	1.13E+01	6.51E-01	7.91E-03
240	FBgn0034381	List	6.51E+00	6.51E-01	6.73E-03
241	FBgn0015039	Cyp9b2	1.08E+01	6.49E-01	2.47E-02
242	FBgn0010395	Itgbetanu	7.46E+00	6.49E-01	9.53E-03
243	FBgn0044452	Atg2	1.12E+01	6.48E-01	1.34E-02
244	FBgn0030347	CG15739	8.69E+00	6.47E-01	1.36E-02
245	FBgn0025692	CG3814	8.19E+00	6.46E-01	3.84E-02
246	FBgn0050424	CG30424	6.31E+00	6.46E-01	2.67E-02
247	FBgn0014031	Spat	1.14E+01	6.46E-01	1.08E-02
248	FBgn0034200	CG11395	1.11E+01	6.46E-01	2.76E-02

249	FBgn0050269	CG30269	7.06E+00	6.44E-01	3.32E-02
250	FBgn0030775	CG9673	9.47E+00	6.40E-01	1.53E-02
251	FBgn0032935	Atg18b	8.77E+00	6.38E-01	1.48E-02
252	FBgn0031538	CG3246	9.89E+00	6.38E-01	1.08E-02
253	FBgn0034909	CG4797	8.85E+00	6.36E-01	6.01E-03
254	FBgn0038211	CG9649	8.81E+00	6.34E-01	6.01E-03
255	FBgn0052687	CG32687	1.09E+01	6.34E-01	8.73E-03
256	FBgn0031523	CG15408	7.81E+00	6.34E-01	2.86E-02
257	FBgn0025687	LKR	8.66E+00	6.33E-01	2.76E-02
258	FBgn0033093	CG3270	9.51E+00	6.31E-01	1.41E-02
259	FBgn0051769	CG31769	9.66E+00	6.29E-01	1.41E-02
260	FBgn0036368	CG10738	8.32E+00	6.23E-01	2.30E-02
261	FBgn0085360	CG34331	9.11E+00	6.16E-01	1.21E-02
262	FBgn0038088	CG10126	7.85E+00	6.11E-01	1.12E-02
263	FBgn0020385	pug	1.30E+01	6.08E-01	3.79E-02
264	FBgn0034497	CG9090	1.06E+01	6.02E-01	4.31E-02
265	FBgn0002569	Mal-A2	1.03E+01	6.00E-01	3.10E-02
266	FBgn0035091	CG3829	9.67E+00	5.99E-01	3.04E-02
267	FBgn0037714	CG9396	9.06E+00	5.99E-01	1.08E-02
268	FBgn0063497	GstE3	8.86E+00	5.97E-01	1.48E-02
269	FBgn0039927	CG11155	8.74E+00	5.87E-01	6.17E-03

270	FBgn0033079	Fmo-2	9.65E+00	5.85E-01	6.89E-03
271	FBgn0003328	scb	1.05E+01	5.76E-01	1.28E-02
272	FBgn0035083	Tina-1	1.09E+01	5.72E-01	4.18E-05
273	FBgn0012034	AcCoAS	1.30E+01	5.70E-01	2.76E-02
274	FBgn0037146	CG7470	1.22E+01	5.68E-01	9.18E-03
275	FBgn0037166	CG11426	8.12E+00	5.68E-01	7.91E-03
276	FBgn0050371	CG30371	8.59E+00	5.66E-01	3.33E-02
277	FBgn0052672	Atg8a	1.23E+01	5.59E-01	3.32E-03
278	FBgn0043841	vir-1	1.25E+01	5.53E-01	2.52E-02
279	FBgn0051663	CG31663	8.16E+00	5.52E-01	1.08E-02
280	FBgn0037007	CG5059	1.12E+01	5.50E-01	4.34E-03
281	FBgn0031381	Npc2a	1.17E+01	5.50E-01	1.30E-03
282	FBgn0037818	CG6465	7.41E+00	5.48E-01	8.10E-03
283	FBgn0037973	CG18547	9.76E+00	5.45E-01	4.37E-03
284	FBgn0038037	Cyp9f2	1.06E+01	5.45E-01	1.91E-03
285	FBgn0051777	CG31777	8.13E+00	5.45E-01	3.82E-02
286	FBgn0040985	CG6115	1.04E+01	5.38E-01	3.97E-04
287	FBgn0023129	aay	1.16E+01	5.34E-01	1.68E-02
288	FBgn0032213	CG5390	1.03E+01	5.27E-01	3.98E-02
289	FBgn0030521	CtsB1	1.30E+01	5.27E-01	5.59E-04
290	FBgn0036831	CG6839	9.41E+00	5.21E-01	1.67E-02

291	FBgn0028562	sut2	5.90E+00	5.21E-01	3.96E-02
292	FBgn0027579	mino	1.24E+01	5.20E-01	4.50E-03
293	FBgn0014417	CG13397	1.21E+01	5.19E-01	4.33E-04
294	FBgn0011705	rost	1.09E+01	5.10E-01	1.38E-03
295	FBgn0030594	CG9509	1.03E+01	5.10E-01	2.75E-02
296	FBgn0037872	cu	1.10E+01	5.00E-01	1.62E-02
297	FBgn0029843	Nep1	7.53E+00	-5.39E-01	5.23E-03
298	FBgn0033294	Mal-A4	1.03E+01	-5.54E-01	1.31E-02
299	FBgn0039030	CG6660	8.57E+00	-5.66E-01	3.20E-02
300	FBgn0033627	CG13204	7.51E+00	-5.77E-01	3.65E-02
301	FBgn0259112	CR42254	6.80E+00	-5.83E-01	4.60E-02
302	FBgn0037923	CG6813	6.51E+00	-5.83E-01	4.08E-02
303	FBgn0027513	ana2	9.88E+00	-5.90E-01	3.33E-03
304	FBgn0000615	exu	1.34E+01	-5.90E-01	1.59E-03
305	FBgn0035985	Cpr67B	8.04E+00	-6.16E-01	1.44E-02
306	FBgn0026263	bip1	1.00E+01	-6.39E-01	2.45E-04
307	FBgn0052554	CG32554	6.37E+00	-6.46E-01	3.70E-02
308	FBgn0035490	CG1136	6.42E+00	-6.50E-01	1.95E-02
309	FBgn0034262	swi2	5.84E+00	-6.64E-01	2.04E-02
310	FBgn0034270	CG6401	8.41E+00	-6.65E-01	6.19E-04
311	FBgn0035791	CG8539	9.12E+00	-6.65E-01	8.70E-03

312	FBgn0015558	tty	7.46E+00	-6.74E-01	1.75E-02
313	FBgn0002571	Mal-A3	1.00E+01	-7.20E-01	4.19E-02
314	FBgn0083945	CG34109	5.89E+00	-7.42E-01	1.66E-02
315	FBgn0023541	Cyp4d14	6.33E+00	-7.53E-01	1.60E-02
316	FBgn0034312	CG10916	7.60E+00	-7.65E-01	3.40E-03
317	FBgn0032896	CG14400	6.33E+00	-7.69E-01	3.89E-02
318	FBgn0031791	AANATL2	5.50E+00	-7.71E-01	4.99E-02
319	FBgn0040342	CG3706	7.69E+00	-8.14E-01	3.98E-02
320	FBgn0085426	Rgk3	5.85E+00	-8.39E-01	4.01E-02
321	FBgn0033836	CG18278	6.76E+00	-8.44E-01	2.45E-02
322	FBgn0039342	CG5107	1.15E+01	-8.46E-01	2.65E-02
323	FBgn0003390	shf	7.40E+00	-8.73E-01	3.48E-04
324	FBgn0039798	CG11313	6.41E+00	-8.81E-01	2.68E-02
325	FBgn0033817	GstE14	5.83E+00	-9.34E-01	2.32E-02
326	FBgn0004360	Wnt2	4.85E+00	-9.48E-01	2.14E-02
327	FBgn0028534	CG7916	1.14E+01	-9.68E-01	2.76E-02
328	FBgn0031533	CG2772	7.86E+00	-9.71E-01	6.76E-03
329	FBgn0034553	CG9993	6.01E+00	-1.00E+00	2.65E-02
330	FBgn0040823	dpr6	6.99E+00	-1.05E+00	1.63E-03
331	FBgn0011722	Tig	8.49E+00	-1.05E+00	3.93E-03
332	FBgn0053109	CG33109	9.47E+00	-1.05E+00	3.14E-02

333	FBgn0039471	CG6295	1.12E+01	-1.06E+00	2.71E-02
334	FBgn0010549	l(2)03659	9.24E+00	-1.06E+00	4.18E-05
335	FBgn0037782	Npc2d	7.48E+00	-1.10E+00	2.77E-02
336	FBgn0042186	CG17239	8.14E+00	-1.10E+00	2.27E-02
337	FBgn0031451	CG9961	5.28E+00	-1.12E+00	4.27E-03
338	FBgn0053301	CG33301	8.20E+00	-1.12E+00	3.49E-04
339	FBgn0039474	CG6283	1.00E+01	-1.15E+00	3.32E-03
340	FBgn0016054	phr6-4	9.01E+00	-1.16E+00	1.53E-02
341	FBgn0050054	CG30054	7.57E+00	-1.18E+00	1.34E-03
342	FBgn0001089	Gal	8.85E+00	-1.19E+00	1.11E-03
343	FBgn0032085	CG9555	7.02E+00	-1.19E+00	6.34E-03
344	FBgn0036024	CG18180	1.24E+01	-1.25E+00	1.14E-02
345	FBgn0040262	Ugt36Ba	5.70E+00	-1.26E+00	4.02E-03
346	FBgn0000055	Adh	6.25E+00	-1.28E+00	3.18E-03
347	FBgn0031930	CG7025	6.34E+00	-1.29E+00	1.65E-02
348	FBgn0053965	CG33965	6.03E+00	-1.30E+00	1.86E-03
349	FBgn0025583	IM2	1.08E+01	-1.31E+00	4.38E-03
350	FBgn0033603	Cpr47Ef	5.21E+00	-1.36E+00	2.10E-02
351	FBgn0034197	Cda9	6.09E+00	-1.41E+00	1.39E-03
352	FBgn0039476	CG6271	5.51E+00	-1.41E+00	3.46E-03
353	FBgn0032891	Oseg5	6.65E+00	-1.46E+00	4.61E-03

354	FBgn0039475	CG6277	9.35E+00	-1.46E+00	5.51E-04
355	FBgn0031944	CG46025	3.70E+00	-1.47E+00	3.65E-02
356	FBgn0033090	CG15909	2.99E+00	-1.49E+00	1.84E-02
357	FBgn0001224	Hsp23	9.90E+00	-1.49E+00	8.30E-03
358	FBgn0039152	Rootletin	6.38E+00	-1.49E+00	4.24E-03
359	FBgn0033096	Zip42C.1	3.93E+00	-1.49E+00	7.81E-03
360	FBgn0034318	CG14500	8.01E+00	-1.50E+00	1.96E-02
361	FBgn0038790	MtnC	9.04E+00	-1.51E+00	2.55E-03
362	FBgn0082987	snoRNA:Psi28S-2444	3.07E+00	-1.51E+00	2.57E-02
363	FBgn0052483	CG32483	6.51E+00	-1.64E+00	7.81E-04
364	FBgn0002869	MtnB	8.53E+00	-1.68E+00	5.04E-03
365	FBgn0003313	sala	2.01E+00	-1.69E+00	2.77E-02
366	FBgn0032066	CG9463	9.95E+00	-1.77E+00	2.47E-02
367	FBgn0033216	CG1946	4.83E+00	-1.78E+00	1.32E-02
368	FBgn0035666	Jon65Aii	7.40E+00	-1.85E+00	1.60E-02
369	FBgn0032507	CG9377	5.43E+00	-1.86E+00	1.44E-03
370	FBgn0037183	CG14451	2.07E+00	-1.92E+00	1.66E-02
371	FBgn0004428	LysE	4.95E+00	-1.92E+00	2.88E-02
372	FBgn0002939	ninaD	5.57E+00	-1.95E+00	1.73E-03
373	FBgn0004429	LysP	7.35E+00	-2.02E+00	7.06E-05
374	FBgn0052984	CG32984	5.05E+00	-2.12E+00	3.97E-04

375	FBgn0036023	CG18179	7.74E+00	-2.13E+00	6.52E-03
376	FBgn0082940	snoRNA:Me28S-C3227a	9.58E-01	-2.14E+00	1.95E-02
377	FBgn0039684	Obp99d	2.87E+00	-2.14E+00	3.92E-02
378	FBgn0032067	CG9465	6.08E+00	-2.18E+00	4.49E-02
379	FBgn0085358	Diedel3	9.33E+00	-2.25E+00	3.97E-04
380	FBgn0040104	lectin-24A	4.01E+00	-2.67E+00	1.03E-02
381	FBgn0051089	CG31089	3.88E+00	-2.94E+00	2.50E-03
382	FBgn0050091	CG30091	2.07E+00	-3.16E+00	9.53E-03
383	FBgn0035886	Jon66Ci	5.61E+00	-3.18E+00	2.63E-03
384	FBgn0020506	Amyrel	5.75E+00	-3.61E+00	7.19E-05

Table A.2: Differentially expressed genes between wildtype flies and *IR-Atg1* flies without DXV infection. Genes presented in the table are selected by log_2 fold Change $>$ 0.5 and p value $<$ 0.05. Gene list is sorted by log_2 fold Change from the largest to the smallest.

Bibliography

Agaisse, H. and Perrimon, N. (2004). The roles of jak/stat signaling in drosophila immune responses. *Immunol Rev*, 198:72–82.

Agaisse, H., Petersen, U. M., Boutros, M., Mathey-Prevot, B., and Perrimon, N. (2003). Signaling role of hemocytes in drosophila jak/stat-dependent response to septic injury. *Dev Cell*, 5(3):441–50.

Alexa, A., Rahnenführer, J., and Lengauer, T. (2006). Improved scoring of functional groups from gene expression data by decorrelating go graph structure. *Bioinformatics*, 22(13):1600–7.

Alirezaei, M., Flynn, C. T., Wood, M. R., and Whitton, J. L. (2012). Pancreatic acinar cell-specific autophagy disruption reduces coxsackievirus replication and pathogenesis in vivo. *Cell Host Microbe*, 11(3):298–305.

Aliyari, R. and Ding, S.-W. (2009). Rna-based viral immunity initiated by the dicer family of host immune receptors. *Immunol Rev*, 227(1):176–88.

Aliyari, R., Wu, Q., Li, H.-W., Wang, X.-H., Li, F., Green, L. D., Han, C. S., Li, W.-X., and Ding, S.-W. (2008). Mechanism of induction and suppression of antiviral immunity directed by virus-derived small rnas in drosophila. *Cell Host Microbe*, 4(4):387–97.

Anders, S. and Huber, W. (2010). Differential expression analysis for sequence count data. *Genome Biol*, 11(10):R106.

Anders, S., Pyl, P. T., and Huber, W. (2014). Htseq - a python framework to work with high-throughput sequencing data. *Bioinformatics*.

Anderson, K. V. (2000). Toll signaling pathways in the innate immune response. *Curr Opin Immunol*, 12(1):13–9.

Arico, S., Petiot, A., Bauvy, C., Dubbelhuis, P. F., Meijer, A. J., Codogno, P., and Ogier-Denis, E. (2001). The tumor suppressor pten positively regulates macroautophagy by inhibiting the phosphatidylinositol 3-kinase/protein kinase b pathway. *J Biol Chem*, 276(38):35243–6.

Arrese, E. L., Mirza, S., Rivera, L., Howard, A. D., Chetty, P. S., and Soulages, J. L. (2008a). Expression of lipid storage droplet protein-1 may define the role of akh as a lipid mobilizing hormone in manduca sexta. *Insect Biochem Mol Biol*, 38(11):993–1000.

Arrese, E. L., Rivera, L., Hamada, M., Mirza, S., Hartson, S. D., Weintraub, S., and Soulages, J. L. (2008b). Function and structure of lipid storage droplet protein 1 studied in lipoprotein complexes. *Arch Biochem Biophys*, 473(1):42–7.

Arthur, J. S. C. and Ley, S. C. (2013). Mitogen-activated protein kinases in innate immunity. *Nat Rev Immunol*, 13(9):679–92.

Au, K. F., Jiang, H., Lin, L., Xing, Y., and Wong, W. H. (2010). Detection of splice junctions from paired-end rna-seq data by splicemap. *Nucleic Acids Res*, 38(14):4570–8.

Auer, P. L., Srivastava, S., and Doerge, R. W. (2012). Differential expression–the next generation and beyond. *Brief Funct Genomics*, 11(1):57–62.

Autret, A., Martin-Latil, S., Mousson, L., Wirotius, A., Petit, F., Arnoult, D., Colbère-Garapin, F., Estaquier, J., and Blondel, B. (2007). Poliovirus induces bax-dependent cell death mediated by c-jun nh2-terminal kinase. *J Virol*, 81(14):7504–16.

Avadhanula, V., Weasner, B. P., Hardy, G. G., Kumar, J. P., and Hardy, R. W. (2009). A novel system for the launch of alphavirus rna synthesis reveals a role for the imd pathway in arthropod antiviral response. *PLoS Pathog*, 5(9):e1000582.

Baroja-Mazo, A., Martín-Sánchez, F., Gomez, A. I., Martínez, C. M., Amores-Iniesta, J., Compan, V., Barberà-Cremades, M., Yagüe, J., Ruiz-Ortiz, E., Antón, J., Buján, S., Couillin, I., Brough, D., Arostegui, J. I., and Pelegrín, P. (2014). The nlrp3 inflammasome is released as a particulate danger signal that amplifies the inflammatory response. *Nat Immunol*, 15(8):738–48.

Basbous, N., Coste, F., Leone, P., Vincentelli, R., Royet, J., Kellenberger, C., and Rousel, A. (2011). The drosophila peptidoglycan-recognition protein lf interacts with

peptidoglycan-recognition protein lc to downregulate the imd pathway. *EMBO Rep*, 12(4):327–33.

Beller, M., Bulankina, A. V., Hsiao, H.-H., Urlaub, H., Jäckle, H., and Kühnlein, R. P. (2010). Perilipin-dependent control of lipid droplet structure and fat storage in drosophila. *Cell Metab*, 12(5):521–32.

Beller, M., Riedel, D., Jänsch, L., Dieterich, G., Wehland, J., Jäckle, H., and Kühnlein, R. P. (2006). Characterization of the drosophila lipid droplet subproteome. *Mol Cell Proteomics*, 5(6):1082–94.

Benjamini, Y. (1995). Controlling the false discovery rate: A practical and powerful approach to multiple testing. *Journal of the Royal Statistical Society*, 57(1):289–300.

Bernstein, E., Caudy, A. A., Hammond, S. M., and Hannon, G. J. (2001). Role for a bidentate ribonuclease in the initiation step of rna interference. *Nature*, 409(6818):363–6.

Berry, D. L. and Baehrecke, E. H. (2007). Growth arrest and autophagy are required for salivary gland cell degradation in drosophila. *Cell*, 131(6):1137–48.

Bi, J., Xiang, Y., Chen, H., Liu, Z., Grönke, S., Kühnlein, R. P., and Huang, X. (2012). Opposite and redundant roles of the two drosophila perilipins in lipid mobilization. *Journal of cell science*, 125(15):3568–3577.

Bickel, P. E., Tansey, J. T., and Welte, M. A. (2009). Pat proteins, an ancient family of lipid droplet proteins that regulate cellular lipid stores. *Biochim Biophys Acta*, 1791(6):419–40.

Bidla, G., Dushay, M. S., and Theopold, U. (2007). Crystal cell rupture after injury in drosophila requires the jnk pathway, small gtpases and the tnf homolog eiger. *J Cell Sci*, 120(Pt 7):1209–15.

Birghan, C., Mundt, E., and Gorbalenya, A. E. (2000). A non-canonical lon proteinase lacking the atpase domain employs the ser-lys catalytic dyad to exercise broad control over the life cycle of a double-stranded rna virus. *EMBO J*, 19(1):114–23.

Bischoff, V., Vignal, C., Boneca, I. G., Michel, T., Hoffmann, J. A., and Royet, J. (2004). Function of the drosophila pattern-recognition receptor pgrp-sd in the detection of gram-positive bacteria. *Nat Immunol*, 5(11):1175–80.

Bischoff, V., Vignal, C., Duvic, B., Boneca, I. G., Hoffmann, J. A., and Royet, J. (2006). Downregulation of the drosophila immune response by peptidoglycan-recognition proteins sc1 and sc2. *PLoS Pathog*, 2(2):e14.

Blommaart, E. F., Krause, U., Schellens, J. P., Vreeling-Sindelárová, H., and Meijer, A. J. (1997). The phosphatidylinositol 3-kinase inhibitors wortmannin and ly294002 inhibit autophagy in isolated rat hepatocytes. *Eur J Biochem*, 243(1-2):240–6.

Blommaart, E. F., Luiken, J. J., Blommaart, P. J., van Woerkom, G. M., and Meijer, A. J. (1995). Phosphorylation of ribosomal protein s6 is inhibitory for autophagy in isolated rat hepatocytes. *J Biol Chem*, 270(5):2320–6.

Bolstad, B. M., Irizarry, R. A., Astrand, M., and Speed, T. P. (2003). A comparison of normalization methods for high density oligonucleotide array data based on variance and bias. *Bioinformatics*, 19(2):185–93.

Bonnefont, J.-P., Djouadi, F., Prip-Buus, C., Gobin, S., Munnich, A., and Bastin, J. (2004). Carnitine palmitoyltransferases 1 and 2: biochemical, molecular and medical aspects. *Mol Aspects Med*, 25(5-6):495–520.

Böttcher, B., Kiselev, N. A., Stel'Mashchuk, V. Y., Perevozchikova, N. A., Borisov, A. V., and Crowther, R. A. (1997). Three-dimensional structure of infectious bursal disease virus determined by electron cryomicroscopy. *J Virol*, 71(1):325–30.

Boutros, M., Agaisse, H., and Perrimon, N. (2002). Sequential activation of signaling pathways during innate immune responses in drosophila. *Dev Cell*, 3(5):711–22.

Brasaemle, D. L. (2007). Thematic review series: adipocyte biology. the perilipin family of structural lipid droplet proteins: stabilization of lipid droplets and control of lipolysis. *J Lipid Res*, 48(12):2547–59.

Brasaemle, D. L., Subramanian, V., Garcia, A., Marcinkiewicz, A., and Rothenberg, A. (2009). Perilipin a and the control of triacylglycerol metabolism. *Mol Cell Biochem*, 326(1-2):15–21.

Bremer, J. (1983). Carnitine–metabolism and functions. *Physiol Rev*, 63(4):1420–80.

Brogden, K. A. (2005). Antimicrobial peptides: pore formers or metabolic inhibitors in bacteria? *Nat Rev Microbiol*, 3(3):238–50.

Bronkhorst, A. W. and van Rij, R. P. (2014). The long and short of antiviral defense: small rna-based immunity in insects. *Curr Opin Virol*, 7C:19–28.

Brown, E. J., Albers, M. W., Shin, T. B., Ichikawa, K., Keith, C. T., Lane, W. S., and

Schreiber, S. L. (1994). A mammalian protein targeted by g1-arresting rapamycin-receptor complex. *Nature*, 369(6483):756–8.

Bruenn, J. A. (1991). Relationships among the positive strand and double-strand rna viruses as viewed through their rna-dependent rna polymerases. *Nucleic Acids Res*, 19(2):217–26.

Bullard, J. H., Purdom, E., Hansen, K. D., and Dudoit, S. (2010). Evaluation of statistical methods for normalization and differential expression in mrna-seq experiments. *BMC Bioinformatics*, 11:94.

Buszczak, M., Lu, X., Segraves, W. A., Chang, T. Y., and Cooley, L. (2002). Mutations in the midway gene disrupt a drosophila acyl coenzyme a: diacylglycerol acyltransferase. *Genetics*, 160(4):1511–8.

Carpenter, J. A., Obbard, D. J., Maside, X., and Jiggins, F. M. (2007). The recent spread of a vertically transmitted virus through populations of drosophila melanogaster. *Mol Ecol*, 16(18):3947–54.

Cermelli, S., Guo, Y., Gross, S. P., and Welte, M. A. (2006). The lipid-droplet proteome reveals that droplets are a protein-storage depot. *Curr Biol*, 16(18):1783–95.

Chang, C.-I., Chelliah, Y., Borek, D., Mengin-Lecreulx, D., and Deisenhofer, J. (2006). Structure of tracheal cytotoxin in complex with a heterodimeric pattern-recognition receptor. *Science*, 311(5768):1761–4.

Chang, Y.-Y. and Neufeld, T. P. (2009). An atg1/atg13 complex with multiple roles in tor-mediated autophagy regulation. *Mol Biol Cell*, 20(7):2004–14.

Chen, Z. and Duan, X. (2011). Ribosomal rna depletion for massively parallel bacterial rna-sequencing applications. *Methods Mol Biol*, 733:93–103.

Chintapalli, V. R., Wang, J., and Dow, J. A. T. (2007). Using flyatlas to identify better drosophila melanogaster models of human disease. *Nat Genet*, 39(6):715–20.

Choe, K.-M., Lee, H., and Anderson, K. V. (2005). Drosophila peptidoglycan recognition protein lc (pgrp-lc) acts as a signal-transducing innate immune receptor. *Proc Natl Acad Sci U S A*, 102(4):1122–6.

Choe, K.-M., Werner, T., Stöven, S., Hultmark, D., and Anderson, K. V. (2002). Requirement for a peptidoglycan recognition protein (pgrp) in relish activation and antibacterial immune responses in drosophila. *Science*, 296(5566):359–62.

Choi, Y. K., Kim, T.-K., Kim, C.-J., Lee, J.-S., Oh, S.-Y., Joo, H. S., Foster, D. N., Hong, K.-C., You, S., and Kim, H. (2006). Activation of the intrinsic mitochondrial apoptotic pathway in swine influenza virus-mediated cell death. *Exp Mol Med*, 38(1):11–7.

Chotkowski, H. L., Ciota, A. T., Jia, Y., Puig-Basagoiti, F., Kramer, L. D., Shi, P.-Y., and Glaser, R. L. (2008). West nile virus infection of drosophila melanogaster induces a protective rnai response. *Virology*, 377(1):197–206.

Chung, H. K., Kordyban, S., Cameron, L., and Dobos, P. (1996). Sequence analysis of the bicistronic drosophila x virus genome segment a and its encoded polypeptides. *Virology*, 225(2):359–68.

Clarke, P., Meintzer, S. M., Wang, Y., Moffitt, L. A., Richardson-Burns, S. M., Johnson,

G. L., and Tyler, K. L. (2004). Jnk regulates the release of proapoptotic mitochondrial factors in reovirus-infected cells. *J Virol*, 78(23):13132–8.

Costa, A., Jan, E., Sarnow, P., and Schneider, D. (2009). The imd pathway is involved in antiviral immune responses in drosophila. *PLoS One*, 4(10):e7436.

Coulibaly, F., Chevalier, C., Gutsche, I., Pous, J., Navaza, J., Bressanelli, S., Delmas, B., and Rey, F. A. (2005). The birnavirus crystal structure reveals structural relationships among icosahedral viruses. *Cell*, 120(6):761–72.

Crawford, S. E., Hyser, J. M., Utama, B., and Estes, M. K. (2012). Autophagy hijacked through viroporin-activated calcium/calmodulin-dependent kinase kinase- signaling is required for rotavirus replication. *Proc Natl Acad Sci U S A*, 109(50):E3405–13.

Cuervo, A. M. and Dice, J. F. (2000). Unique properties of lamp2a compared to other lamp2 isoforms. *J Cell Sci*, 113 Pt 24:4441–50.

Da Costa, B., Chevalier, C., Henry, C., Huet, J.-C., Petit, S., Lepault, J., Boot, H., and Delmas, B. (2002). The capsid of infectious bursal disease virus contains several small peptides arising from the maturation process of pvp2. *J Virol*, 76(5):2393–402.

De Gregorio, E., Spellman, P. T., Tzou, P., Rubin, G. M., and Lemaitre, B. (2002). The toll and imd pathways are the major regulators of the immune response in drosophila. *EMBO J*, 21(11):2568–79.

Delaney, J. R., Stöven, S., Uvell, H., Anderson, K. V., Engström, Y., and Mlodzik, M. (2006). Cooperative control of drosophila immune responses by the jnk and nf-kappab signaling pathways. *EMBO J*, 25(13):3068–77.

Delgado, M. A., Elmaoued, R. A., Davis, A. S., Kyei, G., and Deretic, V. (2008). Toll-like receptors control autophagy. *EMBO J*, 27(7):1110–21.

Dérijard, B., Hibi, M., Wu, I. H., Barrett, T., Su, B., Deng, T., Karin, M., and Davis, R. J. (1994). Jnk1: a protein kinase stimulated by uv light and ha-ras that binds and phosphorylates the c-jun activation domain. *Cell*, 76(6):1025–37.

Dillies, M.-A., Rau, A., Aubert, J., Hennequet-Antier, C., Jeanmougin, M., Servant, N., Keime, C., Marot, G., Castel, D., Estelle, J., Guernec, G., Jagla, B., Jouneau, L., Laloë, D., Le Gall, C., Schaëffer, B., Le Crom, S., Guedj, M., Jaffrézic, F., and French StatOmique Consortium (2013). A comprehensive evaluation of normalization methods for illumina high-throughput rna sequencing data analysis. *Brief Bioinform*, 14(6):671–83.

Dobos, P. (1995). The molecular biology of infectious pancreatic necrosis virus (ipnv). *Annual Review of Fish Diseases*, 5:25–54.

Dostert, C., Jouanguy, E., Irving, P., Troxler, L., Galiana-Arnoux, D., Hetru, C., Hoffmann, J. A., and Imler, J.-L. (2005). The jak-stat signaling pathway is required but not sufficient for the antiviral response of drosophila. *Nat Immunol*, 6(9):946–53.

Dziarski, R. and Gupta, D. (2006). The peptidoglycan recognition proteins (pgrps). *Genome Biol*, 7(8):232.

Edgar, B. A. and Schubiger, G. (1986). Parameters controlling transcriptional activation during early drosophila development. *Cell*, 44(6):871–7.

Egan, J. J., Greenberg, A. S., Chang, M. K., Wek, S. A., Moos, Jr, M. C., and Londos, C. (1992). Mechanism of hormone-stimulated lipolysis in adipocytes: translocation of hormone-sensitive lipase to the lipid storage droplet. *Proc Natl Acad Sci U S A*, 89(18):8537–41.

Elrod-Erickson, M., Mishra, S., and Schneider, D. (2000). Interactions between the cellular and humoral immune responses in drosophila. *Curr Biol*, 10(13):781–4.

Fahey, K. J., O'Donnell, I. J., and Azad, A. A. (1985). Characterization by western blotting of the immunogens of infectious bursal disease virus. *J Gen Virol*, 66 (Pt 7):1479–88.

Falgueras, J., Lara, A. J., Fernández-Pozo, N., Cantón, F. R., Pérez-Trabado, G., and Claros, M. G. (2010). Seqtrim: a high-throughput pipeline for pre-processing any type of sequence read. *BMC Bioinformatics*, 11:38.

Fauny, J. D., Silber, J., and Zider, A. (2005). Drosophila lipid storage droplet 2 gene (lsd-2) is expressed and controls lipid storage in wing imaginal discs. *Dev Dyn*, 232(3):725–32.

Ferrandon, D., Jung, A. C., Criqui, M., Lemaitre, B., Uttenweiler-Joseph, S., Michaut, L., Reichhart, J., and Hoffmann, J. A. (1998). A drosomycin-gfp reporter transgene reveals a local immune response in drosophila that is not dependent on the toll pathway. *EMBO J*, 17(5):1217–27.

Funakoshi, T., Matsuura, A., Noda, T., and Ohsumi, Y. (1997). Analyses of apg13 gene involved in autophagy in yeast, saccharomyces cerevisiae. *Gene*, 192(2):207–13.

Galiana-Arnoux, D., Dostert, C., Schneemann, A., Hoffmann, J. A., and Imler, J.-L. (2006). Essential function in vivo for dicer-2 in host defense against rna viruses in drosophila. *Nat Immunol*, 7(6):590–7.

Gannagé, M., Dormann, D., Albrecht, R., Dengjel, J., Torossi, T., Rämer, P. C., Lee, M., Strowig, T., Arrey, F., Conenello, G., Pypaert, M., Andersen, J., García-Sastre, A., and Münz, C. (2009). Matrix protein 2 of influenza a virus blocks autophagosome fusion with lysosomes. *Cell Host Microbe*, 6(4):367–80.

Garrington, T. P. and Johnson, G. L. (1999). Organization and regulation of mitogen-activated protein kinase signaling pathways. *Curr Opin Cell Biol*, 11(2):211–8.

Gendrin, M., Zaidman-Rémy, A., Broderick, N. A., Paredes, J., Poidevin, M., Roussel, A., and Lemaitre, B. (2013). Functional analysis of pgrp-la in drosophila immunity. *PLoS One*, 8(7):e69742.

Georgel, P., Naitza, S., Kappler, C., Ferrandon, D., Zachary, D., Swimmer, C., Kopczynski, C., Duyk, G., Reichhart, J. M., and Hoffmann, J. A. (2001). Drosophila immune deficiency (imd) is a death domain protein that activates antibacterial defense and can promote apoptosis. *Dev Cell*, 1(4):503–14.

Gibbings, D., Mostowy, S., Jay, F., Schwab, Y., Cossart, P., and Voinnet, O. (2012). Selective autophagy degrades dicer and ago2 and regulates mirna activity. *Nat Cell Biol*, 14(12):1314–21.

Gorbalenya, A. E. and Koonin, E. V. (1988). Birnavirus rna polymerase is related to polymerases of positive strand rna viruses. *Nucleic Acids Res*, 16(15):7735.

Gottar, M., Gobert, V., Michel, T., Belvin, M., Duyk, G., Hoffmann, J. A., Ferrandon, D., and Royet, J. (2002). The drosophila immune response against gram-negative bacteria is mediated by a peptidoglycan recognition protein. *Nature*, 416(6881):640–4.

Grönke, S., Beller, M., Fellert, S., Ramakrishnan, H., Jäckle, H., and Kühnlein, R. P. (2003). Control of fat storage by a drosophila pat domain protein. *Curr Biol*, 13(7):603–6.

Grönke, S., Mildner, A., Fellert, S., Tennagels, N., Petry, S., Müller, G., Jäckle, H., and Kühnlein, R. P. (2005). Brummer lipase is an evolutionary conserved fat storage regulator in drosophila. *Cell Metab*, 1(5):323–30.

Grönke, S., Müller, G., Hirsch, J., Fellert, S., Andreou, A., Haase, T., Jäckle, H., and Kühnlein, R. P. (2007). Dual lipolytic control of body fat storage and mobilization in drosophila. *PLoS Biol*, 5(6):e137.

Guan, J., Stromhaug, P. E., George, M. D., Habibzadegah-Tari, P., Bevan, A., Dunn, Jr, W. A., and Klionsky, D. J. (2001). Cvt18/gsa12 is required for cytoplasm-to-vacuole transport, pexophagy, and autophagy in saccharomyces cerevisiae and pichia pastoris. *Mol Biol Cell*, 12(12):3821–38.

Guo, H. S. and Ding, S. W. (2002). A viral protein inhibits the long range signaling activity of the gene silencing signal. *EMBO J*, 21(3):398–407.

Guo, X. and Lu, R. (2013). Characterization of virus-encoded rna interference suppressors in caenorhabditis elegans. *J Virol*, 87(10):5414–23.

Gutierrez, E., Wiggins, D., Fielding, B., and Gould, A. P. (2007). Specialized hepatocyte-like cells regulate drosophila lipid metabolism. *Nature*, 445(7125):275–80.

Gutierrez, M. G., Master, S. S., Singh, S. B., Taylor, G. A., Colombo, M. I., and Deretic, V. (2004). Autophagy is a defense mechanism inhibiting bcg and mycobacterium tuberculosis survival in infected macrophages. *Cell*, 119(6):753–66.

Guttman, M., Garber, M., Levin, J. Z., Donaghey, J., Robinson, J., Adiconis, X., Fan, L., Koziol, M. J., Gnirke, A., Nusbaum, C., Rinn, J. L., Lander, E. S., and Regev, A. (2010). Ab initio reconstruction of cell type-specific transcriptomes in mouse reveals the conserved multi-exonic structure of lincrnas. *Nat Biotechnol*, 28(5):503–10.

Hardcastle, T. J. and Kelly, K. A. (2010). bayseq: empirical bayesian methods for identifying differential expression in sequence count data. *BMC Bioinformatics*, 11:422.

Harrison, D. A., Binari, R., Nahreini, T. S., Gilman, M., and Perrimon, N. (1995). Activation of a drosophila janus kinase (jak) causes hematopoietic neoplasia and developmental defects. *EMBO J*, 14(12):2857–65.

Harrison, D. A., McCoon, P. E., Binari, R., Gilman, M., and Perrimon, N. (1998). Drosophila unpaired encodes a secreted protein that activates the jak signaling pathway. *Genes Dev*, 12(20):3252–63.

He, C., Song, H., Yorimitsu, T., Monastyrska, I., Yen, W.-L., Legakis, J. E., and Klionsky, D. J. (2006). Recruitment of atg9 to the preautophagosomal structure by atg11 is essential for selective autophagy in budding yeast. *J Cell Biol*, 175(6):925–35.

He, S., Wurtzel, O., Singh, K., Froula, J. L., Yilmaz, S., Tringe, S. G., Wang, Z., Chen, F., Lindquist, E. A., Sorek, R., and Hugenholtz, P. (2010). Validation of two ribosomal rna removal methods for microbial metatranscriptomics. *Nat Methods*, 7(10):807–12.

Heaton, N. S. and Randall, G. (2010). Dengue virus-induced autophagy regulates lipid metabolism. *Cell Host Microbe*, 8(5):422–32.

Hjalmarsson, A., Carlemalm, E., and Everitt, E. (1999). Infectious pancreatic necrosis virus: identification of a vp3-containing ribonucleoprotein core structure and evidence for o-linked glycosylation of the capsid protein vp2. *J Virol*, 73(4):3484–90.

Honti, V., Csordás, G., Kurucz, É., Márkus, R., and Andó, I. (2014). The cell-mediated immunity of drosophila melanogaster: hemocyte lineages, immune compartments, microanatomy and regulation. *Dev Comp Immunol*, 42(1):47–56.

Hou, X. S., Melnick, M. B., and Perrimon, N. (1996). Marelle acts downstream of the drosophila hop/jak kinase and encodes a protein similar to the mammalian stats. *Cell*, 84(3):411–9.

Hudson, P. J., McKern, N. M., Power, B. E., and Azad, A. A. (1986). Genomic structure of the large rna segment of infectious bursal disease virus. *Nucleic Acids Res*, 14(12):5001–12.

Hulo, C., de Castro, E., Masson, P., Bougueleret, L., Bairoch, A., Xenarios, I., and Le Mercier, P. (2011). Viralzone: a knowledge resource to understand virus diversity. *Nucleic Acids Res*, 39(Database issue):D576–82.

Hultmark, D. (1993). Immune reactions in drosophila and other insects: a model for innate immunity. *Trends Genet*, 9(5):178–83.

Huttunen, P., Hyypiä, T., Vihinen, P., Nissinen, L., and Heino, J. (1998). Echovirus 1 infection induces both stress- and growth-activated mitogen-activated protein kinase pathways and regulates the transcription of cellular immediate-early genes. *Virology*, 250(1):85–93.

Ichimura, Y., Kirisako, T., Takao, T., Satomi, Y., Shimonishi, Y., Ishihara, N., Mizushima, N., Tanida, I., Kominami, E., Ohsumi, M., Noda, T., and Ohsumi, Y. (2000). A ubiquitin-like system mediates protein lipidation. *Nature*, 408(6811):488–92.

Ip, Y. T., Reach, M., Engstrom, Y., Kadalayil, L., Cai, H., González-Crespo, S., Tatei, K., and Levine, M. (1993). Dif, a dorsal-related gene that mediates an immune response in drosophila. *Cell*, 75(4):753–63.

Jacinto, E. and Hall, M. N. (2003). Tor signalling in bugs, brain and brawn. *Nat Rev Mol Cell Biol*, 4(2):117–26.

Jackson, W. T., Giddings, Jr, T. H., Taylor, M. P., Mulinyawe, S., Rabinovitch, M., Kopito, R. R., and Kirkegaard, K. (2005). Subversion of cellular autophagosomal machinery by rna viruses. *PLoS Biol*, 3(5):e156.

Janeway, Jr, C. A. (2013). Pillars article: approaching the asymptote? evolution and revolution in immunology. cold spring harb symp quant biol. 1989. 54: 1-13. *J Immunol*, 191(9):4475–87.

Jaskiewicz, L. and Filipowicz, W. (2008). Role of dicer in posttranscriptional rna silencing. *Curr Top Microbiol Immunol*, 320:77–97.

Jin, R., Zhu, W., Cao, S., Chen, R., Jin, H., Liu, Y., Wang, S., Wang, W., and Xiao, G. (2013). Japanese encephalitis virus activates autophagy as a viral immune evasion strategy. *PLoS One*, 8(1):e52909.

Jinks, T. M., Polydorides, A. D., Calhoun, G., and Schedl, P. (2000). The jak/stat signaling pathway is required for the initial choice of sexual identity in drosophila melanogaster. *Mol Cell*, 5(3):581–7.

Jounai, N., Takeshita, F., Kobiyama, K., Sawano, A., Miyawaki, A., Xin, K.-Q., Ishii, K. J., Kawai, T., Akira, S., Suzuki, K., and Okuda, K. (2007). The atg5 atg12 conjugate associates with innate antiviral immune responses. *Proc Natl Acad Sci U S A*, 104(35):14050–5.

Jousset, F. X., Bergoin, M., and Revet, B. (1977). Characterization of the drosophila c virus. *J Gen Virol*, 34(2):269–83.

Jovel, J. and Schneemann, A. (2011). Molecular characterization of drosophila cells persistently infected with flock house virus. *Virology*, 419(1):43–53.

Juhász, G., Érdi, B., Sass, M., and Neufeld, T. P. (2007). Atg7-dependent autophagy promotes neuronal health, stress tolerance, and longevity but is dispensable for metamorphosis in drosophila. *Genes & development*, 21(23):3061–3066.

Juhász, G., Hill, J. H., Yan, Y., Sass, M., Baehrecke, E. H., Backer, J. M., and Neufeld,

T. P. (2008). The class iii pi(3)k vps34 promotes autophagy and endocytosis but not tor signaling in drosophila. *J Cell Biol*, 181(4):655–66.

Kamada, Y., Funakoshi, T., Shintani, T., Nagano, K., Ohsumi, M., and Ohsumi, Y. (2000). Tor-mediated induction of autophagy via an apg1 protein kinase complex. *J Cell Biol*, 150(6):1507–13.

Kaneko, T., Goldman, W. E., Mellroth, P., Steiner, H., Fukase, K., Kusumoto, S., Harley, W., Fox, A., Golenbock, D., and Silverman, N. (2004). Monomeric and polymeric gram-negative peptidoglycan but not purified lps stimulate the drosophila imd pathway. *Immunity*, 20(5):637–49.

Kaneko, T., Yano, T., Aggarwal, K., Lim, J.-H., Ueda, K., Oshima, Y., Peach, C., Erturk-Hasdemir, D., Goldman, W. E., Oh, B.-H., Kurata, S., and Silverman, N. (2006). Pgrp-lc and pgrp-le have essential yet distinct functions in the drosophila immune response to monomeric dap-type peptidoglycan. *Nat Immunol*, 7(7):715–23.

Kapun, M., Nolte, V., Flatt, T., and Schlötterer, C. (2010). Host range and specificity of the drosophila c virus. *PLoS One*, 5(8):e12421.

Ke, P.-Y. and Chen, S. S.-L. (2011). Activation of the unfolded protein response and autophagy after hepatitis c virus infection suppresses innate antiviral immunity in vitro. *J Clin Invest*, 121(1):37–56.

Kelley, D. R., Schatz, M. C., and Salzberg, S. L. (2010). Quake: quality-aware detection and correction of sequencing errors. *Genome Biol*, 11(11):R116.

Kemball, C. C., Alirezaei, M., Flynn, C. T., Wood, M. R., Harkins, S., Kiosses, W. B., and Whitton, J. L. (2010). Coxsackievirus infection induces autophagy-like vesicles and megaphagosomes in pancreatic acinar cells in vivo. *J Virol*, 84(23):12110–24.

Kemp, C., Mueller, S., Goto, A., Barbier, V., Paro, S., Bonnay, F., Dostert, C., Troxler, L., Hetru, C., Meignin, C., Pfeffer, S., Hoffmann, J. A., and Imler, J.-L. (2013). Broad rna interference-mediated antiviral immunity and virus-specific inducible responses in drosophila. *J Immunol*, 190(2):650–8.

Kent, W. J. (2002). Blat–the blast-like alignment tool. *Genome Res*, 12(4):656–64.

Kibenge, F. S. and Dhama, V. (1997). Evidence that virion-associated vp1 of avibirnaviruses contains viral rna sequences. *Arch Virol*, 142(6):1227–36.

Kihara, A., Noda, T., Ishihara, N., and Ohsumi, Y. (2001). Two distinct vps34 phosphatidylinositol 3-kinase complexes function in autophagy and carboxypeptidase y sorting in saccharomyces cerevisiae. *J Cell Biol*, 152(3):519–30.

Kim, J., Dalton, V. M., Eggerton, K. P., Scott, S. V., and Klionsky, D. J. (1999). Apg7p/cvt2p is required for the cytoplasm-to-vacuole targeting, macroautophagy, and peroxisome degradation pathways. *Mol Biol Cell*, 10(5):1337–51.

Kim, L. K., Choi, U. Y., Cho, H. S., Lee, J. S., Lee, W.-b., Kim, J., Jeong, K., Shim, J., Kim-Ha, J., and Kim, Y.-J. (2007). Down-regulation of nf-kappab target genes by the ap-1 and stat complex during the innate immune response in drosophila. *PLoS Biol*, 5(9):e238.

Kim, S.-M., Park, J.-H., Chung, S.-K., Kim, J.-Y., Hwang, H.-Y., Chung, K.-C., Jo, I., Park, S.-I., and Nam, J.-H. (2004). Coxsackievirus b3 infection induces cyr61 activation via jnk to mediate cell death. *J Virol*, 78(24):13479–88.

Kim, T., Yoon, J., Cho, H., Lee, W.-B., Kim, J., Song, Y.-H., Kim, S. N., Yoon, J. H., Kim-Ha, J., and Kim, Y.-J. (2005). Downregulation of lipopolysaccharide response in drosophila by negative crosstalk between the ap1 and nf-kappab signaling modules. *Nat Immunol*, 6(2):211–8.

Kimmel, A. R., Brasaemle, D. L., McAndrews-Hill, M., Sztalryd, C., and Londos, C. (2010). Adoption of perilipin as a unifying nomenclature for the mammalian pat-family of intracellular lipid storage droplet proteins. *J Lipid Res*, 51(3):468–71.

Kirisako, T., Ichimura, Y., Okada, H., Kabeya, Y., Mizushima, N., Yoshimori, T., Ohsumi, M., Takao, T., Noda, T., and Ohsumi, Y. (2000). The reversible modification regulates the membrane-binding state of apg8/aut7 essential for autophagy and the cytoplasm to vacuole targeting pathway. *J Cell Biol*, 151(2):263–76.

Kirkegaard, K. and Jackson, W. T. (2005). Topology of double-membraned vesicles and the opportunity for non-lytic release of cytoplasm. *Autophagy*, 1(3):182–4.

Klionsky, D. J. (2005). The molecular machinery of autophagy: unanswered questions. *J Cell Sci*, 118(Pt 1):7–18.

Klionsky, D. J. and Emr, S. D. (2000). Autophagy as a regulated pathway of cellular degradation. *Science*, 290(5497):1717–21.

Kozarewa, I., Ning, Z., Quail, M. A., Sanders, M. J., Berriman, M., and Turner, D. J. (2009). Amplification-free illumina sequencing-library preparation facilitates improved mapping and assembly of (g+c)-biased genomes. *Nat Methods*, 6(4):291–5.

Kühnlein, R. P. (2012). Thematic review series: Lipid droplet synthesis and metabolism: from yeast to man. lipid droplet-based storage fat metabolism in drosophila. *J Lipid Res*, 53(8):1430–6.

Kuma, A., Mizushima, N., Ishihara, N., and Ohsumi, Y. (2002). Formation of the approximately 350-kda apg12-apg5.apg16 multimeric complex, mediated by apg16 oligomerization, is essential for autophagy in yeast. *J Biol Chem*, 277(21):18619–25.

Kumar, A., Manna, S. K., Dhawan, S., and Aggarwal, B. B. (1998). Hiv-tat protein activates c-jun n-terminal kinase and activator protein-1. *J Immunol*, 161(2):776–81.

Kunz, J., Henriquez, R., Schneider, U., Deuter-Reinhard, M., Movva, N. R., and Hall, M. N. (1993). Target of rapamycin in yeast, tor2, is an essential phosphatidylinositol kinase homolog required for g1 progression. *Cell*, 73(3):585–96.

Kurata, S. (2014). Peptidoglycan recognition proteins in drosophila immunity. *Dev Comp Immunol*, 42(1):36–41.

Kyriakis, J. M., Banerjee, P., Nikolakaki, E., Dai, T., Rubie, E. A., Ahmad, M. F., Avruch, J., and Woodgett, J. R. (1994). The stress-activated protein kinase subfamily of c-jun kinases. *Nature*, 369(6476):156–60.

Lagueux, M., Perrodou, E., Levashina, E. A., Capovilla, M., and Hoffmann, J. A. (2000).

Constitutive expression of a complement-like protein in toll and jak gain-of-function mutants of drosophila. *Proc Natl Acad Sci U S A*, 97(21):11427–32.

Lamb, J. A., Ventura, J.-J., Hess, P., Flavell, R. A., and Davis, R. J. (2003). Jund mediates survival signaling by the jnk signal transduction pathway. *Mol Cell*, 11(6):1479–89.

Lassmann, T., Hayashizaki, Y., and Daub, C. O. (2009). Tagdust–a program to eliminate artifacts from next generation sequencing data. *Bioinformatics*, 25(21):2839–40.

Law, C. W., Chen, Y., Shi, W., and Smyth, G. K. (2014). voom: Precision weights unlock linear model analysis tools for rna-seq read counts. *Genome Biol*, 15(2):R29.

Lee, C.-Y., Clough, E. A., Yellon, P., Teslovich, T. M., Stephan, D. A., and Baehrecke, E. H. (2003). Genome-wide analyses of steroid- and radiation-triggered programmed cell death in drosophila. *Curr Biol*, 13(4):350–7.

Lee, H. K., Lund, J. M., Ramanathan, B., Mizushima, N., and Iwasaki, A. (2007). Autophagy-dependent viral recognition by plasmacytoid dendritic cells. *Science*, 315(5817):1398–401.

Lee, K.-A. and Lee, W.-J. (2014). Drosophila as a model for intestinal dysbiosis and chronic inflammatory diseases. *Dev Comp Immunol*, 42(1):102–10.

Lee, S. B., Park, J., Jung, J. U., and Chung, J. (2005). Nef induces apoptosis by activating jnk signaling pathway and inhibits nf-kappab-dependent immune responses in drosophila. *J Cell Sci*, 118(Pt 9):1851–9.

Legakis, J. E., Yen, W.-L., and Klionsky, D. J. (2007). A cycling protein complex required for selective autophagy. *Autophagy*, 3(5):422–32.

Lemaitre, B. and Hoffmann, J. (2007). The host defense of drosophila melanogaster. *Annu Rev Immunol*, 25:697–743.

Lemaitre, B., Kromer-Metzger, E., Michaut, L., Nicolas, E., Meister, M., Georgel, P., Reichhart, J. M., and Hoffmann, J. A. (1995a). A recessive mutation, immune deficiency (imd), defines two distinct control pathways in the drosophila host defense. *Proc Natl Acad Sci U S A*, 92(21):9465–9.

Lemaitre, B., Meister, M., Govind, S., Georgel, P., Steward, R., Reichhart, J. M., and Hoffmann, J. A. (1995b). Functional analysis and regulation of nuclear import of dorsal during the immune response in drosophila. *EMBO J*, 14(3):536–45.

Lemaitre, B., Nicolas, E., Michaut, L., Reichhart, J. M., and Hoffmann, J. A. (1996). The dorsoventral regulatory gene cassette spätzle/toll/cactus controls the potent antifungal response in drosophila adults. *Cell*, 86(6):973–83.

Lemaitre, B., Reichhart, J. M., and Hoffmann, J. A. (1997). Drosophila host defense: differential induction of antimicrobial peptide genes after infection by various classes of microorganisms. *Proc Natl Acad Sci U S A*, 94(26):14614–9.

Leulier, F., Parquet, C., Pili-Floury, S., Ryu, J.-H., Caroff, M., Lee, W.-J., Mengin-Lecreulx, D., and Lemaitre, B. (2003). The drosophila immune system detects bacteria through specific peptidoglycan recognition. *Nat Immunol*, 4(5):478–84.

Leulier, F., Rodriguez, A., Khush, R. S., Abrams, J. M., and Lemaitre, B. (2000). The drosophila caspase dredd is required to resist gram-negative bacterial infection. *EMBO Rep*, 1(4):353–8.

Leulier, F., Vidal, S., Saigo, K., Ueda, R., and Lemaitre, B. (2002). Inducible expression of double-stranded rna reveals a role for dfadd in the regulation of the antibacterial response in drosophila adults. *Curr Biol*, 12(12):996–1000.

L'Heritier, P. (1958). The hereditary virus of drosophila. *Adv Virus Res*, 5:195–245.

Lhocine, N., Ribeiro, P. S., Buchon, N., Wepf, A., Wilson, R., Tenev, T., Lemaitre, B., Gstaiger, M., Meier, P., and Leulier, F. (2008). Pims modulates immune tolerance by negatively regulating drosophila innate immune signaling. *Cell Host Microbe*, 4(2):147–58.

Li, F. and Ding, S.-W. (2006). Virus counterdefense: diverse strategies for evading the rna-silencing immunity. *Annu Rev Microbiol*, 60:503–31.

Li, H., Li, W. X., and Ding, S. W. (2002). Induction and suppression of rna silencing by an animal virus. *Science*, 296(5571):1319–21.

Li, J., Witten, D. M., Johnstone, I. M., and Tibshirani, R. (2012a). Normalization, testing, and false discovery rate estimation for rna-sequencing data. *Biostatistics*, 13(3):523–38.

Li, J.-K., Liang, J.-J., Liao, C.-L., and Lin, Y.-L. (2012b). Autophagy is involved in the early step of japanese encephalitis virus infection. *Microbes Infect*, 14(2):159–68.

Liang, X. H., Jackson, S., Seaman, M., Brown, K., Kempkes, B., Hibshoosh, H., and Levine, B. (1999). Induction of autophagy and inhibition of tumorigenesis by beclin 1. *Nature*, 402(6762):672–6.

Liang, X. H., Kleeman, L. K., Jiang, H. H., Gordon, G., Goldman, J. E., Berry, G., Herman, B., and Levine, B. (1998). Protection against fatal sindbis virus encephalitis by beclin, a novel bcl-2-interacting protein. *J Virol*, 72(11):8586–96.

Lim, J.-H., Kim, M.-S., Kim, H.-E., Yano, T., Oshima, Y., Aggarwal, K., Goldman, W. E., Silverman, N., Kurata, S., and Oh, B.-H. (2006). Structural basis for preferential recognition of diaminopimelic acid-type peptidoglycan by a subset of peptidoglycan recognition proteins. *J Biol Chem*, 281(12):8286–95.

Lin, L.-T., Dawson, P. W. H., and Richardson, C. D. (2010). Viral interactions with macroautophagy: a double-edged sword. *Virology*, 402(1):1–10.

Lipinski, M. M., Zheng, B., Lu, T., Yan, Z., Py, B. F., Ng, A., Xavier, R. J., Li, C., Yankner, B. A., Scherzer, C. R., and Yuan, J. (2010). Genome-wide analysis reveals mechanisms modulating autophagy in normal brain aging and in alzheimer's disease. *Proc Natl Acad Sci U S A*, 107(32):14164–9.

Liu, C., Gelius, E., Liu, G., Steiner, H., and Dziarski, R. (2000). Mammalian peptidoglycan recognition protein binds peptidoglycan with high affinity, is expressed in neutrophils, and inhibits bacterial growth. *J Biol Chem*, 275(32):24490–9.

Liu, Z. and Huang, X. (2013). Lipid metabolism in drosophila: development and disease. *Acta Biochim Biophys Sin (Shanghai)*, 45(1):44–50.

Lloyd, T. E. and Taylor, J. P. (2010). Flightless flies: Drosophila models of neuromuscular disease. *Ann N Y Acad Sci*, 1184:e1–20.

Lombardo, E., Maraver, A., Castón, J. R., Rivera, J., Fernández-Arias, A., Serrano, A., Carrascosa, J. L., and Rodriguez, J. F. (1999). Vp1, the putative rna-dependent rna polymerase of infectious bursal disease virus, forms complexes with the capsid protein vp3, leading to efficient encapsidation into virus-like particles. *J Virol*, 73(8):6973–83.

Londos, C., Sztalryd, C., Tansey, J. T., and Kimmel, A. R. (2005). Role of pat proteins in lipid metabolism. *Biochimie*, 87(1):45–9.

Longo, N., Amat di San Filippo, C., and Pasquali, M. (2006). Disorders of carnitine transport and the carnitine cycle. *Am J Med Genet C Semin Med Genet*, 142C(2):77–85.

Lu, X., Gruia-Gray, J., Copeland, N. G., Gilbert, D. J., Jenkins, N. A., Londos, C., and Kimmel, A. R. (2001). The murine perilipin gene: the lipid droplet-associated perilipins derive from tissue-specific, mrna splice variants and define a gene family of ancient origin. *Mamm Genome*, 12(9):741–9.

Luo, H., Rose, P., Barber, D., Hanratty, W. P., Lee, S., Roberts, T. M., D'Andrea, A. D., and Dearolf, C. R. (1997). Mutation in the jak kinase jh2 domain hyperactivates drosophila and mammalian jak-stat pathways. *Mol Cell Biol*, 17(3):1562–71.

Luo, L., Liao, Y. J., Jan, L. Y., and Jan, Y. N. (1994). Distinct morphogenetic functions of similar small gtpases: Drosophila drac1 is involved in axonal outgrowth and myoblast fusion. *Genes Dev*, 8(15):1787–802.

Magyar, G. and Dobos, P. (1994). Evidence for the detection of the infectious pancreatic necrosis virus polyprotein and the 17-kda polypeptide in infected cells and of the ns protease in purified virus. *Virology*, 204(2):580–9.

Maillet, F., Bischoff, V., Vignal, C., Hoffmann, J., and Royet, J. (2008). The drosophila peptidoglycan recognition protein pgrp-lf blocks pgrp-lc and imd/jnk pathway activation. *Cell Host Microbe*, 3(5):293–303.

Mamanova, L., Andrews, R. M., James, K. D., Sheridan, E. M., Ellis, P. D., Langford, C. F., Ost, T. W. B., Collins, J. E., and Turner, D. J. (2010). Frt-seq: amplification-free, strand-specific transcriptome sequencing. *Nat Methods*, 7(2):130–2.

Marguerat, S. and Bähler, J. (2010). Rna-seq: from technology to biology. *Cell Mol Life Sci*, 67(4):569–79.

Martin, J. A. and Wang, Z. (2011). Next-generation transcriptome assembly. *Nat Rev Genet*, 12(10):671–82.

Massey, A. C., Zhang, C., and Cuervo, A. M. (2006). Chaperone-mediated autophagy in aging and disease. *Curr Top Dev Biol*, 73:205–35.

Matsuura, A., Tsukada, M., Wada, Y., and Ohsumi, Y. (1997). Apg1p, a novel protein kinase required for the autophagic process in saccharomyces cerevisiae. *Gene*, 192(2):245–50.

McGarry, J. D. and Brown, N. F. (1997). The mitochondrial carnitine palmitoyltransferase system. from concept to molecular analysis. *Eur J Biochem*, 244(1):1–14.

MD, Y. (2012). *Differential Expression for RNA sequencing (RNA-seq) data: Mapping, Summarization, Statistical Analysis and Experimental Design*. Number 169-190. Bioinformatics for High Throughput Sequencing.

Medzhitov, R., Preston-Hurlburt, P., and Janeway, Jr, C. A. (1997). A human homologue of the drosophila toll protein signals activation of adaptive immunity. *Nature*, 388(6640):394–7.

Meijer, A. J. and Codogno, P. (2004). Regulation and role of autophagy in mammalian cells. *Int J Biochem Cell Biol*, 36(12):2445–62.

Meinander, A., Runchel, C., Tenev, T., Chen, L., Kim, C.-H., Ribeiro, P. S., Broemer, M., Leulier, F., Zvelebil, M., Silverman, N., and Meier, P. (2012). Ubiquitylation of the initiator caspase dredd is required for innate immune signalling. *EMBO J*, 31(12):2770–83.

Meléndez, A. and Neufeld, T. P. (2008). The cell biology of autophagy in metazoans: a developing story. *Development*, 135(14):2347–60.

Mellroth, P. and Steiner, H. (2006). Pgrp-sb1: an n-acetylmuramoyl l-alanine amidase with antibacterial activity. *Biochem Biophys Res Commun*, 350(4):994–9.

Metzker, M. L. (2010). Sequencing technologies - the next generation. *Nat Rev Genet*, 11(1):31–46.

Michel, T., Reichhart, J. M., Hoffmann, J. A., and Royet, J. (2001). Drosophila toll is activated by gram-positive bacteria through a circulating peptidoglycan recognition protein. *Nature*, 414(6865):756–9.

Miller, J. R., Koren, S., and Sutton, G. (2010). Assembly algorithms for next-generation sequencing data. *Genomics*, 95(6):315–27.

Miura, S., Gan, J.-W., Brzostowski, J., Parisi, M. J., Schultz, C. J., Londos, C., Oliver, B., and Kimmel, A. R. (2002). Functional conservation for lipid storage droplet association among perilipin, adrp, and tip47 (pat)-related proteins in mammals, drosophila, and dictyostelium. *J Biol Chem*, 277(35):32253–7.

Miyoshi, H., Souza, S. C., Zhang, H.-H., Strissel, K. J., Christoffolete, M. A., Kovsan, J., Rudich, A., Kraemer, F. B., Bianco, A. C., Obin, M. S., and Greenberg, A. S. (2006). Perilipin promotes hormone-sensitive lipase-mediated adipocyte lipolysis via phosphorylation-dependent and -independent mechanisms. *J Biol Chem*, 281(23):15837–44.

Mizuguchi, K., Parker, J. S., Blundell, T. L., and Gay, N. J. (1998). Getting knotted: a model for the structure and activation of spätzle. *Trends Biochem Sci*, 23(7):239–42.

Mizushima, N. and Klionsky, D. J. (2007). Protein turnover via autophagy: implications for metabolism. *Annu Rev Nutr*, 27:19–40.

Mizushima, N., Noda, T., and Ohsumi, Y. (1999). Apg16p is required for the function of the apg12p-apg5p conjugate in the yeast autophagy pathway. *EMBO J*, 18(14):3888–96.

Mizushima, N., Noda, T., Yoshimori, T., Tanaka, Y., Ishii, T., George, M. D., Klionsky, D. J., Ohsumi, M., and Ohsumi, Y. (1998). A protein conjugation system essential for autophagy. *Nature*, 395(6700):395–8.

Morisato, D. and Anderson, K. V. (1995). Signaling pathways that establish the dorsal-ventral pattern of the drosophila embryo. *Annu Rev Genet*, 29:371–99.

Mortazavi, A., Williams, B. A., McCue, K., Schaeffer, L., and Wold, B. (2008). Mapping and quantifying mammalian transcriptomes by rna-seq. *Nat Methods*, 5(7):621–8.

Müller, H., Islam, M. R., and Raue, R. (2003). Research on infectious bursal disease–the past, the present and the future. *Vet Microbiol*, 97(1-2):153–65.

Mundt, E., Beyer, J., and Müller, H. (1995). Identification of a novel viral protein in infectious bursal disease virus-infected cells. *J Gen Virol*, 76 (Pt 2):437–43.

Mundt, E., Köllner, B., and Kretzschmar, D. (1997). Vp5 of infectious bursal disease virus is not essential for viral replication in cell culture. *J Virol*, 71(7):5647–51.

Murrow, L. and Debnath, J. (2013). Autophagy as a stress-response and quality-control mechanism: implications for cell injury and human disease. *Annu Rev Pathol*, 8:105–37.

Myllymäki, H., Valanne, S., and Rämet, M. (2014). The drosophila imd signaling pathway. *J Immunol*, 192(8):3455–62.

Nagy, E. and Dobos, P. (1984a). Coding assignments of drosophila x virus genome segments: in vitro translation of native and denatured virion dsrna. *Virology*, 137(1):58–66.

Nagy, E. and Dobos, P. (1984b). Synthesis of drosophila x virus proteins in cultured drosophila cells. *Virology*, 134(2):358–67.

Nakahira, K., Haspel, J. A., Rathinam, V. A. K., Lee, S.-J., Dolinay, T., Lam, H. C., Englert, J. A., Rabinovitch, M., Cernadas, M., Kim, H. P., Fitzgerald, K. A., Ryter, S. W., and Choi, A. M. K. (2011). Autophagy proteins regulate innate immune responses by inhibiting the release of mitochondrial dna mediated by the nalp3 inflammasome. *Nat Immunol*, 12(3):222–30.

Nakamoto, M., Moy, R. H., Xu, J., Bambina, S., Yasunaga, A., Shelly, S. S., Gold, B., and Cherry, S. (2012). Virus recognition by toll-7 activates antiviral autophagy in drosophila. *Immunity*, 36(4):658–67.

Neyen, C., Poidevin, M., Roussel, A., and Lemaitre, B. (2012). Tissue- and ligand-specific sensing of gram-negative infection in drosophila by pgrp-lc isoforms and pgrp-le. *J Immunol*, 189(4):1886–97.

Noda, T., Kim, J., Huang, W. P., Baba, M., Tokunaga, C., Ohsumi, Y., and Klionsky, D. J. (2000). Apg9p/cvt7p is an integral membrane protein required for transport vesicle formation in the cvt and autophagy pathways. *J Cell Biol*, 148(3):465–80.

Noda, T. and Ohsumi, Y. (1998). Tor, a phosphatidylinositol kinase homologue, controls autophagy in yeast. *J Biol Chem*, 273(7):3963–6.

Oh, J. E. and Lee, H. K. (2014). Pattern recognition receptors and autophagy. *Front Immunol*, 5:300.

Orvedahl, A., MacPherson, S., Sumpter, Jr, R., Tallóczy, Z., Zou, Z., and Levine, B. (2010). Autophagy protects against sindbis virus infection of the central nervous system. *Cell Host Microbe*, 7(2):115–27.

Ozsolak, F. and Milos, P. M. (2011). Rna sequencing: advances, challenges and opportunities. *Nat Rev Genet*, 12(2):87–98.

Palanker, L., Tennessen, J. M., Lam, G., and Thummel, C. S. (2009). Drosophila hnf4 regulates lipid mobilization and beta-oxidation. *Cell Metab*, 9(3):228–39.

Pan, H., Xie, J., Ye, F., and Gao, S.-J. (2006). Modulation of kaposi's sarcoma-associated herpesvirus infection and replication by mek/erk, jnk, and p38 multiple mitogen-activated protein kinase pathways during primary infection. *J Virol*, 80(11):5371–82.

Paquette, N., Broemer, M., Aggarwal, K., Chen, L., Husson, M., Ertürk-Hasdemir, D., Reichhart, J.-M., Meier, P., and Silverman, N. (2010). Caspase-mediated cleavage, iap binding, and ubiquitination: linking three mechanisms crucial for drosophila nf-kappab signaling. *Mol Cell*, 37(2):172–82.

Paredes, J. C., Welchman, D. P., Poidevin, M., and Lemaitre, B. (2011). Negative regulation by amidase pgrps shapes the drosophila antibacterial response and protects the fly from innocuous infection. *Immunity*, 35(5):770–9.

Park, J. M., Brady, H., Ruocco, M. G., Sun, H., Williams, D., Lee, S. J., Kato, Jr, T., Richards, N., Chan, K., Mercurio, F., Karin, M., and Wasserman, S. A. (2004). Targeting of tak1 by the nf-kappa b protein relish regulates the jnk-mediated immune response in drosophila. *Genes Dev*, 18(5):584–94.

Patel, R. T., Soulages, J. L., Hariharasundaram, B., and Arrese, E. L. (2005). Activation of the lipid droplet controls the rate of lipolysis of triglycerides in the insect fat body. *J Biol Chem*, 280(24):22624–31.

Patro, R., Mount, S. M., and Kingsford, C. (2014). Sailfish enables alignment-free isoform quantification from rna-seq reads using lightweight algorithms. *Nat Biotechnol*, 32(5):462–4.

Périès, J., Printz, P., Canivet, M., and Chuat, J. C. (1966). [multiplication of vesicular stomatitis virus in drosophila melanogaster]. *C R Acad Sci Hebd Seances Acad Sci D*, 262(19):2106–7.

Perkins, D., Gyure, K. A., Pereira, E. F. R., and Aurelian, L. (2003). Herpes simplex virus type 1-induced encephalitis has an apoptotic component associated with activation of c-jun n-terminal kinase. *J Neurovirol*, 9(1):101–11.

Persson, C., Oldenvi, S., and Steiner, H. (2007). Peptidoglycan recognition protein lf: a negative regulator of drosophila immunity. *Insect Biochem Mol Biol*, 37(12):1309–16.

Petiot, A., Ogier-Denis, E., Blommaart, E. F., Meijer, A. J., and Codogno, P. (2000). Distinct classes of phosphatidylinositol 3'-kinases are involved in signaling pathways that control macroautophagy in ht-29 cells. *J Biol Chem*, 275(2):992–8.

Prentice, E., Jerome, W. G., Yoshimori, T., Mizushima, N., and Denison, M. R. (2004). Coronavirus replication complex formation utilizes components of cellular autophagy. *J Biol Chem*, 279(11):10136–41.

Rämet, M., Lanot, R., Zachary, D., and Manfruelli, P. (2002a). Jnk signaling pathway is required for efficient wound healing in drosophila. *Dev Biol*, 241(1):145–56.

Rämet, M., Manfruelli, P., Pearson, A., Mathey-Prevot, B., and Ezekowitz, R. A. B.

(2002b). Functional genomic analysis of phagocytosis and identification of a drosophila receptor for e. coli. *Nature*, 416(6881):644–8.

Ramsay, R. R., Gandour, R. D., and van der Leij, F. R. (2001). Molecular enzymology of carnitine transfer and transport. *Biochim Biophys Acta*, 1546(1):21–43.

Ravikumar, B., Vacher, C., Berger, Z., Davies, J. E., Luo, S., Oroz, L. G., Scaravilli, F., Easton, D. F., Duden, R., O'Kane, C. J., and Rubinsztein, D. C. (2004). Inhibition of mtor induces autophagy and reduces toxicity of polyglutamine expansions in fly and mouse models of huntington disease. *Nat Genet*, 36(6):585–95.

Reggiori, F., Shintani, T., Nair, U., and Klionsky, D. J. (2005). Atg9 cycles between mitochondria and the pre-autophagosomal structure in yeasts. *Autophagy*, 1(2):101–9.

Reggiori, F., Tucker, K. A., Stromhaug, P. E., and Klionsky, D. J. (2004). The atg1-atg13 complex regulates atg9 and atg23 retrieval transport from the pre-autophagosomal structure. *Dev Cell*, 6(1):79–90.

Reikine, S., Nguyen, J. B., and Modis, Y. (2014). Pattern recognition and signaling mechanisms of rig-i and mda5. *Front Immunol*, 5:342.

Reinganum, C. (1975). The isolation of cricket paralysis virus from the emperor gum moth, antheraea eucalypti scott, and its infectivity towards a range of insect species. *Intervirology*, 5(1-2):97–102.

Revet, B. and Delain, E. (1982). The drosophila x virus contains a 1-microm double-stranded rna circularized by a 67-kd terminal protein: high-resolution denaturation mapping of its genome. *Virology*, 123(1):29–44.

Robinson, M. D., McCarthy, D. J., and Smyth, G. K. (2010). edger: a bioconductor package for differential expression analysis of digital gene expression data. *Bioinformatics*, 26(1):139–40.

Robinson, M. D. and Oshlack, A. (2010). A scaling normalization method for differential expression analysis of rna-seq data. *Genome Biol*, 11(3):R25.

Rock, F. L., Hardiman, G., Timans, J. C., Kastelein, R. A., and Bazan, J. F. (1998). A family of human receptors structurally related to drosophila toll. *Proc Natl Acad Sci U S A*, 95(2):588–93.

Rodrigue, S., Materna, A. C., Timberlake, S. C., Blackburn, M. C., Malmstrom, R. R., Alm, E. J., and Chisholm, S. W. (2010). Unlocking short read sequencing for metagenomics. *PLoS One*, 5(7):e11840.

Rubio-Gozalbo, M. E., Bakker, J. A., Waterham, H. R., and Wanders, R. J. A. (2004). Carnitine-acylcarnitine translocase deficiency, clinical, biochemical and genetic aspects. *Mol Aspects Med*, 25(5-6):521–32.

Rutschmann, S., Jung, A. C., Zhou, R., Silverman, N., Hoffmann, J. A., and Ferrandon, D. (2000). Role of drosophila ikk gamma in a toll-independent antibacterial immune response. *Nat Immunol*, 1(4):342–7.

Rutschmann, S., Kilinc, A., and Ferrandon, D. (2002). Cutting edge: the toll pathway is required for resistance to gram-positive bacterial infections in drosophila. *J Immunol*, 168(4):1542–6.

Ryu, J.-H., Kim, S.-H., Lee, H.-Y., Bai, J. Y., Nam, Y.-D., Bae, J.-W., Lee, D. G., Shin, S. C., Ha, E.-M., and Lee, W.-J. (2008). Innate immune homeostasis by the homeobox gene caudal and commensal-gut mutualism in drosophila. *Science*, 319(5864):777–82.

Sabin, L. R., Hanna, S. L., and Cherry, S. (2010). Innate antiviral immunity in drosophila. *Curr Opin Immunol*, 22(1):4–9.

Sabin, L. R., Zhou, R., Gruber, J. J., Lukinova, N., Bambina, S., Berman, A., Lau, C.-K., Thompson, C. B., and Cherry, S. (2009). Ars2 regulates both mirna- and sirna-dependent silencing and suppresses rna virus infection in drosophila. *Cell*, 138(2):340–51.

Saitoh, T., Fujita, N., Jang, M. H., Uematsu, S., Yang, B.-G., Satoh, T., Omori, H., Noda, T., Yamamoto, N., Komatsu, M., Tanaka, K., Kawai, T., Tsujimura, T., Takeuchi, O., Yoshimori, T., and Akira, S. (2008). Loss of the autophagy protein atg16l1 enhances endotoxin-induced il-1beta production. *Nature*, 456(7219):264–8.

Sam, L. T., Lipson, D., Raz, T., Cao, X., Thompson, J., Milos, P. M., Robinson, D., Chinnaiyan, A. M., Kumar-Sinha, C., and Maher, C. A. (2011). A comparison of single molecule and amplification based sequencing of cancer transcriptomes. *PLoS One*, 6(3):e17305.

Scaglia, F., Wang, Y., Singh, R. H., Dembure, P. P., Pasquali, M., Fernhoff, P. M., and Longo, N. (1998). Defective urinary carnitine transport in heterozygotes for primary carnitine deficiency. *Genet Med*, 1(1):34–9.

Schlegel, A. and Stainier, D. Y. R. (2007). Lessons from ”lower” organisms: what

worms, flies, and zebrafish can teach us about human energy metabolism. *PLoS Genet*, 3(11):e199.

Schmidt, R. L., Trejo, T. R., Plummer, T. B., Platt, J. L., and Tang, A. H. (2008). Infection-induced proteolysis of pgrp-lc controls the imd activation and melanization cascades in drosophila. *FASEB J*, 22(3):918–29.

Schneider, D. S. and Ayres, J. S. (2008). Two ways to survive infection: what resistance and tolerance can teach us about treating infectious diseases. *Nat Rev Immunol*, 8(11):889–95.

Schneider, D. S., Ayres, J. S., Brandt, S. M., Costa, A., Dionne, M. S., Gordon, M. D., Mabery, E. M., Moule, M. G., Pham, L. N., and Shirasu-Hiza, M. M. (2007). Drosophila eiger mutants are sensitive to extracellular pathogens. *PLoS Pathog*, 3(3):e41.

Schneider, D. S., Jin, Y., Morisato, D., and Anderson, K. V. (1994). A processed form of the spätzle protein defines dorsal-ventral polarity in the drosophila embryo. *Development*, 120(5):1243–50.

Schweiger, M., Schreiber, R., Haemmerle, G., Lass, A., Fledelius, C., Jacobsen, P., Tornqvist, H., Zechner, R., and Zimmermann, R. (2006). Adipose triglyceride lipase and hormone-sensitive lipase are the major enzymes in adipose tissue triacylglycerol catabolism. *J Biol Chem*, 281(52):40236–41.

Scott, R. C., Schuldiner, O., and Neufeld, T. P. (2004). Role and regulation of starvation-induced autophagy in the drosophila fat body. *Dev Cell*, 7(2):167–78.

Seglen, P. O. and Gordon, P. B. (1982). 3-methyladenine: specific inhibitor of autophagic/lysosomal protein degradation in isolated rat hepatocytes. *Proc Natl Acad Sci U S A*, 79(6):1889–92.

Shelly, S., Lukinova, N., Bambina, S., Berman, A., and Cherry, S. (2009). Autophagy is an essential component of drosophila immunity against vesicular stomatitis virus. *Immunity*, 30(4):588–98.

Shi, C.-S., Shenderov, K., Huang, N.-N., Kabat, J., Abu-Asab, M., Fitzgerald, K. A., Sher, A., and Kehrl, J. H. (2012). Activation of autophagy by inflammatory signals limits il-1 production by targeting ubiquitinated inflammasomes for destruction. *Nat Immunol*, 13(3):255–63.

Shintani, T. and Klionsky, D. J. (2004). Cargo proteins facilitate the formation of transport vesicles in the cytoplasm to vacuole targeting pathway. *J Biol Chem*, 279(29):29889–94.

Shintani, T., Mizushima, N., Ogawa, Y., Matsuura, A., Noda, T., and Ohsumi, Y. (1999). Apg10p, a novel protein-conjugating enzyme essential for autophagy in yeast. *EMBO J*, 18(19):5234–41.

Si, X., Luo, H., Morgan, A., Zhang, J., Wong, J., Yuan, J., Esfandiarei, M., Gao, G., Cheung, C., and McManus, B. M. (2005). Stress-activated protein kinases are involved in coxsackievirus b3 viral progeny release. *J Virol*, 79(22):13875–81.

Silverman, N., Zhou, R., Erlich, R. L., Hunter, M., Bernstein, E., Schneider, D., and

Maniatis, T. (2003). Immune activation of nf-kappab and jnk requires drosophila tak1. *J Biol Chem*, 278(49):48928–34.

Simpson, J. T., Wong, K., Jackman, S. D., Schein, J. E., Jones, S. J. M., and Birol, I. (2009). Abyss: a parallel assembler for short read sequence data. *Genome Res*, 19(6):1117–23.

Sinenko, S. A. and Mathey-Prevot, B. (2004). Increased expression of drosophila tetraspanin, tsp68c, suppresses the abnormal proliferation of ytr-deficient and ras/raf-activated hemocytes. *Oncogene*, 23(56):9120–8.

Smyth, G. K. (2004). Linear models and empirical bayes methods for assessing differential expression in microarray experiments. *Stat Appl Genet Mol Biol*, 3:Article3.

Stöven, S., Ando, I., Kadalayil, L., Engström, Y., and Hultmark, D. (2000). Activation of the drosophila nf-kappab factor relish by rapid endoproteolytic cleavage. *EMBO Rep*, 1(4):347–52.

Stoven, S., Silverman, N., Junell, A., Hedengren-Olcott, M., Erturk, D., Engstrom, Y., Maniatis, T., and Hultmark, D. (2003). Caspase-mediated processing of the drosophila nf-kappab factor relish. *Proc Natl Acad Sci U S A*, 100(10):5991–6.

Strømhaug, P. E., Reggiori, F., Guan, J., Wang, C.-W., and Klionsky, D. J. (2004). Atg21 is a phosphoinositide binding protein required for efficient lipidation and localization of atg8 during uptake of aminopeptidase i by selective autophagy. *Mol Biol Cell*, 15(8):3553–66.

Subramani, S. and Malhotra, V. (2013). Non-autophagic roles of autophagy-related proteins. *EMBO Rep*, 14(2):143–51.

Suhy, D. A., Giddings, Jr, T. H., and Kirkegaard, K. (2000). Remodeling the endoplasmic reticulum by poliovirus infection and by individual viral proteins: an autophagy-like origin for virus-induced vesicles. *J Virol*, 74(19):8953–65.

Sun, Y., Li, C., Shu, Y., Ju, X., Zou, Z., Wang, H., Rao, S., Guo, F., Liu, H., Nan, W., Zhao, Y., Yan, Y., Tang, J., Zhao, C., Yang, P., Liu, K., Wang, S., Lu, H., Li, X., Tan, L., Gao, R., Song, J., Gao, X., Tian, X., Qin, Y., Xu, K.-F., Li, D., Jin, N., and Jiang, C. (2012). Inhibition of autophagy ameliorates acute lung injury caused by avian influenza a h5n1 infection. *Sci Signal*, 5(212):ra16.

Suzuki, K., Kubota, Y., Sekito, T., and Ohsumi, Y. (2007). Hierarchy of atg proteins in pre-autophagosomal structure organization. *Genes Cells*, 12(2):209–18.

Swaminathan, C. P., Brown, P. H., Roychowdhury, A., Wang, Q., Guan, R., Silverman, N., Goldman, W. E., Boons, G.-J., and Mariuzza, R. A. (2006). Dual strategies for peptidoglycan discrimination by peptidoglycan recognition proteins (pgrps). *Proc Natl Acad Sci U S A*, 103(3):684–9.

Swanlund, J. M., Kregel, K. C., and Oberley, T. D. (2010). Investigating autophagy: quantitative morphometric analysis using electron microscopy. *Autophagy*, 6(2):270–7.

Sztalryd, C., Xu, G., Dorward, H., Tansey, J. T., Contreras, J. A., Kimmel, A. R., and

Londos, C. (2003). Perilipin a is essential for the translocation of hormone-sensitive lipase during lipolytic activation. *J Cell Biol*, 161(6):1093–103.

Takehana, A., Katsuyama, T., Yano, T., Oshima, Y., Takada, H., Aigaki, T., and Kurata, S. (2002). Overexpression of a pattern-recognition receptor, peptidoglycan-recognition protein-le, activates imd/relish-mediated antibacterial defense and the prophenoloxidase cascade in drosophila larvae. *Proc Natl Acad Sci U S A*, 99(21):13705–10.

Takeuchi, O., Kawai, T., Sanjo, H., Copeland, N. G., Gilbert, D. J., Jenkins, N. A., Takeda, K., and Akira, S. (1999). Tlr6: A novel member of an expanding toll-like receptor family. *Gene*, 231(1-2):59–65.

Tal, M. C., Sasai, M., Lee, H. K., Yordy, B., Shadel, G. S., and Iwasaki, A. (2009). Absence of autophagy results in reactive oxygen species-dependent amplification of rlr signaling. *Proc Natl Acad Sci U S A*, 106(8):2770–5.

Tallóczy, Z., Virgin, 4th, H. W., and Levine, B. (2006). Pkr-dependent autophagic degradation of herpes simplex virus type 1. *Autophagy*, 2(1):24–9.

Tang, W.-F., Yang, S.-Y., Wu, B.-W., Jheng, J.-R., Chen, Y.-L., Shih, C.-H., Lin, K.-H., Lai, H.-C., Tang, P., and Horng, J.-T. (2007). Reticulon 3 binds the 2c protein of enterovirus 71 and is required for viral replication. *J Biol Chem*, 282(8):5888–98.

Taylor, M. P., Burgon, T. B., Kirkegaard, K., and Jackson, W. T. (2009). Role of microtubules in extracellular release of poliovirus. *J Virol*, 83(13):6599–609.

Teixeira, L., Rabouille, C., Rørth, P., Ephrussi, A., and Vanzo, N. F. (2003). Drosophila perilipin/adrp homologue lsd2 regulates lipid metabolism. *Mech Dev*, 120(9):1071–81.

Teninges, D., Ohanessian, A., Richard-Molard, C., and Contamine, D. (1978). Isolation and biological properties of drosophila x virus. *Journal of General Virology*.

Thiam, A. R., Farese, Jr, R. V., and Walther, T. C. (2013). The biophysics and cell biology of lipid droplets. *Nat Rev Mol Cell Biol*, 14(12):775–86.

Trapnell, C., Hendrickson, D. G., Sauvageau, M., Goff, L., Rinn, J. L., and Pachter, L. (2013). Differential analysis of gene regulation at transcript resolution with rna-seq. *Nat Biotechnol*, 31(1):46–53.

Trapnell, C., Pachter, L., and Salzberg, S. L. (2009). Tophat: discovering splice junctions with rna-seq. *Bioinformatics*, 25(9):1105–11.

Trapnell, C., Williams, B. A., Pertea, G., Mortazavi, A., Kwan, G., van Baren, M. J., Salzberg, S. L., Wold, B. J., and Pachter, L. (2010). Transcript assembly and quantification by rna-seq reveals unannotated transcripts and isoform switching during cell differentiation. *Nat Biotechnol*, 28(5):511–5.

Tsukada, M. and Ohsumi, Y. (1993). Isolation and characterization of autophagy-defective mutants of saccharomyces cerevisiae. *FEBS Lett*, 333(1-2):169–74.

Tucker, K. A., Reggiori, F., Dunn, Jr, W. A., and Klionsky, D. J. (2003). Atg23 is essential for the cytoplasm to vacuole targeting pathway and efficient autophagy but not pexophagy. *J Biol Chem*, 278(48):48445–52.

Ulvila, J., Vanha-Aho, L.-M., and Rämet, M. (2011). Drosophila phagocytosis - still many unknowns under the surface. *APMIS*, 119(10):651–62.

Valanne, S., Wang, J.-H., and Rämet, M. (2011). The drosophila toll signaling pathway. *J Immunol*, 186(2):649–56.

van Rij, R. P., Saleh, M.-C., Berry, B., Foo, C., Houk, A., Antoniewski, C., and Andino, R. (2006). The rna silencing endonuclease argonaute 2 mediates specific antiviral immunity in drosophila melanogaster. *Genes Dev*, 20(21):2985–95.

van Vlies, N., Ferdinandusse, S., Turkenburg, M., Wanders, R. J. A., and Vaz, F. M. (2007). Ppar alpha-activation results in enhanced carnitine biosynthesis and octn2-mediated hepatic carnitine accumulation. *Biochim Biophys Acta*, 1767(9):1134–42.

Vaz, F. M. and Wanders, R. J. A. (2002). Carnitine biosynthesis in mammals. *Biochem J*, 361(Pt 3):417–29.

Vereshchagina, N., Ramel, M.-C., Bitoun, E., and Wilson, C. (2008). The protein phosphatase pp2a-b' subunit widerborst is a negative regulator of cytoplasmic activated akt and lipid metabolism in drosophila. *J Cell Sci*, 121(Pt 20):3383–92.

Vereshchagina, N. and Wilson, C. (2006). Cytoplasmic activated protein kinase akt regulates lipid-droplet accumulation in drosophila nurse cells. *Development*, 133(23):4731–5.

von Einem, U. I., Gorbalenya, A. E., Schirrmeier, H., Behrens, S.-E., Letzel, T., and Mundt, E. (2004). Vp1 of infectious bursal disease virus is an rna-dependent rna polymerase. *J Gen Virol*, 85(Pt 8):2221–9.

Wang, C. W., Kim, J., Huang, W. P., Abeliovich, H., Stromhaug, P. E., Dunn, Jr, W. A., and Klionsky, D. J. (2001). Apg2 is a novel protein required for the cytoplasm to

vacuole targeting, autophagy, and pexophagy pathways. *J Biol Chem*, 276(32):30442–51.

Wang, K., Singh, D., Zeng, Z., Coleman, S. J., Huang, Y., Savich, G. L., He, X., Mieczkowski, P., Grimm, S. A., Perou, C. M., MacLeod, J. N., Chiang, D. Y., Prins, J. F., and Liu, J. (2010). Mapsplice: accurate mapping of rna-seq reads for splice junction discovery. *Nucleic Acids Res*, 38(18):e178.

Wang, X.-H., Aliyari, R., Li, W.-X., Li, H.-W., Kim, K., Carthew, R., Atkinson, P., and Ding, S.-W. (2006). Rna interference directs innate immunity against viruses in adult drosophila. *Science*, 312(5772):452–4.

Wang, Z., Gerstein, M., and Snyder, M. (2009). Rna-seq: a revolutionary tool for transcriptomics. *Nat Rev Genet*, 10(1):57–63.

Weber, S., Fichtner, D., Mettenleiter, T. C., and Mundt, E. (2001). Expression of vp5 of infectious pancreatic necrosis virus strain vr299 is initiated at the second in-frame start codon. *J Gen Virol*, 82(Pt 4):805–12.

Wei, L., Zhu, S., Ruan, G., Hou, L., Wang, J., Wang, B., and Liu, J. (2011). Infectious bursal disease virus-induced activation of jnk signaling pathway is required for virus replication and correlates with virus-induced apoptosis. *Virology*, 420(2):156–63.

Welte, M. A., Cermelli, S., Griner, J., Viera, A., Guo, Y., Kim, D.-H., Gindhart, J. G., and Gross, S. P. (2005). Regulation of lipid-droplet transport by the perilipin homolog lsd2. *Curr Biol*, 15(14):1266–75.

Werner, T., Borge-Renberg, K., Mellroth, P., Steiner, H., and Hultmark, D. (2003). Functional diversity of the drosophila pgrp-lc gene cluster in the response to lipopolysaccharide and peptidoglycan. *J Biol Chem*, 278(29):26319–22.

Werner, T., Liu, G., Kang, D., Ekengren, S., Steiner, H., and Hultmark, D. (2000). A family of peptidoglycan recognition proteins in the fruit fly drosophila melanogaster. *Proc Natl Acad Sci U S A*, 97(25):13772–7.

Wilhelm, B. T. and Landry, J.-R. (2009). Rna-seq-quantitative measurement of expression through massively parallel rna-sequencing. *Methods*, 48(3):249–57.

Williams, M. J. (2007). Drosophila hemopoiesis and cellular immunity. *J Immunol*, 178(8):4711–6.

Wu, L. P. and Anderson, K. V. (1998). Regulated nuclear import of rel proteins in the drosophila immune response. *Nature*, 392(6671):93–7.

Wu, Y.-T., Tan, H.-L., Shui, G., Bauvy, C., Huang, Q., Wenk, M. R., Ong, C.-N., Codogno, P., and Shen, H.-M. (2010). Dual role of 3-methyladenine in modulation of autophagy via different temporal patterns of inhibition on class i and iii phosphoinositide 3-kinase. *J Biol Chem*, 285(14):10850–61.

Xi, Z., Ramirez, J. L., and Dimopoulos, G. (2008). The aedes aegypti toll pathway controls dengue virus infection. *PLoS Pathog*, 4(7):e1000098.

Xie, J., Pan, H., Yoo, S., and Gao, S.-J. (2005). Kaposi's sarcoma-associated herpesvirus induction of ap-1 and interleukin 6 during primary infection mediated by multiple mitogen-activated protein kinase pathways. *J Virol*, 79(24):15027–37.

Xu, Y., Jagannath, C., Liu, X.-D., Sharafkhaneh, A., Kolodziejska, K. E., and Eissa, N. T. (2007). Toll-like receptor 4 is a sensor for autophagy associated with innate immunity. *Immunity*, 27(1):135–44.

Yan, R., Small, S., Desplan, C., Dearolf, C. R., and Darnell, Jr, J. E. (1996). Identification of a stat gene that functions in drosophila development. *Cell*, 84(3):421–30.

Yang, Z. and Klionsky, D. J. (2010). Eaten alive: a history of macroautophagy. *Nat Cell Biol*, 12(9):814–22.

Yano, T., Mita, S., Ohmori, H., Oshima, Y., Fujimoto, Y., Ueda, R., Takada, H., Goldman, W. E., Fukase, K., Silverman, N., Yoshimori, T., and Kurata, S. (2008). Autophagic control of listeria through intracellular innate immune recognition in drosophila. *Nat Immunol*, 9(8):908–16.

Yao, K., Goodwin, M. A., and Vakharia, V. N. (1998). Generation of a mutant infectious bursal disease virus that does not cause bursal lesions. *J Virol*, 72(4):2647–54.

Yue, Z., Jin, S., Yang, C., Levine, A. J., and Heintz, N. (2003). Beclin 1, an autophagy gene essential for early embryonic development, is a haploinsufficient tumor suppressor. *Proc Natl Acad Sci U S A*, 100(25):15077–82.

Zachos, G., Clements, B., and Conner, J. (1999). Herpes simplex virus type 1 infection stimulates p38/c-jun n-terminal mitogen-activated protein kinase pathways and activates transcription factor ap-1. *J Biol Chem*, 274(8):5097–103.

Zaidman-Rémy, A., Hervé, M., Poidevin, M., Pili-Floury, S., Kim, M.-S., Blanot, D., Oh, B.-H., Ueda, R., Mengin-Lecreulx, D., and Lemaitre, B. (2006). The drosophila

amidase pgrp-lb modulates the immune response to bacterial infection. *Immunity*, 24(4):463–73.

Zaidman-Rémy, A., Poidevin, M., Hervé, M., Welchman, D. P., Paredes, J. C., Fahlander, C., Steiner, H., Mengin-Lecreulx, D., and Lemaitre, B. (2011). Drosophila immunity: analysis of pgrp-sb1 expression, enzymatic activity and function. *PLoS One*, 6(2):e17231.

Zambon, R. A., Nandakumar, M., Vakharia, V. N., and Wu, L. P. (2005). The toll pathway is important for an antiviral response in drosophila. *Proc Natl Acad Sci U S A*, 102(20):7257–62.

Zambon, R. A., Vakharia, V. N., and Wu, L. P. (2006). Rnai is an antiviral immune response against a dsrna virus in drosophila melanogaster. *Cell Microbiol*, 8(5):880–9.

Zapata, H. J., Nakatsugawa, M., and Moffat, J. F. (2007). Varicella-zoster virus infection of human fibroblast cells activates the c-jun n-terminal kinase pathway. *J Virol*, 81(2):977–90.

Zerbino, D. R. and Birney, E. (2008). Velvet: algorithms for de novo short read assembly using de bruijn graphs. *Genome Res*, 18(5):821–9.

Zhang, Z. and Wang, W. (2014). Rna-skim: a rapid method for rna-seq quantification at transcript level. *Bioinformatics*, 30(12):i283–i292.

Zhirnov, O. P. and Klenk, H. D. (2013). Influenza a virus proteins ns1 and hemagglutinin along with m2 are involved in stimulation of autophagy in infected cells. *J Virol*, 87(24):13107–14.

Zhou, R., Silverman, N., Hong, M., Liao, D. S., Chung, Y., Chen, Z. J., and Maniatis, T. (2005). The role of ubiquitination in drosophila innate immunity. *J Biol Chem*, 280(40):34048–55.

Zhou, R., Yazdi, A. S., Menu, P., and Tschopp, J. (2011). A role for mitochondria in nlrp3 inflammasome activation. *Nature*, 469(7329):221–5.

Zhou, X., Babu, J. R., da Silva, S., Shu, Q., Graef, I. A., Oliver, T., Tomoda, T., Tani, T., Wooten, M. W., and Wang, F. (2007). Unc-51-like kinase 1/2-mediated endocytic processes regulate filopodia extension and branching of sensory axons. *Proc Natl Acad Sci U S A*, 104(14):5842–7.